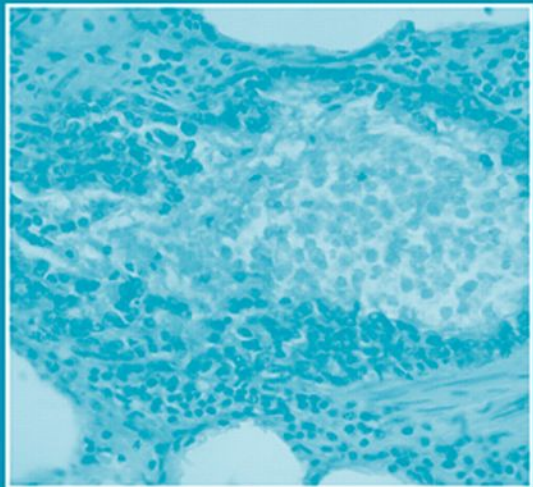


INTERNATIONAL REVIEW OF CYTOLOGY

A SURVEY OF CELL BIOLOGY

Edited by
Kwang W. Jeon



Volume 257



International Review of

Cytology

A Survey of

Cell Biology

VOLUME 257

SERIES EDITORS

Geoffrey H. Bourne	1949–1988
James F. Danielli	1949–1984
Kwang W. Jeon	1967–
Martin Friedlander	1984–1992
Jonathan Jarvik	1993–1995

EDITORIAL ADVISORY BOARD

Isaiah Arkin	Keith Latham
Eve Ida Barak	Bruce D. McKee
Peter L. Beech	Michael Melkonian
Howard A. Bern	Keith E. Mostov
Robert A. Bloodgood	Andreas Oksche
Dean Bok	Thoru Pederson
Hiroo Fukuda	Manfred Schliwa
Ray H. Gavin	Teruo Shimmen
Siamon Gordon	Robert A. Smith
May Griffith	Wildred D. Stein
William R. Jeffery	Nikolai Tomilin

International Review of
Cytology A Survey of
Cell Biology

Edited by

Kwang W. Jeon
Department of Biochemistry
University of Tennessee
Knoxville, Tennessee

VOLUME 257



AMSTERDAM • BOSTON • HEIDELBERG • LONDON
NEW YORK • OXFORD • PARIS • SAN DIEGO
SAN FRANCISCO • SINGAPORE • SYDNEY • TOKYO
Academic Press is an imprint of Elsevier



Front Cover Photograph: Courtesy of Darko Marinkovic:
Faculty of Veterinary Medicine, Belgrade, Serbia

Academic Press is an imprint of Elsevier
525 B Street, Suite 1900, San Diego, California 92101-4495, USA
84 Theobald's Road, London WC1X 8RR, UK

This book is printed on acid-free paper. 

Copyright © 2007, Elsevier Inc. All Rights Reserved.

No part of this publication may be reproduced or transmitted in any form or by any means, electronic or mechanical, including photocopy, recording, or any information storage and retrieval system, without permission in writing from the Publisher.

The appearance of the code at the bottom of the first page of a chapter in this book indicates the Publisher's consent that copies of the chapter may be made for personal or internal use of specific clients. This consent is given on the condition, however, that the copier pay the stated per copy fee through the Copyright Clearance Center, Inc. (www.copyright.com), for copying beyond that permitted by Sections 107 or 108 of the U.S. Copyright Law. This consent does not extend to other kinds of copying, such as copying for general distribution, for advertising or promotional purposes, for creating new collective works, or for resale. Copy fees for pre-2007 chapters are as shown on the title pages. If no fee code appears on the title page, the copy fee is the same as for current chapters.
0074-7696/2007 \$35.00

Permissions may be sought directly from Elsevier's Science & Technology Rights Department in Oxford, UK: phone: (+44) 1865 843830, fax: (+44) 1865 853333, E-mail: permissions@elsevier.com. You may also complete your request on-line via the Elsevier homepage (<http://elsevier.com>), by selecting "Support & Contact" then "Copyright and Permission" and then "Obtaining Permissions."

For information on all Elsevier Academic Press publications
visit our Web site at www.books.elsevier.com

ISBN-13: 978-0-12-373701-4

ISBN-10: 0-12-373701-X

PRINTED IN THE UNITED STATES OF AMERICA
07 08 09 10 9 8 7 6 5 4 3 2 1

Working together to grow
libraries in developing countries

www.elsevier.com | www.bookaid.org | www.sabre.org

ELSEVIER

BOOK AID
International

Sabre Foundation

CONTENTS

Contributors	ix
--------------------	----

Role of CCN2/CTGF/Hcs24 in Bone Growth

Satoshi Kubota and Masaharu Takigawa

I. Introduction	2
II. The CCN Family	2
III. CCN2: A Multiple Regulator of Mesenchymal Tissue Development	8
IV. CCN2 and Bone Cell Biology	12
V. Concluding Remarks	30
References	31

Action Potential in Charophytes

Mary Jane Beilby

I. Introduction	43
II. Historical Background (Up to Late 1990s)	49
III. New Approaches in the New Century	71
IV. Summary	74
References	76

Similarity of the Domain Structure of Proteins as a Basis for the Conservation of Meiosis

Yu. F. Bogdanov, T. M. Grishaeva, and S. Ya. Dadashev

I.	Introduction.....	84
II.	Homomorphism of Cytological Features of Meiosis	86
III.	Functional Analogy of Morphogenetic Proteins in Meiosis	89
IV.	Recombination Enzymes	109
V.	Proteins of the SMC Family	114
VI.	Importance of Secondary Protein Structure for Ultrastructure Morphogenesis.....	122
VII.	Conclusion: Organelle Morphology as Dependent on the Protein Structure.....	130
	References	132

Fibroblast Differentiation in Wound Healing and Fibrosis

Ian A. Darby and Tim D. Hewitson

I.	Introduction.....	144
II.	Inflammation and Wound Healing	144
III.	Fibroblasts and Myofibroblasts	148
IV.	Fibrogenic Mediators.....	157
V.	Regulation of Fibrogenesis.....	166
VI.	Concluding Remarks	170
	References	170

Tumor Hypoxia and Targeted Gene Therapy

Olga Greco and Simon Scott

I.	Introduction.....	181
II.	Hypoxia-Targeted Gene Therapy	184
III.	Combination of Hypoxia Gene Therapy with Conventional Treatments.....	196
IV.	Concluding Remarks	201
	References	201

Cellular Basis of Chronic Obstructive Pulmonary Disease in Horses

Darko Marinkovic, Sanja Aleksic-Kovacevic, and Pavle Plamenac

I. Introduction	214
II. Morpho-Functional Features of Horse Lungs	216
III. Cytological Features of Equine Lungs.....	221
IV. Chronic Obstructive Pulmonary Disease (COPD) in Horses	223
V. Conclusions and Perspectives	238
References	240
Index	249

This page intentionally left blank

CONTRIBUTORS

Numbers in parentheses indicate the pages on which the authors' contributions begin.

Sanja Aleksic-Kovacevic (213), *Department of Pathology, Faculty of Veterinary Medicine, University of Belgrade, Belgrade, Serbia*

Mary Jane Beilby (43), *School of Physics, The University of New South Wales, Sydney, Australia*

Yu. F. Bogdanov (83), *Vavilov Institute of General Genetics, Russian Academy of Sciences, Moscow, Russian Federation*

S. Ya. Dadashev (83), *Vavilov Institute of General Genetics, Russian Academy of Sciences, Moscow, Russian Federation*

Ian A. Darby (143), *School of Medical Sciences, RMIT University, Melbourne, Australia*

Olga Greco (181), *Tumour Microcirculation Group, University of Sheffield, Royal Hallamshire Hospital, Sheffield, United Kingdom*

T. M. Grishaeva (83), *Vavilov Institute of General Genetics, Russian Academy of Sciences, Moscow, Russian Federation*

Tim D. Hewitson (143), *Department of Nephrology, The Royal Melbourne Hospital; Department of Medicine, University of Melbourne, Melbourne, Australia*

Satoshi Kubota (1), *Department of Biochemistry and Molecular Dentistry, Okayama University Graduate School of Medicine, Dentistry and Pharmaceutical Sciences, Okayama, Japan*

Darko Marinkovic (213), *Department of Pathology, Faculty of Veterinary Medicine, University of Belgrade, Belgrade, Serbia*

Pavle Plamenac (213), *Department of Pathology, Faculty of Veterinary Medicine, University of Belgrade, Belgrade, Serbia*

Simon Scott (181), *Medway School of Pharmacy, The University of Kent, Kent, United Kingdom*

Masaharu Takigawa (1), *Department of Biochemistry and Molecular Dentistry, Okayama University Graduate School of Medicine, Dentistry and Pharmaceutical Sciences, Okayama, Japan*

Role of CCN2/CTGF/Hcs24 in Bone Growth

Satoshi Kubota and Masaharu Takigawa*

Department of Biochemistry and Molecular Dentistry, Okayama University Graduate School of Medicine, Dentistry and Pharmaceutical Sciences, Okayama, Japan

Our bones mostly develop through a process called endochondral ossification. This process is initiated in the cartilage prototype of each bone and continues through embryonic and postnatal development until the end of skeletal growth. Therefore, the central regulator of endochondral ossification is the director of body construction, which is, in other words, the determinant of skeletal size and shape. We suggest that CCN2/CTGF/Hcs24 (CCN2) is a molecule that conducts all of the procedures of endochondral ossification. CCN2, a member of the CCN family of novel modulator proteins, displays multiple functions by manipulating the local information network, using its conserved modules as an interface with a variety of other biomolecules. Under a precisely designed four-dimensional genetic program, CCN2 is produced from a limited population of chondrocytes and acts on all of the mesenchymal cells inside the bone callus to promote the integrated growth of the bone. Furthermore, the utility of CCN2 as regenerative therapeutics against connective tissue disorders, such as bone and cartilage defects and osteoarthritis, has been suggested. Over the years, the pathological action of CCN2 has been suggested. Nevertheless, it can also be regarded as another aspect of the physiological and regenerative function of CCN2, which is discussed as well.

KEY WORDS: Bone growth, Endochondral ossification, Bone regeneration, CCN family, Cartilage/chondrocytes, Skeletal development, Connective tissue growth factor (CTGF). © 2007 Elsevier Inc.

*Corresponding author. E-mail address: takigawa@md.okayama-u.ac.jp

I. Introduction

In mammals, the development of most bones in the skeleton is initiated by the preparation of the cartilage prototype and is accomplished through endochondral ossification or its related process. Endochondral ossification occurs mainly by growth plate chondrocytes in a precisely organized architecture with four-dimensional (i.e., temporal and spatial) polarity of cytodifferentiation, in collaboration with vascular endothelial cells and osteoblasts, which invade through the cartilage canal. This complex biological process is under the control of a vast number of systemic hormones and local growth factors. Analogous to a full orchestra that needs a conductor to play polyphonic music with multiple instruments, certain key molecules have to modulate the functioning status of these signaling molecules and integrate the extracellular information in a harmonized manner to maintain the proper biological architecture of the growth plate and to promote the endochondral ossification toward bone growth. We suggest that CCN2, which is a classical member of the CCN protein family and was formerly called the connective tissue growth factor (CTGF)/hypertrophic chondrocyte-specific gene product 24 (Hcs24)/ecogenin, is one such conductor/modulator of bone growth.

The functional characteristics of CCN2 as a conductor/modulator are represented by the fact that CCN2 is capable of promoting both the growth and differentiation of most mesenchymal cells involved in endochondral ossification. This apparently contradictory functionality may explain how CCN2 acts as a central driver of cartilage/bone growth and regeneration. In this article, we first briefly introduce the novel family of modulator proteins, namely the CCN family. Thereafter, we summarize advances in CCN2 research, mainly from the viewpoint of the molecular and cellular biology of bone growth and regeneration.

II. The CCN Family

A. General Structure and Terminology

The acronym “CCN” does not represent any structural or functional aspect of this gene family, but is a simple assemblage of the three classical members recognized earlier. This “family name” was first given in 1993 by Bork from the first letters of Cyr61 (cysteine-rich protein 61), CTGF (connective tissue growth factor), and NOV (nephroblastoma-overexpressed gene). Thereafter, three additional members were newly classified in this family (Brigstock, 1999; Lau and Lam, 1999; Perbal, 2004; Perbal and Takigawa, 2005; Takigawa

et al., 2003). During this emerging period, a number of different names were independently assigned to each member by different research groups, thereby resulting in significant confusion in terminology (Baxter et al., 1998; Grotendorst et al., 2000; Moussad and Brigstock, 2000). To resolve this problem, a unified nomenclature was proposed in 2003, in which each member was renamed numerically under the family name, CCN (Brigstock et al., 2003). The relevance between the unified and original name of each member is summarized in Fig. 1A. Mammals possess six members in their genome so far, and no evidence for another member has yet been described.

Although the genomic organization of the members demonstrates remarkable variety, all of the gene products retain a highly characteristic structure. Except for CCN6, these proteins consist of four conserved protein modules connected in tandem in order, following an N-terminal signal peptide for secretion. It should be noted that these four modules—insulin-like growth

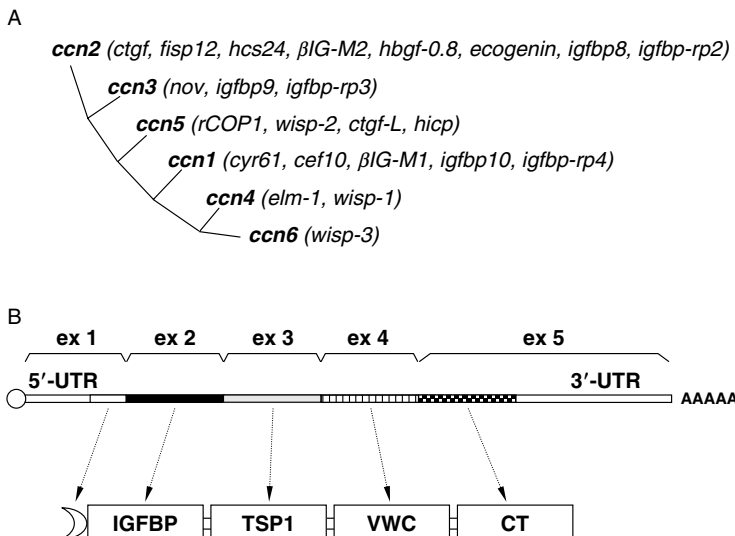


FIG. 1 The CCN family. (A) The six members identified in the mammalian genomes. Previous designations given to each gene member are shown in parentheses. The members are placed based on a genetic dendrogram previously proposed (Perbal and Takigawa, 2005). (B) General structure of the mRNA and the nascent protein of a CCN family member. The mRNA is the assemblage of five exons (top of the panel) with the 5'-cap and 3'-poly(A) tail structures. Exons (ex) 1, 2, 3, 4, and 5 encode the signal peptide for secretion (a crescent), insulin-like growth factor-binding protein module (IGFBP), thrombospondin type 1 repeat module (TSP1), von Willebrand factor type C repeat (VWC) module, and carboxyl terminal cysteine knot (CT) module, respectively, except for CCN5, which lacks the CT module. The open reading frame is flanked by the 5'-untranslated region (UTR) and the 3'-UTR, which are crucial for the posttranscriptional regulation of gene expression in most members.

factor binding protein (IGFBP), von Willebrand factor type C repeat (VWC), thrombospondin type 1 repeat (TSP1), and C-terminal cysteine-knot (CT) modules—contain conserved cysteine residues and are highly interactive with a variety of other molecules, thus providing a structural basis for the multiple functionality of CCN member proteins (Perbal and Takigawa, 2005). Interestingly, each module is encoded by the corresponding single exon, and the boundaries of exons in mRNA strictly correspond to the module boundary in protein (Fig. 1B). Therefore, the CCN members are supposed to have developed by exon shuffling along the course of evolution (Patthy, 1987). In this context, the conserved cysteine residues involved in all of the modules are supposed to determine the proper tertiary structure of each module by intra-modular interactions rather than by intermodular/intermolecular interactions (Brigstock, 1999). In the mRNAs, the coding regions are flanked by 5'- and 3'-untranslated regions (UTR) that contain critical regulatory elements of gene expression, which will be described later (Kubota and Takigawa, 2002).

B. Members of the CCN Family

1. CCN1/Cyr61/Cef10

The first member of the CCN family was identified as one of the immediate-early genes in mouse fibroblasts in 1989. Because of the 38 cysteine residues in the gene product, which is currently recognized to be conserved among all of the CCN family proteins, this gene was designated cysteine-rich 61 (*cyr61*) (O'Brien *et al.*, 1990; Simmons *et al.*, 1989). Mammalian *ccn1* genes are quite compact with relatively short introns, as observed in *ccn2*. In terms of protein structure, CCN1/Cyr61 is uniquely characterized by spacer/hinge amino acid stretches located between the VWC and TSP modules (Bork, 1993). However, the functional significance of this intermodular peptide is still unclear.

The CCN1 protein is known to mediate integrin-associated cell adhesion events while promoting wound healing, angiogenesis, and chondrogenesis, as also observed in the case of CCN2 (Chen *et al.*, 2001a,b; Jedsadayanmata *et al.*, 1999; Kireeva *et al.*, 1997; Schober *et al.*, 2002). In addition, when we stimulated chondrocytic cells with different types of cytokines, *ccn1* and *ccn2* displayed a similar response to all the stimuli examined, thus indicating that they may be engaged in similar missions in the metabolism of skeletal tissues (Moritani *et al.*, 2005). Nevertheless, a difference in their biological roles was also clearly represented by the phenotypic difference between knockout (KO) mice of *ccn1* and *ccn2*. Most of *ccn1* KO mice were reported to be embryonic lethal, due to a failure of embryonic vascular system development in placenta (Mo *et al.*, 2002), whereas skeletal phenotypes of a survived minor population of animals displayed different changes from those observed in the

ccn2 KO mice (Dornbach and Lyons, 2004). In summary, CCN1 may therefore be regarded as a modulator in bone development second to CCN2.

Similarities and differences between the two are also represented in other functional properties. In analogy to *ccn2*, *ccn1* is involved in the determination of malignant phenotypes of several types of tumor cells (Perbal, 2001; Tong *et al.*, 2001; Xie *et al.*, 2001). In contrast, opposite roles of *ccn1* and *ccn2* in the development of renal fibrosis were proposed (Sawai *et al.*, 2003; Yokoi *et al.*, 2001). However, it is at least clear that both are biologically required and neither is dispensable for vertebrates.

2. CCN2/CTGF/Hcs24/Fisp12

This particular member will be described in complete detail in the following sections. Therefore, we briefly describe only the history of CCN2/CTGF research. CCN2/CTGF was first discovered as a mitogenic and chemotactic factor purified from human cultured vein endothelial cell supernatant in 1991 (Bradham *et al.*, 1991). Owing to such effects, it was initially called connective tissue growth factor for fibroblasts. However, before the discovery of human CCN2/CTGF, a murine orthologue had already been isolated from NIH/3T3 and transforming growth factor (TGF)- β -stimulated mouse ARK-2B cells, and designated fibroblast-inducible secreted protein-12 (Fisp12) (Ryseck *et al.*, 1991) and β IG-M2 (Brunner *et al.*, 1991), respectively. After a few years, a cDNA that was specifically expressed in a human chondrocytic cell line was cloned and the corresponding gene was designated the hypertrophic chondrocyte-specific 24 (*hcs24*) gene, since this gene displayed a highly specific expression among the hypertrophic chondrocytes at a particular stage of development in mice (Nakanishi *et al.*, 1997). In relation to these findings, another name, “ecogenin,” was given to its gene product, since its gene product was revealed to be a central promoter of endochondral ossification (Takigawa *et al.*, 2003). As such, since independent research groups analyzed the function of this multifunctional modulator based on different aspects, a number of different names were consequently given to this single molecule (Fig. 1A). The fact that no other member possesses more names than CCN2/CTGF may represent the multiple functionality of this molecule, as described in this article.

3. CCN3/Nov

The original name given to CCN3 stands for nephroblastoma overexpressed gene (*nov*), which indicates that this particular gene was found to be overexpressed in all of the chicken myeloblastosis-associated virus (MAV)-induced nephroblastomas examined so far (Joliot *et al.*, 1992). This MAV-associated form of the CCN3 protein was not a full-length one, but was an N-terminal truncated form due to the retroviral integration of the MAV provirus. Because

of this, CCN3 has been investigated primarily from pathological points of view. In fact, the overexpression of *ccn3* has been reported in various types of tumors; however, its role in tumorigenesis and its relationship to malignant phenotypes are still controversial. Studies have revealed that full-length CCN3 tended to counteract the malignant phenotypes in Ewing sarcoma and glioblastoma cells (Gupta *et al.*, 2001).

Compared to the oncological roles mentioned previously, the physiological functions of CCN3 still remain to be investigated. The angiogenic property of CCN3 has already been proven, in which integrins play a critical role as a CCN3 receptor (Lin *et al.*, 2003). In addition, the expression of CCN3 in hypertrophic chondrocytes in growth cartilage and skeletal muscle tissues suggests a possible involvement of CCN3 in skeletal formation (Lafont *et al.*, 2005; Perbal, 2001; Yu *et al.*, 2003). During development, neuroepithelium and the neural tube show strong *ccn3* expression in chicken embryo (Katsume *et al.*, 2001). Although the function and its mechanism are still unclear, interactions with cell-surface molecules including Notch, connexins, and cadherins may be involved as CCN3 counterparts (Fu *et al.*, 2004; Gellhaus *et al.*, 2004; Sakamoto *et al.*, 2002). The nuclear localization of CCN3 was indicated, suggesting a possible role of CCN3 as an intracellular signaling molecule as well (Planque *et al.*, 2006).

4. CCN4/Elm1/WISP-1

The first report describing this gene appeared in 1998. In that report, a gene was found to be overexpressed in low-metastatic type 1 cells among murine melanomas, and it was thus named *Elm1* (Hashimoto *et al.*, 1998). In the same year, three human CCN family members were simultaneously discovered as Wnt1-inducible secretory proteins (WISP), which included the human *Elm1* orthologue (Pennica *et al.*, 1998). Since then, this new group of CCN family members has tended to be called serially numbered WISP proteins, until the names CCN4–6 were given. Similar to CCN3, most CCN4 research has been conducted in relation to the field of oncology (Soon *et al.*, 2003; Xu *et al.*, 2000). One of the most interesting findings concerning CCN4 is the identification of a novel splicing variant of *ccn4* mRNA, which is associated with malignant phenotypes of scirrhous gastric carcinoma and cholangiocarcinoma (Tanaka *et al.*, 2001, 2003). This splicing variant encodes a truncated form of CCN4 lacking the VWC module. The functional consequence of a deletion of a particular module is of critical interest, since such an event is also observed for CCN3 and CCN6.

Although not fully supported by experimental evidence, it is suspected that CCN4 plays a certain role in skeletalogenesis. First, CCN4 was found to regulate osteoblastic differentiation (French *et al.*, 2004). Second, we confirmed the production of CCN4 in cartilage tissues. Therefore, the role of

CCN2 in bone growth may be comprehensively discussed with those of other CCN family members in the near future.

As anticipated in all of the CCN family proteins, the molecular interaction of CCN4 and other molecules should provide the basis for its biological functions. From this point of view, the specific interaction with proteoglycans is worthy of note (Desnoyers *et al.*, 2001).

5. CCN5/rCOP-1/WISP-2

Among mammalian CCN family members CCN5 is the only one that genetically lacks one of the modules. Since the trimodular structure of CCN5 appears to be quite unusual as a CCN family member, it was once regarded as an endogenous antagonist with dominant-negative phenotypes against the other members. Nevertheless, subsequent research has revealed that CCN5 is also a multifunctional molecule, as summarized later.

The initial name, *Cop1*, was given for rat *ccn5* in 1998 during the investigation of antioncogenic genes that act as a negative regulator for cell transformation (Delmolino *et al.*, 2001; Zhang *et al.*, 1998). As happened in CCN4, the human orthologue was rediscovered as one of the Wnt1-inducible WISP gene products and classified as the second member of this group, WISP2 (Pennica *et al.*, 1998). This molecule was also once considered to be a CCN2-related molecule, which was highly produced in human osteoblasts, and another name, CTGF-L, was also given to it (Kumar *et al.*, 1999).

CCN5 is currently known to be involved in cell proliferation, adhesion, and osteoblastic differentiation. Including vascular smooth muscle cells (Delmolino *et al.*, 2001), research has indicated that *ccn5* gene expression was negatively correlated with cell proliferation in several types of cells, whereas it was promoted in MCF7 breast cancer cells (Delmalino *et al.*, 2001; Zhang *et al.*, 1998; Zoubine *et al.*, 2001). Such a controversial biological outcome by the same gene expression is one of the common characteristics of CCN family members. Regarding bone growth, the expression of *ccn5* was observed in normal osteoblasts, but it was absent in osteosarcoma cells (Kumar *et al.*, 1999). *In vitro* experiments indicated that *ccn5* promoted the adhesion of osteoblasts, while it inhibited osteocalcin production by rat osteoblastic cells (Kumar *et al.*, 1999). As such, biological missions assigned to CCN5 are still difficult to specify. However, together with the truncated forms of CCN3 and 4, future investigations on this trimodular member may provide critical information to help clarify certain specific functions of CCN protein subfragments.

6. CCN6/WISP-3

Unlike the other members, only one name, WISP3, was proposed for this member in 1998 before the establishment of the unified nomenclature (Pennica *et al.*, 1998). It does not necessarily mean that this molecule is an

accessory member, but is merely due to its relatively late discovery. In fact, although few reports are present, both physiological and pathological aspects of CCN6 function are known today. First, CCN6 is the only member that is associated with a distinct human genetic disorder. One year after its discovery, a number of mutations in *ccn6* genes were found in cases of progressive pseudorheumatoid dysplasia (Hurvitz *et al.*, 1999). More recently, a single nucleotide polymorphism analysis revealed an association between *ccn6* point mutations and susceptibility to juvenile idiopathic arthritis (Lamb *et al.*, 2005). These genetic associations were partially supported by the finding that overexpression of *ccn6* in chondrocytic cells induced enhanced production of cartilage matrix components (Sen *et al.*, 2004). These reports strongly indicate critical roles of CCN6 in cartilage development and bone growth. Nevertheless, a study with CCN6 KO mice showed CCN6 was dispensable for skeletal development (Kutz *et al.*, 2005). Obviously, further investigation is required to account for the discrepancy observed between human and murine species. It should also be noted that a splicing variant of CCN6 mRNA lacking coding exons for the TSP and CT modules was present in gastrointestinal carcinomas (Tanaka *et al.*, 2002), which again emphasizes certain functions of CCN subfragments in human malignancies, as suggested in other CCN family members.

III. CCN2: A Multiple Regulator of Mesenchymal Tissue Development

A. Distribution in Normal Tissues

When normal tissue distribution was biochemically analyzed with total organ/tissue preparation, *ccn2* appeared to be expressed in several different organs and tissues and was once supposed to be produced by a number of different types of cells. Even in such an initial investigation, no significant *ccn2* expression was detected in normal liver and peripheral blood leukocytes (Kim *et al.*, 1997; Mukudai *et al.*, 2003). However, more detailed cell biological and histological analyses revealed that the CCN2-producing cell population was highly restricted in normal adult tissues, as represented by the mesenchyme of the cardiovascular and gonadal systems (Friedrichsen *et al.*, 2005; Yamaai *et al.*, 2005). One of the major CCN2 producers is the vascular endothelial cell, which is involved in the tissues that conferred positive signals in biochemical analysis, as stated previously. Although CCN2 is actively produced from normal cells upon tissue regeneration, *ccn2* gene expression seems to remain silent in other tissue components. However interestingly, we do have a huge

reservoir of CCN2 in the bloodstream. In 2004, involvement of a large amount of CCN2 in platelets was uncovered (Cicha *et al.*, 2004; Kubota *et al.*, 2004). These findings emphasize the crucial role of CCN2 in angiogenesis and tissue regeneration in adult mammals.

During development, *ccn2* is distinctly expressed in a limited population of cells at specific differentiation stages, thus indicating its critical role in certain types of tissue development. This finding is best represented in growth plate cartilage. In the initiation of endochondral ossification, CCN2 is produced in a relatively broad range of chondrocytes. Along with long bone growth, expression of *ccn2* becomes restricted among prehypertrophic to hypertrophic chondrocytes (Moritani *et al.*, 2003b; Nakanishi *et al.*, 1997). It is interesting to note that the distribution of the CCN2 molecule does not necessarily correspond to that of the *ccn2* expressing cells. Indeed, an immunohistochemical analysis showed a stronger accumulation of CCN2 protein in terminally differentiated hypertrophic layers of mature growth plates, whereas gene expression was more prominent in prehypertrophic chondrocytes. A similar positional discrepancy was also observed during secondary ossification center formation. This “molecular walking” is supposed to be enabled by the specific interaction of CCN2 with certain proteoglycans that directly bind to CCN2 and are indispensable for cartilage development (Arikawa-Hirasawa *et al.*, 1999; Nishida *et al.*, 2003).

CCN2 is also actively produced in the kidney during the course of development (Friedrichsen *et al.*, 2005; Surveyor and Brigstock, 1999). Since CCN2 is induced upon angiogenesis, every process that requires vascular development may accompany CCN2 production. It is also of particular interest that *ccn2* gene expression was observed in the tooth germ mesenchymes of mouse developing teeth, indicating the possible contribution of CCN2 in the epithelial-mesenchymal signaling involved in tooth development (Shimo *et al.*, 2002; Yamaai *et al.*, 2005). Unexpectedly, the production of CCN2 by megakaryocytes has never previously been confirmed. Therefore, the origin of platelet-encapsulated CCN2 still remains to be clarified.

B. Physiological Roles in Connective Tissues

As represented by the expression pattern of *ccn2* in normal tissues, CCN2 plays a major role in the development and growth of particular tissues, such as cartilage, bone, heart, and kidney. Therefore, CCN2 is estimated to actively continue this mission in certain tissues for as long as the body grows, 20 years in the case of humans. Thereafter, CCN2 is occasionally expressed in the maintenance and regeneration of corresponding tissues, as stated later.

A number of *in vitro* studies have previously revealed the positive effects of CCN2 in the growth of connective tissues, including cartilage and bone. CCN2

actually promotes the proliferation of fibroblasts, chondrocytes, osteoblasts, and vascular endothelial cells *in vitro* (Babic *et al.*, 1999; Grotendorst and Duncan, 2005; Nakanishi *et al.*, 2000; Nishida *et al.*, 2002; Safadi *et al.*, 2003; Shimo *et al.*, 1999). Furthermore, it also promotes the differentiation of those cells with an enhancement of their own mature phenotypes. It should be noted that all of these biological events constitute the endochondral ossification process, which explains why it was once entitled “ecogenin.” In general, it is quite exceptional for a single protein to promote both proliferation and differentiation of the same cells, but CCN2 does both. However, such an ability to yield apparently opposite effects represents the very functional property of CCN proteins as modulators, as stated previously.

C. Involvement in Wound Healing

Since CCN2 was originally identified as a factor that promotes the proliferation and chemotaxis of fibroblasts, the relevance of CCN2 and wound healing was investigated in the relatively early days of CCN2 research mainly by dermatologists. In addition to such *in vitro* findings, *ccn2* gene expression in wounded skin tissues was first reported in 1993, which suggests specific roles of CCN2 in the normal healing process of skin tissue (Igarashi *et al.*, 1993). Finally, the abundant inclusion of CCN2 in platelets and the fact that platelet-rich plasma (PRP) actually promoted wound healing supported these hypothetical roles of CCN2 in wound healing (Laplante *et al.*, 2001).

CCN2 as a conductor of wound healing is also represented in certain skin disorders with hyperplasia and fibrosis. Overexpression of the CCN2 gene was locally observed in keloids, which may be regarded as an overregeneration of fibrotic tissue, and in cases of progressive systemic sclerosis (Igarashi *et al.*, 1996; Sato *et al.*, 2000). In those patients, the susceptibility of the *ccn2* gene to TGF- β was found to be elevated, indicating the involvement of not only CCN2, but also of TGF- β as an upstream signaling molecule in such skin fibrotic diseases (Kikuchi *et al.*, 1995; Mori *et al.*, 1999). The association of CCN2 with fibrosis in a number of other organs and tissues is described in further discussion.

D. CCN2 and Fibrotic Disorders: A Pathological Role

In addition to mitogenic activity, CCN2 also stimulates the production of extracellular matrix (ECM) components, such as collagens and fibronectins, from fibroblasts (Grotendorst and Duncan, 2005; Twigg *et al.*, 2002), which overall indicates that CCN2 is a promoter of fibrous tissue formation. Therefore, once the precise molecular system of CCN2 production is no longer regulated to trigger the overproduction, excessive fibrous tissue formation

might well occur in any organ containing fibroblasts. In line with this assumption, the contribution of CCN2 in fibrotic disorders in a number of organs has been specified. The classical case was reported in skin fibrosis, as stated previously. Subsequently, overexpression of CCN2 has been observed in renal fibrosis (Gupta *et al.*, 2000; Ito *et al.*, 1998), liver cirrhosis (Abou-Shady *et al.*, 2000; Hayashi *et al.*, 2002; Rachfal and Brigstock, 2003), pulmonary fibrosis (Allen *et al.*, 1999; Bonniaud *et al.*, 2003; Lasky *et al.*, 1998), cardiac fibrosis (Dean *et al.*, 2005), and pancreatic fibrosis (di Mola *et al.*, 1999). In addition, other fibrosis-associated human diseases, such as biliary atresia (Tamatani *et al.*, 1998), inflammatory bowel disease (Dammeier *et al.*, 1998a), and atherosclerosis, were also found to be associated with unusual CCN2 gene expression and production (Cicha *et al.*, 2005).

In many such fibrotic disorders including the previously mentioned skin fibrosis, it has been suggested that TGF- β is the upstream driver initiating these pathological events (Gruschwitz *et al.*, 1990; Kothapalli *et al.*, 1997). This hypothesis is supported by two distinct types of evidence. First, the involvement of TGF- β in those lesions was confirmed *in vivo*; second, the transcriptional activation of the CCN2 gene by TGF- β was uncovered by molecular biological investigations *in vitro* (Grotendorst *et al.*, 1996). It is known that TGF- β also stimulates CCN1 gene expression; however, TGF- β -induced CCN1 and CCN2 appear to act in distinct ways to yield an opposite biological outcome in renal fibrosis, where CCN2 plays a negative role, as introduced in the section on CCN1 (Sawai *et al.*, 2003; Yokoi *et al.*, 2001). As such, a structural and functional comparison of CCN1 and CCN2 can provide a breakthrough to clarify the mechanism of CCN2-induced fibrosis in the kidney.

E. Malignant Phenotypes and CCN2 in Tumors

As observed in other CCN family members, the role of CCN2 in tumorigenesis and malignant phenotypes of neoplasm still remains controversial. No evidence has yet indicated that CCN2 directly stimulates the growth of malignancies. It is true that the overexpression of the CCN2 gene has been observed in a number of human malignancies, including breast cancer (Xie *et al.*, 2001), skin cancer (Igarashi *et al.*, 1998), melanoma (Kubo *et al.*, 1998), pancreatic cancer (Wenger *et al.*, 1999), and chondrosarcoma (Shakunaga *et al.*, 2000). Of note, a significant relationship was indicated between CCN2 expression level and prognosis in clinical cases of breast cancer (Xie *et al.*, 2001) and colorectal cancer (Lin *et al.*, 2005). However, overexpression experiments *in vitro* usually resulted in attenuation of cell growth, promotion of differentiation, or induction of apoptosis (Hishikawa *et al.*, 1999; Moritani *et al.*, 2003a). Therefore, the concomitant expression of the *ccn2* gene in those malignancies does not seem to merit the proliferation of tumor cells *per se*.

Nevertheless, studies have helped to clarify the contribution of CCN2 in the invasion and metastasis of tumors. In particular, CCN2 has been shown to be involved in bone metastasis of breast cancer (Kang *et al.*, 2003; Shimo *et al.*, 2006). This finding is supported by the fact that CCN2 promotes angiogenesis upon tumor hypoxia, thereby inducing vascular endothelial cells to produce several catabolic enzymes to destroy the ECM of connective tissue (Kondo *et al.*, 2002). The molecular regulation of the hypoxic induction of CCN2 has been revealed to be exerted in multiple steps, as detailed later (Kondo *et al.*, 2002, 2006).

IV. CCN2 and Bone Cell Biology

A. Structure and Evolution of Bone and CCN2

1. Evolution of Skeleton and Two Modes of Mammalian Skeletal Development

It is widely recognized that mammalian bone consists of two types of bone of different origins (Karaplis, 2002). Most of the skeletal parts are developed through endochondral ossification or its related process, in which bone is initially designed as its own prototypic cartilage. Limited types of skeletal bone, such as the clavicle and cranium, are formed by a distinct biological process called intramembranous ossification. The latter process was established to furnish calcified exoskeleton in an early era of animal evolution, probably more than 300 million years ago. Therefore, the clavicle and cranium may be regarded as examples of fossil tissues in living mammals. In contrast, the other bones that are formed through cartilage by endochondral ossification have been established during the course of the evolution of animals toward vertebrates. In fact, the lamprey, which is widely recognized as one of the most primitive vertebrates on earth, possesses a vertebra that is entirely composed of uncalcified cartilage. Thereafter, the endoskeleton was furnished not only to support body structure and movement, but also for hematopoiesis and calcium phosphate storage as vertebrates were migrating from sea to rivers and finally to land.

In contrast to intramembranous ossification, in which bone is directly produced by osteoblasts from periosteum, endochondral ossification is accomplished by the collaboration of a number of different types of cells (Fig. 2A). The major cells involved are mesenchymal cells—particularly chondrocytes. The initial cartilage prototype consists of apparently uniform chondrocytes. However, once endochondral ossification is initiated, chondrocytes proceed to differentiate, strictly maintaining their polarity. In the

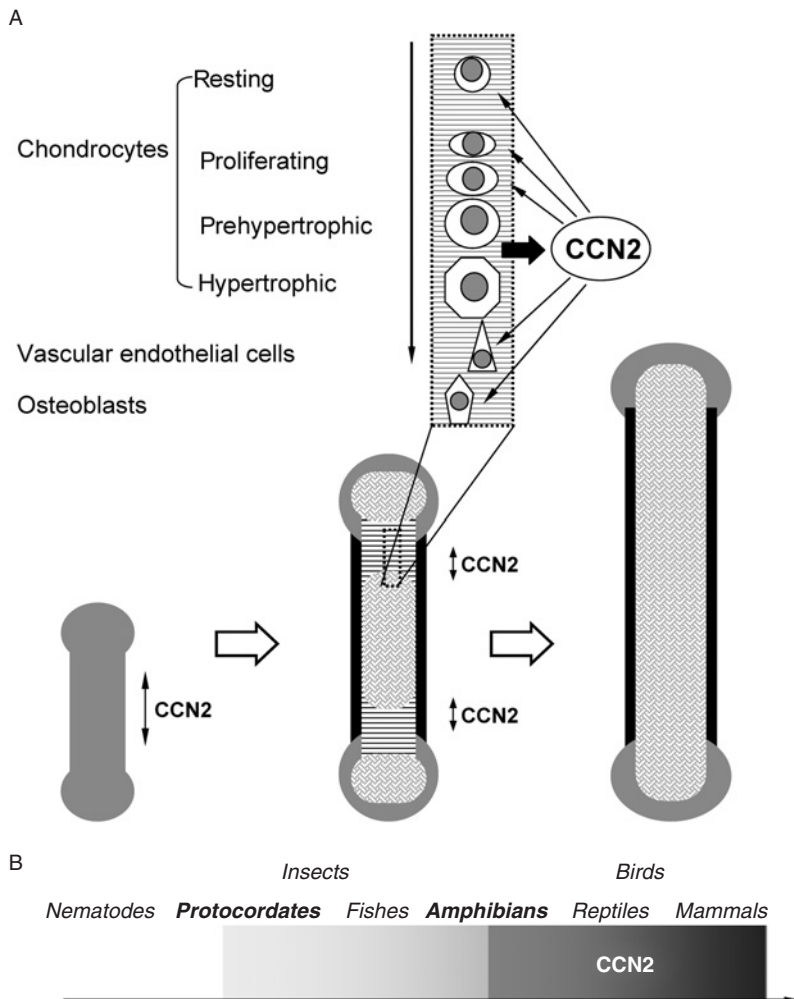


FIG. 2 CCN2 and endochondral ossification. (A) A schematic representation of the endochondral bone formation process and the roles of CCN2 therein. Most mammalian bones are initially constructed as a cartilage prototype (lower panel) and grow through a sophisticated process entitled endochondral ossification (upper panel). In this process, CCN2 is extensively produced by prehypertrophic/hypertrophic chondrocytes (also indicated with bidirectional arrows in the lower panel) that act as a paracrine factor to promote the entire procedure. (B) The emergence of CCN2 during the course of vertebrate evolution. Ancestral orthologues can be specified even in protostomes, such as *Ciona intestinalis* and insects. However, orthologues highly homologous (>80% at the nucleotide level excluding the signal peptide-encoding region) to human *ccn2*, which is thought to be the direct prototype of our *ccn2* gene, are found only in the species after amphibian evolution.

central stage of ossification, chondrocytes first proliferate to extend the body of the bone, and then the cells produce a vast amount of ECM, which is the major phenotype of mature chondrocytes. Finally, the cells reach the very central region where they undergo hypertrophy, thereby producing matrix vesicles and initiating the calcification of ECM. Toward the center of this hypertrophic zone, vascular invasion occurs in order to supply osteoblasts, blood cells, and their progenitors, while hypertrophic chondrocytes are removed after completing their task. As a result, after body growth, chondrocytes in metaphysis disappear, but they later reappear out of necessity from stromal cells—after a bone fracture, for example.

2. Structural and Functional Conservation of CCN2 along with Animal Evolution

In general, the genes that play a critical role in the drastic phenotypical changes that occur during the evolutionary course were prepared in advance for such apparent changes. Since *ccn2* is a critical gene in bone growth, it is a matter of course that this CCN family member is structurally conserved among all of the vertebrates with calcified bones. Moreover, we are able to find *ccn2* orthologues even in certain invertebrates. It is of particular note that *ccn2* can be found in tunicates, which develop through metamorphosis. In their adult body, the endoskeleton is totally absent; however, their larvae do form cartilaginous vertebrate-like structures. Thereafter, vertebrates were born after a long course of pedomorphosis. In summary, *ccn2* is supposed to have been furnished in the genome for the development of endoskeleton, rather than calcified tissues (Fig. 2B).

The functional conservation and compatibility of CCN2 among the mouse, rabbit, and human were confirmed by *in vivo* and *in vitro* studies; similar biological effects of human recombinant CCN2 (Nishida *et al.*, 1998; Asano *et al.*, 2005) were observed not only in human chondrocytic cells, but also in rabbit and mouse chondrocytes (Nakanishi *et al.*, 2000; Nishida *et al.*, 2002, 2004), and the *ccn2* KO mice displayed certain exact phenotypes that were expected by the data obtained in these studies (Ivkovic *et al.*, 2003). The transspecies compatibility of CCN2 is reminiscent of that of hormones, thus representing its major role in extracellular signaling.

3. Expression and Localization of the *ccn2* Gene Product in Developing Bone

Basically, the CCN2 protein is distributed where cartilage and bone are known to grow. As explained previously, in an adult animal after growth, growth plate cartilage is replaced by bone containing osteocytes, osteoblasts, hematopoietic cells, vascular endothelial cells, and their progenitors. No

detectable CCN2 protein is observed inside the callus of the long bones at this stage, except around vascular endothelial cells. However, during development, a vast amount of CCN2 molecules are produced under the strict four-dimensional program of gene expression. In the early stages of long bone development before ossification center formation, CCN2 protein is distributed among most of the chondrocytes except for the resting ones in the cartilage prototype. After the formation of the ossification center, the CCN2-positive chondrocyte population becomes limited around the ossification centers that are composed of hypertrophic/prehypertrophic chondrocytes (Moritani *et al.*, 2003b; Nakanishi *et al.*, 1997). A similar distribution of CCN2 is also observed among the articular chondrocytes facing the secondary ossification center at epiphyses in young animals (M. Oka *et al.*, unpublished observations). As the bone grows, a specific accumulation of CCN2 in hypertrophic/prehypertrophic layers becomes increasingly evident. In the advanced stage of endochondral ossification, CCN2 molecules are occasionally observed most strongly in the prehypertrophic layers, thus suggesting that prehypertrophic chondrocytes act as a major producer of CCN2, while late hypertrophic ones act as its reservoir. Beyond these chondrocytes, osteoblasts are engaging themselves in the construction and remodeling of cancellous bone. In young growing animals, CCN2 protein can be detected in those osteoblasts as well, albeit at reduced levels.

When bone growth is completed, there still is cartilage at the surface of the edge of the bone to construct the joints, which is called permanent articular cartilage. The articular cartilage does contain chondrocyte layers toward bone marrow, but CCN2 protein is usually absent therein, probably because such cartilage is not growing. However, in any situation requiring cartilage and bone regeneration, *ccn2* gene expression recurs, as observed in osteoarthritis (OA) (Kumar *et al.*, 2001; Omoto *et al.*, 2004), fracture, and tooth extraction (Kanyama *et al.*, 2003; Nakata *et al.*, 2002).

B. Roles of CCN2 in Bone Cell Biology

1. Effects on Growth Plate Chondrocytes

Since the rediscovery of *ccn2* as a gene specifically expressed in the human chondrocytic cell line HCS-2/8 (Hattori *et al.*, 1998; Takigawa *et al.*, 1989, 1991) *in vitro* and the hypertrophic layers of the developing mouse growth plate *in vivo* (Nakanishi *et al.*, 1997), the cell biological effects of CCN2 on growth plate chondrocytes has been extensively investigated. As a result of this research, it is now clear that CCN2 promotes the proliferation, maturation, and hypertrophy of growth plate chondrocytes at different stages of differentiation *in vitro*. Indeed, CCN2 promotes DNA and proteoglycan synthesis during the maturation stages with a concomitant increase in collagen type II and aggrecan

core protein gene expression, which are typical markers of mature chondrocytes (Nakanishi *et al.*, 2000). In the later stages of differentiation, CCN2 enhances calcium uptake, alkaline phosphatase activity, and collagen X expression, all of which represent hypertrophic phenotypes toward calcification. These findings were mainly obtained by using primary rabbit growth cartilage cells and highly active human recombinant CCN2 derived from transformed HeLa cells (Asano *et al.*, 2005; Shimo *et al.*, 1999). According to these results, not only the hypertrophic chondrocytes, but also the proliferating and even resting chondrocytes can be the targets of CCN2. Considering that CCN2 is predominantly released by prehypertrophic and hypertrophic chondrocytes, it is anticipated that it acts in an autocrine, paracrine, and matricrine (ECM-associated four-dimensional) manner to drive chondrocytes and other mesenchymal cells during endochondral ossification (Kubota *et al.*, 2001; Nishida *et al.*, 2003). Interestingly, in the early stage before growth plate formation, CCN2 is distributed throughout from proliferating to hypertrophic layers that include chondrocytes other than the CCN2 producers as well. This phenomenon supports the idea of the paracrine and matricrine action of CCN2. At the same time, it is hypothesized that the amount of infiltration of CCN2 in cartilage may be a factor in determining the resultant bone length after growth, which may well vary among individuals.

2. Effects on Osteoblasts and Vascular Endothelial Cells

If CCN2 acts in a paracrine manner, then the CCN2 released from the growth plate may act on osteoblasts and vascular endothelial cells. In fact, it has already been proven by several independent research groups that osteoblasts and endothelial cells are also targets of CCN2. Although the osteoblasts themselves produce little CCN2, an *in vitro* study clearly indicated that CCN2 promoted proliferation; maturation, as evaluated by the expression of a few marker genes, such as osteopontin and osteocalcin; and the mineralization of osteoblastic cells (Nishida *et al.*, 2000; Safadi *et al.*, 2003). These effects were probably mediated by cell-surface receptor molecules that were displayed on these cells. Osteoblasts are the central player in bone formation and remodeling, not only at the last stage of endochondral ossification, but also through intramembranous ossification. As such, CCN2 is therefore now considered to be involved in all of the bone growth processes of mammals.

The effects of CCN2 on vascular endothelial cells are intriguing, but controversial. Using recombinant CCN2, a few groups, including us, have uncovered the angiogenic potential of CCN2, as evaluated by the proliferation, migration, and tube formation of primary endothelial cells *in vitro* and by blood vessel formation *in vivo* (Babic *et al.*, 1999; Shimo *et al.*, 1998, 1999). As represented by the fact that growth plate formation is initiated by

the invasion of blood vessels through cartilage canals, physiological angiogenesis is indispensable for the proper growth of long bones. It should be noted that prior to the formation of the primary ossification center, *ccn2* gene expression was initiated surrounding the point of blood vessel invasion (M. Oka *et al.*, unpublished observations). Therefore, CCN2 seems to act as an angiogenic conductor in cartilage. These findings are supported by the phenotypes of the KO mice (Ivkovic *et al.*, 2003), as described later.

However, CCN2 is by no means the only major angiogenic molecule. Among other such molecules, vascular endothelial cell growth factor (VEGF) is one of the best known. Surprisingly, CCN2 was shown to interact with VEGF and to interfere with angiogenesis by VEGF (Inoki *et al.*, 2002). Since CCN2 is supposed to interact with a vast number of other bioactive molecules, the final outcome of CCN2 should thus be considered as the net output of various molecular interactions, which needs extensive investigation in the future (Fig. 3). In addition, several different malignant neoplasms have also been shown to take advantage of this property of CCN2 (Shimo *et al.*, 2001a,b), as briefly noted previously.

3. Effects on Articular Chondrocytes

Articular cartilage at the edges of long bones is one of the permanent cartilage tissues, including the nasal, auricular, tracheal, and laryngeal cartilage and the *nucleus pulposus* in vertebras. In contrast to growth plate chondrocytes, articular chondrocytes are maintained in articular cartilage as a part of the long bones even after the end of their growth. Their mission is to maintain the elasticity and integrity of the cartilage that is a critical part of joint machinery. Therefore, they have to supply cartilage matrix components and should never go beyond prehypertrophic stages in chondrocytic differentiation, except under pathological conditions.

Since CCN2 also promotes the hypertrophy of growth plate chondrocytes, it could be a specific promoter of pathological hypertrophy therein as well. However, surprisingly, CCN2 never promotes the hypertrophy of cultured articular chondrocytes even under differentiation-inducing conditions, whereas it does promote proliferation and maturation of those cells (Nishida *et al.*, 2002). These *in vitro* data are consistent with the *in vivo* findings that CCN2 production among articular chondrocytes is observed either during bone development (Nawachi *et al.*, 2002) or after cartilage damage (Kumar *et al.*, 2001; Omoto *et al.*, 2004), which thus suggests that CCN2 is required for the development and regeneration of articular cartilage. The differential effects of CCN2 on two distinct types of chondrocytes are probably enabled by the molecular property of CCN2 as a “four-handed modulator.” As a result of the interplay with multiple molecules, CCN2 may drive the whole extracellular signaling network toward the desired direction in each microenvironment. In addition,

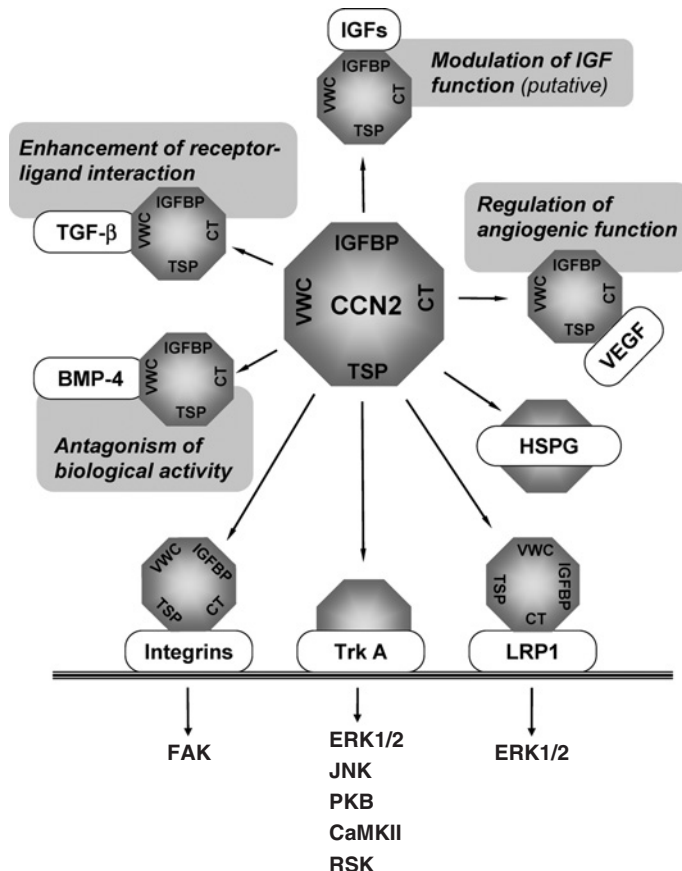


FIG. 3 The multiple interplay of CCN2 with other signaling molecules and its biological outcomes. Interactions with growth factors, cell surface signal transducing receptors, and heparan sulfate proteoglycans (HSPG) are illustrated. The resultant functional alteration by CCN2 is briefly described in the case of growth factors, while specific activation of intracellular signaling kinases is summarized for the cell surface receptors. Other abbreviations are explained in the text.

the differential effects of CCN2 on growth plate and articular chondrocytes also provide critical information to answer the basic question concerning the properties of chondrocytes. Are articular and growth plate chondrocytes basically the same and able to transdifferentiate each other, or are they already committed to their own differentiation pathways? Based on the previously stated data, an affirmative answer can be given to the latter question, at least after the formation of the secondary ossification center.

4. Effects on Bone Marrow Mesenchymal Stromal Cells

The adult bone marrow stroma contains a number of mesenchymal stem cells that are capable of differentiating into osteoblasts, chondrocytes, myoblasts, and adipocytes. Therefore, bone marrow stromal cells are attracting the interest of a number of medical scientists, as they are an excellent source for the regeneration of mesenchymal tissues. In 2004, Nishida *et al.*, reported the successful regeneration of the full-thickness defect in rat articular cartilage by CCN2 with a gelatin hydrogel carrier, which enabled gradual and continuous release of CCN2. As a part of this study, the effect of CCN2 on the chondrogenic differentiation of mouse mesenchymal stromal cells was also evaluated. The long-term culture of those cells in the presence of recombinant CCN2 significantly induced the chondrocytic differentiation therein, as evaluated by cartilage matrix-specific staining and marker gene expression (Nishida *et al.*, 2004). Therefore, it is clear that CCN2 promotes chondrocytic differentiation of mesenchymal stromal cells. In addition, CCN2 was found to mediate the Wnt3A and bone morphogenetic protein (BMP) 9 signals toward osteoblast differentiation of mesenchymal stem cells at early stages of differentiation (Luo *et al.*, 2004). However, whether it also promotes myogenic and adipogenic differentiation as well, or it specifically promotes chondrogenic/osteogenic differentiation only, still remains unclear. Of note, a study analyzing the expression of CCN family member genes revealed the sustained expression of the CCN2 gene along with osteogenic, adipogenic, and chondrogenic differentiation of mesenchymal stem cells (Schutze *et al.*, 2005). These findings indicate certain roles of CCN2 in all three differentiation pathways, thus suggesting that CCN2 may promote all of these pathways simultaneously.

5. Phenotypes of *ccn2*^{-/-} Mice

Until now, a conventional type of *ccn2* knockout mice had been generated and their phenotypes were analyzed and reported by Ivkovic *et al.*, (2003). Although mice possess the five other family members as well, which might compensate for a single depletion of any member, the removal of CCN2 conferred distinct abnormal phenotypes, particularly in the growth plate. The embryos of *ccn2* null mice grow until birth, but they are lethal upon delivery, owing to respiratory failure. Respiratory failure is estimated to be due to the hypoplasia of the rib cage, which is caused by abnormal endochondral ossification.

Impaired endochondral ossification was observed throughout the entire skeleton, thus resulting in systemic skeletal dysmorphism. According to histological analysis of the growth plates, chondrocyte hypertrophy was severely affected by *ccn2* depletion. Morphologically, the hypertrophic layers

were remarkable enlarged, without proper vascular invasion. The matrix deposition, matrix metalloproteinase production, and VEGF gene expression by those cells all decreased, emphasizing the role of CCN2 in chondrocyte differentiation and angiogenesis. Importantly, the observed abnormality is totally consistent with the results of the *in vitro* evaluation of CCN2 function, confirming the integrity of both investigations from different approaches. However, no remarkable phenotypic changes were observed in *ccn2* heterozygous KO mice, which does not necessarily indicate that a single *ccn2* locus is biologically sufficient, but it may be a result of compensation by the other *ccn* family members.

6. Cell Surface Receptors

Because of the characteristic tetramodular structure as a CCN family member, CCN2 is capable of interacting with a vast number of other molecules, which at the same time indicates that multiple different cell surface molecules should be assigned for the receptors of CCN2 (Fig. 3). In fact, in 1998, Nishida already reported a specific receptor–ligand complex on the chondrocytic and osteoblastic cell surface, which was actually phosphorylated upon CCN2 stimulation (Nishida *et al.*, 1998, 2000). To date, the best known cell surface CCN2 receptors are integrins. Accumulated experimental data showed that integrins $\alpha_M\beta_2$, $\alpha_6\beta_1$, and $\alpha_{IIb}\beta_3$ mediated the cell adhesion of monocytes, fibroblasts, and platelets, respectively, under direct interaction with CCN2 (Chen *et al.*, 2001a; Jedsadayanmata *et al.*, 1999; Schober *et al.*, 2002). It is also interesting to note that another type of integrin, $\alpha_v\beta_3$, was reported to assist CCN2 in inducing angiogenesis (Babic *et al.*, 1999). This $\alpha_v\beta_3$ molecule was reported to mediate the adhesion of hepatic stellate cells under an interaction with the CT module (Gao and Brigstock, 2004). Therefore, particular types of integrins are supposed to be the direct receptors of the CT module.

Among these integrins, $\alpha_6\beta_1$ could activate intracellular phosphorylation signaling via focal adhesion kinase (FAK) in skin fibroblasts. This finding is of particular interest, since the activation of specific signaling pathways through mitogen-activated protein kinases (MAPKs) is involved in transmitting CCN2-emitted signals for chondrocyte proliferation and differentiation, as indicated in the next section. Other signal transducing cell surface CCN2 receptors were also identified on the surface of kidney mesangial cells (Wahab *et al.*, 2005a). These receptors, Trk A and $p75^{\text{NTR}}$, had already been identified as the specific receptors for neurotrophins. Surprisingly, CCN2 was found to bind to these molecules and induce autophosphorylation of the tyrosine residue in Trk A as well as the original ligands, even though its biological outcome still remains to be investigated (Wahab *et al.*, 2005a). To our regret, all of the previous findings were obtained with nonosteogenic cells. Considering the central role of CCN2 in bone growth, certain receptors

specific on chondrocytes and/or osteoblasts are expected. We previously confirmed the strong expression of Trk A on hypertrophic chondrocytes that appeared in bone fracture lesions (Asaumi *et al.*, 2000). Therefore, although no signal transducing cell surface receptor has yet been defined in osteogenic cells including chondrocytes, Trk A continues to be one of the most probable candidates for such CCN2 receptors.

In addition to these receptors, several different molecules on chondrocytes have been proposed to initiate the intracellular signaling of CCN2 receptors to promote endochondral ossification. The low-density lipoprotein receptor-like protein 1 (LRP-1) was identified as a binding protein of the CCN2 molecule (Segarini *et al.*, 2001), and subsequent investigations clarified that LRP-1 mediated the transmission of the CCN2 signal to the extracellular signal-regulated kinase (ERK) signaling pathway in promoting myofibroblastic differentiation (Yang *et al.*, 2004). We also confirmed the display of LRP-1 molecules on chondrocytes both *in vivo* and *in vitro*; it is therefore highly probable that LRP-1 plays a significant role in cartilage biology in collaboration with CCN2 (Kawata *et al.*, 2006). Another intriguing candidate is ErbB4, which is also a tyrosine kinase-type receptor for one of the neurotrophins and is expressed among chondrocytes (Nawachi *et al.*, 2002). In this way, CCN2 has been shown to utilize multiple receptors when exerting its multiple functions, as we have previously expected.

Finally, it should be noted that not only the direct receptors specific for CCN2, but also the indirect effects of CCN2 via other extracellular molecules should not be overlooked. These molecules include growth factors (Abreu *et al.*, 2002; Inoki *et al.*, 2002) and proteoglycans (Nishida *et al.*, 2003), several of which may be regarded as coreceptors. Such findings again indicate that CCN2 is a driver of a signaling network in a microenvironment rather than a growth factor that can deliver a few messages.

7. MAPK and Upstream Kinases in the Transduction of CCN2 Signals

As mentioned in the last section, CCN2 is capable of activating multiple intracellular phosphorylation signals in a variety of target cells. In 2001, Yosimichi *et al.*, reported that two classical MAPKs, p38 MAPK and ERK1/2, mediated the CCN2-emitted signals to promote the differentiation and proliferation of chondrocytes, respectively (Yosimichi *et al.*, 2001). The extensive study also revealed the contribution of another major member of MAPK, Jun N-terminal kinase (JNK) to CCN2 signal transduction for both the proliferation and differentiation of chondrocytes (Yosimichi *et al.*, 2006). In addition to these well-known MAPK pathways, the involvement of the phosphatidylinositol-3 kinase (PI3K)-protein kinase B/Akt pathway in

transmitting the CCN2 signal to promote chondrocyte hypertrophy has been elucidated. Furthermore, a study has demonstrated that protein kinase C (PKC), particularly PKC α , is a major secondary messenger kinase that mediates most of these CCN2 signals described, except for those to JNK (Yosimichi *et al.*, 2006). In contrast to the accumulating findings on chondrocytes, little is known concerning such intracellular signal mediators in osteoblasts. Even in the case of chondrocytes, the relationship between the cell surface receptors as intracellular signal donors and the kinases as signal recipients still remains unclear.

However, in other types of cells, the CCN2 signal transduction cascades from the cell surface receptor to the MAPKs have been gradually elucidated (Fig. 3). In skin fibroblasts and hepatic stellate cells, integrin $\alpha_6\beta_1$ translates CCN2 binding to the phosphorylation of ERK1/2 (Chen *et al.*, 2001a). In renal mesangial cells, Trk A is autophosphorylated by CCN2 binding, which initiates the signal transduction to multiple downstream kinases. These kinases include PKC α and δ , MEK-ERK1/2, JNK, PKB, p90-ribosomal S6 kinase (RSK), and calmodulin kinase II (CaMKII), most of which can be inhibited by a specific inhibitor of Trk (Wahab *et al.*, 2005a). Through the activation of these kinases, a TGF- β -inducible early gene (TIEG), which is a nuclear transcription factor, was eventually induced after CCN2 stimulation (Wahab *et al.*, 2005b). The transmembrane transduction mechanism of the CCN2 signals to target genes through MAPKs in chondrocytes will be clarified in the near future, employing a strategy similar to that utilized for other types of cells.

8. Endocytotic Incorporation and Possible Intracellular Functions of CCN2

All of the CCN protein members are furnished with N-terminal signal peptide sequences, and they are basically secretory proteins; hence they are believed to play major roles as extracellular signaling modulators. However, as reported in the case of other growth factors, intracellular CCN2 may well play significant biological roles in particular states. From this point of view, it is of particular interest that extracellular CCN2 can be taken up by endocytosis (Wahab *et al.*, 2001). Endocytotic transportation was first observed in renal mesangial cells. In these cells, exogenous CCN2 was incorporated inside of the cells and finally reached the nucleus. A similar finding was also confirmed in chondrocytic cells by us (Kawata *et al.*, 2006). After endocytosis, molecules encapsulated in endosomes can be directed to a few distinct destinations. The most classical pathway leads to lysosomes, where the incorporated molecules are to be degraded. However, certain endosomal populations, designated as recycling endosomes, may shuttle back to the plasma membrane to recycle their components. This system is

considered to provide a basis for transcytosis that enables the transcellular transport of extracellular molecules. Furthermore, a study revealed that adaptor protein containing the PH domain, TB domain, and leucine zipper motif (APPL) proteins transported into the nucleus through endocytosis plays a role in the regulation of gene expression (Miaczynska *et al.*, 2004). Therefore, the biological significance of CCN2 endocytosis in endochondral ossification should not be overlooked. Indeed, LRP-1, one of the CCN2 receptors, is widely known to be a key player in endocytotic events, which further emphasizes this point.

Regardless of the pathway, the intracellular function of CCN2 has been suggested mostly by overexpression studies. Generally, the overexpression of CCN2 tends to attenuate cell growth. In human breast cancer cells, CCN2 induced apoptosis (Hishikawa *et al.*, 1999), while it restrained the proliferation of human oral squamous carcinoma cells (Moritani *et al.*, 2003a). Notably, human CCN2 overexpressed in monkey Cos-7 cells has been shown to accumulate in a perinuclear organelle corresponding to the microtubule organization center without being secreted and thereby inducing G₂–M arrest of those cells (Kubota *et al.*, 2000a). Taking these findings together with the fact that a dense accumulation of CCN2 is observed in quiescent hypertrophic chondrocytes, intracellular CCN2 may be a critical factor in stopping the proliferation of chondrocytes in terminal hypertrophic differentiation.

C. Regulation of *ccn2* Gene Expression

1. Controlled Expression of *ccn2* During Endochondral Ossification

Differentiation stage-dependent CCN2 gene expression observed in the growth plate is perfectly reproducible in cell culture systems with primary growth plate chondrocytes. As previously described, the baseline of *ccn2* gene expression is kept at low levels in immature growth plate chondrocytes, whereas it is strongly induced around the onset of hypertrophic differentiation *in vivo* (H. Kawaki *et al.*, unpublished observations). According to several *in vitro* studies, the peak of *ccn2* expression is observed in chondrocytes at prehypertrophic stages, preceding the peak of type X collagen gene expression, which is a typical marker of hypertrophic chondrocytes. The mechanism by which this differentiation-dependent induction/silencing of *ccn2* gene expression occurs has been uncovered through a variety of molecular biological approaches.

Gene expression is regulated through multiple steps from chromatin remodeling to protein translation. Little had been known concerning the role of epigenetic regulation, for example, by histone/DNA modification to turn on/off the corresponding locus, in *ccn2* gene regulation. However, significant progress has been made in clarifying the involvement of transcriptional

and posttranscriptional regulatory systems in the precisely controlled expression of the *ccn2* gene during the endochondral ossification process. The next two sections briefly describe advances in the research on such regulatory systems of *ccn2* gene expression, which regulates the organized development of the growth plate for the proper growth of most bones in vertebrates.

2. Human *ccn2* Proximal Promoter and Transcriptional Regulation

As is generally observed in a number of eukaryotic protein-encoding genes, the CCN2 gene is primarily driven by a classical core promoter segment of the gene containing a typical TATA box (Grotendorst *et al.*, 1996). Around the core promoter, several functional and putative *cis* elements have been identified, or predicted, which together constitute the CCN2 proximal promoter. The involvement of the proximal promoter region in the induction/silencing of CCN2 gene expression in response to a variety of stimuli, including TGF- β and endothelin-1 (ET-1), has been indicated, thus leading to the identification of a few *cis* elements therein (Grotendorst *et al.*, 1996; Xu *et al.*, 2004). The TGF- β response element/basal control element 1 (TbRE/BCE-1) is a critical element that determines basal promoter activity in mesangial cells and mediates gene regulation by TGF- β in fibroblasts and chondrocytes (Eguchi *et al.*, 2001; Grotendorst *et al.*, 1996). Juxtaposing the TbRE, a Smad binding element (SBE) has also been located and it has been shown to play a significant role in modulating TGF- β signaling in mesangial cells (Wahab *et al.*, 2005b). According to a study, SBE mediates the transcriptional activation of *ccn2* by sphingosine 1-phosphate in rat mesangial cells as well (Katsuma *et al.*, 2005). Moreover, the proximal promoter contains the third *cis* element to mediate a certain part of the multiple intracellular signals emitted by TGF- β . This element is characterized by the retention of a tandem repeat of the TEF-1 binding consensus sequence and is structurally distinct from the two mentioned previously (Leask *et al.*, 2003). Therefore, the proximal promoter transcriptionally regulates *ccn2* gene expression through multiple signaling pathways, transcription factors, and *cis* elements upon TGF- β stimulation in a variety of cells (Fig. 4).

In terms of bone growth, our series of investigations revealed another *cis* element that is critical for mediating the chondrocyte-specific induction of *ccn2* gene expression. This element, designated transcriptional enhancer dominant in chondrocytes (TRENDIC), was discovered in the proximal promoter region, forming a cluster with TbRE and SBE (Fig. 4) (Eguchi *et al.*, 2001, 2002). TRENDIC is required to maintain high level CCN2 expression in the chondrocytic cell line HCS-2/8. This element also acts as

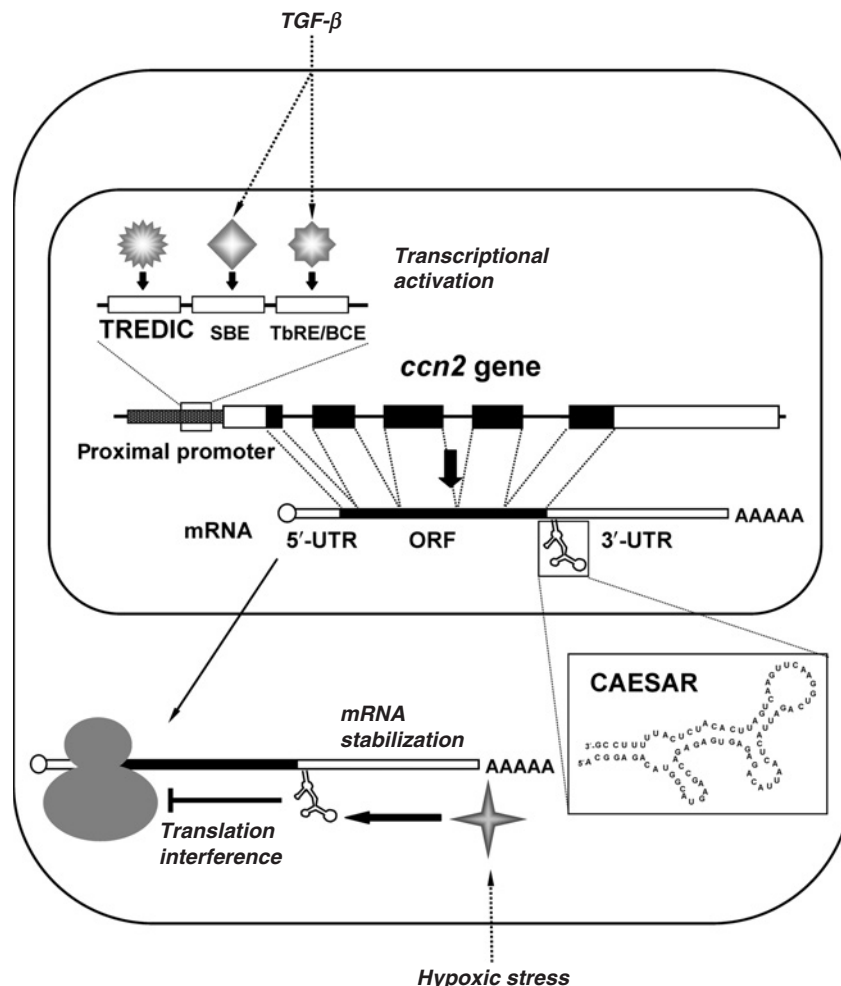


FIG. 4 Transcriptional and posttranscriptional regulation of the human *ccn2* gene in chondrocytes. The TGF- β signal is mediated by a few *cis*-elements including SBE and TbRE/BCE in chondrocytes as well as in fibroblasts, whereas the chondrocyte-specific enhancement of transcription is enabled by a novel enhancer, TREDIC. The dual functional posttranscriptional regulatory element CAESAR acts as a constitutive translational silencer and a dynamic regulatory element of mRNA stability upon hypoxic stress conditions. The primary structure and predicted secondary structure of CAESAR are also illustrated.

an enhancer in several different types of cells; nevertheless, among all the cells examined, its effect was strongest in chondrocytic cells.

It should also be noted that transcriptional induction is not necessarily mediated by the elements in the proximal promoter region. In fact, the effect

of glucocorticoid to strongly enhance CCN2 transcription was generally recognized (Dammeier *et al.*, 1998b), which was confirmed by a nuclear run-on assay. However, no *cis*-acting element in the proximal promoter area longer than 1500 base pairs was found to mediate this effect by glucocorticoid so far (Kubota *et al.*, 2003; H. Kawaki *et al.*, unpublished observations). Similarly, although a number of extracellular stimuli, including nitric oxides (Keil *et al.*, 2002), statins [3-hydroxy-3-methylglytaryl coenzyme A (HMG-CoA) reductase inhibitor] (Heusinger-Ribeiro *et al.*, 2004), α -tocopherol (Villacorta *et al.*, 2003), and mechanical stresses (Grimshaw and Mason, 2001), have been shown to modulate the *ccn2* transcript level, no significant contribution of the proximal promoter has been described therein. Two possibilities are left to be addressed to resolve these issues. First, *cis* elements may be well scattered outside of the proximal promoter, even in the introns of the CCN2 gene. Second, unless a nuclear run-on assay could directly show that the observed change in mRNA level should occur at the transcriptional stage, such a change may be an outcome of posttranscriptional regulation, as detailed in the next section.

3. 3'-UTR-Mediated Posttranscriptional Regulation

Posttranscriptional regulation can be conducted in multiple steps. After the transcription of the mRNA precursors, they undergo a series of modifications and then become mature mRNAs. This process includes addition of a 5'-methylguanyl cap and polyadenyl tail, and mRNA splicing. Currently, the regulation of *ccn2* gene expression through alternative slicing events has not yet been elucidated. Afterward, mature mRNA is actively exported out from the cell nucleus to the ribosome in the cytoplasm. The regulation by selective nucleocytoplasmic transport can be conducted at the nuclear pores, and the stability of mature mRNA is another determinant of the steady-state level of mRNA. In the case of CCN2, regulation through the nuclear export process is still not known either. However, the current investigation indicated that the half-life of CCN2 mRNA is dynamically regulated through particular RNA *cis* elements in chick and human chondrocytes, as described later. After the journey to the ribosome, cytoplasmic mature RNA is captured in the ribosomal translation initiation complex, and protein molecules are finally produced there. The *ccn2* gene expression is also regulated at this final step through an RNA *cis* element on the *ccn2* mRNA. Surprisingly, in human cells, a single RNA *cis* element is regulating both mRNA stability and translation. In 2000, we identified and designated this element as a *cis*-acting element of structure-anchored repression (CAESAR: Fig. 4) in both human (Kubota *et al.*, 2000b) and mouse (Kondo *et al.*, 2000) *ccn2* genes.

It is widely recognized that the 3'-untranslated region (3'-UTR) plays a major role in mediating such posttranscriptional gene regulation (Kubota

et al., 1999). A number of *cis* elements that are the targets of specific binding proteins to conduct mRNA degradation and transport have been identified in the 3'-UTR of various eukaryotic mRNAs (Asaoka-Taguchi *et al.*, 1999; Brewer, 1991; Moallem *et al.*, 1998). More recently, the micro-RNA (miRNA) has been attracting the interest of biologists all over the world. The target sequences of miRNAs are also located in the 3'-UTR and mediate specific degradation and/or translation interference (Harfe, 2005). The CAESAR is also located in the 3'-UTR of human CCN2 mRNA, facing the junction with the open reading frame. It is a secondary-structured RNA element 84 bases in length. The involvement of CAESAR itself represses basal gene expression at a low level by interfering with efficient mRNA translation, which probably contributes to restricted CCN2 expression *in vivo*. This constitutive repressive effect is considered to be the static function of CAESAR (Kubota *et al.*, 2005). The repressive potential of CAESAR does not depend on the primary nucleotide sequence, but instead depends greatly on the secondary structure, which provided the basis of the nomenclature (Kubota *et al.*, 2000b). This static aspect of CAESAR function, which appears to be a general event, occurs in most of the cells *in vivo*. In contrast, the dynamic regulation of *ccn2* gene expression is observed among particular types of cells including chondrocytes, in which *ccn2* plays a critical biological role. Upon hypoxic exposure, both the steady-state level of *ccn2* mRNA and CCN2 protein production increases, without any increase in the transcription rate (Kondo *et al.*, 2006). This apparent increase in the *ccn2* mRNA upon hypoxia is ascribed to the increased mRNA stability realized by the interaction of CAESAR and specific binding protein(s). These findings suggest that CAESAR plays a role in regulated *ccn2* gene expression in developing cartilage that is avascular, and thus it tends to undergo hypoxic conditions.

Clearer evidence indicating an active role of the 3'-UTR in the differentiation-dependent expression of the CCN2 gene along with endochondral ossification has been demonstrated by utilizing chicken primary sternum chondrocytes. In 2005, Mukudai *et al.* identified a novel 50-base-long RNA *cis* element in the 3'-UTR of the chicken CCN2 gene at a location distinct from that of CAESAR in the human *ccn2* gene. This element also represses gene expression in *cis*; however, the repressive activity in the chondrocytes decreases toward hypertrophic differentiation, thus resulting in increased *ccn2* gene expression in prehypertrophic-hypertrophic stages. It was also clarified that a protein with a molecular weight of 40 kDa specifically interacted with this RNA element, and the amount of interaction was negatively related to the resultant *ccn2* mRNA stability. Therefore, the 40-kDa protein is believed to destabilize chicken *ccn2* mRNA by binding to the 50-base-long RNA element. The identification and functional characterization of this protein will provide critical insight into the precise mechanism of this posttranscriptional regulation of *ccn2* gene expression.

D. Utility of CCN2 in Regenerative Therapy of Bone

1. Expression of *ccn2* upon Bone Damage and Repair

When connective tissues suffer physical damage, several growth factors are then supplied for their prompt regeneration. Shortly after such damage, the tissue defect is initially filled with fibrous tissue, which will eventually be replaced by authentic tissue. This process can partly occur in parallel with the damage to certain tissues, which occasionally results in a pathological outcome, such as liver cirrhosis and other fibrotic disorders. CCN2 is a key player in all of these cases.

In the case of a bone fracture, CCN2 is supplied by two independent sources (Fig. 5). One is the endogenous production of CCN2 by the bone-forming cells around the lesion. During fracture healing, enhanced *ccn2* gene expression and protein production are observed in the hypertrophic and proliferative chondrocytes in regenerating cartilage, proliferating periosteal cells around the fracture site, and fibroblast-like stromal cells in a rat rib fracture model (Nakata *et al.*, 2002). In summary, almost all bone-repairing cells are directed to produce CCN2 upon fracture, indicating that CCN2 plays a critical role during bone regeneration. In addition to this endogenous production, exogenous CCN2 is immediately and abundantly delivered to the fracture lesion by utilizing platelets as capsules. Indeed, activated platelets release more CCN2 than any other growth factor involved (Kubota *et al.*, 2004). Therefore, CCN2 is readily supplied to any tissue upon injury, if only hemorrhaging occurs and the coagulation process is initiated. Since bone is a vascular connective tissue, a bone defect is promptly filled with a clot that is mainly composed of polymerized fibrin fibers with plenty of CCN2. It is important to note that polymerized fibrin serves as a natural carrier of CCN2, which thus enables its gradual and prolonged release around the lesion. Even if *ccn2* is a so-called immediate-early gene, the endogenous production of a sufficient amount of CCN2 requires a significant period of time. The immediate supply and prolonged release of exogenous CCN2 perfectly collaborate with the endogenous CCN2 supply system in accomplishing the regeneration of bone after fracture.

2. Accelerated Regeneration of Articular Cartilage and Bone with CCN2

Owing to the sophisticated combination system of CCN2 supply, a regular bone fracture does not require specific therapy to support the tissue regeneration itself. As previously indicated, CCN2 promotes the proliferation and differentiation of chondrocytes as well as osteoblasts. However, in tissue such as cartilage, an exogenous CCN2 supply is hardly expected, since cartilage is an avascular tissue. This structural property may account for the general

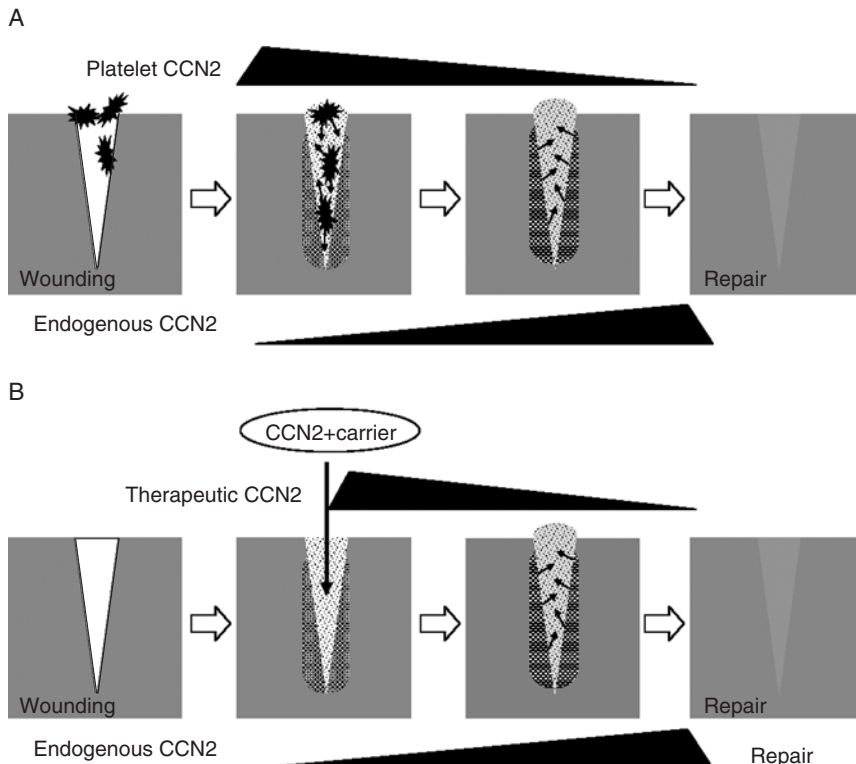


FIG. 5 Regeneration of bone and cartilage by CCN2. (A) Spontaneous regeneration process accomplished by platelet-derived exogenous CCN2 together with the endogenous induction in bone. The amorphous burr-shaped objects indicate platelets. (B) The therapeutic regeneration of articular cartilage by a carrier-adsorbed recombinant CCN2 together with the endogenous induction in cartilage. The change in the amount of CCN2 from two different origins during tissue regeneration is schematically represented above or below each panel, respectively.

observation that spontaneous repair of injured cartilage is seldom observed. Therefore, if only exogenous CCN2 is artificially supplied, mimicking the microenvironment of the regenerating bone fracture lesion, even cartilage defects can be regenerated. Based on this idea, we examined the effects of CCN2 on articular cartilage regeneration in rat OA and full-layer articular cartilage defect models *in vivo* (Fig. 5). To enable the prolonged and gradual release of CCN2, we employed a gelatin hydrogel carrier as a better substitute for the fibrin in the clot. As a result, the application of the gelatin hydrogel-adsorbed CCN2 remarkably accelerated the regeneration of the damaged cartilage in OA and thereby helped to ensure the repair of a full-thickness cartilage defect that did not occur without CCN2 (Nishida *et al.*, 2004).

As such, CCN2 was proven to be a promising tool for the regenerative therapy of such cartilage disorders.

Although bone regeneration usually occurs spontaneously, certain types of bone defects may well experience significant difficulties in completing the whole repair process. This deficiency in bone defect healing can be caused by either systemic or local conditions. Several disorders in the endocrine system affect the regeneration potential of bone through disregulated metabolism of bone components. The most common cases of defective bone repair are observed in the alveolar bone after tooth extraction, which is known as a "dry socket." Similar to the cartilage defect cases, the local application of CCN2 is expected to assist in repairing such bone defects with an attenuated regeneration potential. Our current research with a rat model has demonstrated the significant effects of the CCN2–gelatin hydrogel complex on the accelerated regeneration of persisting tibial bone defects (K. Kikuchi *et al.*, unpublished observations).

V. Concluding Remarks

Even today, a significant number of scientists regard CCN2 as an etiological factor of fibrotic disorders, instead of recognizing its authentic role in the living body. It is a matter of course for certain biomolecules to be first identified as factors associated with particular disorders, which usually determines the initial terminology of such molecules. Thereafter, in most cases, the physiological role of the "disease-associated" molecule is clarified, showing that this molecule is indispensable for life. Such an example can be commonly found in oncogene products. In this report, we showed that CCN2, formerly known as connective tissue growth factor, is a central participant in endochondral ossification, which determines the shape and size of most of the bones in vertebrates. Based on this knowledge, we further uncovered the fact that CCN2 is a key participant in connective tissue regeneration. Although fibrosis can be consequently pathogenic, it can even be considered as a mode of compensatory regeneration of damaged tissue, which results in functional failure. Therefore, we should first emphasize the primary property of CCN2 as a local modulator of bone growth and regeneration, as discussed later.

The living human body is composed of a set of organs executing its own specific mission. Strictly organized tissue constitutes each organ to construct a functional mechanism. Bone is one of these organs; it not only constructs the skeleton to support the whole body, but also a reservoir of calcium and a hematopoietic center. As briefly introduced, the growth plate that builds up the bone from inside has a highly ordered structure with a precise alignment of differentiating chondrocytes, vascular endothelial cells, and osteoblasts.

Obviously, to construct and maintain this sophisticated architecture, an excellent molecular organizer of the local cell society is required. In general, for well-balanced improvement in any part of a society, negotiation is one of the most efficient means. CCN2 interacts with a number of growth factors, ECM components, and cell surface molecules to promote all of the stages of endochondral ossification. As a result, CCN2 is thus considered to be an excellent molecular negotiator in the mesenchymal cell society. Because negotiators have to appear only when requested, the transcriptional and posttranscriptional regulatory systems have been furnished for the CCN2 gene. To promote the growth and regeneration of bone and cartilage, a total and balanced activation of the cell society is required. Rather than a single factor of limited and strong effects that may cause an imbalance in the cell society, a negotiator that promotes balanced tissue growth should be a better choice for regenerative therapy. CCN2 is obviously one such candidate. Exploring the therapeutic approaches with the external application of the CCN2 protein, or the internal induction/reduction by external stimuli, is therefore expected to control the growth and regeneration of mesenchymal tissues, and even the occurrence of ectopic fibrosis in other tissues.

Acknowledgments

This work was supported by Grants-in-Aid for Scientific Research (S) (to M.T.) and (C) (to S.K.) and for Exploratory Research (M.T.) from the Ministry of Education, Culture, Sports, Science and Technology of Japan and the Japan Society for the Promotion of Science; the Foundation for Growth Science in Japan (M.T.); the Sumitomo Foundation (M.T.); the Ryobi-teien Memorial Foundation (S.K.); and the Kurozumi Medical Foundation (S.K.). We also thank Ms. Yuki Nonami for her valuable secretarial assistance.

REFERENCES

Abou-Shady, M., Friess, H., Zimmermann, A., di Mola, F. F., Guo, X. Z., Baer, H. U., and Buchler, M. W. (2000). Connective tissue growth factor in human liver cirrhosis. *Liver* **20**, 296–304.

Abreu, J. G., Kotpura, N. I., Reversade, B., and De Robertis, E. M. (2002). Connective-tissue growth factor (CTGF) modulates cell signalling by BMP and TGF-beta. *Nat. Cell Biol.* **4**, 599–604.

Allen, J. T., Knight, R. A., Bloor, C. A., and Spiteri, M. A. (1999). Enhanced insulin-like growth factor binding protein-related protein 2 (Connective tissue growth factor) expression in patients with idiopathic pulmonary fibrosis and pulmonary sarcoidosis. *Am. J. Respir. Cell Mol. Biol.* **21**, 693–700.

Arikawa-Hirasawa, E., Watanabe, H., Takami, H., Hassell, J. R., and Yamada, Y. (1999). Perlecan is essential for cartilage and cephalic development. *Nat. Genet.* **23**, 354–358.

Asano, M., Kubota, S., Nakanishi, T., Nishida, T., Yamaai, T., Yosimichi, G., Ohyama, K., Sugimoto, T., Murayama, Y., and Takigawa, M. (2005). Effect of connective tissue growth factor (CCN2/CTGF) on proliferation and differentiation of mouse periodontal ligament-derived cells. *Cell Commun. Signal.* **5**, 11.

Asaoka-Taguchi, M., Yamada, M., Nakamura, A., Hanyu, K., and Kobayashi, S. (1999). Maternal Pumilio acts together with Nanos in germline development in *Drosophila* embryos. *Nat. Cell Biol.* **1**, 431–437.

Asaumi, K., Nakanishi, T., Asahara, H., Inoue, H., and Takigawa, M. (2000). Expression of neurotrophins and their receptors (TRK) during fracture healing. *Bone* **26**, 625–633.

Babic, A. M., Chen, C. C., and Lau, L. F. (1999). Fisp12/mouse connective tissue growth factor mediates endothelial cell adhesion and migration through integrin alphavbeta3, promotes endothelial cell survival, and induces angiogenesis *in vivo*. *Mol. Cell. Biol.* **19**, 2958–2966.

Baxter, R. C., Binoux, M. A., Clemons, D. R., Conover, C. A., Drop, S. L., Holly, J. M., Mohan, S., Oh, Y., and Rosenfeld, R. G. (1998). Recommendations for nomenclature of the insulin-like growth factor binding protein superfamily. *Endocrinology* **139**, 4036.

Bonniaud, P., Margetts, P. J., Kolb, M., Haberberger, T., Kelly, M., Robertson, J., and Gauldie, J. (2003). Adenoviral gene transfer of connective tissue growth factor in the lung induces transient fibrosis. *Am. J. Respir. Crit. Care Med.* **168**, 770–778.

Bork, P. (1993). The modular architecture of a new family of growth regulators related to connective tissue growth factor. *FEBS Lett.* **327**, 125–130.

Bradham, D. M., Igarashi, A., Potter, R. L., and Grotendorst, G. R. (1991). Connective tissue growth factor: A cysteine-rich mitogen secreted by human vascular cells is related to the SRC-induced immediate early gene product CEF-10. *J. Cell Biol.* **114**, 1285–1294.

Brewer, G. (1991). An A + U-rich element RNA-binding factor regulates c-myc mRNA stability *in vitro*. *Mol. Cell. Biol.* **11**, 2460–2466.

Brigstock, D. R. (1999). The connective tissue growth factor/cysteine-rich 61/nephroblastoma overexpressed (CCN) family. *Endocr. Rev.* **20**, 189–206.

Brigstock, D. R., Goldschmeding, R., Katsube, K. I., Lam, S. C., Lau, L. F., Lyons, K., Naus, C., Perbal, B., Riser, B., Takigawa, M., and Yeger, H. (2003). Proposal for a unified CCN nomenclature. *Mol. Pathol.* **56**, 127–128.

Brunner, A., Chinn, J., Neubauer, M., and Purchio, A. F. (1991). Identification of a gene family regulated by transforming growth factor-beta. *DNA Cell Biol.* **10**, 293–300.

Chen, C. C., Chen, N., and Lau, L. F. (2001a). The angiogenic factors Cyr61 and connective tissue growth factor induce adhesive signaling in primary human skin fibroblasts. *J. Biol. Chem.* **276**, 10443–10452.

Chen, C. C., Mo, F. E., and Lau, L. F. (2001b). The angiogenic factor Cyr61 activates a genetic program for wound healing in human skin fibroblasts. *J. Biol. Chem.* **276**, 47329–47337.

Cicha, I., Garlich, C. D., Daniel, W. G., and Goppelt-Strube, M. (2004). Activated human platelets release connective tissue growth factor. *Thromb. Haemost.* **91**, 755–760.

Cicha, I., Yilmaz, A., Klein, M., Raithel, D., Brigstock, D. R., Daniel, W. G., Goppelt-Strube, M., and Garlich, C. D. (2005). Connective tissue growth factor is overexpressed in complicated atherosclerotic plaques and induces mononuclear cell chemotaxis *in vitro*. *Arterioscler. Thromb. Vasc. Biol.* **25**, 1008–1013.

Dammeier, J., Brauchle, M., Falk, W., Grotendorst, G. R., and Werner, S. (1998a). Connective tissue growth factor: A novel regulator of mucosal repair and fibrosis in inflammatory bowel disease? *Int. J. Biochem. Cell Biol.* **30**, 909–922.

Dammeier, J., Beer, H. D., Brauchle, M., and Werner, S. (1998b). Dexamethasone is a novel potent inducer of connective tissue growth factor expression. Implications for glucocorticoid therapy. *J. Biol. Chem.* **273**, 18185–18190.

Dean, R. G., Balding, L. C., Candido, R., Burns, W. C., Cao, Z., Twigg, S. M., and Burrell, L. M. (2005). Connective tissue growth factor and cardiac fibrosis after myocardial infarction. *J. Histochem. Cytochem.* **53**, 1245–1256.

Delmolino, L. M., Stearns, N. A., and Castellot, J. J., Jr. (2001). COP-1, a member of the CCN family, is a heparin-induced growth arrest specific gene in vascular smooth muscle cells. *J. Cell. Physiol.* **188**, 45–55.

Desnoyers, L., Arnott, D., and Pennica, D. (2001). WISP-1 binds to decorin and biglycan. *J. Biol. Chem.* **276**, 47599–47607.

di Mola, F. F., Friess, H., Martignoni, M. E., Di Sebastiano, P., Zimmermann, A., Innocenti, P., Gruber, H., Gold, L. I., Korc, M., and Buchler, M. W. (1999). Connective tissue growth factor is a regulator for fibrosis in human chronic pancreatitis. *Ann. Surg.* **230**, 63–71.

Dornbach, L. M., and Lyons, K. M. (2004). Regulation of skeletal development by CCN1 and CCN2. Third International Workshop on the CCN Family of Genes. St. Malo, France, 20–23 October 2004, Abstract p. 26.

Eguchi, T., Kubota, S., Kondo, S., Shimo, T., Hattori, T., Nakanishi, T., Kuboki, T., Yatani, H., and Takigawa, M. (2001). Regulatory mechanism of human connective tissue growth factor (CTGF/Hcs24) gene expression in a human chondrocytic cell line, HCS-2/8. *J. Biochem. (Tokyo)* **130**, 79–87.

Eguchi, T., Kubota, S., Kondo, S., Kuboki, T., Yatani, H., and Takigawa, M. (2002). A novel *cis*-element that enhances connective tissue growth factor gene expression in chondrocytic cells. *Biochem. Biophys. Res. Commun.* **295**, 445–451.

French, D. M., Kaul, R. J., D'Souza, A. L., Crowley, C. W., Bao, M., Frantz, G. D., Filvaroff, E. H., and Desnoyers, L. (2004). WISP-1 is an osteoblastic regulator expressed during skeletal development and fracture repair. *Am. J. Pathol.* **165**, 855–867.

Friedrichsen, S., Heuer, H., Christ, S., Cuthill, D., Bauer, K., and Raivich, G. (2005). Gene expression of connective tissue growth factor in adult mouse. *Growth Factors* **23**, 43–53.

Fu, C. T., Bechberger, J. F., Ozog, M. A., Perbal, B., and Naus, C. C. (2004). CCN3 (NOV) interacts with connexin43 in C6 glioma cells: Possible mechanism of connexin-mediated growth suppression. *J. Biol. Chem.* **279**, 36943–36950.

Gao, R., and Brigstock, D. R. (2004). Connective tissue growth factor (CCN2) induces adhesion of rat activated hepatic stellate cells by binding of its C-terminal domain to integrin alpha(v)beta(3) and heparan sulfate proteoglycan. *J. Biol. Chem.* **279**, 8848–8855.

Gellhaus, A., Dong, X., Propson, S., Maass, K., Klein-Hitpass, L., Kibschull, M., Traub, O., Willecke, K., Perbal, B., Lye, S. J., and Winterhager, E. (2004). Connexin43 interacts with NOV: A possible mechanism for negative regulation of cell growth in choriocarcinoma cells. *J. Biol. Chem.* **279**, 36931–36942.

Grimshaw, M. J., and Mason, R. M. (2001). Modulation of bovine articular chondrocyte gene expression in vitro by oxygen tension. *Osteoarthritis Cartilage* **9**, 357–364.

Grotendorst, G. R., and Duncan, M. R. (2005). Individual domains of connective tissue growth factor regulate fibroblast proliferation and myofibroblast differentiation. *FASEB J.* **19**, 729–738.

Grotendorst, G. R., Okochi, H., and Hayashi, N. (1996). A novel transforming growth factor beta response element controls the expression of the connective tissue growth factor gene. *Cell Growth Differ.* **7**, 469–480.

Grotendorst, G. R., Lau, L. F., and Perbal, B. (2000). CCN proteins are distinct from and should not be considered members of the insulin-like growth factor-binding protein superfamily. *Endocrinology* **141**, 2254–2256.

Gruschwitz, M., Muller, P. U., Sepp, N., Hofer, E., Fontana, A., and Wick, G. (1990). Transcription and expression of transforming growth factor type beta in the skin of progressive systemic sclerosis: A mediator of fibrosis? *J. Invest. Dermatol.* **94**, 197–203.

Gupta, N., Wang, H., McLeod, T. L., Naus, C. C., Kyurkchiev, S., Advani, S., Yu, J., Perbal, B., and Weichselbaum, R. R. (2001). Inhibition of glioma cell growth and tumorigenic potential by CCN3 (NOV). *Mol. Pathol.* **54**, 293–299.

Gupta, S., Clarkson, M. R., Duggan, J., and Brady, H. R. (2000). Connective tissue growth factor: Potential role in glomerulosclerosis and tubulointerstitial fibrosis. *Kidney Int.* **58**, 1389–1399.

Harfe, B. D. (2005). MicroRNAs in vertebrate development. *Curr. Opin. Genet. Dev.* **15**, 410–415.

Hashimoto, Y., Shindo-Okada, N., Tani, M., Nagamachi, Y., Takeuchi, K., Shiroishi, T., Toma, H., and Yokota, J. (1998). Expression of the Elm1 gene, a novel gene of the CCN (connective tissue growth factor, Cyr61/Cef10, and neuroblastoma overexpressed gene) family, suppresses in vivo tumor growth and metastasis of K-1735 murine melanoma cells. *J. Exp. Med.* **187**, 289–296.

Hattori, T., Fujisawa, T., Sasaki, K., Yutani, Y., Nakanishi, T., Takahashi, K., and Takigawa, M. (1998). Isolation and characterization of a rheumatoid arthritis-specific antigen (RA-A47) from a human chondrocytic cell line (HCS-2/8). *Biochem. Biophys. Res. Commun.* **245**, 679–683.

Hayashi, N., Kakimura, T., Soma, Y., Grotendorst, G. R., Tamaki, K., Harada, M., and Igarashi, A. (2002). Connective tissue growth factor is directly related to liver fibrosis. *Hepatogastroenterology* **49**, 133–135.

Heusinger-Ribeiro, J., Fischer, B., and Goppelt-Struebe, M. (2004). Differential effects of simvastatin on mesangial cells. *Kidney Int.* **66**, 187–195.

Hishikawa, K., Oemar, B. S., Tanner, F. C., Nakaki, T., Luscher, T. F., and Fujii, T. (1999). Connective tissue growth factor induces apoptosis in human breast cancer cell line MCF-7. *J. Biol. Chem.* **274**, 37461–37466.

Hurvitz, J. R., Suwairi, W. M., Van Hul, W., El-Shanti, H., Superti-Furga, A., Roudier, J., Holderbaum, D., Pauli, R. M., Herd, J. K., Van Hul, E. V., Rezai-Delui, H., Legius, E., et al. (1999). Mutations in the CCN gene family member WISP3 cause progressive pseudorheumatoid dysplasia. *Nat. Genet.* **23**, 94–98.

Igarashi, A., Okochi, H., Bradham, D. M., and Grotendorst, G. R. (1993). Regulation of connective tissue growth factor gene expression in human skin fibroblasts and during wound repair. *Mol. Biol. Cell* **4**, 637–645.

Igarashi, A., Nashiro, K., Kikuchi, K., Sato, S., Ihn, H., Fujimoto, M., Grotendorst, G. R., and Takehara, K. (1996). Connective tissue growth factor gene expression in tissue sections from localized scleroderma, keloid, and other fibrotic skin disorders. *J. Invest. Dermatol.* **106**, 729–733.

Igarashi, A., Hayashi, N., Nashiro, K., and Takehara, K. (1998). Differential expression of connective tissue growth factor gene in cutaneous fibrohistiocytic and vascular tumors. *J. Cutan. Pathol.* **25**, 143–148.

Inoki, I., Shiomi, T., Hashimoto, G., Enomoto, H., Nakamura, H., Makino, K., Ikeda, E., Takata, S., Kobayashi, K., and Okada, Y. (2002). Connective tissue growth factor binds vascular endothelial growth factor (VEGF) and inhibits VEGF-induced angiogenesis. *FASEB J.* **16**, 219–221.

Ito, Y., Aten, J., Bende, R. J., Oemar, B. S., Rabelink, T. J., Weening, J. J., and Goldschmeding, R. (1998). Expression of connective tissue growth factor in human renal fibrosis. *Kidney Int.* **53**, 853–861.

Ivkovic, S., Yoon, B. S., Popoff, S. N., Safadi, F. F., Libuda, D. E., Stephenson, R. C., Daluiski, A., and Lyons, K. M. (2003). Connective tissue growth factor coordinates chondrogenesis and angiogenesis during skeletal development. *Development* **130**, 2779–2791.

Jedsadayanmata, A., Chen, C-C., Kireeva, M. L., Lau, L. F., and Lam, S. C-T. (1999). Activation-dependent adhesion of human platelets to Cyr61 and Fisp12/mouse connective

tissue growth factor is mediated through integrin alpha(IIb)beta(3). *J. Biol. Chem.* **274**, 24321–24327.

Joliot, V., Martinerie, C., Dambrine, G., Plassiart, G., Brisac, M., Crochet, J., and Perbal, B. (1992). Proviral rearrangements and overexpression of a new cellular gene (nov) in myeloblastosis-associated virus type 1-induced nephroblastomas. *Mol. Cell. Biol.* **12**, 10–21.

Kang, Y., Siegel, P. M., Shu, W., Drobniak, M., Kakonen, S. M., Cordon-Cardo, C., Guise, T. A., and Massague, J. (2003). A multigenic program mediating breast cancer metastasis to bone. *Cancer Cell* **3**, 537–549.

Kanyama, M., Kuboki, T., Akiyama, K., Nawachi, K., Miyauchi, F. M., Yatani, H., Kubota, S., Nakanishi, T., and Takigawa, M. (2003). Connective tissue growth factor expressed in rat alveolar bone regeneration sites after tooth extraction. *Arch. Oral. Biol.* **48**, 723–730.

Karaplis, A. C. (2002). Embryonic development of bone and the molecular regulation of intramembranous and endochondral bone formation. In “Principles of Bone Biology” (J. P. Bilezikian, L. G. Raisz, and G. A. Rodan, Eds.), Vol. 1, pp. 33–58. Academic Press, New York.

Katsume, K., Chuai, M. L., Liu, Y. C., Kabasawa, Y., Takagi, M., Perbal, B., and Sakamoto, K. (2001). The expression of chicken NOV, a member of the CCN gene family, in early stage development. *Brain Res. Gene Expr. Patterns* **1**, 61–65.

Katsuma, S., Ruike, Y., Yano, T., Kimura, M., Hirasawa, A., and Tsujimoto, G. (2005). Transcriptional regulation of connective tissue growth factor by sphingosine 1-phosphate in rat cultured mesangial cells. *FEBS Lett.* **579**, 2576–2582.

Kawata, K., Eguchi, T., Kubota, S., Kawaki, H., Oka, M., Minagi, S., and Takigawa, M. (2006). Possible role of LRPI, a CCN2 receptor, in chondrocytes. *Biochem. Biophys. Res. Commun.* **345**, 552–559.

Keil, A., Blom, I. E., Goldschmeding, R., and Rupprecht, H. D. (2002). Nitric oxide down-regulates connective tissue growth factor in rat mesangial cells. *Kidney Int.* **62**, 401–411.

Kikuchi, K., Kadono, T., Ihn, H., Sato, S., Igarashi, A., Nakagawa, H., Tamaki, K., and Takehara, K. (1995). Growth regulation in scleroderma fibroblasts: Increased response to transforming growth factor-beta 1. *J. Invest. Dermatol.* **105**, 128–132.

Kim, H. S., Nagalla, S. R., Oh, Y., Wilson, E., Roberts, C. T., Jr., and Rosenfeld, R. G. (1997). Identification of a family of low-affinity insulin-like growth factor binding proteins (IGFBPs): Characterization of connective tissue growth factor as a member of the IGFBP superfamily. *Proc. Natl. Acad. Sci. USA* **94**, 12981–12986.

Kireeva, M. L., Latinkic, B. V., Kolesnikova, T. V., Chen, C. C., Yang, G. P., Abler, A. S., and Lau, L. F. (1997). Cyr61 and Fisp12 are both ECM-associated signaling molecules: Activities, metabolism, and localization during development. *Exp. Cell Res.* **233**, 63–77.

Kondo, S., Kubota, S., Eguchi, T., Hattori, T., Nakanishi, T., Sugahara, T., and Takigawa, M. (2000). Characterization of a mouse ctgf 3'-UTR segment that mediates repressive regulation of gene expression. *Biochem. Biophys. Res. Commun.* **278**, 119–124.

Kondo, S., Kubota, S., Shimo, T., Nishida, T., Yosimichi, G., Eguchi, T., Sugahara, T., and Takigawa, M. (2002). Connective tissue growth factor increased by hypoxia may initiate angiogenesis in collaboration with matrix metalloproteinases. *Carcinogenesis* **23**, 769–776.

Kondo, S., Kubota, S., Mukudai, Y., Moritani, N., Nishida, T., Matsushita, H., Matsumoto, S., Sugahara, T., and Takigawa, M. (2006). Hypoxic regulation of stability of connective tissue growth factor/CCN2 mRNA by 3'-untranslated region interacting with a cellular protein in human chondrosarcoma cells. *Oncogene* **25**, 1099–1110.

Kothapalli, D., Frazier, K. S., Welply, A., Segarini, P. R., and Grotendorst, G. R. (1997). Transforming growth factor beta induces anchorage-independent growth of NRK fibroblasts via a connective tissue growth factor-dependent signaling pathway. *Cell Growth Differ.* **8**, 61–68.

Kubo, M., Kikuchi, K., Nashiro, K., Kakinuma, T., Hayashi, N., Nanko, H., and Tamaki, K. (1998). Expression of fibrogenic cytokines in desmoplastic malignant melanoma. *Br. J. Dermatol.* **139**, 192–197.

Kubota, S., and Takigawa, M. (2002). Driving the driver: Molecular regulation of CTGF/Hcs24/CCN2 that regulates chondrocyte growth and differentiation. In “Recent Research Developments in Biophysics and Biochemistry,” pp. 995–1012. Research Signpost, Trivandrum, Kerala, India.

Kubota, S., Hattori, T., Nakanishi, T., and Takigawa, M. (1999). Involvement of *cis*-acting repressive element(s) in the 3'-untranslated region of human connective tissue growth factor gene. *FEBS Lett.* **450**, 84–88.

Kubota, S., Hattori, T., Shimo, T., Nakanishi, T., and Takigawa, M. (2000a). Novel intracellular effects of human connective tissue growth factor expressed in Cos-7 cells. *FEBS Lett.* **474**, 58–62.

Kubota, S., Kondo, S., Eguchi, T., Hattori, T., Nakanishi, T., Pomerantz, R. J., and Takigawa, M. (2000b). Identification of an RNA element that confers post-transcriptional repression of connective tissue growth factor/hypertrophic chondrocyte specific 24 (ctgf/hcs24) gene: Similarities to retroviral RNA-protein interactions. *Oncogene* **19**, 4773–4786.

Kubota, S., Eguchi, T., Shimo, T., Nishida, T., Hattori, T., Kondo, S., Nakanishi, T., and Takigawa, M. (2001). Novel mode of processing and secretion of connective tissue growth factor/ecogenin (CTGF/Hcs24) in chondrocytic HCS-2/8 cells. *Bone* **29**, 155–161.

Kubota, S., Moritani, N. H., Kawaki, H., Mimura, H., Minato, M., and Takigawa, M. (2003). Transcriptional induction of connective tissue growth factor/hypertrophic chondrocyte-specific 24 gene by dexamethasone in human chondrocytic cells. *Bone* **33**, 694–702.

Kubota, S., Kawata, K., Yanagita, T., Doi, H., Kitoh, T., and Takigawa, M. (2004). Abundant retention and release of connective tissue growth factor (CTGF/CCN2) by platelets. *J. Biochem. (Tokyo)* **136**, 279–282.

Kubota, S., Mukudai, Y., Moritani, N. H., Nakao, K., Kawata, K., and Takigawa, M. (2005). Translational repression by the *cis*-acting element of structure-anchored repression (CAESAR) of human ctgf/ccn2 mRNA. *FEBS Lett.* **579**, 3751–3758.

Kumar, S., Hand, A. T., Connor, J. R., Dodds, R. A., Ryan, P. J., Trill, J. J., Fisher, S. M., Nuttall, M. E., Lipshutz, D. B., Zou, C., Hwang, S. M., Votta, B. J., et al. (1999). Identification and cloning of a connective tissue growth factor-like cDNA from human osteoblasts encoding a novel regulator of osteoblast functions. *J. Biol. Chem.* **274**, 17123–17131.

Kumar, S., Connor, J. R., Dodds, R. A., Halsey, W., Van Horn, M., Mao, J., Sathe, G., Mui, P., Agarwal, P., Badger, A. M., Lee, J. C., Gowen, M., et al. (2001). Identification and initial characterization of 5000 expressed sequenced tags (ESTs) each from adult human normal and osteoarthritic cartilage cDNA libraries. *Osteoarthritis Cartilage* **9**, 641–653.

Kutz, W. E., Gong, Y., and Warman, M. L. (2005). WISP3, the gene responsible for the human skeletal disease progressive pseudorheumatoid dysplasia, is not essential for skeletal function in mice. *Mol. Cell. Biol.* **25**, 414–421.

Lafont, J., Jacques, C., Le Dreau, G., Calhabeu, F., Thibout, H., Dubois, C., Berenbaum, F., Laurent, M., and Martinerie, C. (2005). New target genes for NOV/CCN3 in chondrocytes: TGF-beta2 and type X collagen. *J. Bone Miner. Res.* **20**, 2213–2223.

Lamb, R., Thomson, W., Ogilvie, E., and Donn, R. British Society of Paediatric and Adolescent Rheumatology. (2005). Wnt-1-inducible signaling pathway protein 3 and susceptibility to juvenile idiopathic arthritis. *Arthritis. Rheum.* **52**, 3548–3553.

Laplante, A. F., Germain, L., Auger, F. A., and Moulin, V. (2001). Mechanisms of wound reepithelialization: Hints from a tissue-engineered reconstructed skin to long-standing questions. *FASEB J.* **15**, 2377–2389.

Lasky, J. A., Ortiz, L. A., Tonthat, B., Hoyle, G. W., Corti, M., Athas, G., Lungarella, G., Brody, A., and Friedman, M. (1998). Connective tissue growth factor mRNA expression is upregulated in bleomycin-induced lung fibrosis. *Am. J. Physiol.* **275**, L365–L371.

Lau, L. F., and Lam, S. C. (1999). The CCN family of angiogenic regulators: The integrin connection. *Exp. Cell Res.* **248**, 44–57.

Leask, A., Holmes, A., Black, C. M., and Abraham, D. J. (2003). Connective tissue growth factor gene regulation. Requirements for its induction by transforming growth factor-beta 2 in fibroblasts. *J. Biol. Chem.* **278**, 13008–13015.

Lin, B. R., Chang, C. C., Che, T. F., Chen, S. T., Chen, R. J., Yang, C. Y., Jeng, Y. M., Liang, J. T., Lee, P. H., Chang, K. J., Chau, Y. P., and Kuo, M. L. (2005). Connective tissue growth factor inhibits metastasis and acts as an independent prognostic marker in colorectal cancer. *Gastroenterology* **128**, 9–23.

Lin, C. G., Leu, S. J., Chen, N., Tebeau, C. M., Lin, S. X., Yeung, C. Y., and Lau, L. F. (2003). CCN3 (NOV) is a novel angiogenic regulator of the CCN protein family. *J. Biol. Chem.* **278**, 24200–24208.

Luo, Q., Kang, Q., Si, W., Jiang, W., Park, J. K., Peng, Y., Li, X., Luu, H. H., Luo, J., Montag, A. G., Haydon, R. C., and He, T. C. (2004). Connective tissue growth factor (CTGF) is regulated by Wnt and bone morphogenetic proteins signaling in osteoblast differentiation of mesenchymal stem cells. *J. Biol. Chem.* **279**, 55958–55968.

Miaczynska, M., Christoforidis, S., Giner, A., Shevchenko, A., Uttenweiler-Joseph, S., Habermann, B., Wilm, M., Parton, R. G., and Zerial, M. (2004). APPL proteins link Rab5 to nuclear signal transduction via an endosomal compartment. *Cell* **116**, 445–456.

Mo, F. E., Muntean, A. G., Chen, C. C., Stolz, D. B., Watkins, S. C., and Lau, L. F. (2002). CYR61 (CCN1) is essential for placental development and vascular integrity. *Mol. Cell. Biol.* **22**, 8709–8720.

Moallem, E., Kilav, R., Silver, J., and Naveh-Many, T. (1998). RNA-protein binding and post-transcriptional regulation of parathyroid hormone gene expression by calcium and phosphate. *J. Biol. Chem.* **273**, 5253–5259.

Mori, T., Kawara, S., Shinozaki, M., Hayashi, N., Kakinuma, T., Igarashi, A., Takigawa, M., Nakanishi, T., and Takehara, K. (1999). Role and interaction of connective tissue growth factor with transforming growth factor-beta in persistent fibrosis: A mouse fibrosis model. *J. Cell. Physiol.* **181**, 153–159.

Moritani, N. H., Kubota, S., Nishida, T., Kawaki, H., Kondo, S., Sugahara, T., and Takigawa, M. (2003a). Suppressive effect of overexpressed connective tissue growth factor on tumor cell growth in a human oral squamous cell carcinoma-derived cell line. *Cancer Lett.* **192**, 205–214.

Moritani, N. H., Kubota, S., Eguchi, T., Fukunaga, T., Yamashiro, T., Takano-Yamamoto, T., Tahara, H., Ohyama, K., Sugahara, T., and Takigawa, M. (2003b). Interaction of AP-1 and the ctgf gene: A possible driver of chondrocyte hypertrophy in growth cartilage. *J. Bone Miner. Metab.* **21**, 205–210.

Moritani, N. H., Kubota, S., Sugahara, T., and Takigawa, M. (2005). Comparable response of ccn1 with ccn2 genes upon arthritis: An *in vitro* evaluation with a human chondrocytic cell line stimulated by a set of cytokines. *Cell Commun. Signal.* **3**, 6.

Moussad, E. E., and Brigstock, D. R. (2000). Connective tissue growth factor: What's in a name? *Mol. Genet. Metab.* **71**, 276–292.

Mukudai, Y., Kubota, S., and Takigawa, M. (2003). Conserved repressive regulation of connective tissue growth factor/hypertrophic chondrocyte-specific gene 24 (ctgf/hcs24) enabled by different elements and factors among vertebrate species. *Biol. Chem.* **384**, 1–9.

Mukudai, Y., Kubota, S., Eguchi, T., Kondo, S., Nakao, K., and Takigawa, M. (2005). Regulation of chicken ccn2 gene by interaction between RNA cis-element and putative trans-factor during differentiation of chondrocytes. *J. Biol. Chem.* **280**, 3166–3177.

Nakanishi, T., Kimura, Y., Tamura, T., Ichikawa, H., Yamaai, Y., Sugimoto, T., and Takigawa, M. (1997). Cloning of a mRNA preferentially expressed in chondrocytes by differential display-PCR from a human chondrocytic cell line that is identical with connective tissue growth factor (CTGF) mRNA. *Biochem. Biophys. Res. Commun.* **234**, 206–210.

Nakanishi, T., Nishida, T., Shimo, T., Kobayashi, K., Kubo, T., Tamatani, T., Tezuka, K., and Takigawa, M. (2000). Effects of CTGF/Hcs24, a product of a hypertrophic chondrocyte-specific gene, on the proliferation and differentiation of chondrocytes in culture. *Endocrinology* **141**, 264–273.

Nakata, E., Nakanishi, T., Kawai, A., Asaumi, K., Yamaai, T., Asano, M., Nishida, T., Mitani, S., Inoue, H., and Takigawa, M. (2002). Expression of connective tissue growth factor/hypertrophic chondrocyte-specific gene product 24 (CTGF/Hcs24) during fracture healing. *Bone* **31**, 441–447.

Nawachi, K., Inoue, M., Kubota, S., Nishida, T., Yosimichi, G., Nakanishi, T., Kanyama, M., Kuboki, T., Yatani, H., Yamaai, T., and Takigawa, M. (2002). Tyrosine kinase-type receptor ErbB4 in chondrocytes: Interaction with connective tissue growth factor and distribution in cartilage. *FEBS Lett.* **528**, 109–113.

Nishida, T., Nakanishi, T., Shimo, T., Asano, M., Hattori, T., Tamatani, T., Tezuka, K., and Takigawa, M. (1998). Demonstration of receptors specific for connective tissue growth factor on a human chondrocytic cell line (HCS-2/8). *Biochem. Biophys. Res. Commun.* **247**, 905–909.

Nishida, T., Nakanishi, T., Asano, M., Shimo, T., and Takigawa, M. (2000). Effects of CTGF/Hcs24, a hypertrophic chondrocyte-specific gene product, on the proliferation and differentiation of osteoblastic cells *in vitro*. *J. Cell. Physiol.* **184**, 197–206.

Nishida, T., Kubota, S., Nakanishi, T., Kuboki, T., Yosimichi, G., Kondo, S., and Takigawa, M. (2002). CTGF/Hcs24, a hypertrophic chondrocyte-specific gene product, stimulates proliferation and differentiation, but not hypertrophy of cultured articular chondrocytes. *J. Cell. Physiol.* **192**, 55–63.

Nishida, T., Kubota, S., Fukunaga, T., Kondo, S., Yosimichi, G., Nakanishi, T., Takano-Yamamoto, T., and Takigawa, M. (2003). CTGF/Hcs24, hypertrophic chondrocyte-specific gene product, interacts with perlecan in regulating the proliferation and differentiation of chondrocytes. *J. Cell. Physiol.* **196**, 265–275.

Nishida, T., Kubota, S., Kojima, S., Kuboki, T., Nakao, K., Kushibiki, T., Tabata, Y., and Takigawa, M. (2004). Regeneration of defects in articular cartilage in rat knee joints by CCN2 (connective tissue growth factor). *J. Bone Miner. Res.* **19**, 1308–1319.

O'Brien, T. P., Yang, G. P., Sanders, L., and Lau, L. F. (1990). Expression of *cyr61*, a growth factor-inducible immediate-early gene. *Mol. Cell. Biol.* **10**, 3569–3577.

Omoto, S., Nishida, K., Yamaai, Y., Shibahara, M., Nishida, T., Doi, T., Asahara, H., Nakanishi, T., Inoue, H., and Takigawa, M. (2004). Expression and localization of connective tissue growth factor (CTGF/Hcs24/CCN2) in osteoarthritic cartilage. *Osteoarthritis Cartilage* **12**, 771–778.

Patthy, L. (1987). Intron-dependent evolution: Preferred types of exons and introns. *FEBS Lett.* **214**, 1–7.

Pennica, D., Swanson, T. A., Welsh, J. W., Roy, M. A., Lawrence, D. A., Lee, J., Brush, J., Taneyhill, L. A., Deuel, B., Lew, M., Watanabe, C., Cohen, R. L., et al. (1998). WISP genes are members of the connective tissue growth factor family that are up-regulated in *wnt-1*-transformed cells and aberrantly expressed in human colon tumors. *Proc. Natl. Acad. Sci. USA* **95**, 14717–14722.

Perbal, B. (2001). NOV (nephroblastoma overexpressed) and the CCN family of genes: Structural and functional issues. *Mol. Pathol.* **54**, 57–79.

Perbal, B. (2004). CCN proteins: Multifunctional signalling regulators. *Lancet* **363**, 62–64.

Perbal, B., and Takigawa, M. (2005). “CCN Proteins—a New Family of Cell Growth and Differentiation Regulators.” Imperial College Press, London.

Planque, N., Long Li, C., Saule, S., Bleau, A.-M., and Perbal, B. (2006). Nuclear addressing provides a clue for the transforming activity of amino-truncated CCN proteins. *J. Cell. Biochem.* **99**, 105–116.

Rachfal, A. W., and Brigstock, D. R. (2003). Connective tissue growth factor (CTGF/CCN2) in hepatic fibrosis. *Hepatol. Res.* **26**, 1–9.

Ryseck, R. P., Macdonald-Bravo, H., Mattei, M. G., and Bravo, R. (1991). Structure, mapping, and expression of fisp-12, a growth factor-inducible gene encoding a secreted cysteine-rich protein. *Cell Growth Differ.* **2**, 225–233.

Safadi, F. F., Xu, J., Smock, S. L., Kanaan, R. A., Selim, A. H., Odgren, P. R., Marks, S. C., Jr., Owen, T. A., and Popoff, S. N. (2003). Expression of connective tissue growth factor in bone: Its role in osteoblast proliferation and differentiation *in vitro* and bone formation *in vivo*. *J. Cell. Physiol.* **196**, 51–62.

Sakamoto, K., Yamaguchi, S., Ando, R., Miyawaki, A., Kabasawa, Y., Takagi, M., Li, C. L., Perbal, B., and Katsube, K. (2002). The nephroblastoma overexpressed gene (NOV/ccn3) protein associates with Notch1 extracellular domain and inhibits myoblast differentiation via Notch signaling pathway. *J. Biol. Chem.* **277**, 29399–29405.

Sato, S., Nagaoka, T., Hasegawa, M., Tamatani, T., Nakanishi, T., Takigawa, M., and Takehara, K. (2000). Serum levels of connective tissue growth factor are elevated in patients with systemic sclerosis: Association with extent of skin sclerosis and severity of pulmonary fibrosis. *J. Rheumatol.* **27**, 149–154.

Sawai, K., Mori, K., Mukoyama, M., Sugawara, A., Suganami, T., Koshikawa, M., Yahata, K., Makino, H., Nagae, T., Fujinaga, Y., Yokoi, H., Yoshioka, T., et al. (2003). Angiogenic protein Cyr61 is expressed by podocytes in anti-Thy-1 glomerulonephritis. *J. Am. Soc. Nephrol.* **14**, 1154–1163.

Schober, J. M., Chen, N., Grzeszkiewicz, T. M., Jovanovic, I., Emeson, E. E., Ugarova, T. P., Ye, R. D., Lau, L. F., and Lam, S. C. (2002). Identification of integrin alpha(M)beta(2) as an adhesion receptor on peripheral blood monocytes for Cyr61 (CCN1) and connective tissue growth factor (CCN2): Immediate-early gene products expressed in atherosclerotic lesions. *Blood* **99**, 4457–4465.

Schutze, N., Noth, U., Schneidereit, J., Hendrich, C., and Jakob, F. (2005). Differential expression of CCN-family members in primary human bone marrow-derived mesenchymal stem cells during osteogenic, chondrogenic and adipogenic differentiation. *Cell Commun. Signal.* **3**, 5.

Segarini, P. R., Nesbitt, J. E., Li, D., Hays, L. G., Yates, J. R., 3rd, and Carmichael, D. F. (2001). The low density lipoprotein receptor-related protein/alpha2-macroglobulin receptor is a receptor for connective tissue growth factor. *J. Biol. Chem.* **276**, 40659–40667.

Sen, M., Cheng, Y. H., Goldring, M. B., Lotz, M. K., and Carson, D. A. (2004). WISP3-dependent regulation of type II collagen and aggrecan production in chondrocytes. *Arthritis Rheum.* **50**, 488–497.

Shakunaga, T., Ozaki, T., Ohara, N., Asaumi, K., Doi, T., Nishida, K., Kawai, A., Nakanishi, T., Takigawa, M., and Inoue, H. (2000). Expression of connective tissue growth factor in cartilaginous tumors. *Cancer* **89**, 1466–1473.

Shimo, T., Kubota, S., Yoshioka, N., Ibaragi, S., Isowa, S., Eguchi, T., Sasaki, A., and Takigawa, M. (2006). Pathogenic role of connective tissue growth factor (CTGF/CCN2) in osteolytic metastasis of breast cancer. *J. Bone Miner. Res.* **21**, 1045–1059.

Shimo, T., Nakanishi, T., Kimura, Y., Nishida, T., Ishizeki, K., Matsumura, T., and Takigawa, M. (1998). Inhibition of endogenous expression of connective tissue growth factor by its antisense oligonucleotide and antisense RNA suppresses proliferation and migration of vascular endothelial cells. *J. Biochem. (Tokyo)* **124**, 130–140.

Shimo, T., Nakanishi, T., Nishida, T., Asano, M., Kanyama, M., Kuboki, T., Tamatani, T., Tezuka, K., Takemura, M., Matsumura, T., and Takigawa, M. (1999). Connective tissue

growth factor induces the proliferation, migration, and tube formation of vascular endothelial cells *in vitro*, and angiogenesis *in vivo*. *J. Biochem. (Tokyo)* **126**, 137–145.

Shimo, T., Nakanishi, T., Nishida, T., Asanao, M., Sasaki, A., Kanyama, M., Kuboki, T., Matsumura, T., and Takigawa, M. (2001a). Involvement of CTGF, a hypertrophic chondrocyte-specific gene product, in tumor angiogenesis. *Oncology* **61**, 315–322.

Shimo, T., Kubota, S., Kondo, S., Nakanishi, T., Sasaki, A., Mese, H., Matsumura, T., and Takigawa, M. (2001b). Connective tissue growth factor as a major angiogenic agent that is induced by hypoxia in a human breast cancer cell line. *Cancer Lett.* **174**, 57–64.

Shimo, T., Wu, C., Billings, P. C., Piddington, R., Rosenbloom, J., Pacifici, M., and Koyama, E. (2002). Expression, gene regulation, and roles of Fisp12/CTGF in developing tooth germs. *Dev. Dyn.* **224**, 267–278.

Simmons, D. L., Levy, D. B., Yannoni, Y., and Erikson, R. L. (1989). Identification of a phorbol ester-repressible v-src-inducible gene. *Proc. Natl. Acad. Sci. USA* **86**, 1178–1182.

Soon, L. L., Yie, T. A., Shvarts, A., Levine, A. J., Su, F., and Tchou-Wong, K. M. (2003). Overexpression of WISP-1 down-regulated motility and invasion of lung cancer cells through inhibition of Rac activation. *J. Biol. Chem.* **278**, 11465–11470.

Surveyor, G. A., and Brigstock, D. R. (1999). Immunohistochemical localization of connective tissue growth factor (CTGF) in the mouse embryo between days 7.5 and 14.5 of gestation. *Growth Factors* **17**, 115–124.

Takigawa, M. (2003). CTGF/Hcs24 as a multifunctional growth factor for fibroblasts, chondrocytes and vascular endothelial cells. *Drug News Perspect.* **16**, 11–21.

Takigawa, M., Tajima, K., Pan, H. O., Enomoto, M., Kinoshita, A., Suzuki, F., Takano, Y., and Mori, Y. (1989). Establishment of a clonal human chondrosarcoma cell line with cartilage phenotypes. *Cancer Res.* **49**, 3996–4002.

Takigawa, M., Pan, H. O., Kinoshita, A., Tajima, K., and Takano, Y. (1991). Establishment from a human chondrosarcoma of a new immortal cell line with high tumorigenicity *in vivo*, which is able to form proteoglycan-rich cartilage-like nodules and to respond to insulin *in vitro*. *Int. J. Cancer* **48**, 717–725.

Takigawa, M., Nakanishi, T., Kubota, S., and Nishida, T. (2003). Role of CTGF/HCS24/egogenin in skeletal growth control. *J. Cell. Physiol.* **194**, 256–266.

Tamatani, T., Kobayashi, H., Tezuka, K., Sakamoto, S., Suzuki, K., Nakanishi, T., Takigawa, M., and Miyano, T. (1998). Establishment of the enzyme-linked immunosorbent assay for connective tissue growth factor (CTGF) and its detection in the sera of biliary atresia. *Biochem. Biophys. Res. Commun.* **251**, 748–752.

Tanaka, S., Sugimachi, K., Saeki, H., Kinoshita, J., Ohga, T., Shimada, M., Maehara, Y., and Sugimachi, K. (2001). A novel variant of WISP1 lacking a Von Willebrand type C module overexpressed in scirrhous gastric carcinoma. *Oncogene* **20**, 5525–5532.

Tanaka, S., Sugimachi, K., Shimada, M., Maehara, Y., and Sugimachi, K. (2002). Variant WISPs as targets for gastrointestinal carcinomas. *Gastroenterology* **123**, 392–393.

Tanaka, S., Sugimachi, K., Kameyama, T., Maehara, S., Shirabe, K., Shimada, M., Wands, J. R., and Maehara, Y. (2003). Human WISP1v, a member of the CCN family, is associated with invasive cholangiocarcinoma. *Hepatology* **37**, 1122–1129.

Tong, X., Xie, D., O'Kelly, J., Miller, C. W., Muller-Tidow, C., and Koeffler, H. P. (2001). Cyr61, a member of CCN family, is a tumor suppressor in non-small cell lung cancer. *J. Biol. Chem.* **276**, 47709–47714.

Twigg, S. M., Joly, A. H., Chen, M. M., Tsubaki, J., Kim, H. S., Hwa, V., Oh, Y., and Rosenfeld, R. G. (2002). Connective tissue growth factor/IGF-binding protein-related protein-2 is a mediator in the induction of fibronectin by advanced glycosylation end-products in human dermal fibroblasts. *Endocrinology* **143**, 1260–1269.

Villacorta, L., Graca-Souza, A. V., Ricciarelli, R., Zingg, J. M., and Azzi, A. (2003). Alpha-tocopherol induces expression of connective tissue growth factor and antagonizes tumor

necrosis factor-alpha-mediated downregulation in human smooth muscle cells. *Circ. Res.* **92**, 104–110.

Wahab, N. A., Brinkman, H., and Mason, R. M. (2001). Uptake and intracellular transport of the connective tissue growth factor: A potential mode of action. *Biochem. J.* **359**, 89–97.

Wahab, N. A., Weston, B. S., and Mason, R. M. (2005a). Connective tissue growth factor CCN2 interacts with and activates the tyrosine kinase receptor TrkA. *J. Am. Soc. Nephrol.* **16**, 340–351.

Wahab, N. A., Weston, B. S., and Mason, R. M. (2005b). Modulation of the TGFbeta/Smad signaling pathway in mesangial cells by CTGF/CCN2. *Exp. Cell Res.* **307**, 305–314.

Wenger, C., Ellenrieder, V., Alber, B., Lacher, U., Menke, A., Hameister, H., Wilda, M., Iwamura, T., Beger, H. G., Adler, G., and Gress, T. M. (1999). Expression and differential regulation of connective tissue growth factor in pancreatic cancer cells. *Oncogene* **18**, 1073–1080.

Xie, D., Nakachi, K., Wang, H., Elashoff, R., and Koeffler, H. P. (2001). Elevated levels of connective tissue growth factor, WISP-1, and CYR61 in primary breast cancers associated with more advanced features. *Cancer Res.* **61**, 8917–8923.

Xu, L., Corcoran, R. B., Welsh, J. W., Pennica, D., and Levine, A. J. (2000). WISP-1 is a Wnt-1- and beta-catenin-responsive oncogene. *Genes Dev.* **14**, 585–595.

Xu, S. W., Howat, S. L., Renzoni, E. A., Holmes, A., Pearson, J. D., Dashwood, M. R., Bou-Gharios, G., Denton, C. P., du Bois, R. M., Black, C. M., Leask, A., and Abraham, D. J. (2004). Endothelin-1 induces expression of matrix-associated genes in lung fibroblasts through MEK/ERK. *J. Biol. Chem.* **279**, 23098–23103.

Yamaai, T., Nakanishi, T., Asano, M., Nawachi, K., Yoshimichi, G., Ohyama, K., Komori, T., Sugimoto, T., and Takigawa, M. (2005). Gene expression of connective tissue growth factor (CTGF/CCN2) in calcifying tissues of normal and cbfa1-null mutant mice in late stage of embryonic development. *J. Bone Miner. Metab.* **23**, 280–288.

Yang, M., Huang, H., Li, J., Li, D., and Wang, H. (2004). Tyrosine phosphorylation of the LDL receptor-related protein (LRP) and activation of the ERK pathway are required for connective tissue growth factor to potentiate myofibroblast differentiation. *FASEB J.* **18**, 920–921.

Yokoi, H., Sugawara, A., Mukoyama, M., Mori, K., Makino, H., Saganami, T., Nagae, T., Yahata, K., Fujinaga, Y., Tanaka, I., and Nakao, K. (2001). Role of connective tissue growth factor in profibrotic action of transforming growth factor-beta: A potential target for preventing renal fibrosis. *Am. J. Kidney Dis.* **38**, S134–S138.

Yoshimichi, G., Nakanishi, T., Nishida, T., Hattori, T., Takano-Yamamoto, T., and Takigawa, M. (2001). CTGF/Hcs24 induces chondrocyte differentiation through a p38 mitogen-activated protein kinase (p38MAPK), and proliferation through a p44/42 MAPK/extracellular-signal regulated kinase (ERK). *Eur. J. Biochem.* **268**, 6058–6065.

Yoshimichi, G., Kubota, S., Nishida, T., Kondo, S., Yanagita, T., Nakao, K., Takano-Yamamoto, T., and Takigawa, M. (2006). Roles of PKC, PI3K and JNK in multiple transduction of CCN2/CTGF signals in chondrocytes. *Bone* **38**, 853–863.

Yu, C., Le, A. T., Yeger, H., Perbal, B., and Alman, B. A. (2003). NOV (CCN3) regulation in the growth plate and CCN family member expression in cartilage neoplasia. *J. Pathol.* **201**, 609–615.

Zhang, R., Averboukh, L., Zhu, W., Zhang, H., Jo, H., Dempsey, P. J., Coffey, R. J., Pardee, A. B., and Liang, P. (1998). Identification of rCop-1, a new member of the CCN protein family, as a negative regulator for cell transformation. *Mol. Cell. Biol.* **18**, 6131–6141.

Zoubine, M. N., Banerjee, S., Saxena, N. K., Campbell, D. R., and Banerjee, S. K. (2001). WISP-2: A serum-inducible gene differentially expressed in human normal breast epithelial cells and in MCF-7 breast tumor cells. *Biochem. Biophys. Res. Commun.* **282**, 421–425.

This page intentionally left blank

Action Potential in Charophytes

Mary Jane Beilby

School of Physics, The University of New South Wales,
Sydney, Australia

The plant action potential (AP) has been studied for more than half a century. The experimental system was provided mainly by the large charophyte cells, which allowed insertion of early large electrodes, manipulation of cell compartments, and inside and outside media. These early experiments were inspired by the Hodgkin and Huxley (HH) work on the squid axon and its voltage clamp techniques. Later, the patch clamping technique provided information about the ion transporters underlying the excitation transient. The initial models were also influenced by the HH picture of the animal AP. At the turn of the century, the paradigm of the charophyte AP shifted to include several chemical reactions, second messenger-activated channel, and calcium ion liberation from internal stores. Many aspects of this new model await further clarification. The role of the AP in plant movements, wound signaling, and turgor regulation is now well documented. Involvement in invasion by pathogens, chilling injury, light, and gravity sensing are under investigation.

KEY WORDS: Action potential, Voltage clamp, Patch clamp, Perfusion, Cytoplasmic streaming, Cl^- channels, Ca^{2+} channels, K^+ channels, Pharmacological dissection, Internal Ca^{2+} stores, IP_3 activation, Ca^{2+} pump, Hodgkin Huxley model.

© 2007 Elsevier Inc.

I. Introduction

A. Defining Features of the Action Potential

The action potential (AP) is also referred to as excitation transient or just excitation. The AP involves rapid decrease (depolarization) of the negative membrane potential difference (PD) followed by a slower repolarization

(Fig. 1). Sufficient similarities exist between the animal and plant AP to suggest that we are looking at related phenomena:

- AP is elicited, when the membrane PD is depolarized to a definite threshold level.
- Once the threshold PD is reached, the AP form and amplitude are independent of the amplitude of the stimulus (all-or-none response; Fig. 2A).
- There is a refractory period following an AP, when a new AP cannot be stimulated (Fig. 2B).
- The AP initiated in one part of the cell propagates along the cell, sometimes several cells.
- An increase in temperature makes the AP faster (Fig. 3).

The Nobel Prize winning Hodgkin and Huxley (HH) model of the squid axon (Hodgkin and Huxley, 1952a–d) has influenced the early analysis of the plant AP. The AP in the nerve is generated by two opposing ionic fluxes: Sodium (Na^+) inflow and Potassium (K^+) outflow. The increase of the Na^+ conductance is the initial response to the stimulus, which depolarizes the membrane PD. The delayed increase in K^+ conductance and the spontaneous decrease in Na^+ conductance repolarize the membrane back to the resting state. The mathematical model and its application to *Chara* AP are outlined in Section II.J.3. The HH modeling was made possible by the technique of voltage clamping, in which the membrane PD is held at a selected level by passing a current through the membrane. The AP was also fixed in space by a thin current-supplying electrode placed along the axis of the cylindrical cell. Similar technology was applied to charophytes (Section II.A.1).

However, there are also some marked differences between excitation in plant and animal cells. The time scale in plants is longer by a factor of 10^3 (compare Fig. 1A and B). In plants there are two membranes, the outer plasmalemma and the inner tonoplast. Both membranes usually undergo excitation (Fig. 4A). The contributions from two membranes and the variation of ion concentration in both cytoplasmic and vacuolar compartments are the probable reasons for the shape of the plant AP being more variable (Fig. 1A). The evolutionary pressures on the animal AP are greater to keep the shape constant (Johnson *et al.*, 2002). The plant AP peak remains at negative PDs, crossing into positive region only under unusual circumstances (Beilby and MacRobbie, 1984; Findlay, 1962). The AP peak in the squid axon usually becomes positive. (This is not apparent in Fig. 1B, as both Hodgkin and Huxley and Cole replotted APs by relabeling the negative membrane resting PD as zero and treating the AP as a positive change in PD.) The outflow of chloride ions instead of inflow of sodium ions is responsible for the

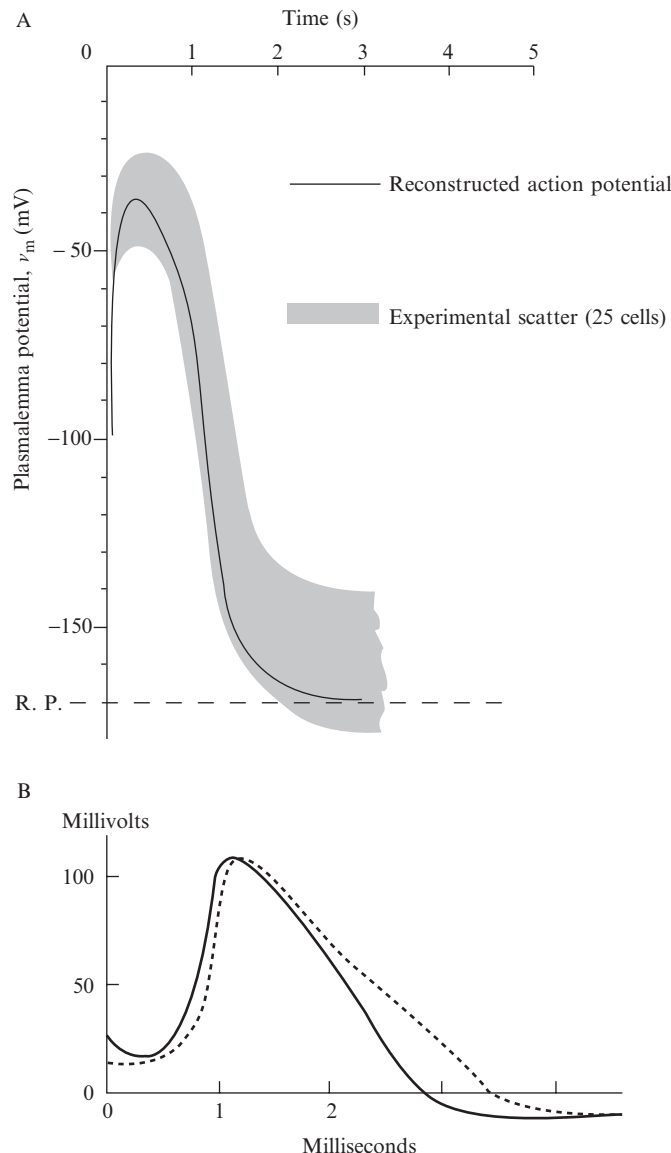


FIG. 1 Comparison of plant and nerve AP. (A) The plant AP reconstructed using HH equations (full line). The shaded area shows the variation of the AP form observed in 25 cells (Beilby and Coster, 1979b), R. P. = resting potential. (B) The axon AP data (dashed line) and HH simulation (continuous line), Cole (1968). Note the difference in time scales between (A) and (B).

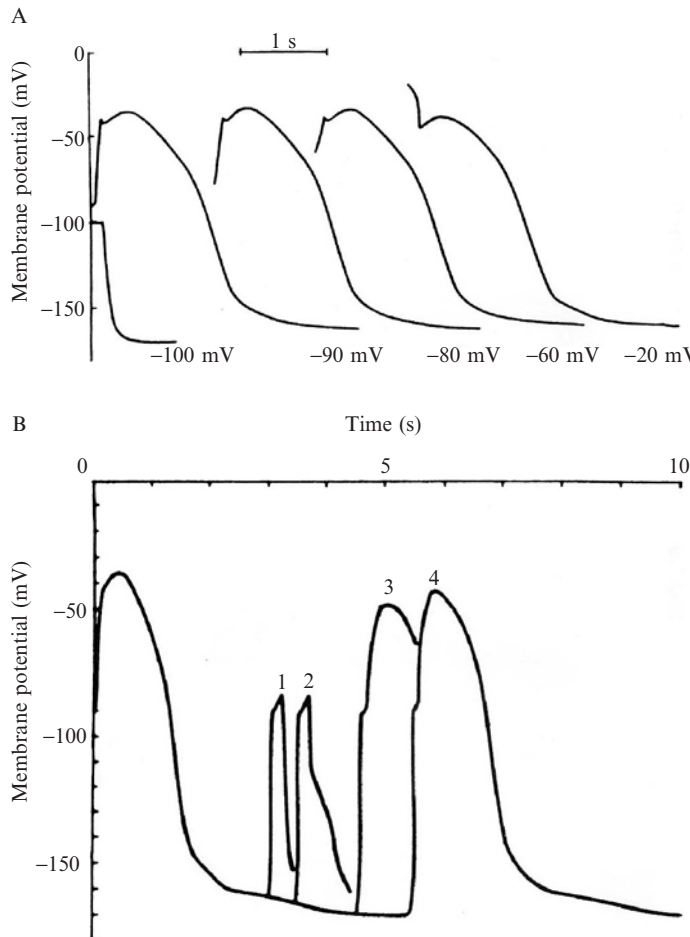


FIG. 2 (A) All-or-none behavior of the simulated AP (Beilby and Coster, 1979b). For the stimulating pulse-width of 0.15 s, there is no excitation at -100 mV, but AP does occur at -90 mV. If the stimulating current depolarized the membrane PD to levels more positive than the threshold (levels shown next to each curve), the form of the AP is not changed. The calculated threshold PD is slightly more positive than experimental threshold of ~ -115 mV. (B) The simulated refractory period (Beilby and Coster, 1979b). No excitation occurs when the simulated pulse is applied up to 3 s after previous excitation (response 1 and 2). After 5 s APs can be elicited, but they do not reach their full amplitude (response 3 and 4). The experimental refractory period varied from 6 to 60 s.

depolarizing stage in plants. Calcium ion plays an important part in the AP of most charophytes (see Sections II.E.1–2).

The HH picture of the axon excitation is so good, that it dominated our approach to analysis of charophyte (and other plant) excitation for almost

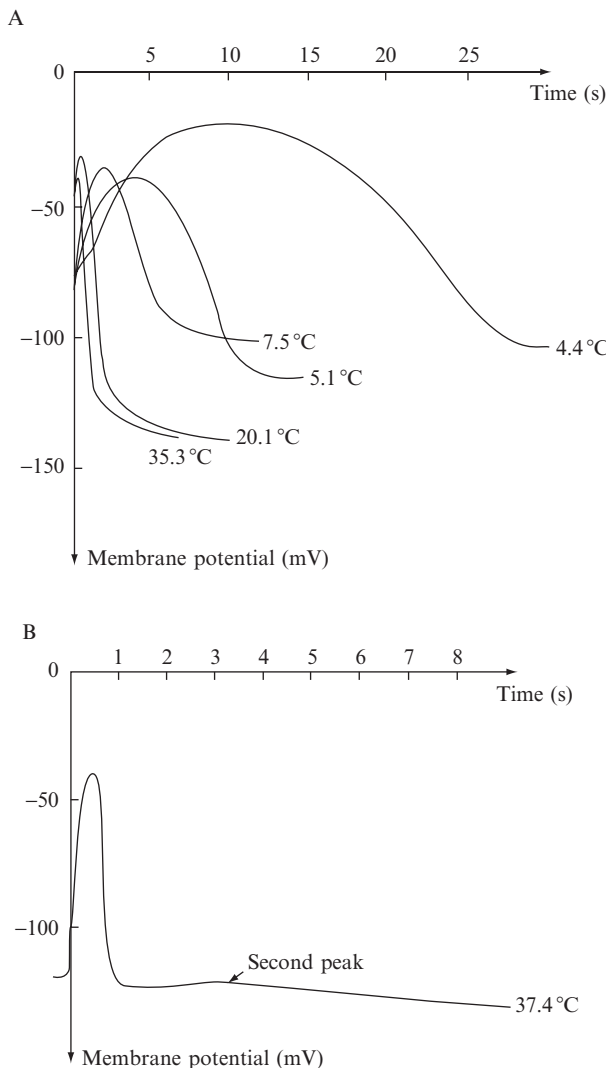
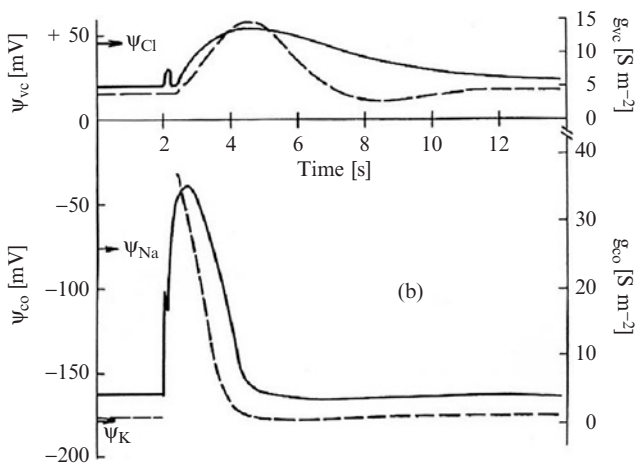


FIG. 3 (A) The variation of the AP duration as a function of temperature (Beilby and Coster, 1976). (B) At high temperature of 37.4°C, the AP measured across both membranes of *C. corallina* cell shows the two superimposed responses clearly (Beilby, 1978).

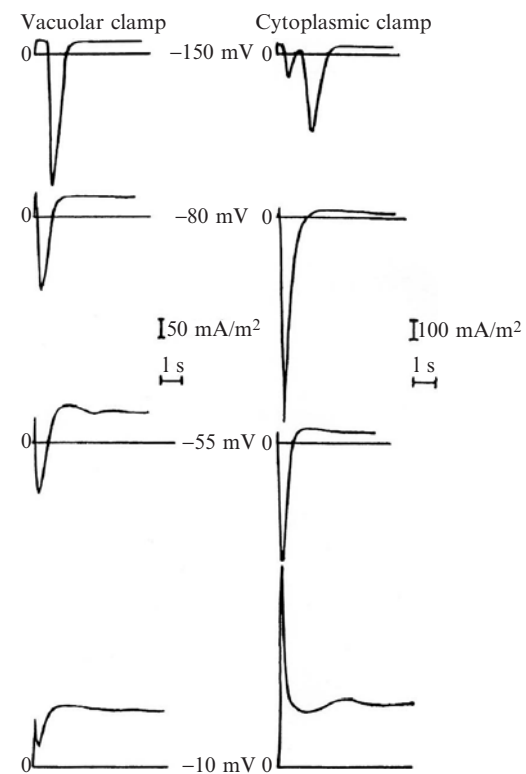
half a century. It is becoming apparent that other mechanisms underlie the plant AP and their intricacies are now emerging from the shadow of the animal AP (Biskup *et al.*, 1999; Thiel *et al.*, 1990; Wacke and Thiel, 2001; Wacke *et al.*, 2003).

A



(b)

B



B. Why Is the Study of Charophyte AP Important

Because of their large cell size, charophytes have been the subject of many electrophysiological studies, leading to an extensive body of information about them. The “green plants” or Viridiplantae are now viewed as containing two evolutionary lineages or clades, the Charophyta and the Chlorophyta (Karol *et al.*, 2001). The charophyte clade contains the charophyte algae and embryophytes (land plants). This close relationship indicates that knowledge gained on the charophyte system will be applicable to a wide range of land plants.

APs play an important role in signal transmission, not only in animal tissue such as nerve and muscle, but also in plant systems. Touch-sensitive plants (*Mimosa pudica*) and carnivorous plants (*Dionaea*) respond to a mechanical stimulus, which evoke APs that propagate to motor tissues, where turgor-aided movement is initiated (Pickard, 1973; Sibaoka, 1969; Simons, 1981). AP-like prolonged response to hypotonic stress enables salt-tolerant charophyte *Lamprothamnium* to regulate its turgor (Beilby and Shepherd, 2006). APs are also implicated in transmission of wound signals (Shimmen, 1996, 1997a,b,c). The stoppage of the cytoplasmic streaming triggered by the AP prevents leakage of cytoplasm from injured cells (Kamitsubo and Kikuyama, 1992; Kamitsubo *et al.*, 1989). Further, Davies (1987) suggested that most plants are capable of producing APs and that these play a major role in intercellular and intracellular communication alongside hormonal and other chemical signaling. The changes in ion concentrations, turgor, and water flow may result in modified activities of enzymes in the cell wall and changes in the membranes and the cytoplasm. There is a likely role for APs in chilling injury, invasion by pathogens, and light and gravity sensing. These electrical signaling cascades await future research.

II. Historical Background (Up to Late 1990s)

A. Experimental Techniques

1. Voltage Clamp

The voltage clamp technique was adopted in charophytes independently by Findlay (1961) and Kishimoto (1961, 1964). The results became easier to

FIG. 4 (A) Action potentials recorded simultaneously across the plasmalemma (Ψ_{co}) and tonoplast (Ψ_{vc}) of a *Chara corallina* cell (Findlay and Hope, 1964a). Note the resting PDs at each membrane. The dashed lines are the approximate time-courses of plasmalemma conductance, g_{co} , and tonoplast conductance, g_{vc} . (B) A comparison of the transient currents in *C. corallina* cell with both membranes clamped (left column) and plasmalemma clamp only (right column) (Beilby and Coster, 1979a).

interpret, once the space-clamp was introduced and the two membranes were voltage clamped separately (Findlay, 1964b).

In four-terminal voltage clamp, one pair of electrodes is used to measure the membrane PD, while the other pair of electrodes delivers the current. The measured PD is fed into an input of a comparator operational amplifier, while the other input receives a command voltage, which can be set to a single level or a complex function, such as a ramp, bipolar staircase, or the AP shape. As long as the membrane PD is different from the command, the comparator provides current (I) in the appropriate direction to decrease the difference. Modern electronics can facilitate this negative feedback process in several ms (for more details, see Beilby, 1989; Beilby and Beilby, 1983). To fix the excitation in space (space-clamp), the current electrode was made from a thin wire, extending throughout the length of a cylindrical cell (Findlay, 1964c; for review on methodology see Beilby, 1989). To voltage clamp each membrane alone, the PD measuring electrodes are placed into cytoplasm and outside medium (plasmalemma) or cytoplasm and vacuole (tonoplast). When the voltage clamp is applied across both membranes (PD-measuring electrodes are placed in vacuole and outside medium), the PD across each membrane distributes itself according to the membrane resistance—thus neither membrane is clamped to the command PD (Findlay, 1964c).

Some researchers used more complex voltage clamp commands. Kishimoto (1972) and later other Japanese researchers employed linearly depolarizing ramp command for voltage clamp (Fig. 5A). Thiel (1995) produced “AP clamp.” This technique utilized the computer control of the command voltage for the voltage clamp circuitry. The AP was recorded and then replayed as command voltage, while a range of blocking agents was applied (Thiel, 1995; Thiel *et al.*, 1997).

2. Compartment Manipulation

The large size of the charophyte cells facilitates manipulation of various cell compartments. These techniques are a two-edged sword, because while much greater control can be exercised over some cell compartments, the degree of disruption of normal cell structure and function is much greater than the simple electrode insertion or even voltage clamping and the results can be misleading. The control over internal media is limited, as cells do not survive if the changes from natural sap or cytoplasm are too extreme. More details of the various techniques described later can be found in an excellent review by Shimmen *et al.* (1994).

a. Vacuolar Perfusion In this technique the cell is placed into a three-compartment holder, where the compartments are electrically insulated by grease. The cell ends in the two outer compartments are cut off and the cell

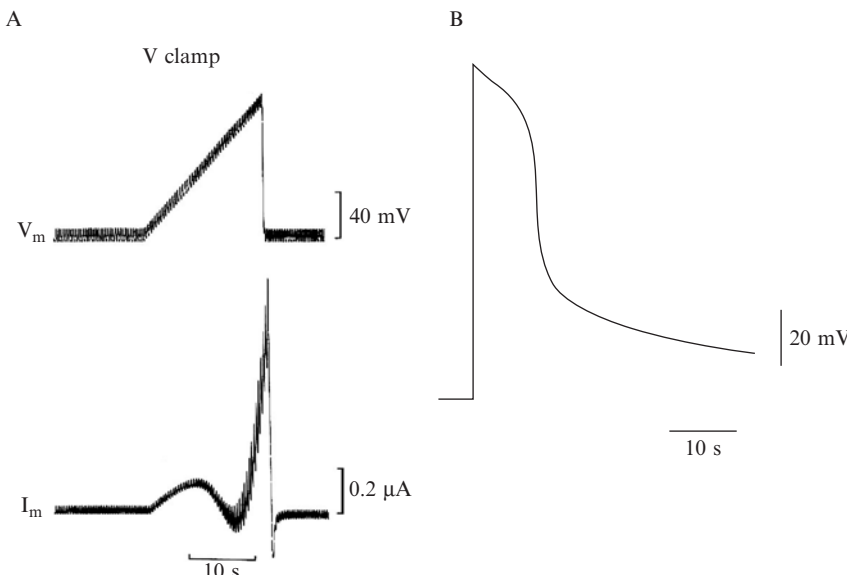


FIG. 5 Excitation in tonoplast free cells. (A) Excitation in a cell with a low Cl^- concentration (0.01 mM) in internal medium. The ramp-command clamp and the N-shaped current response, typical of excitation (Shimmen and Tazawa, 1980). (B) The cells perfused with medium with 100 mM K^+ produced an AP similar to that observed in intact cells (Shimmen and Tazawa, 1980).

sap is replaced by an artificial medium. The middle compartment is left empty until the perfusion is complete to prevent plasmolysis. Subsequently it is filled by outside medium, which is made isotonic to the perfusion medium by adding sorbitol or mannitol. The cell PD is simply measured by dipping the outside electrode into the middle pool and the "inside" electrode into one of the outer pools. Such cells have no turgor pressure, but can be exposed to a series of different solutions in a short time (Tazawa *et al.*, 1975). For the turgor pressure to develop, the ends of the cells can be ligated tightly by silk or synthetic thread. The cells can then be treated as ordinary cells and inside electrode has to be inserted into the cell. Such cells can be perfused only once and if they are left over time, they will alter the perfusion medium to be as similar as possible to the natural vacuolar sap. To retain the tonoplast, the perfusion medium must contain more than 1 mM Ca^{2+} (Tazawa, 1964).

b. Tonoplast Removal The removal of the tonoplast can be achieved mechanically by fast flow (Williamson, 1975) or chemically by including the

Ca^{2+} chelator EGTA (Tazawa *et al.*, 1976). The tonoplast-free cells can be used in the open-vacuole mode or ligated mode. However, as most of the cell cytoplasm is washed away, the cells lack cytoplasmic crystals and organelles for efficient wound healing and electrode insertion has to be done very carefully. There are many recipes for the artificial cytoplasmic medium (Shimmen *et al.*, 1994), which needs to contain Mg^{2+} and ATP for the cell to achieve negative membrane PD, streaming, and APs.

c. Cytoplasm-Enriched Fragments Long internodal cells (~ 10 cm) can be centrifuged at ~ 1 g for 20 min (Beilby and Shepherd, 1989; Hirono and Mitsui, 1981). The cytoplasm moves to one end of the cell. The cell is then wilted slightly and the cytoplasm-rich end is ligated and cut off (Beilby, 1989), obtaining a short (1.0–2.0 mm) cytoplasm-rich fragment. These can survive indefinitely, forming new vacuoles in a matter of hours. However, the cytoplasmic layer remains much thicker than in the intact cells and easily accessible to multiple electrode impalements.

d. Plasma-Membrane Permeabilization This system is prepared by plasmolyzing the cell with media of high osmolarity to irreversibly detach the plasma membrane from the cell wall. The integrity of the membrane is then destroyed by exposure to ice-cold Ca^{2+} chelator EGTA (Shimmen and Tazawa, 1983a). Any complex molecule that can pass through the cell wall can then access the cytoplasmic side of the tonoplast.

3. Patch Clamp

a. Tonoplast Membrane Cytoplasmic droplets can be created spontaneously by cutting the charophyte cells. The membrane surrounding the droplets are believed to be derived from the tonoplast (Luhring, 1986; Sakano and Tazawa, 1986). The cell wall does not form and most frequently found K^+ channels are well characterized (e.g., see Laver, 1990). Chloride (Cl^-) channels were described by Tyerman and Findlay (1989), Katsuhara and Tazawa (1992), and Beilby *et al.* (1999).

b. Plasma Membrane The charophyte cells are too large for the wall to be removed by wall-digesting enzymes. Microsurgical methods of cutting the wall have been successfully applied to access the plasma membrane (Coleman, 1986; Laver, 1991; Okihara *et al.*, 1991; Thiel *et al.*, 1993). Both the “cell-attached” and free patch configurations have been used.

B. The Stimulus

Although the most usual stimulus is facilitated by passing a current to reduce (depolarize) the membrane PD to the threshold level, there are many other ways to achieve this. Ohkawa and Kishimoto (1975) found that if the membrane PD is made more negative (hyperpolarized) by passing an inward current, the membrane PD overshoots the previous resting level once the current is turned off. The overshoot in depolarizing direction increased with the degree of previous hyperpolarization until the excitation threshold was reached. A similar effect was observed in the squid axon, where it was called “anode break excitation” (Hodgkin and Huxley, 1952a). Findlay and Hope (1976) reviewed several methods of stimulating an AP in plants: a sudden change in temperature by $\sim -15^{\circ}\text{C}$ or $\sim +25^{\circ}\text{C}$ (Harvey, 1942a; Hill, 1935), irradiation with intense UV light (Harvey, 1942b), or irradiation with alpha particles (Gaffey, 1972). The last technique caused membrane PD to hyperpolarize and stimulated APs by anode break once the radiation was turned off.

Kishimoto (1968) elicited APs by mechanical stimulation. Receptor PDs, proportional to the magnitude of the stimulus, depolarized the membrane PD. When the threshold PD was reached, AP was observed. This AP was of the same form as those obtained by electrical stimulus. Kishimoto also found that a number of subthreshold stimuli added up to excite APs. Later, Shimmen (1996, 1997a,b,c) made a more detailed study of mechano-stimulation. In charophytes growing in their natural environment, with rain, water currents and walking or swimming animals, the mechanical stimulus is the most likely source of excitation. Another way of mechano-stimulation is to change the cell turgor via the inserted pressure probe. Zimmermann and Beckers (1978) found that both increasing and decreasing pressure stimulated APs.

Any chemical agent that causes depolarization of the membrane PD is likely to stimulate APs, unless it also affects the channels involved in the AP process. Kishimoto (1966a) exposed *Nitella flexilis* cells to 10–100 mM of NaCl or LiCl and observed periodic trains of spontaneous APs. Spontaneous APs were also obtained by adding 1-mM EDTA or 2-mM ATP.

The definite threshold PD was a source of fascination to many researchers. Changing only a few mV near the threshold PD caused a large change in the electrical characteristics of the membrane (Fig. 2A). Such phenomena can serve as illustrations of chaos and catastrophe theories (Thom, 1975). Fujita and Mizuguchi (1955), Findlay (1959), and Gaffey (1972) showed that in *Nitella* the stimulating current pulse obeyed the classical strength-duration relationship (Katz, 1937). For longer pulses the threshold PD became more negative, for shorter pulses more positive. However, there are limiting levels, in which no time extension of the wide current pulse and no amplitude

increase of the very short current pulse, produce excitation. The relationship is based on a minimum quantity of electric charge (product of stimulus current and pulse width), needed to discharge the membrane capacitance and depolarize the membrane PD to threshold level.

In voltage clamp experiments the membrane PD is usually clamped to a depolarized level for some seconds and the excitation threshold manifests itself by flow of negative (inward) current (see Fig. 4B). Kishimoto (1964, 1966b) replotted the excitation currents at different times after the start of each clamp, obtaining N-shaped current-voltage (I/V) characteristics (see Fig. 5A). Similar results were obtained by using a ramp voltage command (Kishimoto, 1972). Kishimoto observed that as the rate of the voltage ramp was varied from 150 mV/sec to 30 mV/sec, the excitation transient appeared at more positive PDs. This is known as accommodation and can be observed in nerve and muscle tissue (Hodgkin and Huxley, 1952a). Thus in case of a ramp, there is a minimum rate of depolarization to produce an AP.

C. Coupling to Streaming Stoppage

The cytoplasm of charophyte cells rotates steadily around the cell at speeds near 100 $\mu\text{m/s}$ depending on the medium temperature. The streaming mechanism is now understood in terms of myosin, attached to barium sulphate crystals in the cytoplasm, which leapfrogs along the actin helix, propelling the crystal. The crystals stir the viscous flowing cytoplasm moving it along. The streaming can be detected by observing the movement of the organelles and particles present in the cytoplasmic phase, providing a beautiful and mesmerizing sight. At the time of excitation, the streaming stops suddenly and slowly recovers its original speed in 5–10 min (Kamiya, 1959). While the cells are not streaming, other APs can be stimulated. Tazawa and Kishimoto (1968) found that the viscosity of the cytoplasm does not increase at the time of the stoppage, but the motive force disappears. Tazawa and Kishimoto (1964) perfused *Nitella* cell vacuole with artificial sap and demonstrated that about 3-mM Ca^{2+} was necessary for normal cyclosis, but high concentration of 50 mM had an inhibitive effect. This early finding suggested the role of Ca^{2+} in cytoplasmic streaming. Beilby (1984a) observed streaming stoppage in *Chara*, even when Ca^{++} in the medium was replaced by Mg^{++} . The removal of the tonoplast in the intracellular perfusion by mechanical (Williamson, 1975) or chemical (Tazawa *et al.*, 1976) method made the cytoplasmic compartment accessible. First, this technique established the need for ATP and Mg^{2+} in millimolar concentrations. Williamson (1975) showed that in the tonoplast-free cells rise in Ca^{2+} concentration above 10^{-6} M retards

streaming substantially. Tazawa *et al.* (1976) disrupted the tonoplast by including calcium chelator EGTA in the perfusion medium. In such cells cytoplasmic streaming did not stop at the time of the AP. Hayama *et al.* (1979) made cytoplasm-enriched cell fragments and demonstrated that the excitation at the plasma membrane is only enough to cause streaming stoppage. They also demonstrated that tonoplast-free perfused cells could be reperfused with media without EGTA and various concentrations of Ca^{2+} . High Ca^{2+} concentrations (1 mM) permanently inhibited streaming. This concentration was taken as the minimum amount for total cytoplasmic stoppage. Tominaga and Tazawa (1981) found that in their perfusion experiments the threshold Ca^{2+} concentration for streaming inhibition was lower at 0.5 mM. Kikuyama and Tazawa (1983) suggested that the perfusion technique induced changes in the motile system making it less sensitive to Ca^{2+} . Later, the steady state $[\text{Ca}^{2+}]_{\text{cyt}}$ was measured at ~ 200 nM, rising to ~ 700 nM at the peak of the AP (Plieth and Hansen, 1996; Williamson and Ashley, 1982). In salt-tolerant *Lamprothamnium succinctum*, the steady state $[\text{Ca}^{2+}]_{\text{cyt}}$ was 80 nM and streaming was not inhibited at $[\text{Ca}^{2+}]_{\text{cyt}}$ below 200 nM, but strongly inhibited above 500 nM (Okazaki *et al.*, 2002). So clearly, the AP does involve a transient rise in $[\text{Ca}^{2+}]_{\text{cyt}}$ and Section II.E.1 reviews the evidence on the sources of the Ca^{2+} .

D. Resolving Responses at Plasmalemma and Tonoplast

Plant cells have a cytoplasmic layer sandwiched between plasmalemma and tonoplast. Even in giant charophyte cells, the cytoplasm is only about 10- μm thick and opinions vary on how difficult it is to place an electrode there. If the cell is stimulated, the excitation occurs at both membranes. Findlay and Hope (1964a) were the first to record the excitation transients simultaneously at both membranes in *Chara* (Fig. 4A). When the AP is measured between the vacuole and the outside medium, the two transients superimpose on each other. At high temperature, it is possible to resolve the peaks of the transient at each membrane (Fig. 3B). Findlay and Hope (1964a) also measured the resting resistance of both membranes as $12.1 \pm 2.5 \text{ k}\Omega\text{.cm}^2$ and $1.1 \pm 0.1 \text{ k}\Omega\text{.cm}^2$ for plasmalemma and tonoplast, respectively. The resistances fell to about $300 \Omega\text{.cm}^2$ for both membranes. Similar excitation responses at both membrane were measured in a brackish charophyte *Nitellopsis obtusa* (Findlay, 1970).

However, as greater variety of charophytes became the subject of electrophysiological studies, several trends emerged. Kikuyama (1986b) found that *N. axilliformis* exhibited negative-going PD transient across the tonoplast. In *N. flexilis*, the plasmalemma and tonoplast transients can be resolved even

when the data are gathered by inserting the inside microelectrode into the vacuole (Kikuyama and Shimmen, 1997; Shimmen and Nishikawa, 1988). The tonoplast excitation could only be observed when $[Ca^{2+}]_{cyt}$ increased. The $[Ca^{2+}]_{cyt}$ was monitored by injecting aequorin into the cytoplasm. The timing of the rise in $[Ca^{2+}]_{cyt}$ was closely correlated with the plasmalemma AP, but the plasmalemma AP was not affected by lack of Ca^{2+} in the outside medium.

Findlay (1970) compared the excitation currents measured by voltage-clamping the plasmalemma alone and both membranes in series. A comparison at several PD levels is shown in Fig. 4B. Beilby (1990) made a detailed comparison of the data measured with the PD-measuring electrode in the vacuole and cytoplasm, with the short segment of the cell compartment-clamped or short cell space-clamped with a thin wire electrode. For most steady state currents, the plasmalemma resistance is much greater than that of the tonoplast. Thus most of the clamp PD will be across plasmalemma and the vacuole/outside data will be a good approximation of the plasmalemma characteristics. However, at the peak of the transient current, the plasmalemma may be equally or more conductive than the tonoplast and that is why the current transients are different with the electrode placement (Fig. 4B). Note particularly two peaks at PDs near the threshold level and the sharp positive peak near 0 PD in the plasmalemma-only clamp series.

Removal of the tonoplast in the cell perfusion (see Section II.A.2) also isolated the plasmalemma response. Although this technique answered several questions, it also introduced new puzzles. By washing out the intricate cytoplasmic phase with its many organelles, the system was irreversibly altered. Shimmen *et al.* (1976) found that the shape of the AP in tonoplast-free cells became rectangular and the duration varied from more than a minute to a fraction of a minute in repeated stimulations by an outward (depolarizing) current (Fig. 6A). No refractory period was observed. Beilby *et al.* (1993) measured membrane currents, while the membrane PD was clamped at levels more positive than excitation threshold in cells of tonoplast-free *Nitellopsis obtusa*. The currents also exhibited very slow inactivation compared to the intact cells (Fig. 6B and C). As the K^+ concentration in the medium was increased from 0.1 mM in artificial pond water (APW) to between 3–10 mM, it was possible to shift the membrane PD between two stable states by a short depolarizing or hyperpolarizing pulse (see Fig. 6A). Often the increase in medium K^+ caused the shift to depolarized level, while K^+ being replaced by Ca^{2+} repolarized the membrane PD.

Coster *et al.* (1974) inserted two microelectrodes into the *Chara* cytoplasm, one filled with 2-M KCl, the other with various dilute solutions of KCl or NaCl. The variation of the PD between the two electrodes with KCl or NaCl concentration was consistent with the cytoplasm behaving as a Donnan phase with 0.1–0.2 M negative fixed charges. At the time of excitation the

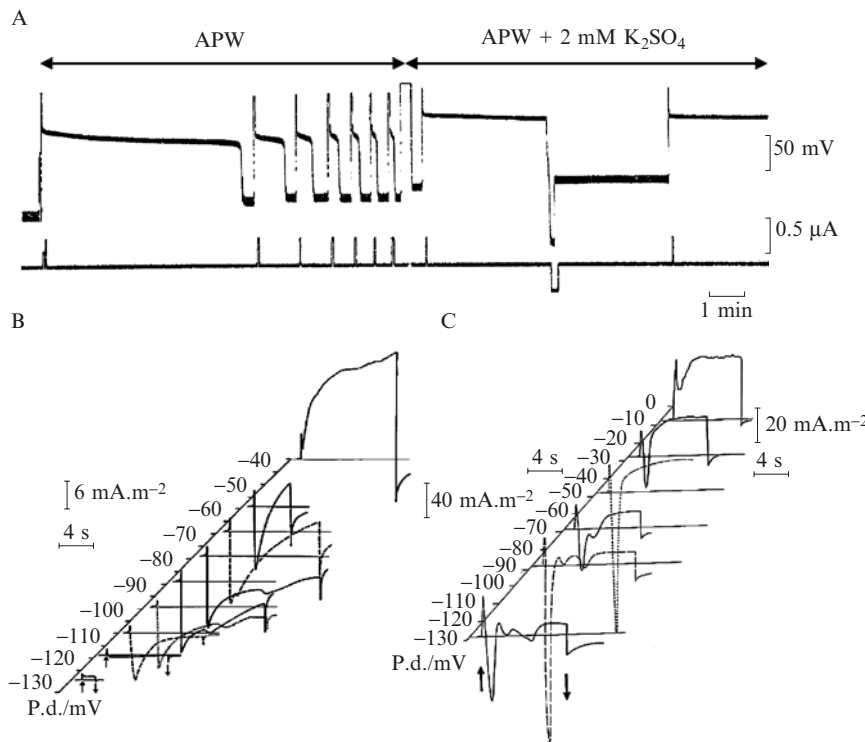


FIG. 6 Excitation in tonoplast free cells. (A) The record of PD in APW shows the prolonged AP, with decreasing duration upon repeated stimulation. Upon addition of 2-mM K₂SO₄, the membrane PD could be manipulated between two levels by hyperpolarizing and depolarizing pulse, respectively (Shimmen *et al.*, 1976). Comparison of the excitation clamp currents in *Nitellopsis obtusa* (Beilby *et al.*, 1993), (B) perfused tonoplast-free ligated cell, and (C) intact cell. The cells were voltage clamped at their resting PD, then to a PD level indicated (upward arrow) on the scale and finally back to the preclamp resting PD (downward arrow).

Donnan potential disappeared, suggesting a loss of fixed negative charges. How do these fixed charges arise? Do they play a role in electroneutrality at the time of AP? This interesting direction in research needs to be continued.

E. Resolving Individual Transporters

1. Calcium Channels

What ion flows produce the AP? The peak of the AP is found at small negative PDs (Fig. 1A). Thus Na⁺ was eliminated early, as the equilibrium (Nernst) PD was too negative. Both Cl⁻ and Ca²⁺ have positive equilibrium PDs.

The involvement of Ca^{2+} was obvious from quite early experiments. Osterhout and Hill (1933) performed experiments with *Nitella* and reported loss of excitability (anesthesia), when medium was replaced with distilled water. The choice of this ion was also attractive from an historical point of view, as only animals more advanced than Coelenterates have Na^+ based AP. The more ancient AP mechanism is Ca^{2+} based (Hille, 1992; Wayne, 1994). The Australian researchers, Hope (1961a,b) and Findlay (1961, 1962), correlated the increased amplitude of the AP spike to greater concentration of Ca^{2+} in the medium. They suggested that an inflow of Ca^{2+} carried the inward current of the depolarizing phase of the AP. However, they were unable to observe any changes in $^{45}\text{Ca}^{2+}$ influx (Hope and Findlay, 1964) and so correctly assumed that Cl^- is the main depolarizing ion, and that Ca^{2+} is needed for activation. Interestingly, if Ca^{2+} was the depolarizing ion, it might not have been detected, as only in later years the difficulty with wall bound Ca^{2+} became known (Reid and Smith, 1992). Fifteen years later, Hayama *et al.* (1979) did detect Ca^{2+} influx, but not large enough to account for the AP transient or the streaming stoppage. So, Ca^{2+} influx is involved in many types of charophytes, but mainly to increase the cytoplasmic concentration, which in turn opens the Cl^- channels on both plasmalemma and tonoplast and K^+ channels on the tonoplast. As most charophytes need Ca^{2+} or (Sr^{2+}) in the medium to be excitable, it is a reasonable assumption that at least some of the Ca^{2+} comes from the outside through Ca^{2+} selective channels. Beilby and Coster (1979a), while voltage clamping *Chara*, observed two transient currents, when the membrane PD was clamped just a little more positive than the excitation threshold (Fig. 4B). They thought that the second transient could be due to Ca^{2+} flow, but this timing was not right for the scheme of Ca^{2+} -activation of Cl^- channels. Lunevsky *et al.* (1983), voltage clamping the plasmalemma of *Nitellopsis*, inhibited the large transient current by Cl^- channel blocker, ethacrynic acid (see Fig. 7B). A small prompt transient was revealed at the beginning of the excitation. This transient seemed a better candidate for the Ca^{2+} inflow. However, the channel that passes the first transient current was found not to be selective. An increase in concentration of K^+ and Na^+ in the medium affects the first transient, but as these are low in the normal APW, Ca^{2+} is then the preferred ion (Lunevsky *et al.*, 1983).

Shimmen and Tazawa (1980), using tonoplast-free *Chara* cells, found that the AP peak was not sensitive to internal Cl^- concentration. Thus excitation occurred with very low Cl^- inside the cell or with EGTA, which prevented Ca^{2+} concentration inside the cell to rise (Fig. 5A). Kikuyama *et al.* (1984) could not detect Cl^- efflux from tonoplast-free cells containing abundant Cl^- . Mimura and Tazawa (1983) found that if *Nitellopsis* cells were reperfused with media containing varying concentrations of Ca^{2+} , membrane PD depolarized and membrane resistance decreased, but Cl^- efflux did not increase. Shiina and Tazawa (1987) tested Ca^{2+} and Cl^- channel inhibitors (see Section II.F.3 and

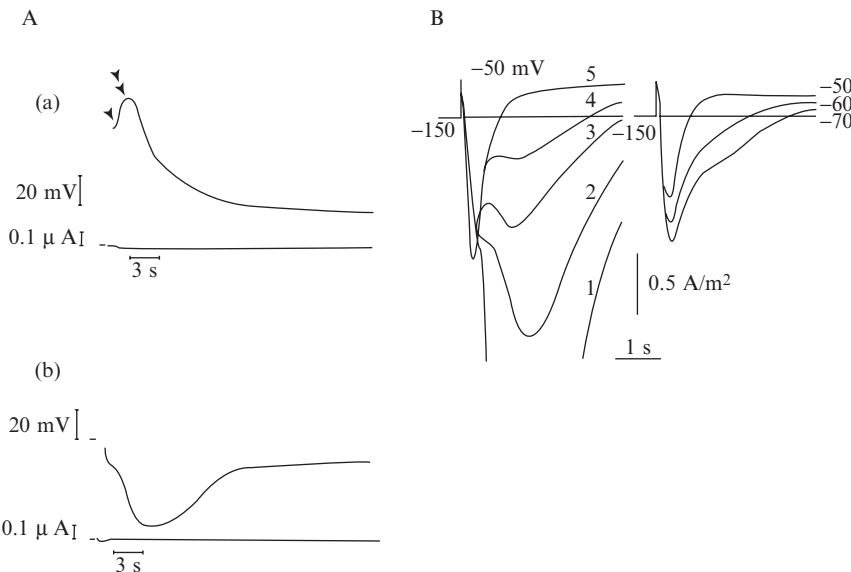


FIG. 7 (A) The dependence of the tonoplast AP in *Nitella pulchella* on Cl^- concentration of the vacuolar sap. The PD measuring electrode was in the vacuole. (a) Cell containing the natural cell sap. Single arrow shows the plasmalemma AP, double arrow the tonoplast AP. (b) The natural cell sap was replaced with an artificial medium lacking Cl^- . The AP reversed in a negative (downward) direction (Kikuyama and Tazawa, 1976). (B) Inhibition of the excitation Cl^- clamp current (curve 1) by ethacrynic acid (curves 2–5 taken in 10 min intervals) in *Nitellopsis obtusa*. The current through cation channels is revealed and can be explored at different clamp PDs (Lunevsky *et al.*, 1983).

the results were consistent with Ca^{2+} carrying the excitation current. The Japanese researchers suggested that under some circumstances Ca^{2+} inflow alone is responsible for the AP in tonoplast-free cells.

Using the patch clamp technique, is it possible to detect Ca^{2+} channels in the plasmalemma? The answer is not simple. Thiel *et al.* (1993) employed cell-attached configuration and found nonselective low conductance (4 pS) channel, which could conduct Ca^{2+} . However, the activity of these channels did not correlate with the activity of the Cl^- channels. Thiel *et al.* (1997) suggested that the cytoplasmic side of the plasma membrane contains stores for Ca^{2+} , which are replenished by the non-selective channels. A release of Ca^{2+} is favored by depolarizing the membrane PD. The cytoplasmic Ca^{2+} concentration rises locally and Cl^- channels in the vicinity are activated. The AP is a superposition of such stochastic microscopic events, the voltage dependence of the Cl^- channel (as modeled by Beilby and Coster, 1979b) being an illusion. The refractory period correlates with the time needed to refill the internal stores.

This picture was supported by elegant experiments of Plieth *et al.* (1998) with Mn^{2+} -induced quenching of fluorescent Ca^{2+} indicator fura-dextran. The addition of Mn^{2+} to the external medium or injection into the vacuole did not cause fluorescence quenching at the time of AP. As it was expected that Mn^{2+} can permeate through the Ca^{2+} channels, the result suggested that Ca^{2+} increase at the time of AP was due to release from internal stores. This hypothesis was further supported by preincubating *Chara* cells in high Mn^{2+} medium (25–30 mM). Such cells exhibited transient quenching of fura fluorescence at the time of AP in Mn^{2+} -free solutions. It was assumed that Mn^{2+} was taken up into the internal stores and released at the time of AP. Plieth *et al.* (1998) suggest that the Ca^{2+} store might be the endoplasmic reticulum (ER). The importance of Ca^{2+} -filled internal stores for normal AP to occur can explain several observations from other experiments. Williamson and Ashley (1982) observed slow regeneration of Ca^{2+} rise at the time of excitation after transfer of cells from Mg^{2+} - to a Ca^{2+} -containing medium. The Ca^{2+} channel blocker La^{3+} takes several hours to abolish excitation (Beilby, 1984b; Tsutsui *et al.*, 1986, 1987). These effects can be explained by the need to fill or to empty the Ca^{2+} internal stores.

2. Chloride Channels

Gaffey and Mullins (1958), Mullins (1962), and Hope and Findlay (1964) loaded cells with $^{36}Cl^-$ and found efflux from excited cells 100 times greater ($\sim 1 \times 10^{-6} \text{ mol m}^{-2} \text{ s}^{-1}$) than that in the resting cells. Mailman and Mullins (1966) improved time resolution by using a Ag/AgCl electrode. Later the increased Cl^- efflux at the time of excitation was measured using other methods (Haapnen and Skoglund, 1967; Kikuyama, 1986a,b, 1987; Oda, 1976; for other references see Shimmen *et al.*, 1994). In fact, this seemed to be one of the favorite experiments during the 1960s, 1970s and 1980s. Using the Goldman equation, Wayne (1994) estimates the rise of Cl^- permeability about 100× at the time of the AP.

The experiments with tonoplast-free cells provided a wealth of data, but also some confusion, as under some circumstances, the Ca^{2+} influx seems to be wholly responsible for excitation (see previous section on Ca^{2+}). Shiina and Tazawa (1988), using *Nitellopsis*, measured time-independent increase in Cl^- efflux upon increasing Ca^{2+} in the perfusion medium to pCa 5.4 ($\sim 4.0 \mu\text{M}$). They concluded, that in experiments of Mimura and Tazawa (1983), EGTA concentration in the perfusion medium prevented Ca^{2+} increase and Cl^- channel activation. Mimura and Shimmen (1994), using *Chara*, and Kataev *et al.* (1984), using *Nitellopsis*, found Ca^{2+} -dependent membrane PD depolarization accompanied by transient efflux of Cl^- . The peak membrane PD depolarization saturated at pCa of ~ 4 . The peak Cl^- efflux increased more gradually with Ca^{2+} concentration and saturated at pCa of ~ 3.0 . Kataev

et al. (1984) suggested that Cl^- channels may be inactivated by the continuous exposure to high Ca^{2+} , which might act on the cytoskeleton. They argued that at the time of AP, the exposure to high Ca^{2+} is too short for this inhibition to occur and the Cl^- current is simply inactivated by Ca^{2+} -concentration decrease.

The patch clamp technique was employed to find Cl^- channels that underlie the AP. Several types of Cl^- channels have been observed in charophyte plasmalemma (Coleman, 1986; Laver, 1991; McCulloch *et al.*, 1997), but their properties did not make them obvious candidates for the depolarizing phase of the AP. Okihara *et al.* (1991, 1993) found two types of Cl^- channels in the inside-out patches from the *Chara* plasmalemma. One of these, type A, was quite selective for Cl^- and required 1- μM Ca^{2+} for optimum activation. Higher or lower Ca^{2+} concentration caused channel inactivation. The voltage dependence exhibited inward rectification and greater open probability at PDs above -160 mV.

Thiel and coworkers (Homann and Thiel, 1994; Thiel, 1995; Thiel *et al.*, 1993, 1997) used cell-attached configuration and also observed two types of Cl^- channels with unitary conductances of 15 and 38 pS, respectively, with 100-mM Cl^- in the pipette. The advantage of cell-attached mode was the ability to check whether the cell was undergoing excitation. Both types of channels had a very low open probability in nonexcited cells. The open probability increased transiently at the time of an AP and up to ~ 100 Cl^- channels per patch would activate within 1–2 s. However (see previous section), the patch clamp data did not show depolarization-activated Ca^{2+} channels at the beginning of the AP. Thiel *et al.* (1997) concluded that while the depolarization of the membrane PD favors excitation, it is not sufficient for Cl^- -channel activation. Extracellular Ca^{2+} also favors excitation, but there are no visible patch clamp currents just prior to excitation to document an inflow of Ca^{2+} into the cytoplasm. Thus some cytoplasmic factor, possibly Ca^{2+} released from internal stores, facilitates the Cl^- channel activation. Kikuyama *et al.* (1993) observed sparklike random spots of high Ca^{2+} appearing at the time of AP in *Nitella*, suggesting that the AP is a superposition of local Ca^{2+} increases, that in turn activate spikes of Cl^- current. It was obvious that the channel, which provides the depolarizing phase of the AP, is gated in a different way than the axon Na^+ channel. Thiel and coworkers started to design experiments to reveal the mechanism by which the Ca^{2+} was released from internal stores when the membrane PD was depolarized (see Section III.A).

3. Potassium Channels

The increase of both Cl^- and K^+ effluxes at the time of AP has been measured by many researchers (Haapanen and Skoglund, 1967; Hope and Findlay, 1964; Kikuyama, 1986a, 1987a,b; Kikuyama *et al.*, 1984; Oda, 1975, 1976).

Kikuyama *et al.* (1984) calculated K^+ permeability at the time of *Chara* AP and found no increase compared to that at resting state. They suggested that the K^+ efflux arose from the depolarization of the membrane PD.

In *N. axillaris* (Barry, 1968; Kamitsubo, 1980) and *N. axilliformis* (Shimmen and Tazawa, 1983b), the repolarizing PD often overshot the pre-AP resting level. This behavior became known as “after-hyperpolarization.” This effect only occurred if the initial resting PD was more positive than E_K and was inhibited by K^+ channel blocker tetra ethyl ammonium (TEA). Thus K^+ channel activation was postulated.

Thiel and coworkers (Homann and Thiel, 1994; Thiel, 1995; Thiel *et al.*, 1993, 1997) used *Chara* cell-attached configuration and found K^+ channels with linear conductance of about 40 pS. They showed (by comparing patches in excited cells and cells with depolarized PD) that these channels are activated by depolarization. The channels were identified as the K^+ selective outward rectifier, which is not sensitive to TEA. Beilby and Coster (1979a) found that TEA had no effect on the shape of the AP in *Chara*.

How can we reconcile data from *Chara* and *N. axillaris* and *N. axilliformis*? *Chara* plasmalemma contains large conductance K^+ channels, which are sensitive to TEA (Beilby, 1985). These channels are activated by depolarization and K^+ concentration in the medium above about 1 mM. It is not probable that these channels are activated at the time of the AP, while the cells are in APW (0.1-mM K^+). The large conductance K^+ channels might be faster to activate in *N. axillaris* or *N. axilliformis*, or the outward rectifier has a slow inactivation and sensitivity to TEA.

4. Proton Pump

Kishimoto *et al.* (1985) suggested that the pump conductance decreases and the pump current increases at the time of the AP. Both of these effects follow from the I/V profile of the pump and the depolarization of the membrane PD due to the increased conductances of the Cl^- and K^+ channels. The I/V profile of the pump was obtained by fitting the HGSS model (Hansen *et al.*, 1981) with stoichiometry of $2H^+$ per 1 ATP. Similar interpretation applies for a model with the stoichiometric ratio $1H^+$ per 1 ATP (Beilby, 1984b). Working with cells in K^+ state (in which large conductance K^+ channels dominate the plasmalemma electrical characteristics), Beilby found that the H^+ pump appeared to “switch off” in this state and reactivated slowly as the K^+ channels were closed by decreasing K^+ in the outside medium (Beilby, 1985). It was also found that prolonged voltage clamping to depolarized PDs for 5–10 min resulted in decline of the pump activity (Beilby, unpublished). Although the transient depolarization due to the AP is shorter (~ 5 s), there is still a transient effect on the pump conductance as found by Smith and Beilby (1983). The actual mechanism by which the pump is inhibited is not known.

In the case of the AP, the transient rise of Ca^{2+} in the cytoplasm might inhibit the pump. However, in K^+ state, the streaming rate is fast (indicating low Ca^{2+} in the cytoplasm), but the pump needs many minutes to recover after the K^+ state is terminated by lowering the K^+ concentration (Beilby, 1985).

Employing the AP-clamp (see Section II.A.1), Thiel (1995) selectively inhibited the K^+ or the Cl^- current. To balance the charge lost, the two currents should be symmetrical as functions of time. However, the Cl^- current was not balanced by the K^+ current in the first 2 s of the AP. Later in the AP the K^+ current dominates over the Cl^- current. Thiel *et al.* (1997) suggested the excess of Cl^- current may be balanced by the increase in the pump current.

F. Manipulating Inside and Outside Media

1. Ion Concentrations

Changes of medium Cl^- or Ca^{2+} were used in very early experiments (Findlay, 1962; Findlay and Hope, 1964a,b; Kishimoto, 1964, 1966b) to distinguish which of these ions is responsible for the depolarizing phase of the AP. Hope (1961a) and Findlay (1961, 1962) found that the peak PD of the AP (measured between the vacuole and outside) was a linear function of $\log [\text{Ca}^{2+}]_o$, whereas changes in the $[\text{Cl}^-]_o$ between 0–10 mM had little effect. Kishimoto (1966b), working on *N. axillaris*, found that the N-shaped part of the I/V curve became smaller in high Cl^- and more pronounced in high Ca^{2+} . Beilby and Coster (1979a) observed an increase in the second transient peak of the voltage clamp current near the excitation threshold and a reversal of the prompt sharp peak at very depolarized PDs. None of these results were clear-cut and it was the measurements of the Cl^- outflow that identified Cl^- as the depolarizing ion (see Section II.E.2). Now we interpret the effect of high medium Ca^{2+} as increasing the amount of Ca^{2+} in the internal stores and activating more Cl^- channels upon release (Plieth *et al.*, 1998). Shiina and Tazawa (1987) repeated the changes of medium Cl^- or Ca^{2+} to study excitation in tonoplast-free cells and concluded that Ca^{2+} is the main depolarizing ion in this case (see also Section II.D).

An increase in K^+ concentration of the medium above 1 mM opens the large conductance K^+ channels (Beilby, 1985; Smith and Walker, 1981). Cells in K^+ state can be excitable if the resting PD is not too depolarized (Beilby, 1985).

Different divalent ions invoke a range of responses in various charophytes. In *C. corallina* replacing the Ca^{2+} in the APW (artificial pond water) by 5-mM Sr^{2+} reversibly decreased the tonoplast AP after 16 h (Kikuyama, 1986b).

The plasmalemma AP exhibited a wide flat peak in Sr^{2+} APW (Findlay and Hope, 1964a). The streaming stopped at the time of excitation. Using 5-mM Ba^{2+} , Mg^{2+} , or Mn^{2+} reversibly abolished excitation at both membranes. Beilby (1984a) observed that the excitation clamp currents were abolished in Mg^{2+} APW, but not the streaming stoppage. Barry (1968) worked with *N. axillaris* and found that the cells produced APs in 6 mM of CaCl_2 , SrCl_2 , MgCl_2 , and BaCl_2 . Streaming stoppage was observed in CaCl_2 and SrCl_2 only. Cells were not excitable in MnCl_2 or ZnCl_2 . The shape of the AP became progressively more rectangular in Sr^{2+} , Mg^{2+} , and Ba^{2+} . Kikuyama (1986b) used *N. axilliformis* and this charophyte exhibited APs in Ba^{2+} , Mg^{2+} , or Mn^{2+} APW, but the tonoplast AP was reversibly abolished after repeated stimulation. The streaming did not stop. Injection of Ca^{2+} into the cytoplasm induced an AP at both membranes in *Chara* and *N. axilliformis*, whereas injection of Cl^- had no effect. Kikuyama and Tazawa (1976) perfused the vacuole of *N. pulchella* and found that the amplitude and direction of the tonoplast AP was strongly dependent on $[\text{Cl}^-]_{\text{vac}}$ (Fig. 7A).

Beilby (1981) diminished the cytoplasmic Cl^- concentration by Cl^- starvation. The transient voltage clamp currents decreased as a result. Shimmen and Tazawa (1980), using tonoplast-free *Chara*, varied internal K^+ and Cl^- concentrations in tonoplast-free cells. They found that the duration of the AP is strongly dependent on intracellular K^+ concentration. At 100-mM K^+ , the AP resembles that of intact cells (Fig. 5B). Na^+ could substitute for K^+ , but the effect was weaker. AP occurred with very low Cl^- inside the cell or with EGTA, which prevented Ca^{2+} concentration inside the cell to rise. The Japanese researchers assumed the under some circumstances, Ca^{2+} inflow alone produced the depolarizing phase of the AP (see Section II.D). At the other extreme, if the internal concentration of Cl^- increased above 29 mM, the cells lost excitability. The result suggests a low concentration of Cl^- in the cytoplasm of intact cells. Coster (1966) measured cytoplasmic Cl^- in *Chara* as 10 mM.

2. pH

The pH of “normal” charophyte medium, such as artificial pond water (APW), is usually between pH 7.0 and 7.5. Beilby (1982) and Beilby and Bisson (1992) studied excitation in *Chara* in a large range of medium pH from 4.5 to 11.5. The pH 4.5 is the lower limit for excitability: the resting PD approached—100 mV and excitation disappeared after about 60 min at this pH. The excitation currents appeared at more positive voltage clamp levels and with longer initial delay than at higher pH. The time scale was longer. The differences were much less pronounced at more depolarized levels (at and above -35 mV). Consistently, the AP form was also stretched with time.

Above pH 10, *Chara* cells enter the H^+/OH^- state (Bisson and Walker, 1980), in which H^+/OH^- channels dominate the plasmalemma conductance. The form of the AP was conserved at high pH. Under voltage clamp conditions, some differences in the excitation transients emerged. Although the currents at very depolarized PD levels did not show large effects, the currents near the threshold appeared after longer delays and with slower rise and fall times. The changes developed over many minutes.

Tazawa and Shimmen (1982) explored the variation of the internal pH in tonoplast-free cells. *Chara* remained excitable between internal pH limits from pH 6.0 to 9.0, whereas *Nitellopsis* exhibited a narrower range between pH 6.6 and 7.9. The peak PD of the AP was almost independent of the internal pH.

As both internal and external pH deviations from “normal” values caused depolarization of the membrane resting PD, the changes in excitation might stem from this rather than the pH change itself.

3. Inhibitors, Antagonists, and Agonists

Tsutsui *et al.* (1986, 1987a) tested effects of Ca^{2+} channel blockers, La^{3+} and verapamil, Ca^{2+} chelating agent ethylene glycol bis (beta-aminoethyl ether)-*N*, *N*, *N'*, *N'*-tetraacetic acid (EGTA), and calmodulin antagonists W-7 and trifluoperazine (TFP) on the AP and the current-voltage (I/V) profiles of intact cells of *C. corallina*. In small concentrations of 10- μM LaCl_3 and 100- μM verapamil, the resting PD depolarized, the amplitude of the AP decreased irreversibly, and the streaming did not stop at the time of excitation. At 100- μM TFP, the resting PD depolarized and the AP lost amplitude (AP peak at more negative PD) with longer time scale. The streaming did not stop. A similar effect was observed with 40- μM W-7. Tsutsui *et al.* (1987b) employed the ramp voltage clamp command and found that 20- μM LaCl_3 removed the excitable N-shaped part of the I/V profile, 75- μM *N*, *N'*-dicyclohexylcarbodiimide (DCCD) affected the proton pump, without disturbing the excitation channels. 0.5-mM EGTA reversibly depolarized the resting PD and removed excitability. The calmodulin antagonists, TFP (10 μM) and W-7 (20 μM), depolarized membrane PD, reduced excitation, and shifted it to more positive PDs. The effects were partially reversible. Beilby and MacRobbie (1984b) exposed *Chara* cells to 5 μM of TFP. They also found depolarization and slowing of the excitation transients. However, in their experiments the peak of the AP became positive and cells exhibited spontaneous APs with concurrent slowing of cytoplasmic streaming. Beilby (1984b) found that 100 μM LaCl_3 irreversibly removed excitation and the cells could then be returned to APW for collecting I/V profiles over wide PD window.

The effect of putative Ca^{2+} blockers was explicable in terms of no Ca^{2+} inflow, either directly at the time of excitation or to replenish the internal stores. Calmodulin binds Ca^{2+} and the complex then influences ATPases and protein kinases in animal cells (Cheung, 1980). The antagonists TFP and W-7 interfere with these functions. However, the effects of these substances on excitation are not easily explicable in terms of any model. Perhaps, the most significant correlation is that 40- μM W-7, TFP, or CPZ abolished the patch-clamp currents of the Ca^{2+} -dependent Cl^- channel (Okihara *et al.*, 1991).

Lunevsky *et al.* (1983) used Cl^- channel blocker ethacrynic acid to reveal a prompt transient at the beginning of excitation clamp currents across plasmalemma of *Nitellopsis obtusa* (Fig. 7B). They were able to show that this current component responded not only to Ca^{2+} , but also to a range of divalent and monovalent cation concentration changes. They suggested that the underlying channel is a cation channel, activated by depolarization, which passes Ca^{2+} at the time of excitation.

As mentioned earlier (Section II.E.3), "after-hyperpolarization" was observed after the AP in *N. axillaris* (Barry, 1968; Kamitsubo, 1980), *N. axilliformis* (Shimmen and Tazawa, 1983b), and *N. flexilis* (Belton and Van Nettan, 1971). In the first two experimental systems, the effect was abolished by K^+ channel blocker TEA. In *N. flexilis* the after-hyperpolarization was abolished by procaine hydrochloride (which reduced K^+ and Na^+ current activation in animal AP). The AP duration was not affected. The exposure to TEA and BaCl_2 , on the other hand, did prolong the AP duration.

Thiel (1995) and Thiel *et al.* (1997) employed the AP clamp on intact *Chara* cells while blocking the Cl^- current with niflumic acid and/or the K^+ current with Ba^{2+} . They were able to resolve the time-dependence of these currents at the time of the excitation.

Shiina and Tazawa (1987) employed ramp voltage clamp command to study excitability of tonoplast-free cells of *Nitellopsis obtusa*. Cl^- channel blocker 4, 4'-di-isothiocyanostil-bene-2, 2'-disulphonate (DIDS) did not suppress the inward excitation current component of the I/V curve, whereas Ca^{2+} channel blockers La^{3+} and nifedipine removed it irreversibly. Ca^{2+} channel agonist BAY K8644 enhanced excitation. The authors concluded that excitability in tonoplast-free cells is based on activation of Ca^{2+} channels alone.

Shiina *et al.* (1988) suggested that the Ca^{2+} channel is inhibited by protein phosphorylation and activated by protein dephosphorylation. Agents enhancing dephosphorylation, protein kinase inhibitor, or phosphoprotein phosphatase-1, -2A, were perfused into tonoplast-free cells of *Nitellopsis obtusa*, causing the plasma membrane to depolarize and become more conductive. The reverse effect was obtained by agents enhancing phosphorylation, phosphoprotein phosphatase inhibitor I, or alpha-naphthylphosphate. These results were challenged by Zherelova (1989), who found that Ca^{2+} channels

were activated by phosphorylation via protein kinase C. Polymyxin B, which inhibits protein kinase C, blocked the Ca^{2+} current in *N. syncarpa*.

G. Effect of Temperature

Kishimoto (1972) changed medium temperature from 4.5°C to 30°C, while he applied ramp voltage clamp command to cells of *C. australis*. He found that the resting PD became slightly more positive as temperature decreased. The amplitude of negative current decreased with temperature, while the threshold PD became more positive. Excitation disappeared altogether at about 8°C.

Blatt (1974) changed medium temperature between 3°C and 28°C and observed the resting PD and the AP in *N. flexillis*. Both the resting PD and the AP amplitude declined with decreasing temperature. The threshold became more positive and the refractory period was longer at lower temperature. The rise and decay times increased two orders of magnitude with falling temperature, but the form of the AP did not change. Arrhenius plot of the rise and fall times showed a relatively sharp break at 13.5°C. The author suggested that the discontinuity might be related to a “phase change” of the membrane.

Beilby and Coster (1976) studied the temperature dependence of excitation of *C. corallina* (Fig. 3). The duration both of the vacuolar AP and the vacuolar excitation clamp currents increased with decreasing temperature from ~1 s at 40°C to ~30 s at 3.5°C. The peak PD of the AP did not change greatly with temperature. The resting PD depolarized by about 70 mV between 20°C and 5°C. Consequently, the amplitude of the AP decreased with temperature. Similar to Blatt (1974), the authors found that the AP form did not change. The change of duration was quantified by taking the AP or clamp current at 20°C as standard and finding a factor F by which the transients at different temperature have to be shrunk or expanded. The Arrhenius plot of F was curved with no obvious breaks. Activation enthalpies varied from ~7 kJ/mol for temperatures above 20°C to ~350 kJ/mol for temperature less than 7°C. The authors suggested that as temperature increased, a smaller degree of dehydration was necessary for the ions to permeate through the channels that underlie excitation.

H. Signal Propagation

Similarly to the nerve AP, the plant AP propagates along the cell. The conduction velocity in moist air of 0.3–2.3 cm/s was measured in *N. mucronata* (Umrath, 1933), 1.1–2.1 cm/s in *N. translucens* (Auger, 1933), 4.4 cm/s in

N. flexilis, and 1.4 cm/s in *C. braunii* (Sibaoka, 1958). Tabata and Sibaoka (1987) found that the speed of AP propagation in *C. braunii* increased from 0.21 cm/s in moist air to 1.5 cm/s in APW. The AP propagated at almost constant velocity along the cell, but near the end of the cell the velocity in APW increased. The increase was of the right order of magnitude to that predicted by conduction velocity equations (Hodgkin, 1954). The AP in charophytes can be transmitted from cell to cell (Sibaoka and Tabata, 1981; Tabata, 1990).

I. Capacitance at the Time of Excitation

The capacitance of many animal and plant membranes has been estimated as 0.01 F/m^2 (e.g., see Cole, 1970). However, Kishimoto (1972) superimposed small sinusoidal current on the voltage clamp command and measured the phase angle of the resulting clamp current. He concluded that the capacitance increased at the peak of the current transient. Beilby and Beilby (1983) utilized greater computing power to calculate capacitance at the time of voltage clamp to excitable levels, finding transient decrease followed by an increase. The full meaning of these measurements still awaits interpretation.

J. Early Models

1. States of Plasmalemma of Tonoplast-Free Cells

Shimmen *et al.* (1976) explained the behavior of the tonoplast-free cells using the Tasaki (1968) two-state hypothesis, which proposed that negatively charged sites on the outer membrane surface are occupied by divalent cations in resting state and by monovalent cations in excited state. The Japanese researchers viewed the depolarized level as an “excited” level (see Fig. 8A). The excited level was further split into +ATP and -ATP.

This data may be interpreted another way. In tonoplast-free cells, the APs and the transient-clamp currents inactivated very slowly (Fig. 6A and B). However, the excitation-clamp currents in tonoplast-free cells did diminish with time (Beilby *et al.*, 1993). Consequently, although the AP may be prolonged, the excitation state is never stable in low medium K^+ . In high medium K^+ the membrane appeared to have two stable states: depolarized and hyperpolarized. The increase of medium K^+ together with depolarization opens the large conductance K^+ channels (sometime called maxi K^+) at the plasmalemma. These channels become the dominant membrane conductance and the membrane behaves as a K^+ electrode (K^+ state). The maxi K^+ channels can be activated in the tonoplast-free *Chara* cells (Smith, 1984; Smith and Walker, 1981). These channels are closed by increase in medium Ca^{2+} and hyperpolarization of the membrane PD (Beilby, 1985, 1986a,b;

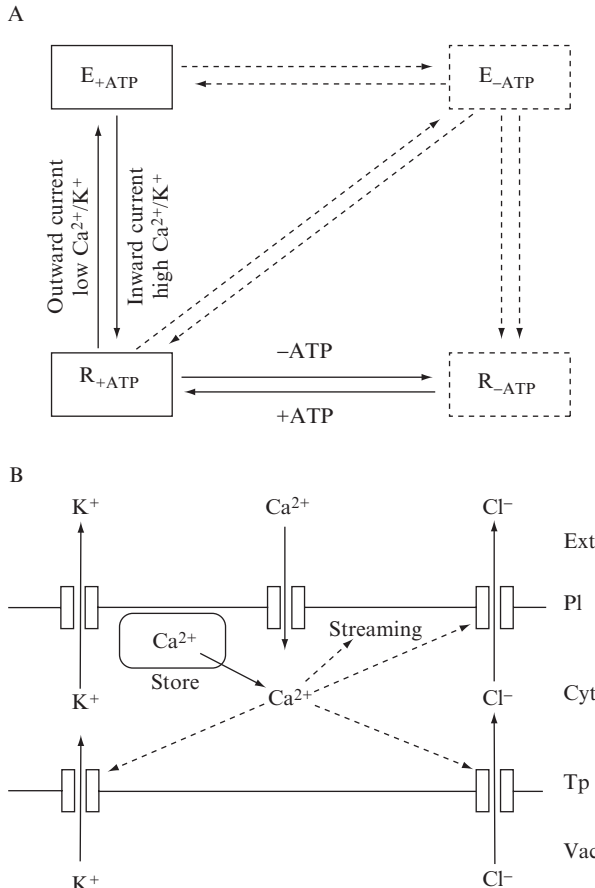


FIG. 8 Models of excitation and membrane states. (A) Four stable states of *Chara* plasmalemma in tonoplast free cells. R and E refer to resting and excited states, respectively (Tazawa and Shimmen, 1980). (B) Ionic events occurring during a charophyte AP. Solid line arrows show net fluxes of ions, dashed line arrows indicate Ca^{2+} activation of other channels (Shimmen *et al.*, 1994).

Smith, 1984). Furthermore, the I/V characteristics of the membrane in K^+ state display region of negative conductance: N-shaped curve, which is similar to that of excitation (e.g., Fig. 5A). The negative conductance is not an exclusive signature of excitation: it arises with any channel with strong PD dependence if the membrane PD is swept through the activation PD of the channel (Beilby, 1986b). Consequently, the steady “excited state” is probably K^+ state. Tazawa and Shimmen (1980) found that the excitability is lost after about 10 min of perfusion with HK medium to remove ATP. My interpretation is that after the Ca^{2+} in the internal store becomes depleted, ATP is necessary

to replenish it. Thus no excitation occurs if no ATP is available in the cytoplasm and consequently, there is no $-ATP$ -excited state.

2. Ionic Events at the Time of Excitation

By the 1990s it was obvious that the initial response to depolarization past the threshold PD is inflow of Ca^{2+} from the outside medium through cation channels (which are probably not very selective). The increase of Ca^{2+} in the cytoplasm induces Ca^{2+} release from internal stores close to the inner face of the plasmalemma (Fig. 8B). Once the Ca^{2+} concentration reaches a certain level, the Cl^- channels are activated on both plasmalemma and tonoplast, producing a flow of anions out of the cell and making membrane PD more positive. The depolarization activates the outward rectifier channels, causing K^+ outflow. At the same time the Ca^{2+} level in the cytoplasm starts to drop and the Cl^- channels inactivate. The reason for the Ca^{2+} level dropping has not been adequately addressed, but emptying of the internal stores was suggested. While the Cl^- channels on both plasmalemma and tonoplast are Ca^{2+} activated, it is not clear whether the tonoplast K^+ channels need cytoplasmic Ca^{2+} increase. The patch clamp studies on cytoplasmic droplets of *Chara* suggest Ca^{2+} involvement (Laver and Walker, 1991), although the analysis of the hypotonic effect in *Lamprothamnium* revealed increase in K^+ conductance at both membranes in lanthanised cells, where the streaming did not stop.

3. Adaptation of Hodgkin-Huxley Model

The equations describing the Na^+ transient in the nerve (Hodgkin and Huxley, 1952a) have been adapted to describe the Cl^- transient and the putative Ca^{2+} transient (Beilby and Coster, 1979b,c).

$$I_{Cl^-} = g_{Cl^-} (E_m - E_{Cl^-}) \quad (1)$$

where I_{Cl^-} is chloride current, g_{Cl^-} is the chloride conductance, E_m is the membrane PD, and E_{Cl^-} is the equilibrium potential for Cl^- .

$$g_{Cl^-} = m^3 h g_{max} \quad (2)$$

where g_{max} is the maximum conductance, m and h are activation and inactivation parameters, respectively.

$$m = m_\infty - (m_\infty - m_0) \exp[(\delta_{Cl^-} - t)/\tau_m] \quad (3)$$

$$h = h_\infty - (h_\infty - h_0) \exp[(\delta_{Cl^-} - t)/\tau_h] \quad (4)$$

where t is time and δ_{Cl^-} is a delay before excitation begins. Delays were later found in the nerve by Keynes and Rojas (1976). Equations 3 and 4 describe how the m and h parameters evolve from their resting values m_0 and h_0 , to the long time values m_∞ and h_∞ with time constants τ_m and τ_h , respectively.

Similar set of equations was used for the second transient. As the membrane PD depolarizes, the outward rectifier is activated and K^+ flows out restoring the resting PD (together with Cl^- inactivation). The PD-dependent activation of the outward rectifier is much faster than the other currents and is taken as “instantaneous.”

The AP can be reconstructed:

$$\frac{dV}{dt} = -\frac{1}{C} [g_{Cl^-}(E_m - E_{Cl^-}) + g_{Ca^{++}}(E_m - E_{Ca^{++}}) + I_{ss}] \quad (5)$$

where I_{ss} is “steady stream current,” which was measured at each PD level.

The AP shape is well approximated by Equation 5. A similar approach was taken by Hirono and Mitsui (1981) in describing excitation in single membrane constructs of *N. axilliformis*. The resting PD restoring current appears to activate more gradually in this charophyte and was fitted with an equation similar to that used in the HH for the nerve.

$$I_K = g_K^* n^4 (V - V_K) \quad (6)$$

$$n = n_\infty - (n_\infty - n_0) \exp[(\delta_K - t)/\tau_n] \quad (7)$$

where g_K^* is the maximum K^+ conductance, V_K is the equilibrium PD for K^+ , and n is the activation parameter.

The fit of the HH equations has been very useful to quantify many aspects of excitation in plants. For instance, Beilby and Coster (1979c) analyzed the temperature dependence of the time constants obtaining activation enthalpies of ~ 60 kJ/mol for activation process and ~ 40 kJ/mol for the inactivation process. They found that the enthalpies are independent of membrane PD and do not involve movement of charged moieties normal to the membrane. The delays in excitation indicate existence of intermediate step(s) before excitation channels can be activated. These ideas are compatible with data on the cytoplasmic second messenger taking part in the plant AP and the new models necessary to describe them.

III. New Approaches in the New Century

A. IP_3 (Inositol 1,4,5, -triphosphate) and Ca^{2+} from Internal Stores

The experiments with Mn^{2+} as a quencher of fura-2 fluorescence (Plieth *et al.*, 1998) confirmed the importance of internal stores as the main source of Ca^{2+} at the time of the AP (see Section II.E.1). Further, the elevation of inositol-1,4,5-triphosphate (IP_3) in the cytoplasm was able to elicit APs

(Thiel *et al.*, 1990). The enzyme phospholipase C (PLC) is responsible for mobilizing IP₃ from its membrane-bound precursor phosphatidyl inositol 4,5-biphosphate (PIP₂). Inhibitors of PLC, Neomycin, and U73122 inhibited excitation in *Chara* (Biskup *et al.*, 1999).

The Ca²⁺ concentration in the cytoplasm was monitored, while the depolarizing pulses of varying height and width were applied. A sharp threshold existed in the Ca²⁺ concentration rise with respect to the strength/duration of the stimulus (Wacke and Thiel, 2001). The response in the Ca²⁺ rise was all or none. If two subthreshold pulses were applied in a certain regime, the full response was also obtained. The experimental results supported the hypothesis that a second messenger, such as IP₃, is produced by the stimulating voltage step and has to reach a critical concentration to liberate Ca²⁺ from internal stores. The double pulse experiments provided information about the dynamics of IP₃ formation and decay into IP₂, as well as refilling of the PIP₂ pool. The double subthreshold pulse produced a response only if the interval between pulses was shorter than ~3 s. This time was within the lifetime of IP₃ in the cytoplasmic compartment and the IP₃ produced by the first pulse was added to the IP₃ produced by the second pulse, reaching the threshold concentration. If the pulses come too close together (less than ~0.3 s), the PIP₂ pool has not been replenished and no further IP₃ was produced.

Wacke *et al.* (2003) borrowed another animal model (Othmer, 1997) to set up a quantitative description of *Chara* AP mediated by IP₃ activated Ca²⁺ channels and Ca²⁺ pumps on the endomembranes of internal stores, such as the ER. Othmer (1997) described the IP₃-sensitive Ca²⁺ channels as having four states: (1) unbound, (2) bound to IP₃, (3) bound to IP₃ and activating Ca²⁺ molecule, and (4) bound to IP₃ and to a second inactivating Ca²⁺ molecule. The channel is only conductive in state 3 and as Ca²⁺ concentration in the cytoplasm rises, the channels undergo transition into inactivated state 4. For the channels to be activated by IP₃ again, the transition into state 1 is necessary. Using sophisticated periodic stimulation technique, Wacke *et al.* (2003) established that the long lifetime of state 4 was responsible for the refractory period. In the simulation using many parameter values from Othmer's animal model, the refractory period was about 30 s. The model also confirmed the previous assumptions (Wacke and Thiel, 2001), that the all-or-none response and the steep dependence of Ca²⁺ response on strength/duration of the stimulatory pulse arises from the dynamics of the model variables.

Although the Wacke *et al.* (2003) modeling of the AP looks very encouraging, Tazawa and Kikuyama (2003) failed to duplicate some of the preceding experiments in *Chara*. Their injection of IP₃ into cytoplasm did not produce Ca²⁺ release; and inhibitors of PLC, U73122, and neomycin, did not affect generation of the AP. An inhibitor of the IP₃ receptor, 2APB, did make

cells inexcitable, but the same effect was observed in tonoplast-free cells, in which the AP transient is thought to be carried by inflow of Ca^{2+} from the outside. The authors suggested, that the inhibitor affects the plasma membrane rather than Ca^{2+} channels on the endomembranes. More experiments will be necessary to understand why the different results were obtained by the German and Japanese groups.

B. Involvement of AP in Wound Signaling

Wounding induces a range of responses in plants. One of the earliest reactions is localized depolarization of membrane PD in cells close to the site of damage. There are also APs and variation potentials that propagate away from the injury site. The experiments with complex tissues of higher plants are too difficult to analyze. Consequently, Shimmen (2001, 2002) employed a much simpler two *Chara* cell system, in which one cell (victim cell) was cut off and the reaction of the other cell (receptor cell) was measured. The receptor cell generated four kinds of depolarization: (1) rapid component, (2) slow and long-lasting component, (3) action potential, and (4) small spikes. The first two responses were observed in most experiments and their origin is assumed to be at the nodal end. The APs and the small spikes were not always present. The AP was generated on the flank of the receptor cell near the cut end and propagated to the far end.

C. AP and Turgor Regulation

Beilby and Shepherd (2006) measured the I/V characteristics of the Ca^{2+} -activated Cl^- channels at the time of hypotonic regulation in *Lamprothamnium succinctum*. They suggest that the same Cl^- channels participate in the hypotonic effect and in the excitation. However, the Ca^{2+} increase at the time of hypotonic effect lasts for more than 10 min (Okazaki *et al.*, 2002). This is far too long for the dynamics of IP_3 -activated Ca^{2+} channels, which close within 15 s (Thiel *et al.*, 1997). Experiments of Kikuyama and Tazawa (2001) suggest that the Ca^{2+} -containing cytoplasmic organelles become mechanically distorted by the hypotonic stress and that there are stretch-activated channels that allow Ca^{2+} to flow into the cytoplasm. This might be an alternative mode of cytoplasmic Ca^{2+} increase, independent of the IP_3 signal cascade.

Similarly to the AP, the fast hypotonic regulation involves outflow of Cl^- and K^+ . In *Lamprothamnium* the Ca^{2+} -activated Cl^- channels open first, followed by the K^+ channels. In this case the large conductance K^+ channels, rather than the outward rectifier, are involved (Beilby and Shepherd, 1996).

In *C. longifolia*, the sequence of channel activation is reversed (Stento *et al.*, 2000). As the loss of KCl is the prime objective of the hypotonic regulation, the sequence of channel activation is not important.

Hoffmann and Bisson (1990) observed APs in *C. longifolia* upon exposure to hypertonic medium. This was not observed at the time of hypertonic regulation of *L. succinctum* (Beilby and Shepherd, 2001). Although *C. longifolia* is able to regulate its turgor and survive in a range of salinities, there is a similarity to salt-sensitive charophytes, which respond with APs when faced with increase in medium salinity (Kishimoto, 1966b; Shepherd *et al.*, in preparation).

IV. Summary

My scientific career started by investigating the charophyte AP (Beilby and Coster, 1976, 1979a,b,c). I have moved on to other transporters in charophyte and other giant-celled organisms, but I kept up my interest in the AP research. So, it was a great pleasure for me to refresh in my memory all the elegant experiments investigating excitation over many years. I hope that the readers will get the same enjoyment, following the intricate story of the charophyte AP. I have described the research up to the mid-1990s in greater detail, as the papers are not available on the World Wide Web and are likely to be less accessible to young researchers.

The late-1990s saw a paradigm shift for the charophyte AP: from PD-activated plasmalemma channel mechanisms, described so well by HH equations, to a combination of several chemical reactions and second messenger-activated channel, liberating Ca^{2+} from internal stores (Biskup *et al.*, 1999; Wacke and Thiel, 2001; Wacke *et al.*, 2003). IP_3 can diffuse freely in the cytoplasm, whereas Ca^{2+} is not mobile (Trewavas, 1999). It is thought that the involvement of IP_3 produces Ca^{2+} waves in many types of cells and enables the AP to travel along the cell. The dynamics of IP_3 production and decay can account for the shape of the AP (Fig. 9), delays between the stimulus and excitation onset, the multiple peaks in the clamp current and for the refractory period. New questions that we have to ask include how is IP_3 release triggered by a threshold PD change across plasmalemma? What can we learn about the Ca^{2+} pumps that return the cytoplasmic Ca^{2+} to a low level after excitation? How is accommodation produced by the IP_3 model? Why do salt-sensitive charophytes, exposed to concentrated saline media, exhibit repetitive firing? The removal of the tonoplast greatly changes the AP form, removes refractory period, but the threshold behavior is retained. The excitation currents are much slower to turn off. Is IP_3 still involved? Can Ca^{2+} diffuse in tonoplast free cells? What happens to ER in these cells? Clearly, the charophyte cells are an

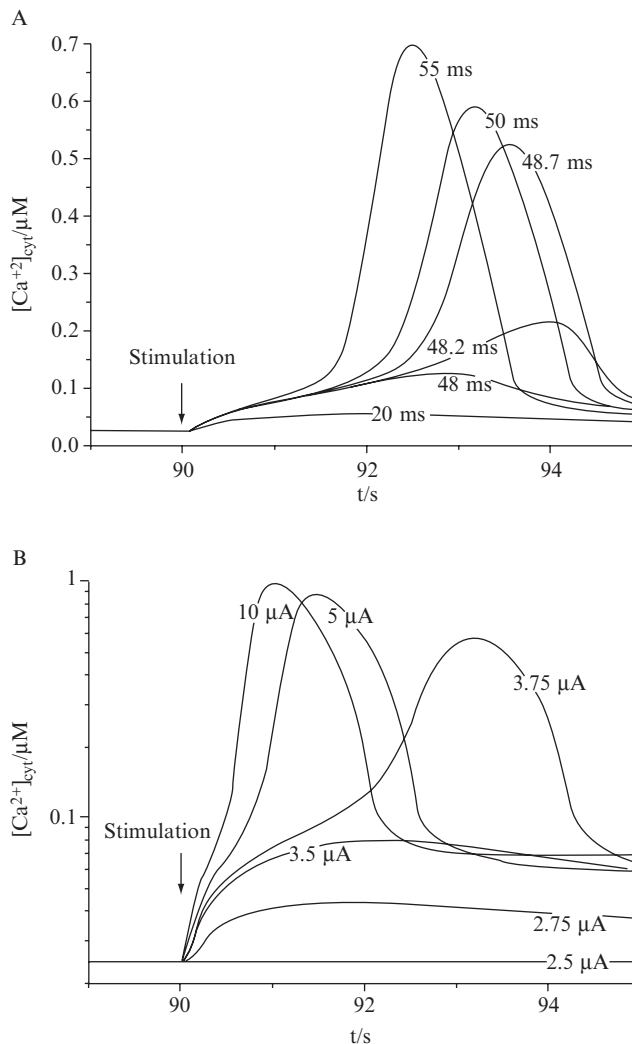


FIG. 9 Simulated transient Ca^{2+} concentration rise as a result of IP_3 -activated endomembrane Ca^{2+} channels. (A) Effect of pulse duration. (B) Effect of pulse strength (Wacke *et al.*, 2003).

excellent system for this research. Cell perfusion combined with inhibitors of IP_3 production and decay, fluorescence microscopy, and electrophysiology will lead us to the understanding of the synergy of structural elements, biochemical reactions, and ion flows that produce the plant AP.

Acknowledgments

Dedicated to G. P. Findlay, whose work continues to provide me with a lot of inspiration.

REFERENCES

Auger, D. (1933). Contribution à l'étude de la propagation de la variation électrique chez les Characees. *Comp. Rend. Soc. Biol.* **113**, 1437–1440.

Barry, W. H. (1968). Coupling of excitation and cessation of cyclosis in *Nitella*: Role of divalent cations. *J. Cell. Physiol.* **72**, 153–159.

Beilby, M. J. (1981). Excitation-revealed changes in cytoplasmic Cl^- concentration in “ Cl^- -starved” *Chara* cells. *J. Membr. Biol.* **62**, 207–218.

Beilby, M. J. (1982). Cl^- channels in *Chara*. *Phil. Trans. R. Soc. Lond. B* **299**, 435–445.

Beilby, M. J. (1984a). Calcium and plant action potentials. *Plant Cell Environ.* **7**, 415–421.

Beilby, M. J. (1984b). Current-voltage characteristics of the proton pump at *Chara* plasmalemma: I. pH dependence. *J. Membr. Biol.* **81**, 113–125.

Beilby, M. J. (1985). Potassium channels at *Chara* plasmalemma. *J. Exp. Bot.* **36**, 228–239.

Beilby, M. J. (1986a). Potassium channels and different states of *Chara* plasmalemma. *J. Membr. Biol.* **89**, 241–249.

Beilby, M. J. (1986b). Factors controlling the K^+ conductance in *Chara*. *J. Membr. Biol.* **93**, 187–193.

Beilby, M. J. (1989). Electrophysiology of giant algal cells. *Methods in Enzymology* **174**, 403–443.

Beilby, M. J., and Beilby, B. N. (1983). Potential dependence of the admittance of *Chara* plasmalemma. *J. Membr. Biol.* **74**, 229–245.

Beilby, M. J., and Bisson, M. A. (1992). *Chara* plasmalemma at high pH: Voltage dependence of the conductance at rest and during excitation. *J. Membr. Biol.* **125**, 25–39.

Beilby, M. J., and Coster, H. G. L. (1976). The action potential in *Chara corallina*: Effect of temperature. *Aust. J. Plant Physiol.* **3**, 275–289.

Beilby, M. J., and Coster, H. G. L. (1979a). The action potential in *Chara corallina*: II. Two activation-inactivation transients in voltage clamps of the plasmalemma. *Aust. J. Plant Physiol.* **6**, 323–335.

Beilby, M. J., and Coster, H. G. L. (1979b). The action potential in *Chara corallina*: III. The Hodgkin-Huxley parameters for the plasmalemma. *Aust. J. Plant Physiol.* **6**, 337–353.

Beilby, M. J., and Coster, H. G. L. (1979c). The action potential in *Chara corallina*: IV. Activation enthalpies of the Hodgkin-Huxley gates. *Aust. J. Plant Physiol.* **6**, 355–365.

Beilby, M. J., and MacRobbie, E. A. C. (1984). Is calmodulin involved in electrophysiology of *Chara corallina*? *J. Exp. Bot.* **35**, 568–580.

Beilby, M. J., and Shepherd, V. A. (1989). Cytoplasm-enriched fragments of *Chara*: Structure and electrophysiology. *Protoplasma* **148**, 150–163.

Beilby, M. J. (1990). Current-voltage curves for plant membrane studies: A critical analysis of the method. *J. Exp. Bot.* **41**, 165–182.

Beilby, M. J., and Shepherd, V. A. (1996). Turgor regulation in *Lamprothamnium papulosum*: I. I/V analysis and pharmacological dissection of the hypotonic effect. salt-tolerant charophyte *Lamprothamnium*. *Plant Cell Environ.* **19**, 837–847.

Beilby, M. J., Cherry, C. A., and Shepherd, V. A. (1999). Dual turgor regulation response to hypotonic stress in *Lamprothamnium papulosum*. *Plant Cell Environ.* **22**, 347–360.

Beilby, M. J., and Shepherd, V. A. (2001). Modeling the current-voltage characteristics of charophyte membranes: II. The effect of salinity on membranes of *Lamprothamnium papulosum*. *J. Membrane Biol.* **181**, 77–89.

Beilby, M. J., and Shepherd, V. A. (2006). The characteristics of Ca^{2+} -activated Cl^- channels of the salt-tolerant charophyte *Lamprothamnium*. *Plant Cell Environ.* **29**, 764–777.

Beilby, M. J., Mimura, T., and Shimmen, T. (1993). The proton pump, high pH channels, and excitation: Voltage clamp studies of intact and perfused cells of *Nitellopsis obtusa*. *Protoplasma* **175**, 144–152.

Belton, P., and Van Netten, C. (1971). The effects of pharmacological agents on the electrical responses of cells of *Nitella flexilis*. *Can. J. Physiol. Pharmacol.* **49**, 824–832.

Biskup, B., Gradmann, D., and Thiel, G. (1999). Calcium release from IP_3 -sensitive stores initiates action potential in *Chara*. *FEBS Letters* **453**, 72–76.

Bisson, M. A., and Walker, N. A. (1980). The *Chara* plasmalemma at high pH: Electrophysiological measurements show rapid specific passive uniport of H^+ or OH^- . *J. Membr. Biol.* **56**, 1–7.

Blatt, F. J. (1974). Temperature dependence of the action potential in *Nitella flexilis*. *Biochim. Biophys. Acta* **339**, 382–389.

Cheung, W. Y. (1980). Calmodulin plays a pivotal role in cellular regulation. *Science* **207**, 19–27.

Cole, K. S. (1968). "Membranes, Ions, Impulses." University of California Press, Berkeley.

Cole, K. S. (1970). Dielectric properties of living membranes. In "Physical principles of biological membranes" (J. Snell, G. Wolken, Iverson, and J. Lam, Eds.), Proceedings of the Coral Gables Conference on Physical Principles of Biological Membranes, pp. 1–15. Gordon and Breach, New York.

Coleman, H. A. (1986). Chloride currents in *Chara*—a patch clamp study. *J. Membr. Biol.* **93**, 55–61.

Coster, H. G. L. (1966). Chloride in cells of *Chara australis*. *Aust. J. Biol. Sci.* **19**, 545–554.

Coster, H. G. L., George, E. P., and Rendle, V. (1974). Potential developed at a solution–cytoplasm interface in *Chara corallina* during rest and excitation. *Aust. J. Plant. Physiol.* **1**, 459–471.

Davies, E. (1987). Action potentials as multifunctional signals in plants: A unifying hypothesis to explain apparently disparate wound responses. *Plant Cell Environ.* **10**, 623–631.

Findlay, G. P. (1959). Studies of action potentials in the vacuole and cytoplasm of *Nitella*. *Australian J. Biol. Sci.* **12**, 412–426.

Findlay, G. P. (1961). Voltage clamp experiments with *Nitella*. *Nature (London)* **191**, 812–814.

Findlay, G. P. (1962). Calcium ions and the action potential in *Nitella*. *Aust. J. Biol. Sci.* **15**, 69–82.

Findlay, G. P. (1970). Membrane electrical behaviour in *Nitellopsis obtusa*. *Aust. J. Biol. Sci.* **23**, 1033–1045.

Findlay, G. P., and Hope, A. B. (1964a). Ionic relations of cells of *Chara australis*: VII. The separate electrical characteristics of the plasmalemma and tonoplast. *Aust. J. Biol. Sci.* **17**, 62–77.

Findlay, G. P., and Hope, A. B. (1964b). Ionic relations of cells of *Chara australis*. VIII. Membrane currents during a voltage clamp. *Aust. J. Biol. Sci.* **17**, 388–399.

Findlay, G. P., and Hope, A. B. (1964c). Ionic relations of cells of *Chara australis*: IX. Analysis of transient membrane currents. *Aust. J. Biol. Sci.* **17**, 400–411.

Findlay, G. P., and Hope, A. B. (1976). Electrical properties of plant cells: Methods and Findings. In "Encyclopedia of Plant Physiology, Transport in Plants II" (U. Luttge and M. G. Pitman, Eds.). Volume 2, Part A. Springer-Verlag, Berlin, Heidelberg, New York.

Fujita, M., and Mizuguchi, K. (1955). Excitation in *Nitella*, especially in relation to electric stimulation. *Cytologia (Tokyo)* **21**, 135–145.

Gaffey, C. T., and Mullins, L. J. (1958). Ion fluxes during the action potential in *Chara*. *J. Physiol.* **144**, 505–524.

Gaffey, C. T. (1972). Stimulation of action potentials with radiation in single cells of *Nitella gracilis*. *Intern. J. Radiation Biol.* **21**, 11–29.

Haapanen, L., and Skoglund, C. R. (1967). Recording of the ionic efflux during single action potentials in *Nitellopsis obtusa* by means of high-frequency reflectometry. *Acta Physiol. Scand.* **69**, 51–68.

Hansen, U.-P., Gradmann, D., Sanders, D., and Slayman, C. L. (1981). Interpretation of current-voltage relationships for “active” ion transport systems: I. Steady-state reaction-kinetic analysis of class-I mechanisms. *J. Memb. Biol.* **63**, 1, 65–190.

Harvey, E. N. (1942a). Hydrostatic pressure and temperature in relation to stimulation and cyclosis in *Nitella flexilis*. *J. Gen. Physiol.* **25**, 855–863.

Harvey, E. N. (1942b). Stimulation of cells by intense flashes of ultraviolet light. *J. Gen. Physiol.* **25**, 431–445.

Hayama, T., Shimmura, T., and Tazawa, M. (1979). Participation of Ca^{2+} in cessation of cytoplasmic streaming induced by membrane excitation in characean internodal cells. *Protoplasma* **99**, 305–321.

Hill, S. E. (1935). Stimulation by cold in *Nitella*. *J. Gen. Physiol.* **18**, 357–367.

Hill, B. (1992). “Ionic channels of excitable membranes.” ED. 2. Sinauer Associates. Sunderland, Massachusetts.

Hirono, C., and Mitsui, T. (1981). Time course of activation in plasmalemma of *Nitella axilliformis*. In “Nerve Membrane: Biochemistry and function of channel proteins” (G. Matsumoto and M. Kotani, Eds.).

Hodgkin, A. L. (1954). A note on conduction velocity. *J. Physiol.* **125**, 221–224.

Hodgkin, A. L., and Huxley, A. F. (1952a). A quantitative description of membrane current and its application to conduction and excitation in nerve. *J. Physiol.* **117**, 500–544.

Hodgkin, A. L., and Huxley, A. F. (1952b). The dual effect of membrane potential on sodium conductance in the giant axon of *Loligo*. *J. Physiol.* **116**, 497–506.

Hodgkin, A. L., and Huxley, A. F. (1952c). Currents carried by sodium and potassium ions through the membrane of the giant axon of *Loligo*. *J. Physiol.* **116**, 449–472.

Hodgkin, A. L., and Huxley, A. F. (1952d). The components of membrane conductance in the giant axon of *Loligo*. *J. Physiol.* **116**, 473–496.

Hoffmann, R., and Bisson, M. A. (1990). *Chara buckelii*, a euryhaline charophyte from unusual saline environment. III. Time course of turgor regulation. *Plant Physiol.* **93**, 122–127.

Hope, A. B. (1961a). Ionic relations of cells of *Chara corallina*. V. The action potential. *Austral. J. Biol. Sci.* **14**, 312–322.

Hope, A. B. (1961b). The action potential in cells of *Chara*. *Nature* **191**, 811–812.

Hope, A. B., and Findlay, G. P. (1964). The action potential in *Chara*. *Plant Cell Physiol.* **5**, 377–379.

Johnson, B. R., Wyttenbach, R. A., Wayne, R., and Hoy, R. R. (2002). Action potentials in giant algal cell: A comparative approach to mechanisms and evolution of excitability. *The Journal of Undergraduate Neuroscience Education (JUNE)*, Fall 2002, **1**, A23–A27.

Kamitsubo, E. (1980). Cytoplasmic streaming in characean cells: Role of subcortical fibrils. *Can. J. Bot.* **58**, 760–765.

Kamitsubo, E., and Kikuyama, M. (1992). Immobilization of endoplasm flowing continuous to the actin cables upon electrical stimulus in *Nitella* internodes. *Protoplasma* **168**, 82–86.

Kamitsubo, E., Ohashi, Y., and Kikuyama, M. (1989). Cytoplasmic streaming in internodal cells of *Nitella* under centrifugal acceleration: A study done with a newly constructed centrifuge microscope. *Protoplasma* **152**, 148–155.

Kamiya, N. (1959). Protoplasmic streaming. *Protoplasmatologia. Handbuch der Protoplasma-forschung VIII/3 a*. Wien: Springer.

Karol, K. G., McCourt, R. M., Cimino, M. T., and Delwiche, C. F. (2001). The closest living relatives of land plants. *Science* **294**, 2351–2353.

Katsuhara, M., and Tazawa, M. (1992). Calcium-regulated channels and their bearing on physiological activities in Characean cells. *Philos. Trans. R. Soc. Lond. Ser. B. Biol. Sci.* **338**, 19–29.

Katz, B. (1937). Experimental evidence for a non-conducted response of nerve to sub-threshold stimulation. *Proc. Roy. Soc. (London). Ser. B* **124**, 244–276.

Keynes, R. D., and Rojas, E. (1976). The temporal and steady-state relationships between activation of the sodium conductance and movement of the gating particles in the squid giant axon. *J. Physiol.* **255**, 157–189.

Kikuyama, M. (1986a). Ion effluxes during excitation of characeae. *Plant Cell Physiol.* **27**, 1213–1216.

Kikuyama, M. (1986b). Tonoplast action potential of characeae. *Plant Cell Physiol.* **27**, 1461–1468.

Kikuyama, M. (1987). Ion efflux during a single action potential of *Nitella axilliformis* in medium lacking Ca^{2+} . *Plant Cell Physiol.* **28**, 179–186.

Kikuyama, M., Shimada, K., and Hiramoto, Y. (1993). Cessation of cytoplasmic streaming follows an increase of cytoplasmic Ca^{2+} during action potential in *Nitella*. *Protoplasma* **174**, 142–146.

Kikuyama, M., Oda, K., Shimmen, T., Hayama, T., and Tazawa, M. (1984). Potassium and chloride effluxes during excitation of characeae cells. *Plant Cell Physiol.* **25**, 965–974.

Kikuyama, M., and Shimmen, T. (1997). Role of Ca^{2+} on triggering tonoplast action potential in intact *Nitella flexilis*. *Plant Cell Physiol.* **38**, 941–944.

Kikuyama, M., and Tazawa, M. (1976). Tonoplast action potential in *Nitella* in relation to vacuolar chloride concentration. *J. Membr. Biol.* **29**, 95–110.

Kikuyama, M., and Tazawa, M. (1983). Transient increase of intracellular Ca^{2+} during excitation of tonoplast-free *Chara* cells. *Protoplasma* **117**, 62–67.

Kikuyama, M., and Tazawa, M. (2001). Mechanosensitive Ca^{2+} release from intracellular stores in *Nitella flexilis*. *Plant Cell Physiol.* **42**, 358–365.

Kishimoto, U. (1961). Current voltage relations in *Nitella*. *Biol. Bull.* **121**, 370–371.

Kishimoto, U. (1964). Current voltage relations in *Nitella*. *Jap. J. Physiol.* **14**, 515–527.

Kishimoto, U. (1966a). Repetitive action potentials in *Nitella* internodes. *Plant Cell Physiol.* **7**, 547–558.

Kishimoto, U. (1966b). Action potential of *Nitella* internodes. *Plant Cell Physiol.* **7**, 559–572.

Kishimoto, U. (1968). Response of *Chara* internodes to mechanical stimulation. *Ann. Rept. Biol. Works Fac. Sci., Osaka Univ.* **16**, 61–66.

Kishimoto, U. (1972). Characteristics of the excitable *Chara* membrane. *Avan. Biophys.* **3**, 199–226.

Kishimoto, U., Takeuchi, Y., Ohkawa, T., and Kami-ika, N. (1985). A kinetic analysis of the electrogenic pump of *Chara corallina*: intelliIII. Pump activity during action potential. *J. Membr. Biol.* **86**, 27–36.

Laver, D. R. (1990). Coupling of K^+ -gating and permeation with Ca^{2+} block in the Ca^{2+} -activated K^+ channel in *Chara australis*. *J. Membr. Biol.* **118**, 55–67.

Laver, D. R. (1991). A surgical method for accessing the plasma-membrane of *Chara australis*. *Protoplasma* **161**, 79–84.

Laver, D. R., and Walker, N. A. (1991). Activation by Ca^{2+} and block by divalent ions of the K^+ channel in the membrane of the cytoplasmic drops from *Chara australis*. *J. Membr. Biol.* **120**, 131–139.

Luhring, H. (1986). Recording of single K^+ channels in the membrane of cytoplasmic drop of *Chara australis*. *Protoplasma* **133**, 19–27.

Lunevsky, V. Z., Zherelova, O. M., Vostrikov, I. Ya., and Berestovsky, G. N. (1983). Excitation of Characeae cell membranes as a result of activation of calcium and chloride channels. *J. Membr. Biol.* **72**, 43–58.

Mailman, D. S., and Mullins, L. J. (1966). The electrical measurement of chloride fluxes in *Nitella*. *Aust. J. Biol. Sci.* **19**, 385–398.

McCulloch, S. R., Laver, D. R., and Walker, N. A. (1997). Anion channel activity in the *Chara* plasma membrane: Cooperative subunit phenomena and a model. *J. Exp. Bot.* **48**, 383–398.

Mimura, T., and Shimmen, T. (1994). Characterisation of the Ca^{2+} -dependent Cl^- efflux in perfused *Chara* cells. *Plant Cell Physiol.* **35**, 7, 93–800.

Mimura, T., and Tazawa, M. (1983). Effect of intracellular Ca^{2+} on membrane potential and membrane resistance in tonoplast-free cells of *Nitellopsis Obtusa*. *Protoplasma* **118**, 49–55.

Mullins, L. J. (1962). Efflux of chloride ions during the action potential of *Nitella*. *Nature* **196**, 986–987.

Oda, K. (1976). Simultaneous recording of potassium and chloride effluxes during an action potential in *Chara corallina*. *Plant Cell Physiol.* **17**, 1085–1088.

Oda, K. (1975). Recording of the potassium efflux during a single action potential in *Chara corallina*. *Plant Cell Physiol.* **16**, 525–528.

Ohkawa, T., and Kishimoto, U. (1975). Anode break excitation in *Chara* membrane. *Plant Cell Physiol.* **16**, 83–91.

Okazaki, Y., Ishigami, M., and Iwasaki, N. (2002). Temporal relationship between cytosolic free Ca^{2+} and membrane potential during hypotonic turgor regulation in a brackish water charophyte *Lamprothamnium succinctum*. *Plant Cell Physiol.* **43**, 1027–1035.

Okihara, K., Ohkawa, T., and Kasai, M. (1993). Effect of calmodulin on Ca^{2+} -dependent Cl^- sensitive anion channels in the *Chara* plasmalemma: a patch-clamp study. *Plant Cell Physiol.* **34**, 75–82.

Okihara, K., Ohkawa, T., Tsutsui, I., and Kasai, M. (1991). A Ca^{2+} - and voltage-dependent Cl^- sensitive anion channel in the *Chara* plasmalemma: A patch-clamp study. *Plant Cell Physiol.* **32**, 593–601.

Osterhout, W. J. V., and Hill, S. E. (1933). Anesthesia produced by distilled water. *J. Gen. Physiol.* **17**, 87–98.

Othmer, H. G. (1997). Signal transduction and second messenger systems. In “Case Studies in Mathematical Modeling—Ecology, Physiology and Cell Biology” (H. G. Othmer, F. R. Adler, M. A. Lewis, and J. Dallon, Eds.). Prentice Hall, Englewood Cliffs, NJ.

Pickard, B. G. (1973). Action potentials in higher plants. *Botan. Rev.* **39**, 172–201.

Plieth, C., Sattelmacher, B., Hansen, U.-P., and Thiel, G. (1998). The action potential in *Chara*: Ca^{2+} release from internal stores visualised by Mn^{2+} -induced quenching of fura dextran. *Plant J.* **13**, 167–175.

Plieth, C., and Hansen, U.-P. (1996). Methodological aspects of pressure loading of Fura-2 into characean cells. *J. Exp. Bot.* **47**, 1601–1612.

Reid, R. J., and Smith, F. A. (1992). Measurement of calcium fluxes in plants using ^{45}Ca . *Planta* **186**, 558–566.

Sakano, K., and Tazawa, T. (1986). Tonoplast origin of the membranes of cytoplasmic droplets prepared from *Chara* internodal cells. *Protoplasma* **131**, 247–249.

Shiina, T., Wayne, R., Tung, H. Y. L., and Tazawa, M. (1988). Possible involvement of protein phosphorylation/dephosphorylation in the modulation of Ca^{2+} channel in tonoplast-free cells of *Nitellopsis*. *J. Membr. Biol.* **102**, 255–264.

Shiina, T., and Tazawa, M. (1987). Demonstration and characterisation of Ca^{2+} channel in tonoplast-free cells of *Nitellopsis obtusa*. *J. Membr. Biol.* **96**, 263–276.

Shiina, T., and Tazawa, M. (1988). Ca^{2+} -dependent Cl^- efflux in tonoplast-free cells of *Nitellopsis obtusa*. *J. Membr. Biol.* **106**, 135–139.

Shimmen, T. (1996). Studies on mechano-perception in characean cells: Development of monitoring apparatus. *Plant Cell Physiol.* **37**, 590–597.

Shimmen, T. (1997a). Studies on mechano-perception in characean cells: Pharmacological analysis. *Plant Cell Physiol.* **38**, 139–148.

Shimmen, T. (1997b). Studies on mechano-perception in characean cells: Effects of external Ca^{2+} and Cl^- . *Plant Cell Physiol.* **38**, 691–697.

Shimmen, T. (1997c). Studies on mechano-perception in characean cells: Decrease in membrane electrical resistance in receptor potentials. *Plant Cell Physiol.* **38**, 1298–1301.

Shimmen, T., Mimura, T., Kikuyama, M., and Tazawa, M. (1994). Characean cells as a tool for studying electrophysiological characteristics of plant cells. *Cell Structure and Function* **19**, 263–278.

Shimmen, T., and Nishikawa, S. (1988). Studies on the tonoplast action potential in *Nitella flexillis*. *J. Membr. Biol.* **101**, 133–140.

Shimmen, T., Kikuyama, M., and Tazawa, M. (1976). Demonstration of two stable potential states of plasmalemma of *Chara* without tonoplast. *J. Membr. Biol.* **30**, 249–270.

Shimmen, T., and Tazawa, M. (1980). Intracellular chloride and potassium ions in relation to excitability of *Chara* membrane. *J. Membr. Biol.* **55**, 223–232.

Shimmen, T., and Tazawa, M. (1983a). Control of cytoplasmic streaming by ATP, Mg⁺⁺ and cytochalasin B in permeabilised characean cell. *Protoplasma* **115**, 18–24.

Shimmen, T., and Tazawa, M. (1983b). Activation of K⁺ channel in membrane excitation of *Nitella axilliformis*. *Plant Cell Physiol.* **24**, 1511–1524.

Shimmen, T. (2001). Electrical perception of “Death message” in *Chara*: Involvement in turgor pressure. *Plant Cell Physiol.* **42**, 366–373.

Shimmen, T. (2002). Electrical perception of “Death message” in *Chara*: Analysis of rapid component and ionic process. *Plant Cell Physiol.* **43**, 1575–1584.

Sibaoka, T. (1958). Conduction of action potential in a plant cell. *Trans. Bose Res. Inst. (Calcutta)* **22**, 43–56.

Sibaoka, T. (1969). Physiology of rapid movements in higher plants. *Annual review of Plant Physiol.* **20**, 165–184.

Sibaoka, T., and Tabata, T. (1981). Electrotonic coupling between adjacent internodal cells in *Chara braunii*: Transmission of action potentials beyond the node. *Plant Cell Physiol.* **22**, 397–411.

Simons, P. J. (1981). The role of electricity in plant movements. *New Phytologist* **87**, 11–37.

Smith, J. R., and Beilby, M. J. (1983). Inhibition of electrogenic transport associated with the action potential in *Chara*. *J. Membr. Biol.* **71**, 131–140.

Smith, P. T. (1984). Electrical evidence from perfused and intact cells for voltage-dependent K⁺ channels in the plasmalemma of *Chara australis*. *Aust. J. Plant Physiol.* **11**, 304–318.

Smith, P. T., and Walker, N. A. (1981). Studies on the perfused plasmalemma of *Chara corallina*: I. Current—voltage curves: ATP and potassium dependence. *J. Membr. Biol.* **60**, 223–236.

Stento, N. A., Ryba, N. G., Kiegle, E. A., and Bisson, M. A. (2000). Turgor regulation in the salt-tolerant alga *Chara longifolia*. *Plant Cell Environ.* **23**, 629–637.

Tabata, T. (1990). Ephaptic transmission and conduction velocity of an action potential in *Chara* internodal cells placed in parallel and in contact with one another. *Plant Cell Physiol.* **31**, 575–579.

Tabata, T., and Sibaoka, T. (1987). Conduction velocity and blockage of action potential in *Chara* internodal cells. *Plant Cell Physiol.* **28**, 1187–1194.

Tasaki, I. (1968). “Nerve Excitation.” C. C. Thomas, Springfield, IL.

Tazawa, M. (1964). Studies on *Nitella* having artificial cell sap. I. Replacement of the cell sap with artificial solutions. *Plant Cell Physiol.* **5**, 33–43.

Tazawa, M., Kikuyama, M., and Nakagawa, S. (1975). Open -vacuole method for measuring membrane potential and membrane resistance of Characeae cells. *Plant Cell Physiol.* **16**, 611–622.

Tazawa, M., Kikuyama, M., and Shimmen, T. (1976). Electric characteristics and cytoplasmic streaming of Characeae cells lacking tonoplast. *Cell Struct. Funct.* **1**, 165–175.

Tazawa, M., and Kishimoto, U. (1964). Studies on *Nitella* having artificial cell sap. II. Rate of cyclosis and electrical potential. *Plant Cell Physiol.* **5**, 45–59.

Tazawa, M., and Kishimoto, U. (1968). Cessation of cytoplasmic streaming of *Chara* internodes during action potential. *Plant Cell Physiol.* **9**, 361–368.

Tazawa, M., and Shimmen, T. (1980). Action potential in Characeae: Some characteristics revealed by internal perfusion studies. In “Plant Membrane Transport: Current Conceptual Issues” (R. M. Spanswick, W. J. Lucas, and J. Dainty, Eds.). Elsevier, New York.

Tazawa, M., and Shimmen, T. (1982). Artificial control of cytoplasmic pH and its bearing on cytoplasmic streaming, electrogenesis and excitability of characeae cells. *Bot. Mag. Tokyo* **95**, 147–150.

Tazawa, M., and Kikuyama, M. (2003). Is Ca^{2+} released from internal stores involved in membrane excitation in characean cells? *Plant Cell Physiol.* **44**, 518–526.

Thiel, G. (1995). Dynamics of chloride and potassium currents during the action potential in *Chara* studied with action potential clamp. *European Biophysical Journal* **24**, 85–92.

Thiel, G., Homann, U., and Plieth, C. (1997). Ion channel activity during the action potential in *Chara*: New insights with new techniques. *J. Exp. Bot.* **48**, 609–622.

Thiel, G., Homann, U., and Gradmann, D. (1993). Microscopic elements of electrical excitation in *Chara*: Transient activity of Cl^- channels in the plasma membrane. *J. Membr. Biol.* **134**, 53–66.

Thiel, G., MacRobbie, E. A. C., and Hanke, D. E. (1990). Raising the intracellular level of inositol 1,4, 5 -triphosphate changes plasma membrane ion transport in characean algae. *EMBO J.* **9**, 1737–1741.

Thom, R. (1975). “Structural stability and morphogenesis.” Benjamin, Reading, MA.

Tominaga, Y., and Tazawa, M. (1981). Reversible inhibition of cytoplasmic streaming by intracellular Ca^{2+} in tonoplast free cells of *Chara australis*. *Protoplasma* **109**, 103–111.

Tsutsui, I., Ohkawa, T., Nagai, R., and Kishimoto, U. (1986). Inhibition of Cl^- channel activation in *Chara corallina* membrane by lanthanum ion. *Plant Cell Physiol.* **27**, 1197–1200.

Tsutsui, I., Ohkawa, T., Nagai, R., and Kishimoto, U. (1987a). Role of calcium ion in the excitability and electrogenic pump activity of *Chara corallina* membrane. I. Effect of La^{3+} , verapamil, EGTA, W-7, and TFP on the action potential. *J. Membr. Biol.* **96**, 65–73.

Tsutsui, I., Ohkawa, T., Nagai, R., and Kishimoto, U. (1987b). Role of calcium ion in the excitability and electrogenic pump activity of *Chara corallina* membrane. II. Effect of La^{3+} , EGTA, and calmodulin antagonists on the current-voltage relation. *J. Membr. Biol.* **96**, 75–84.

Trewavas, A. (1999). Le Calcium, C'est la Vie: Calcium Makes Waves. *Plant Physiol.* **120**, 1–6.

Tyerman, S. D., and Findlay, G. P. (1989). Current-voltage curves of single Cl^- channels which coexist with two types of K^+ channel in the tonoplast of *Chara corallina*. *J. Exp. Bot.* **40**, 105–117.

Umrath, K. (1933). Der Erregungsvorgang bei *Nitella mucronata*. *Protoplasma* **17**, 258–300.

Wacke, M., and Thiel, G. (2001). Electrically triggered all-or-none Ca^{2+} liberation during action potential in the giant alga, *Chara*. *J. Gen. Physiol.* **118**, 11–12.

Wacke, M., Thiel, G., and Hütt, M.-T. (2003). Ca^{2+} dynamics during membrane excitation of green alga *Chara*: Model simulations and experimental data. *J. Membr. Biol.* **191**, 179–192.

Wayne, R. (1994). The excitability of plant cells: With a special emphasis on characean internodal cells. *Botan. Rev.* **60**, 265–367.

Williamson, R. E. (1975). Cytoplasmic streaming in *Chara*: A cell model activated by ATP and inhibited by cytochalasin B. *J. Cell Sci.* **17**, 655–668.

Williamson, R. E., and Ashley, C. C. (1982). Free Ca^{2+} and cytoplasmic streaming in alga *Chara*. *Nature* **296**, 647–651.

Zherelova, O. M. (1989). Protein kinase C is involved in regulation of Ca^{2+} channels in plasmalemma of *Nitella syncarpa*. *FEBS Lett.* **242**, 330–332.

Zimmermann, U., and Beckers, F. (1978). Generation of action potentials in *Chara corallina* by turgor pressure changes. *Planta* **138**, 173–179.

Similarity of the Domain Structure of Proteins as a Basis for the Conservation of Meiosis¹

Yu. F. Bogdanov,² T. M. Grishaeva, and S. Ya. Dadashev

Vavilov Institute of General Genetics, Russian Academy of Sciences,
Moscow, Russian Federation

Meiosis is conserved in all eucaryotic kingdoms, and homologous rows of variability are revealed for the cytological traits of meiosis. To find the nature of these phenomena, we reviewed the most-studied meiosis-specific proteins and studied them with the methods of bioinformatics. We found that synaptonemal complex proteins have no homology of amino-acid sequence, but are similar in the domain organization and three-dimensional (3D) structure of functionally important domains in budding yeast, nematode, *Drosophila*, *Arabidopsis*, and human. Recombination proteins of Rad51/Dmc1 family are conserved to the extent which permits them to make filamentous single-strand deoxyribonucleic acid (ssDNA)-protein intermediates of meiotic recombination. The same structural principles are valid for conservation of the ultrastructure of kinetochores, cell gap contacts, and nuclear pore complexes, such as in the cases when ultrastructure 3D parameters are important for the function. We suggest that self-assembly of protein molecules plays a significant role in building-up of all biological structures mentioned.

KEY WORDS: Meiosis, Synaptonemal complex, Protein domains, Self-assembly, 3D-structure, SMC proteins, Cohesins, Connexins, Innexins, Nuclear pore complex, Recombination.

© 2007 Elsevier Inc.

¹Dedicated to Professor M. J. Moses on the occasion of the 50-year anniversary of the discovery of synaptonemal complex.

²Corresponding author: Yu. F. Bogdanov.

³Supported by the Russian Foundation for Basic Research, project #05-04-49052, and by the Russian Academy of Sciences Program “Biodiversity and dynamics of gene pools.”

I. Introduction

It is well known that the general scheme of meiosis is evolutionarily conserved. The cytological pattern of meiosis is essentially similar in protists, fungi, plants, and animals, although some details vary. Mutations of specific meiotic genes have been found in representatives of all these kingdoms. Such mutations cause morphologically similar cell phenotypes, that is, meiotic abnormalities with similar cytological expression at the light-microscopic and ultrastructural levels. What are the cytological and molecular events occurring in the meiotic cell that are advantageous for meiosis to the extent of determining their existence for thousands and millions of years and their fixation in all kingdoms of eukaryotes?

The molecular basis of meiosis is provided by several tightly associated events, which distinguish meiosis from mitosis and occur in the first meiotic division (meiosis I). The events include (1) synapsis and recombination of homologous chromosomes; (2) the formation of chiasmata, physically linking two nonsister chromatids; and (3) the lack of centromere splitting in meiosis I. The cytological consequences of these events are nondisjunction of sister chromatids and segregation of homologous chromosomes in meiosis I. As a result, cells carrying replicated chromosomes are haploidized. Meiosis II does not require chromosome replication; it leads to segregation of sister chromatids with recombinant alleles located distally of a single (or an odd) chiasma.

It is possible to consider conservation of morphological traits of meiosis as an example of the general biological law of homologous series of variation, which N. I. Vavilov formulated in the 1920s and continued to refine and improve for about 10 more years. This fundamental biological law was formulated on the basis of studies on the variation in plants. More recently, Vavilov extended the law to the animal world. In 1930, one of his formulations described a homologous series as “a biological phenomenon consisting in the fact that different species and even genera of plants or animals include repeating, analogous, parallel series of forms (i.e., forms similar in morphological and physiological features)” (Vavilov, 1987). In his book *Law of Homologous Series in Hereditary Variation* (Vavilov, 1935; reissued as Vavilov, 1987), Vavilov noted that this law is true for larger taxa (families and classes), and gave examples of the homology of morphogenetic processes in ascomycetes and basidiomycetes, in the class Infusoria, in fossil cephalopods, and in insects, amphibians, and mammals (Vavilov, 1935; reissued as Vavilov, 1987).

In all these cases, homology was deduced from the similarity of variation of features, namely, from discrete changes that formed series. This description of the fundamental phenomenon of homology implied the homology of

genes. Of real interest is the question as to how the similarity of intracellular structures in taxonomically distant organisms is ensured at the molecular level. This question concerns all cell structures from chromosomes to all organelles involved in cell division. Rapidly progressing genomics has already developed its own understanding of this problem and quantitative estimation of homology. The homology of genes is considered essential when their nucleotide sequences coincide by no less than 80% (Chervitz *et al.*, 1998; Rubin *et al.*, 2000). Such homology is characteristic of genes coding for functionally important proteins, enzymes in particular, and is, as a rule, followed within the limits of a taxonomic class.

Homology of proteins, especially those fulfilling morphogenetic functions rather than that of genes, is more important for the purpose of this paper. In view of the redundancy of genetic codes, one could expect that the nucleotide sequences of homologous genes are more variable than amino-acid sequences of their products in various organisms. There are mutations that change the course of meiosis, including mutations of specific meiotic genes. Tens of such genes have been identified in model organisms studied to the greatest extent. Judging by the data for *Saccharomyces cerevisiae*, the best-studied model species, meiosis should be governed by hundreds of genes, including those common for meiosis and mitosis (common genes of cell division) and those specific for each of these processes (Bogdanov, 2003). Table I lists specific meiotic genes identified so far in various species. Meiotic mutations are similar in phenotypic expression in different species. Published data on morphological changes in the picture of meiosis allow us to speak about

TABLE I
Number of Specific Meiotic Genes Identified in Different Species

Species	Number of known meiotic genes		
	Total	Studied at the molecular level	References
Yeast <i>Saccharomyces cerevisiae</i>	~300	~300	Priming <i>et al.</i> , 2000
Fly <i>Drosophila melanogaster</i>	~330	~120	Grishaeva (personal communication); Manheim and McKim, 2003
Maize <i>Zea mays</i>	~50	7	Hamant <i>et al.</i> , 2005; Pawlowski <i>et al.</i> , 2004
Rye <i>Secale cereale</i>	21	—	Sosnikhina <i>et al.</i> , 2005
Wall-cress <i>Arabidopsis thaliana</i>	~20	~10–12	Higgins <i>et al.</i> , 2005; Jones <i>et al.</i> , 2003; Schwarzacher, 2003

homologous series of variation in meiotic features in a wide range of taxa, including the kingdoms (Bogdanov, 2003). It is possibly more correct to speak about homomorphism of these features. Let us consider several examples.

II. Homomorphism of Cytological Features of Meiosis

The *compact chromosomes* mutation found in barley *Hordeum vulgare* (Moh and Nilan, 1954) and rye *Secale cereale* (Sosnikhina *et al.*, 2005) leads to supercondensation of chromosomes in metaphase I, but is not expressed in somatic cells (Fig. 1). The condensation of chromosomes during mitosis

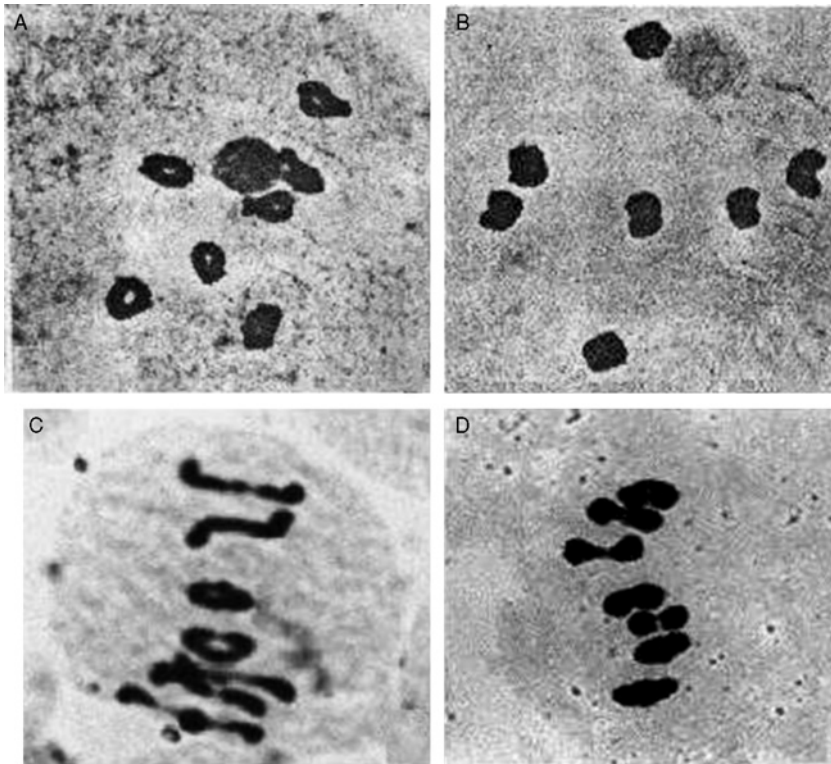


FIG. 1 Chromosomes in meiosis in normal plants (A, C) and in *compact chromosomes* meiotic mutants (B, D) of barley (A, B) and rye (C, D) with equal magnification. (A, B): diakinesis; (C, D): metaphase I. (A and B from Moh and Nilan, 1954, with the permission of the Japan Mendelian Society; C and D courtesy of S. P. Sosnikhina.)

and meiosis depends on specific chromatin proteins, condensins. One of these proteins, meiosis-specific, is possibly affected by the aforementioned mutation.

The example of the *compact chromosomes* mutation refers to plants of one family, Poaceae; yet phenotypically similar mutations of meiotic genes have been identified in other plant families as well. For instance, meiosis-specific mutations leading to synapsis of nonhomologous chromosomes in prophase I were found in diploid onion *Allium cepa* (Liliaceae), diploid maize and rye, and hexaploid wheat *Triticum aestivum*, all belonging to Poaceae. The presence of a gene(s) responsible for strict homology of synapsis in hexaploid wheat seems self-evident, because the chromosomes should be protected against nonhomologous (heterologous) synapsis in cells carrying three homologous genomes: AA, BB, and DD. The discovery of such genes in diploid maize, onion, and rye (Fedotova *et al.*, 1994; Jenkins and Okumus, 1992; Timofeeva and Golubovskaya, 1991) is highly important. This means homology of synapsis is strongly controlled by special genes even in the diploid chromosome set.

Examples exist illustrating homomorphism of some gross cytological features of meiosis in taxonomically distant organisms. In plants and animals, the Rabl configuration, with centromeric chromosome regions clustering in the vicinity of the nuclear membrane and chromosome ends being dispersed throughout the nucleus, changes during early meiotic stages to the bouquet configuration, with the ends of all chromosomes clustering on the nuclear membrane and the centromeres being dispersed (Fig. 2). These events start at premeiotic interphase, and the bouquet configuration is visible from leptotene to late zygotene. Leptotene is difficult to visualize by light microscopy in many higher plants because their chromosomes are extremely long and are packed closely. Light microscopy of zygotene of many cereals (e.g., rye and maize) reveals a chromosome knot (called a synizetic knot) in place of a distinct bouquet characteristic of meiosis in animals, especially in insects. On this evidence, the existence of the meiotic bouquet of chromosomes in flowering plants was questioned in some early reviews and textbooks (Rhoades, 1961; Swanson, 1960) and the synizetic knot was considered to be analogous or even an alternative to the bouquet.

Electron microscopy (EM) of ultrathin sections and microspreads of pollen mother cells has shown (Fig. 3) that the ends of synaptonemal complexes actually cluster on a limited area of the internal nuclear membrane in leptotene and zygotene nuclei of rye (Fedotova *et al.*, 1994). Later, clustering in wheat (Martinez-Perez *et al.*, 1999) and maize (Carlton and Cande, 2002) was documented by fluorescent *in situ* hybridization (FISH) confirming EM findings reported in some earlier works with these plants referred by these authors. Bouquet configurations of meiotic chromosomes have been reported for plants much earlier (Kihara, 1927).

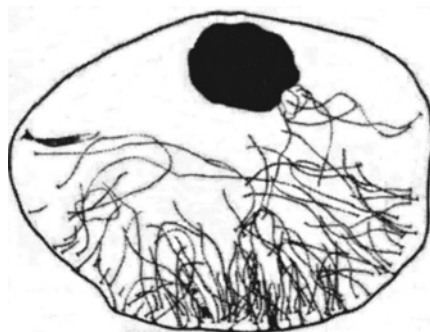


FIG. 2 A "bouquet" of axial elements and synaptonemal complexes and chromosomes at the early zygotene stage of meiosis in *Bombyx mori* oocyte. 3D-reconstruction of serial ultrathin sections; axial elements of chromosomes have been drawn. Out of 112 ends (telomere regions) of chromosomes, 102 ends contact with the inner side of the nuclear envelope in a restricted region, and form the base of bouquet; six ends are just involved in formation of short synaptonemal complexes marked in black (after Rasmussen and Holm, 1981).

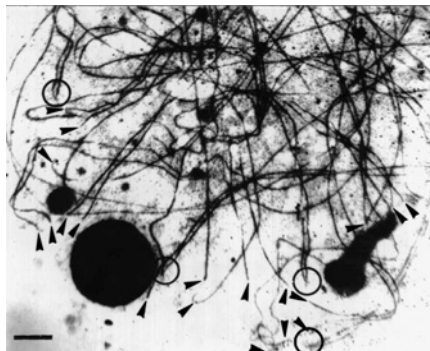


FIG. 3 Spread synaptonemal complexes from rye *Secale cereale* at the zygotene stage of meiosis. Telomeres are grouped in one area (bouquet). Telomeres of synapsed chromosomes are encircled; not-yet-synapsed telomeres are marked with arrowheads. Bar 1 μ . (Courtesy of Yu S. Fedotova.)

Elegant evidence has been obtained for the genetic control of the formation of the chromosome bouquet in leptotene and zygotene in rye (Mikhailova *et al.*, 2001) and maize (Golubovskaya *et al.*, 2002). In addition, a yeast gene is known that codes for a protein located in the telomeric regions of chromosomes. The protein ensures the clustering of the telomeric regions on the inner

side of the nuclear membrane in prophase I (Trelles-Sticken *et al.*, 2000). Thus, the clustering of chromosomes on the nuclear membrane in early prophase I and the resulting bouquet organization of meiotic chromosomes in prophase occur in all eukaryotic kingdoms and are probably an ancient feature of meiosis. This complex feature has been analyzed in detail (Zickler, 2006; Zickler and Kleckner, 1998). Its genetic control is most probably polygenic. It is difficult to say whether the genes responsible for the feature are homologous between yeasts and higher plants. Yet it is safe to say that these genes are analogous, at least functionally, and determine the similarity of the feature in the Vavilovian sense and that there are mutations leading to the same phenotypic variation of the feature. The rule of the telomere clustering in meiosis has several exceptions, for example, flies, including those of the genus *Drosophila*. The exceptions have proper explanations and are a subject for a separate discussion.

Thus, many features of meiosis (expression of specific meiotic genes) in evolutionarily distant species obey Vavilov's law of homologous series of variation. Does this mean that the meiotic genes are homologous? It was already mentioned that, in terms of modern genomics, homology is defined as similarity of the primary structure of deoxyribonucleic acid (DNA) and proteins. However, such homology is lacking among many genes determining similar phenotypes in different plants and animals. These genes code for the proteins that differ in primary structure and yet play similar functions.

III. Functional Analogy of Morphogenetic Proteins in Meiosis

Analogy of phenotypes can be followed in distant taxa and at the molecular level. The structural proteins of synaptonemal complexes (SCs), skeletal structures of prophase meiotic chromosomes, are the most interesting class of proteins specific for meiosis and involved in variation of meiotic features. SC is a nucleoprotein complex with a tight DNA–protein association. Proteins are the major SC component and account for more than 90% of its weight (Gorach *et al.*, 1985). The scheme of SC structure is similar in protists, fungi, plants, and animals, but its ultrastructural elements are formed by proteins differing in primary structure. The primary structures of the mouse, hamster, and human proteins coincide by 60–80%, whereas the budding yeast and *Drosophila* proteins have nothing in common with their mammalian analogs.

A complex polypeptide composition was first demonstrated for rat spermatocyte SC by SDS electrophoresis by C. Heyting and her group (Heyting,

1996). The preparations contained 5–10 major proteins ranging 26–190 kDa. More recently, genes for several SC proteins were cloned and sequenced from the rodent, human (Dobson *et al.*, 1994; Meuwissen *et al.*, 1992; Schalk *et al.*, 1999), and *Saccharomyces cerevisiae* (Chua and Roeder, 1998; Sym *et al.*, 1993) genomes. At present, three major mammalian meiosis-specific proteins of the synaptonemal complex are well studied. These were first found in rat SC and termed SC proteins (SCP) 1, 2, and 3 (Lammers *et al.*, 1994; Meuwissen *et al.*, 1992). Chinese hamster analogs of SCP1 and SCP3 are respectively known as SYN1 and COR1 (Dobson *et al.*, 1994). Human and mouse homologs of SCP1 and SCP2 were found (Meuwissen *et al.*, 1997; Schalk, 1999). The amino-acid sequences of mouse, rat, hamster, and human SCP1 have 74–93% homology (Meuwissen *et al.*, 1992, 1997). The rat and human SCP2 sequences have 63% homology (Schalk, 1999). The *S. cerevisiae* SC proteins are Zip1, Zip2, Red1, and Hop1 (Chua and Roeder, 1998; Hollingsworth *et al.*, 1990; Smith and Roeder, 1997; Sym *et al.*, 1993).

A. Ultrastructure of Synaptonemal Complexes

The SC size varies within a certain range in plants and animals, and depends on the genome size. The total width of the tripartite SC structure is species-specific, ranging 76–240 nm. The SC length corresponds to the bivalent length in meiotic prophase I (Kleckner *et al.*, 2003; Solari, 1998). It is important that the width of the central space, located between the lateral elements, is within the narrow range from 70 to 120 nm in all organisms (Solari, 1998; Zickler and Kleckner, 1999).

Detailed EM imaging of the SC showed that the organization of the central space, is essentially the same in rat, female *D. melanogaster*, and beetle *Blaps cribrosa* (Schmekel *et al.*, 1993a,b) (Fig. 4). The structural unit of the insect central space consists of similar transversal filaments, which extend from one lateral element to the other and have two symmetrical thickenings, known as pillars (Figs. 4 and 5A). Fibrillar bridges link the pillars to produce two parallel bars, which together form a central element. The central space harbors three to five layers of parallel (transversal) filaments, which are similarly linked via fibrillar bridges between the pillars. The SC structure of other eukaryotes has been studied in less detail (Zickler and Kleckner, 1999 for review). Although the tripartite structure of the SC is conserved among most species, its details are species-specific (Schmekel and Daneholt, 1995; von Wettstein *et al.*, 1984). The lateral SC elements of three *Ascobolus* fungi display species-specific banding; their proteins are probably species-specific as well (von Wettstein *et al.*, 1984; Zickler, 1973; Zickler and Kleckner, 1999 for review). Distinct subunit organization is visible in the

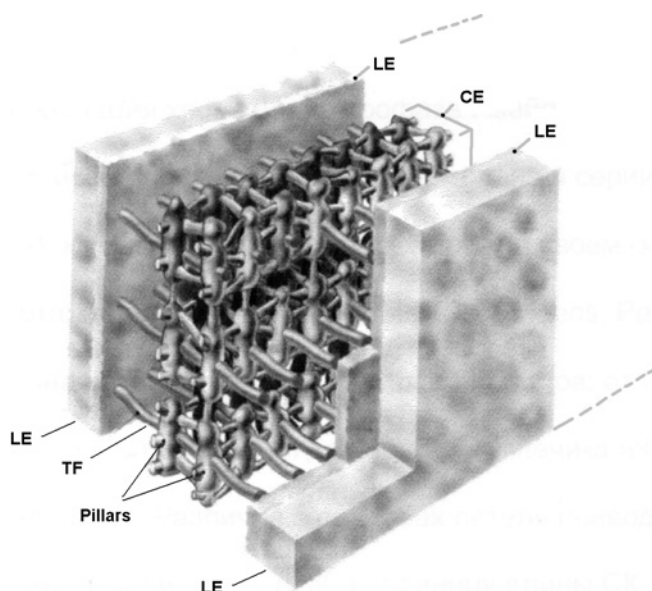


FIG. 4 Three-dimensional model of the central region in the synaptonemal complex of *Blaps cibrosa*. The central region of the SC is schematically displayed with numerous structural units organized side by side into three layers stacked in register. A fibrous network connects the pillars of the individual units. The central element (CE) is demarcated, and the lateral elements (LEs) are depicted as plates. TF, transversal filament. (Derived from Schmekel and Daneholt, 1995, with permission from Elsevier.)

lateral element of the house cricket (Fig. 5B). Electron-dense nodules represent another structure tightly associated with the SC (Carpenter, 1988, 1994; Hawley *et al.*, 1993). These nodules, known as meiotic nodules, play an important role in meiosis. Depending on the time of appearance in prophase I, nodules are classed into two types: early (detectable in leptotene and in zygotene) and late (detectable in the mature SC in pachytene). Compared with the latter, early nodules are more numerous and sometimes vary in shape. The number and distribution of late nodules along the SC proved to correlate with the number and distribution of crossover sites and chiasmata (Carpenter, 1994; Hawley *et al.*, 1993; Sherman and Stack, 1995). On the strength of this observation, a hypothesis was advanced that late nodules are multienzyme complexes that catalyze crossing-over, whereas early nodules mark sites in which DNA strand exchange is initiated in early recombination (Bishop, 1994; Page and Hawley, 2004; Roeder, 1997; Zickler and Kleckner, 1999). At present, the hypothesis can be considered proved. Late nodules

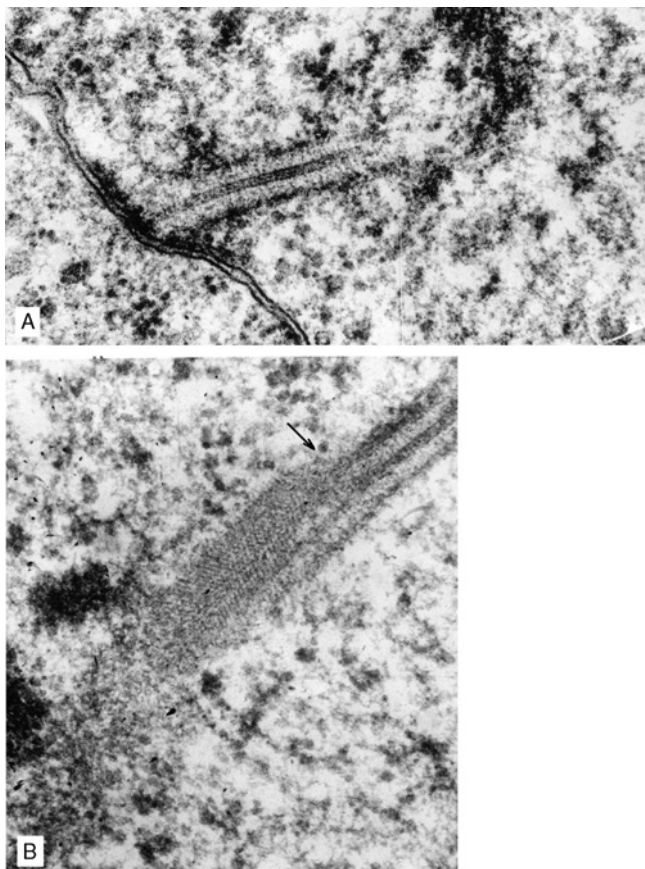


FIG. 5 Electron micrographs of synaptonemal complexes of the cricket *Achaeta domesticus*. Ultrathin sections of prophase I spermatocyte. (A) A fragment of SC attached to the nuclear membrane. Double-line central element is visible. (B) SC makes a twist at the point marked with arrow. The left-side (upper) lateral element is sectioned in tangential planes after the twist, and it is visible that the lateral element consist of numerous dotlike subunits, arranged like a Christmas tree. Presumably, they are large protein molecules/polymers composing the lateral element. (From Yu S. Chentsov and Yu F. Bogdanov, unpublished.)

occur in the SC central space, whereas some early nodules are attached to the axial cores of not yet synapsed chromosomes in early zygotene (Havekes *et al.*, 1994). Late nodules have been named recombination nodules.

The key role in synapsis of homologous chromosomes is played by the protein forming a “zipper” between two lateral SC elements, that is, between homologous chromosomes. It is called a synapsis protein.

B. Proteins of the SC Central Space

Synapsis proteins have been isolated and extensively studied in four mammals (SCP1) and yeast (Zip1). The proteins SCP1 and Zip1 have no homology in primary structure; yet they have similar structural plans and physico-chemical properties (Heyting, 1996; Penkina *et al.*, 2002) and belong to intermediate structural proteins. A description of SCP1 as it was summarized by Penkina *et al.* (2002) follows.

These proteins contain 870–990 amino-acid residues and consist of three domains. Each domain is similar in secondary and tertiary structures to the corresponding domain of similar proteins of other organisms compared (Table II).

Polyclonal antibodies revealed SCP1 (SYN1) in the SC in pachytene, when the SC central space is formed (Meuwissen *et al.*, 1992). The SCP1 gene is transcribed only in meiotic prophase I (Meuwissen *et al.*, 1997). As deduced from its cDNA sequence, SCP1 is 111 kDa, is enriched in positively charged residues such as Lys (14.5%) and Gln (16.3%), and has isoelectric point (pI) 5.5 (Meuwissen *et al.*, 1992).

On evidence of amino-acid sequence analysis, SCP1 consists of three domains: a short proline-rich nonstructured N-terminal domain (52 residues); a central amphipathic domain (700 residues), which is potentially able to form α -helices; and a globular DNA-binding C-terminal domain (194 residues) (Meuwissen *et al.*, 1992). The C-terminal domain is enriched in basic residues (pI 9.8) and contains S/T-P motifs (Meuwissen *et al.*, 1997). Presumably, these motifs cause a β -turn so that the peptide chain forms a loop, which is embedded into the DNA minor groove and contacts its sugar-phosphate backbone (Meuwissen *et al.*, 1997). On *in vitro* evidence, the C end of SCP1 nonspecifically binds with DNA (Dobson *et al.*, 1994; Meuwissen *et al.*, 1997).

The putative secondary structure of SCP1 is similar to that of intermediate proteins such as myosin, keratin, etc. These proteins interact through their amphipathic α -helices to form hetero- and homotypic dimers, which polymerize to yield filaments (Shoeman and Traub, 1993; Stewart, 1993). The computed length of two SCP1 molecules oriented “head to head” is 100 nm, equal to the distance between the SC lateral elements. Hence, the SCP1 filament is theoretically able to bridge the SC central space. Intermediate proteins form dimers 2 nm across and filaments 7–15 nm across (Steinert, 1990). These values are well consistent with the diameter of SC transversal elements (Dong and Roeder, 2000; Solari, 1998), which ranges 2–10 nm. In addition, thick transversal elements were observed to split into thin fibrils at the site of their attachment to the SC lateral elements. All these data made it possible to assume that SCP1 is the major protein of the SC transversal elements (Meuwissen *et al.*, 1992; Schmekel *et al.*, 1996).

TABLE II
Known and Predicted Proteins Forming Transversal Filaments of the SC Central Space

Species and corresponding proteins forming SC transversal filaments	Size of protein molecules and α -helical domains, a.a.			Isoelectric points of whole proteins and their domains				Domain size	
	Size of whole molecule	Size of α -helical domain	Width of the SC central space, nm	Whole molecule	N-end	Central domain	C-end	N-end	C-end
<i>Homo sapiens</i> SCP 1	973	677	100	5,7	5,0	5,4	9,7	120	176
<i>Rattus norvegicus</i> SCP 1	946	717	100	5,6	4,2	5,3	9,8	55	174
<i>Mus musculus</i> SCP 1	993	713	100	5,8	5,9	5,3	9,7	104	176
<i>Oryzias latipes</i> SCP1 (BAE 45256)	895	620	135	6,2	7,7	5,3	10,2	100	175
<i>Danio rerio</i> XP 684182	1000	690	135	6,5	9,6	5,3	10,1	110	200
<i>Saccharomyces cerevisiae</i> Zip 1	875	632	115	6,4	4,8	6,1	10,1	174	124
<i>Kluyveromyces lactis</i> Zip 1	755	545	115	5,4	4,9	5,2	10,1	130	80
<i>Drosophila melanogaster</i> C(3)G/ CG17604	744	495	109	5,9	10,0	4,9	9,7	155	94
<i>Arabidopsis thaliana</i> ZYP 1a	871	650	100–120	5,9	10,0	5,4	9,3	55	166
<i>Oryza sativa</i> CAE 75876	920	590	100–120	5,9	9,5	5,1	9,5	140	190
<i>Caenorhabditis elegans</i> SYP-1	489	355	70–85	6,1	3,7	8,1	10,0	47	87
<i>Caenorhabditis elegans</i> Q 11102	1132	938	70–85	5,5	11,9	5,1	11,0	120	75

A search for predicted proteins (designated by accession numbers) and/or their analysis was carried out by Bogdanov *et al.* specifically for this chapter. Details in the text.

This assumption was confirmed by two experiments. One involved EM with mono- and polyclonal antibodies to the N, C, and central domains of SCP1 (Schmekel *et al.*, 1996). The N domain was localized to the SC central element, and the C domain was observed close to and within an SC lateral element. Affinity-purified antibodies against the SCP1 central domain were in the space between the central and lateral elements. Second, analysis with the two-hybrid system, which reports the *in vivo* protein interaction, showed that SCP1 molecules interact with each other through their N domains (Liu *et al.*, 1996). No interaction was observed between two C domains or between the N and C domains.

Basing on the properties of SCP1, the following organization was assumed for the SC central space (Liu *et al.*, 1996; Schmekel *et al.*, 1996). SCP1 is the major protein of SC transversal elements (Fig. 6), which are formed by similarly oriented SCP1 dimers. The C domains of SCP1 are anchored in the lateral element and, possibly, interact with DNA. The N-terminal domains of SCP1 are directed inward (in the SC central space) to face the N-terminal domains of molecules forming the opposite zipper tooth (Heyting, 1996). Possibly, such interaction of the two opposite teeth provides for the formation of the SC central element (CE) (Fig. 7), which is clearly seen on EM images of ultrathin cell sections or surface spreads of isolated

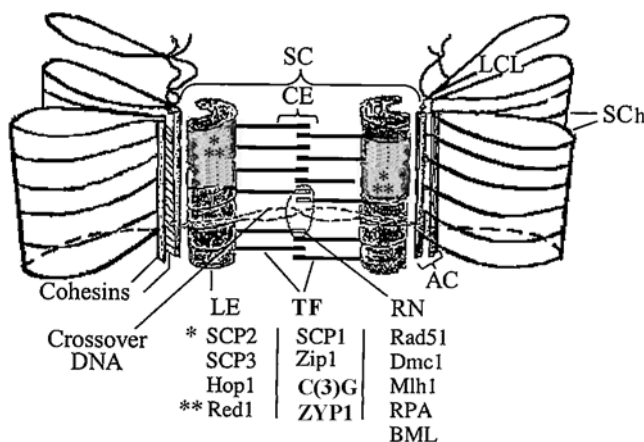


FIG. 6 Hypothetical scheme of the synaptonemal complex (SC) structure in budding yeast, *Drosophila*, and mammals. LCL, lateral chromatin loops; SCh, sister chromatids; CE, central SC element; LE, lateral SC element; TF, transversal filaments between two LEs ("teeth" of the zipper); RN, recombination nodule; AC, chromosome axial cores contained in LEs; SCP1, SCP2, SCP3, proteins forming structural SC elements in mammals; Hop1, Red1, Zip1, their functional counterparts in yeast; C(3)G, in *Drosophila*, ZYP1, in *Arabidopsis thaliana*. Rad51, Dmc1, Mlh1, RPA, BLM, enzymes participating in recombination and production of crossover DNA molecules in yeast, *Drosophila*, and mammals.

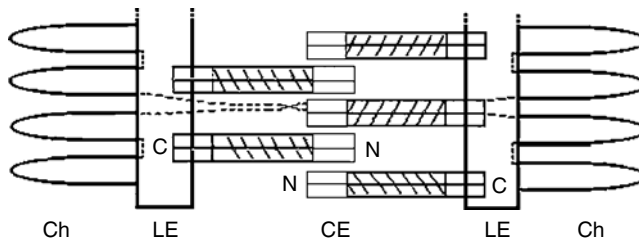


FIG. 7 Scheme of the central space of synaptonemal complex in mammals, yeast, and *Drosophila*. Ch, chromatin loops; LE, lateral element (protein axes of homologous chromosomes); CE, central element; C and N designate C- and N-terminal domains of protein molecules forming transversal filaments (“zipper” teeth). Central, rod-shaped domains of the protein molecules are shaded.

SCs of various organisms. However, this structure of the CE is probably not universal. As Schmekel and Daneholt (1995) have shown by EM imaging of SC of beetle *B. cibrosa*, transversal filaments “can pass as continuous filaments from one lateral element, through the central element, to the opposite lateral element.”

1. Yeast Zip1 Protein

The *S. cerevisiae* SC central-space protein, Zip1, was also studied in detail (Sym *et al.*, 1993). Sequence analysis of the gene *ZIP1* did not reveal any homology between proteins Zip1 and mammalian SCP1. However, proteins Zip1 and SCP1 are similar in secondary structure, suggesting a common role in SC transversal elements. To study the roles of individual Zip1 domains, the SC morphology was analyzed in mutants with deletions or insertions in *ZIP1* gene (Sym and Roeder, 1995; Tung and Roeder, 1998). A structure assumed as a result for the *S. cerevisiae* SC central space is similar to that of mammals.

One more central-space protein, Zip2, was found in *S. cerevisiae* (Chua and Roeder, 1998). Zip2 consists of 704 residues and shows no structural similarity to other proteins in computer analysis of databases. On evidence of special studies, Zip2 may initiate chromosome synapsis by organizing polymerization foci for Zip1 and for other possible components of the SC central space. As deduced from the *S. cerevisiae* Zip1 sequence, the N end (pI 4.8) of the protein may interact with the basic N-subterminal region (residues 200–300, pI 9.6) of the coiled coil (Bogdanov *et al.*, 2003). This conclusion is based on computations performed using the CHARGE program (from the package “Protein Sequence Analysis,” l’Institut Pasteur [<http://bioweb.pasteur.fr/seqanal/interfaces/charge.html>]).

Specific mutations preventing the SC assembly distort the formation of the SC central element. This leads to chromosome asynapsis in prophase I and reduces the crossing over frequency. Such mutations include *c(3)G* in *Drosophila melanogaster* (Smith and King, 1968), *asy* in wheat *Triticum durum* (La Cour and Wells, 1970) and maize *Zea mays* (Maguire and Riess, 1996), *sy1* in rye *Secale cereale* (Sosnikhina *et al.*, 1992), *as6* in tomato (Havekes *et al.*, 1994), and *zip1* in *S. cerevisiae* (Sym and Roeder, 1995). Tung and Roeder (1998) have shown that *zip1* allelic mutations result in various deletions from Zip1, and that the transversal filament length and the SC central space width decrease depending on the size and position of a deletion.

Grishaeva *et al.* (2001) analyzed the data reported by Tung and Roeder (1998) on Zip1, along with the data on mammalian SCP1 (Dobson *et al.*, 1994; Liu *et al.*, 1996; Meuwissen *et al.*, 1992, 1997), and found that the central space width in yeast and mammals correlates well with the size (in amino-acid residues) of the protein molecule forming a transversal filament ($r = 0.85$; $p < 0.001$) (Fig. 8). The correlation was even better with the size of their central rod-shaped coiled-coil domain ($r = 0.90$, $p < 0.001$) (Fig. 9). The rather high coefficient of correlation means that the SC central space width strongly depends on the length of the rod-shaped central domain of the proteins constituting SC transversal filaments (Bogdanov *et al.*, 2002a; Grishaeva *et al.*, 2001). Taking advantage of this correlation and the simple

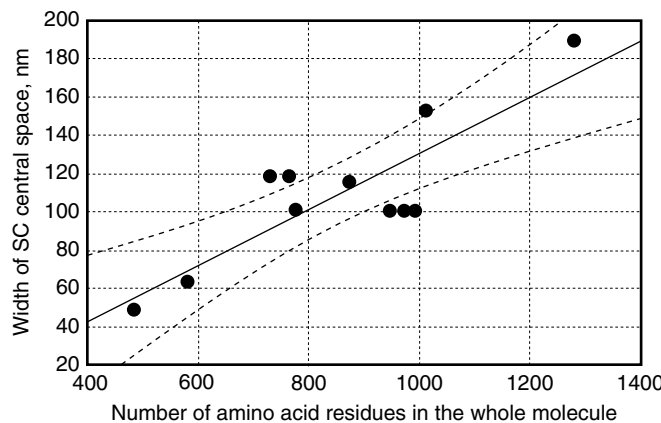


FIG. 8 The relationship between the SC central space width (nm) and size of the total protein molecules (number of amino-acid residues), forming the transverse filaments. Solid circles correspond to proteins SCP1 (human, rat, mouse) (Heyting, 1996; Liu *et al.*, 1996) and Zip1 with internal deletions and duplications in yeast (Tung and Roeder, 1998). The sloping solid line shows the regression for the given characters. Dashed lines show the confidence limits of regression at the 95% confidence interval. (From Bogdanov *et al.*, 2002a.)

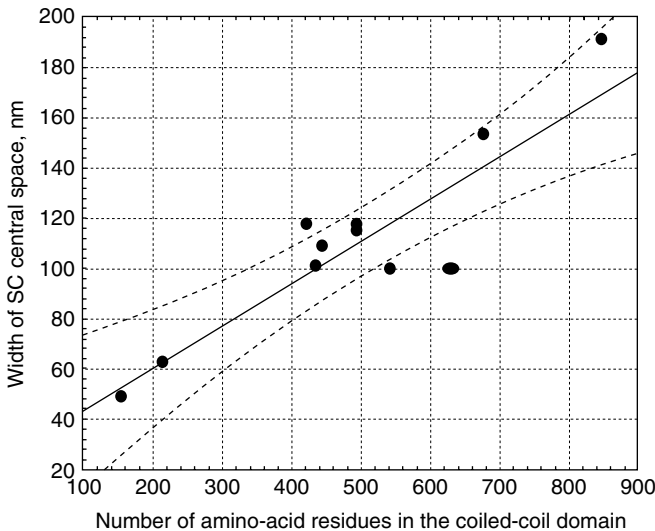


FIG. 9 The relationship between the SC central space width (nm) and size of the α -helical domain of SCP1/Zip1/C(3)G proteins. Designations as in Fig. 8. (From Bogdanov *et al.*, 2002a.)

three-domain protein organization with an inevitable rod-shaped central domain, we used bioinformatic methods to analyze and even predict transversal filament proteins in other organisms with sequenced genomes. The prediction was justified at least in one case, namely, that of *D. melanogaster* (Bogdanov *et al.*, 2002a; Grishaeva *et al.*, 2001; Page and Hawley, 2001).

2. Protein C(3)G of *Drosophila melanogaster*

In *D. melanogaster*, the *c(3)G* (*crossover suppressor on 3 of Gowen*) mutation causes the same ultrastructural alterations of the SC (Hawley *et al.*, 1993) as some mutation in *zip1* locus do in *S. cerevisiae* (Tung and Roeder, 1998). Hence the virtual protein encoded by *c(3)G*⁺ could be considered as a candidate transversal-filament protein. This prediction was borne out. Using elements of the procedure for searching for functional analogs, particularly the ProtParam Tool program, Grishaeva *et al.* (2001) and Bogdanov *et al.* (2002a) showed that, among 78 putative genes present in the *c(3)G* region of chromosome 3, only one, *CG17604*, codes for a protein similar in physicochemical properties to Zip1p and SCP1. The C(3)G/CG17604 virtual protein consists of 744 amino-acid residues and contains three domains, the central one forming an α -helical coiled coil with the length corresponding to the half width of the SC central space in *D. melanogaster*. The protein has

other properties (isoelectric points of the domains, sites of the ATPase activity in the coiled-coil domain, etc.), which also testify to its structural analogy to Zip1p and SCP1.

Page and Hawley (2001) have experimentally established the function of the *c(3)G⁺* protein product. Recombinant constructs harboring *c(3)G⁺* fused with the green fluorescence protein (GFP) gene were obtained and used to transform homozygotes for the *c(3)G* synaptic mutation. In transformants, chromosomes restored the ability to form bivalents in meiotic cells. Moreover, green fluorescence was observed in the central region of the bivalents, fluorescence foci producing a ladderlike pattern similar to that of SC transversal filaments. These data testified to the role of the *c(3)G⁺* product in the formation of SC transversal filaments.

Unlike in SCP1 and Zip1, the N-terminal domain of C(3)G has a high isoelectric point (Table II); that is, its total electrostatic charge is high. The question arises whether this feature prevents C(3)G from forming a zipper, which is presumably characteristic of SCP1 and Zip1. To answer this question, we studied *in silico* the charge distribution along the molecule for all three proteins (Grishaeva, unpublished data; see the next section). As analysis has shown, C(3)G is similar in size, domain organization, and secondary structure of the domains to SCP1 and Zip1, and the lack of sequence homology can hardly prevent the three proteins from playing similar roles in morphologically and functionally similar structures of the cell nucleus, that is, in the SC (Bogdanov, 2003; Bogdanov *et al.*, 2002a,b).

3. Charge Distribution Along the Molecules of Transversal-Filament Proteins

The study employed the CHARGE program (l'Institut Pasteur). The distribution of electrostatic charges along the molecule was compared for mouse and human SCP1, yeast Zip1, and fly C(3)G (Fig. 10). Several common features were found. First, while the total N-terminal domain is generally negative—with the exception of *D. melanogaster* C(3)G—its first amino-acid residues are positively charged in all proteins. Second, the C end is positive in total and has a local peak of a high negative charge (“spur”). Third, charges alternate at a high frequency along the molecule. We constructed a simple model of the zipper interactions between two oppositely directed molecules of the proteins that form, actually or presumably, transversal filaments of the SC. For instance, in the case of C(3)G, complementary electrostatic interactions can occur between peak (1) of one molecule and peak (2) of an oppositely directed molecule or between a pair of peaks: (1) and (3) of one molecule and peaks (4) and (2) of another one (Fig. 11).

Similar examination of SCP1 and Zip1 revealed a regularity, which can also be inferred via thorough analysis of the data reported for the yeast *zip1*

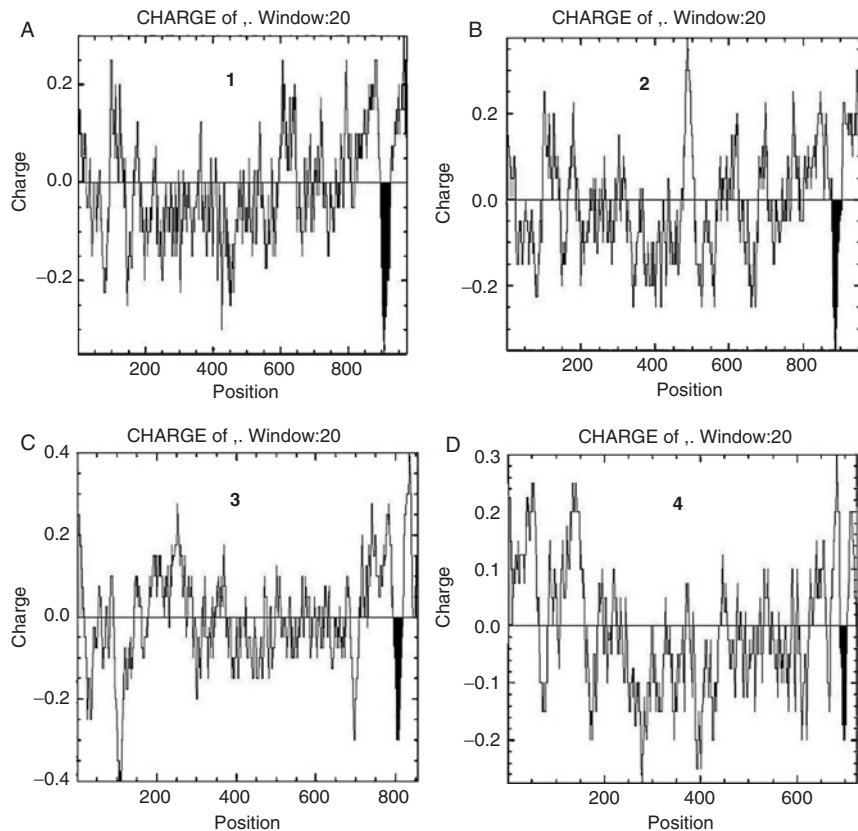


FIG. 10 Distribution of electrostatic charge along protein molecules: mouse and human SCP1 (A, B), yeast Zip1 (C), and C(3)G from *Drosophila* (D). Abscissa shows size of protein molecules (a.a.), ordinate—magnitude of positive (up) and negative (down) charges. Diagnostic peaks are black.

deletion mutants by Tung and Roeder (1998). The SC is not formed in such mutants when the deletion involves a considerable part of the N-terminal domain or the adjacent α -helical region. As modeling showed, the α -helix can be involved in forming the central element when two protein dimers overlap. Several (usually, two) variants of complementary interactions are possible as it was previously discussed about charge peaks of C(3)G molecules (Fig. 11). One can see that there are positive and negative charge “spurs” at N-termini of all the proteins presented in Fig. 10 which can complementary interact as zipper teeth. We analyzed the correlation between the width of the central space and the length of two protein molecules for two possible overlaps in all known and putative SC proteins (Grishaeva *et al.*, 2004). The coefficient of

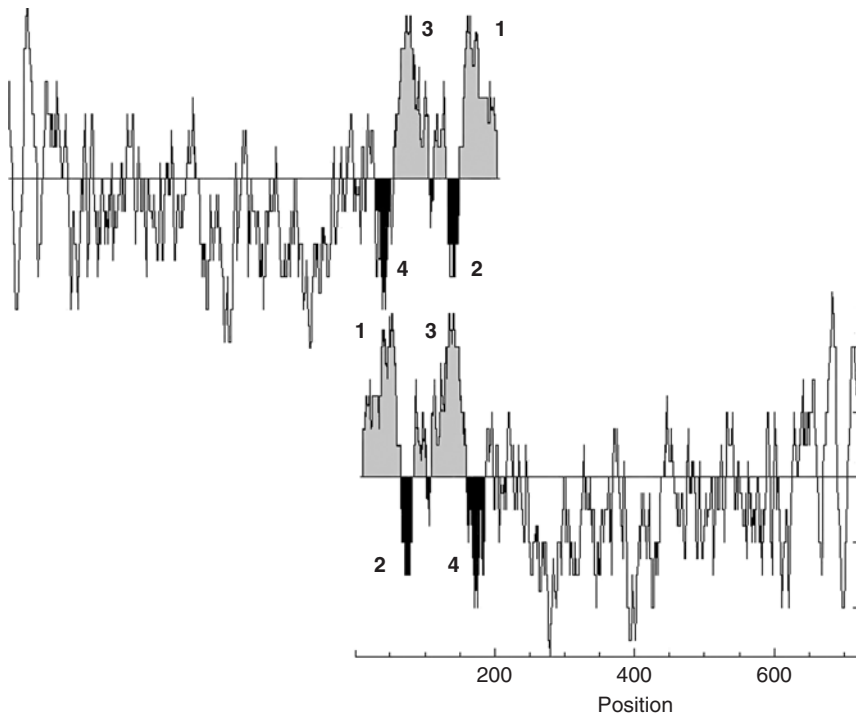


FIG. 11 Modeling of electrostatic interaction of two protein dimer molecules—C(3)G—forming transversal filaments. For details see the text.

correlation was 0.80 ($p \leq 0.001$) for the shorter overlap of the spurs and 0.83 ($p \leq 0.001$) for the longer overlap. The latter coincides with the coefficient of correlation computed for single molecules of all known and hypothetical SC proteins. Thus, the *in silico* modeling of the electrostatic interactions probably reflects the interactions between the proteins *in situ*.

4. *Caenorhabditis elegans* Proteins of the SC Central Space

MacQueen *et al.* (2002) have experimentally found that the *syp-1* gene of *C. elegans* (chromosome V) codes for protein F26D2.2 of 489 amino-acid residues. The size and other features of SYP-1 (GenBank accession no. AF515883) were deduced from the revised gene structure, which has been derived from sequencing cDNAs obtained by RT-PCR and 5'RACE and is consistent with the structure suggested by the EST alignment data present in WormBase. The region between residues 48 and 402 of the protein has been predicted to contain α -helical coiled coils. On immune staining, antibodies to N- and C-terminal parts of SYP-1 have been detected at the interface

between synapsed homologs along their full length in meiotic prophase-I *C. elegans* cells. This provides decisive evidence for the role of SYP-1 in forming the SC central space in *C. elegans*. MacQueen *et al.* (2002) noted that SYP-1 is approximately half the size of Zip1 or SCP1. Because the SC width in *C. elegans* is comparable with that in mammals, yeast, and *Drosophila*, MacQueen *et al.* (2002) have assumed “that SYP-1 exhibits an organization within the SC central region that is distinct from that of Zip1, or SCP1, α -helix and/or that additional structural proteins work in conjunction with SYP-1 to form the mature central region of the *C. elegans* SC.”

In view of these findings, we noted that the ultrastructure of the SC central space in *C. elegans* is unusual and differs from that in yeasts and mammals (Bogdanov *et al.*, 2003). The distinctive feature of *C. elegans* SC is a lack of a clearly defined central element and the absence of a pattern resembling zipper teeth. Whereas the central element is seen as an electron-dense filament located in the central space in many organisms (Zickler and Klecner, 1999), in *C. elegans*, transversal filaments look like continuous connections between the lateral elements that do not cross the central element on the way from one lateral element to the other (Dernburg *et al.*, 1998). This suggests a different type of molecular organization for *C. elegans* transversal filaments. If Model 1 is the organization of transversal filaments in yeast, mammals, and *Drosophila*, then Model 2 describes this structure in *C. elegans*. Probably, a long molecule, rather than two molecules with a zipperlike connection, extends from one to the other lateral element in *C. elegans*. Schmekel *et al.* (1993a,b) and Schmekel and Daneholt (1995) proposed this model for *B. cibrosa* transversal elements. Electron microphotographs of the SC allow a similar interpretation of the morphology of transversal filaments in *C. elegans*. If this is the case, both terminal domains of the protein forming *C. elegans* transversal filaments should be basic to associate with DNA in the SC lateral elements, and the coiled coil must be twice longer than in SCP1 or Zip1.

In view of this, it is worthwhile to mention another *in silico* finding (Bogdanov *et al.*, 2003; Grishaeva *et al.*, 2004). We searched the *C. elegans* proteome for proteins fitting either model. Three more ORFs were found to code for potential SCP1 and Zip1 analogs T26844, T27907, and Q11102. Each of these virtual proteins has a coiled coil suiting either Model 1 (T26844, T27907) or Model 2 (Q11102). However, the C-terminal domain of T26844 or T27907 has a low pI (5.3–5.7) and, therefore, cannot interact with DNA. Hence these proteins were rejected. The third one, Q11102, suits Model 2. Interestingly, the length of the coiled coil corresponds to the complete central-space width of the *C. elegans* SC. Both terminal domains of Q11102 are basic (Table II), meeting the other requirement of Model 2. Thus, Q11102 is a candidate for protein making continuous connections (transverse filaments) between lateral elements in the *C. elegans* SC, if such filaments exist.

In spite of researcher confidence in the *in situ* data, Proteome Inc. has reported that the *C. elegans* protein Z81586 is analogous to Zip1p. Using all criteria described earlier, we found that Z81586 may indeed be a functional analog of Zip1p as judged from its total size, domain structure, the size of the central coiled-coil domain, and physico-chemical properties of the C-terminal domain (see Table II). The protein Z81586 fits Model 1.

Two types of transversal filaments may actually be found on a single SC microphotograph, one representing a continuous connection between the lateral elements (Model 2) and another resembling zipperlike teeth. The former corresponds to the Q11102 putative protein, whereas the latter is possibly SYP-1. Taking the findings of MacQueen *et al.* (2002) into account, both proteins can take part in the construction of transversal filaments to fit Model 1. This statement is true, if the width of the central SC space in *C. elegans* is about 100 nm, as MacQueen *et al.* assume. If the width of the central space is within the range of 75–85 nm, a single protein molecule like Z81586 or SYP-1 can cover this distance and fit well to the regression line shown in (Fig. 8). Regrettably, precise estimation of the width of the central space in *C. elegans* is problematic.

To decide between the two proteins, we analyzed the genetic surroundings of the two candidate genes with the WormBase software. The region was -4 ± 1 on the genetic map of chromosome 1 in the case of the *z81586* gene and -10 ± 3.5 of the X chromosome in the case of the *q11102* gene. Neither region proved to contain a gene annotated in WormBase as responsible for normal meiosis. Thus, the answer is still unclear. Based on the unusual morphology of the SC central space in *C. elegans*, we believe that Q11102 is the *C. elegans* functional analog of SCP1 and Zip1p. We assumed that long molecules of this protein extend over the SC central space to form continuous transversal filaments in *C. elegans* (Bogdanov *et al.*, 2003). Toothlike transversal filaments can be composed of experimentally found SYP-1, putative Z8158, or both, because the SC central space is 3D and, in addition to transversal filaments, contains pillars and other filaments running perpendicular to transversal filaments.

5. *Arabidopsis thaliana* Proteins of the SC Central Space

The strategy of searching for proteins of the SC central space (Bogdanov *et al.*, 2003), which is based on the similar domain organization postulated for all such proteins in eukaryotes, was to a certain extent employed in laboratory studies. However, experimental studies of the proteins involved in the SC central space in *A. thaliana* (Higgins *et al.*, 2005) revealed a protein other than that predicted by *in silico* analysis by Bogdanov *et al.* (2003). Based on the data on transversal filament proteins of mammals, yeasts, and *C. elegans*, Higgins *et al.* (2005) searched the *A. thaliana* proteome for an

analogous protein with the use of the BLAST program (<http://www.ncbi.nlm.nih.gov/BLAST/>). The search yielded 220 proteins, which were ranked using the same program. Higgins *et al.* considered the structural characteristic of transversal filaments of the *A. thaliana* SC and deduced that the protein of interest should consist of 866 amino-acid residues and have a molecular weight of 100 kDa and an isoelectric point (pI) of 6. The protein contains an extended coiled coil flanked at both sides by globular domains, which are at the C and N ends of the molecule. The C-terminal domain has an extremely high pI (10) and contains the putative S/TPXX repeat (Suzuki and Yagi, 1991). These features were observed for two proteins ranking 30 and 40 according to the BLAST results.

The *At1g22260* and *At1g22275* genes (Higgins *et al.*, 2005), which have been designated *ZYP1a* and *ZYP1b*, respectively, are on different DNA strands in a 13-kb region of chromosome 1 (Higgins *et al.*, 2005, Fig. 1B). The start codons are 2 kb apart; the genes are transcribed in opposite directions. For each gene, cDNA clones were obtained by RT-PCR combined with 3' и 5'RACE-PCR. *ZYP1a* codes for a 2920-b mRNA as reported by Higgins *et al.* (2005), including a 2616-b coding region. *ZYP1b* is transcribed to yield a 2874-b mRNA, including a 2571-b coding region. The genes have 93% sequence homology. *ZYP1a* codes for a protein of 871 amino-acid residues, and *ZYP1b*, a protein of 856 residues (Higgins *et al.*, 2005, Fig. 1C). The N-terminal globular domains are basic and consist of 55 amino-acid residues. The domains have 83% similarity. The central coiled-coil domains consist of 650 residues in both proteins and have 95% similarity. The C-terminal globular domains of *ZYP1a* and *ZYP1b* consist of 166 and 151 residues, respectively, and have 75% similarity. RT-PCR analysis showed that the genes are expressed in flower buds but not in leaves.

6. *Oryza sativa* Protein of the SC Central Space

Using the same method, just for this review, we searched the rice *Oryza sativa* proteome for a protein involved in SC transversal filaments. As a reference protein, we used *A. thaliana* *ZYP1*. BLAST analysis revealed two highly homologous proteins (probably paralogs). One of these, CAE75876 of 920 amino-acid residues, was examined. Its secondary structure proved to be typical for transversal filament proteins. Namely, CAE75876 consists of three domains. An extended α -helical domain (590 residues) is flanked by small globular regions. The isoelectric point was estimated at 5.88 for the total protein, 9.48 for its C-terminal domain, 9.46 for the N-terminal domain, and 5.13 for the central domain. A similar secondary structure and physico-chemical properties are characteristic of *A. thaliana* *ZYP1*: pI = 5.9, 9.3, 9.99, and 5.39, respectively (our data). These values are typical for transversal

filament proteins (Table II), apart from high pI of the N-terminal domain. The plant proteins are similar in this feature to their *D. melanogaster* analog.

As for the distribution of electrostatic charges along the molecule, *A. thaliana* ZYP1 and *O. sativa* CAE75876 are similar to each other and to Zip1, SCP1, and C(3)G. The only differences are that the terminus of the N domain is charged negatively, rather than positively, and that the diagnostic spur (a small peak of a negative charge at the N end) is displaced to the terminus of the molecule. These features possibly reflect the specificity of interactions between SC transversal filaments with the lateral element proteins in plants. Taken together, these findings suggest that deduced CAE75876 forms the SC transversal filaments in *O. sativa* as experimentally demonstrated for *A. thaliana* ZYP1, yeast Zip1, mammalian SCP1, and *D. melanogaster* C(3)G.

C. Proteins of SC Lateral Elements

Although the data on the proteins involved in the SC central space are uniform and the domain organization of the proteins forming the SC transversal filaments is conserved, data on the proteins involved in the SC lateral elements form two groups and one exceptional case (Table III). One group accumulates experimentally revealed proteins Hop1 and Red1 in lower eukaryotes (mostly yeasts) and in plants, with Hop1 corresponding to ASY1 in *A. thaliana* and *Brassica* and PAIR2 in *O. sativa* (Armstrong *et al.*, 2002; Higgins *et al.*, 2005; Lorenz *et al.*, 2004; Nonomura, 2004; Smith and Roeder, 2000; Woltering *et al.*, 2000). The other group includes proteins of higher eukaryotes that possess SCP2 and SCP3, which differ from Hop1 and Red1 both in size and in primary and secondary structures (Botelho *et al.*, 2001; Lammers *et al.*, 1994; Martinez-Garay *et al.*, 2002; Offenberg *et al.*, 1998; Pelttari *et al.*, 2001). The exception is a protein of *D. melanogaster*. The only protein, C(2)M (570 a.a.), was identified as a component of the SC lateral elements or a protein contacting them. C(2)M is distantly related to the cohesin Rec8, which is absent from *D. melanogaster* (Anderson *et al.*, 2005; Heidman *et al.*, 2004).

The Hop1 proteins and their coding sequences from different organisms display only low similarity. For instance, the similarity is no more than 40% even between the *S. cerevisiae* and *Kluyveromyces lactis* proteins and is only 30% between *C. elegans* HIM-3 and *S. cerevisiae* Hop1 (Smith and Roeder, 2000; Zetka *et al.*, 1999). Greater conservation is characteristic of the HORMA domain, which is about 200 residues and is close to the N end. This domain, which is responsible for chromatin structuring, was found in all Hop1 orthologs. The smallest ortholog HIM-3 (291 residues) consists almost exclusively of the HORMA domain. In lower eukaryotes, the relevant

TABLE III
Known and Predicted Proteins of SC Lateral Elements

Species	Proteins of SC lateral elements				
	Hop1	Red1	SCP2	SCP3	Other SC proteins
<i>Saccharomyces cerevisiae</i>	+(HORMA, ZnF)	+(coiled coil)			Zip2, Zip3, Mek1 ^a
<i>Schizosaccharomyces pombe</i>	SPBC1718.02 (HORMA, ZnF) ^b	Rec10 (coiled coil) ^b			
<i>Kluyveromyces lactis</i>	+(HORMA, ZnF)	+			
<i>Drosophila melanogaster</i>					C(2)M, ORD
<i>Caenorhabditis elegans</i>	HIM-3 (HORMA)				SYP-2 ^c
<i>Arabidopsis thaliana</i>	ASY1, ASY2 (HORMA, SWIRM)				
<i>Oryza sativa</i>	PAIR2, BAD 00095 (HORMA)	+			Mek1, ^d BAC 20118
<i>Brassica oleracea</i>	ASY1				
<i>Mus musculus</i>	BAB30406, NP_080765 (HORMA)		+	+	
<i>Rattus norvegicus</i>	XP_228333 (HORMA)		+	+	
<i>Homo sapiens</i>	CT46/HORMAD1 (HORMA)		+	+	
<i>Oryzias latipes</i>					BAD 36840
<i>Mesocricetus auratus</i>					COR1

^aAnuradha and Muniyappa, 2004.

^bLorenz *et al.*, 2004.

^cMacQueen *et al.*, 2002.

^dNonomura *et al.*, 2004.

HORMA, SWIRM, ZnF—conserved protein domains.

Proteins found in databases by Bogdanov *et al.* specially for this chapter are designated by their accession numbers. Details in the text.

protein is at least 600 amino-acid residues in size and, in addition to the HORMA domain, contains one or two zinc fingers, acting as DNA-binding sites (Smith and Roeder, 2000). ASY1 of *A. thaliana* contains SWIRM, a small α -helical domain, which is close to the N end and is responsible for protein–protein interactions (data from a computer-aided search). Consistently, there is evidence that Hop1 functions as an oligomer in the cell (Anuradha and Muniyappa, 2004).

A protein involved in the SC lateral elements was identified in *O. sativa* and termed PAIR2. This protein is 610 amino-acid residues in size and has 53% identity to *A. thaliana* ASY1; the genes of the two proteins are similar in exon number (22). At the same time, similarity to Hop1 is only 16%. PAIR2 also possesses the HORMA domain. Expression of its gene during meiosis was demonstrated cytochemically. Mutants for the PAIR2 gene display asynapsis of homologous chromosomes (Nonomura *et al.*, 2004).

The other yeast protein of the SC lateral elements, Red1, has no functional domains other than short α -helical regions found in yeasts. Red1 is more than 800 residues in size. Like Hop1, Red1 is nonconserved between *S. cerevisiae* and *K. lactis*: homology is only 26%. Higher similarity (60%) is characteristic of the C-terminal domains of the two proteins (Lorenz *et al.*, 2004). It is possible that Hop1 and Red1 are not the only components of the SC lateral elements. Some researchers believe that the two proteins do not form a basis of the lateral elements (Zetka *et al.*, 1999), especially as concerns Hop1, which is in mobile association with Red1 (Anuradha and Muniyappa, 2005). Orthologs of Red1 in higher eukaryotes are unknown. Vice versa, orthologs of SCP2 and SCP3 were not found in primitive eukaryotes (Anuradha and Muniyappa, 2005; Smith and Roeder, 2000).

All SCP3 proteins identified so far are highly similar in secondary structure and in size (200–255 amino-acid residues); their primary structure is conserved. The C-terminal half of the molecule forms extended α -helices. It is thought that SCP3 attaches the SC to a chromosome, while SCP2 maintains the structure of lateral elements via binding to SCP3, but not to SCP1, which forms the SC transversal filaments. SCP3 interacts with the cohesins Rec8, SMC1 β , and SMC3 (Lee *et al.*, 2003). SCP2 is larger than SCP3 and lacks known domains and extended α -helical regions. Its size is much the same (about 1500 residues) in different mammals. Like SCP3, SCP2 interacts with cohesin, but its partners are SMC1L1 and SMC3. Rat SCP2 harbors two clusters of S/T-P motifs, which are involved in DNA binding, and eight binding sites for cAMP/cGMP protein kinase (Pelttari *et al.*, 2001).

A special place is occupied by C(2)M (570 residues), which has been identified as an SC component in *D. melanogaster*. Evidence suggests that C(2)M belongs to the α -kleisin family and is distantly related to the meiotic cohesin Rec8. The N end of C(2)M is localized in the SC central space in the immediate vicinity of the lateral elements (Anderson *et al.*, 2005). Because the

SC is not formed in *c(2)M* mutants, it is thought that C(2)M is responsible for the attachment of C(3)G to the lateral elements. It is still unclear whether C(2)M itself is a component of the lateral elements. Possibly, the lateral elements of the *D. melanogaster* SC contain ORD, which is involved in sister chromatid cohesion and may functionally substitute REC8, absent from *D. melanogaster*. Studies have revealed the interaction between C(2)M with the cohesin SMC3 *in vivo* (Heidmann *et al.*, 2004).

As previously mentioned, proteins similar to Hop1 in domain organization and possibly representing its orthologs were identified in mammals (see Table III). One of the human genes coding for a so-called group of cancer-testis (CT) antigens, which includes SCP3, SCP1, and Spo11, codes for CT46/HORMAD1, which is similar to HOP1 and ASY1. This protein consists of 394 amino-acid residues (Chen *et al.*, 2005). Similarity reaches 30% in one region. The *CT46/HORMAD1* gene is expressed in the testes and in cancer cells. Its orthologs were found in macaque, mouse, rat, and even rice. High (up to 90%) similarity among all these proteins was observed in the HORMA region.

In view of this, it is possible to expect that lower eukaryotes possess orthologs of SCP2 and SCP3, whereas higher eukaryotes have orthologs of Hop1 and Red1. If so, the SC lateral elements consist of the proteins that are functionally and structurally conserved the level of protein domain organization and secondary structure of these domains without any conservation of the primary structure, as is the case with the transversal filaments. The only exception is provided by *D. melanogaster*. *In silico*, we found two proteins containing the HORMA domain in *D. melanogaster*. Yet their genes are orthologous to other genes (*mad2*, *rev7*), whose protein products possess the HORMA domain, but do not play a role in meiotic chromosome synapsis. It is possible that *D. melanogaster* does not need a *HOP1* ortholog, because several other mechanisms expedite primary recognition of homologs (Anuradha and Muniyappa, 2005).

D. Evolutionary Mystery of SC Proteins

As noted, the yeast SC proteins perform analogous functions and lack sequence homology to the corresponding mammalian proteins. This is quite conceivable if we consider only the morphology of the SC, because the evolutionary distance between mammals and Ascomycetes is great. Given that the SC in these and other distant taxa have a common general organization, their absolute sizes (e.g., width), the fine structure of the SC central space, and the ultrastructure of its lateral elements are specific for orders and classes and considerably differ between taxonomic types.

Another surprising circumstance concerns the SC proteins (an analogous circumstance for kinetochore proteins is discussed later). It is surprising that structurally nonhomologous proteins are used to assemble the SC of the same structure and function in evolutionarily distant taxa. The analogy can be drawn between the principles of SC formation in different organisms and house building: houses of different sizes are built from different materials and for different climates, but they all are designed according to one principle (i.e., having walls, a roof, and windows) and share the function of sheltering their inhabitants. In the same fashion, the SC serves as a shelter for recombining chromosome sites. Importantly, the SC must align parallel homologous chromosomes, maintain some space between them (the central SC space) so that as the DNA molecules of homologous chromosomes could recombine within the central SC space, and maintain these conditions as long as required to complete recombination and chiasma formation.

Interestingly, the SC assembly in evolutionarily distant organisms, such as yeast *S. cerevisiae* and mammals, involves “standardized” construction elements. For instance, the transversal filaments (“beams”) connecting the SC lateral elements (“walls” of the “house”) have the same construction. They consist of rather simple proteins (Zip1 in yeast and SCP1 in mammals) belonging to the class of intermediary proteins. Each of these proteins contains three polypeptide domains, the central of which is rod-shaped owing to a long coiled coil. The length of this rod-shaped domain and the distance between the SC lateral elements (i.e., the width of the central space) are strongly correlated. Collectively, these data indicate that the species-specific structure of SC proteins, as well as ultrastructure of the SC, is neutral in the context of macroevolution. Thus, the enigma exists of how evolutionarily distant organisms had acquired these proteins?

IV. Recombination Enzymes

A. Recombination Nodules as Compartments for Recombination Enzymes

In zygotene and pachytene, the central space of each SC contains recombination nodules (RNs). It was shown that the RN number in late pachytene corresponds to the chiasma number in various organisms (Anderson *et al.*, 2003; Pigozzi and Solari, 1999; Zickler and Kleckner, 1999). RNs consist of DNA and proteins. Using immunocytochemical methods, RNs were shown to contain enzymes required for recombination of DNA molecules. Studies conducted with various model organisms (fungi, plants, and animals) demonstrated that chiasmata are formed precisely at the chromosome loci where RNs

are located (Stack and Anderson, 2001; Zickler and Kleckner, 1999). RNs serve as ultrastructural compartments of recombination enzymes, or, returning to the house analogy, “kitchen space” within the “house,” that is, the SC (Fig. 12). Several “processors” (“kitchen robots”)—recombination enzymes (for conversion and crossing over)—successively operate in RNs

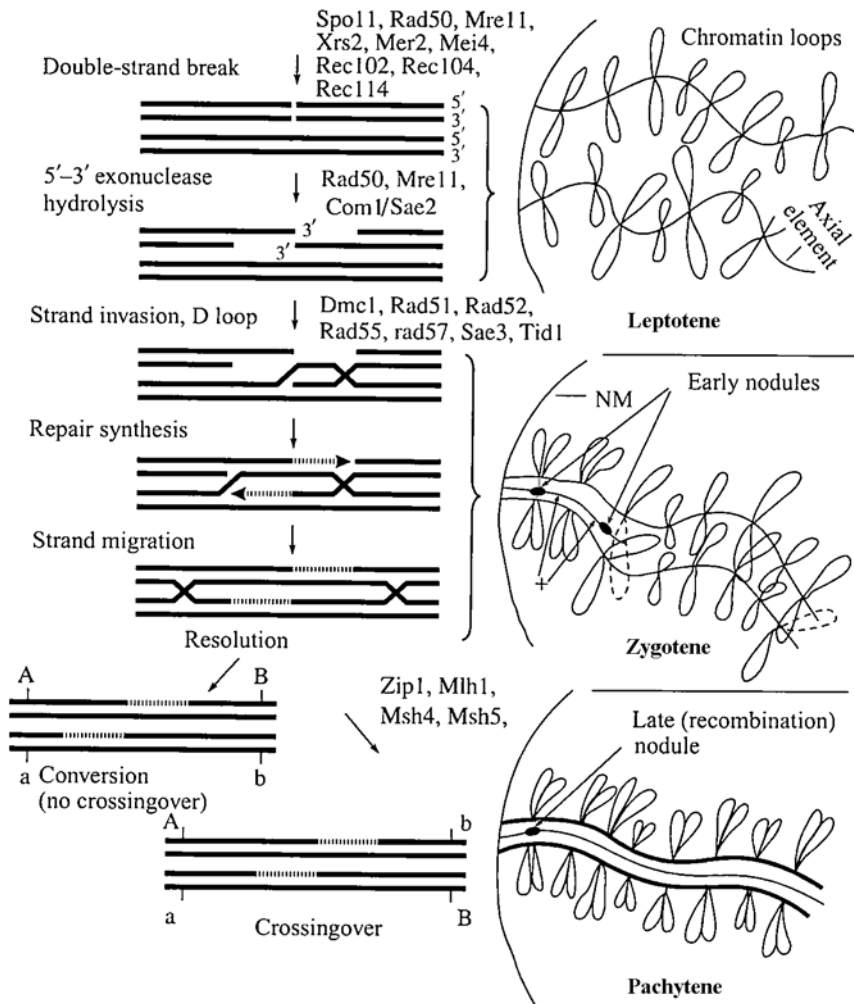


FIG. 12 Correlation between steps in DNA recombination and in SC formation and function. Recombination enzymes, stages of meiotic prophase I, and morphological structures of chromosomes and SC are given; (+) indicates the forming SC central element; NM is the nuclear membrane. (From Bogdanov, 2003.)

(Bishop, 1994; Moens *et al.*, 2002; Tarsounas *et al.*, 1999). Some of the recombination enzymes are borrowed by meiotic cells from somatic ones, which use the molecular mechanism of recombination to repair double-strand DNA breaks; some others of these enzymes are specific for meiosis. The meiosis-specific enzymes serve to increase the efficiency of meiotic recombination. Figure 12 shows the progression of DNA recombination as the SC forms and functions and the operation of some recombination enzymes during meiotic prophase I.

The recombination rate in meiosis is 100–1000 times higher than in mitosis. This is because meiotic recombination is programmed by a set of genes whose protein products cause site-specific double-strand breaks in recombination hot spots. A complex of these proteins is located in early meiotic nodules, which are in the SC central space. Of all recombination proteins, we will consider those of the RecA-Rad51 family, because they are probably crucial for homologous recombination in all kingdoms of prokaryotes and eukaryotes. These proteins are of interest in the context of this discussion because, during recombination, they form large nucleoprotein recombination intermediates in which an important role is played not only by the primary structure, but also by the capability of producing 3D structures.

B. RecA-Rad51 Protein Family

In contrast to evolutionarily neutral SC proteins, recombination enzymes exhibit considerable homology even between members of different kingdoms. The key recombination enzyme, Rad51, is a RecA-like protein inherited by eukaryotes from bacteria. RecA plays a key role in homologous recombination in prokaryotes, being essential for transferring single-stranded DNA (ssDNA) and integrating it in double-stranded DNA. This role has been reproduced *in vitro*. RecA cooperatively interacts with DNA in the presence of ATP. About 100 RecA molecules cover ssDNA in the form of a right-hand helix (Roca and Cox, 1997) so that ssDNA is 1.5-fold longer as compared with double-stranded DNA in the B conformation. RecA expedites a search for a homologous sequence in double-stranded DNA, and the ssDNA-RecA complex is considered to be a key intermediate in homology searching (Egelman, 2001). The *recA* gene has been isolated from more than 65 eubacteria (Eisen, 1995) and three archaebacteria (Sandler *et al.*, 1996). Archaeabacteria have RadA, a RecA homolog. In eukaryotes, RecA-like proteins proved to be similarly essential for homologous recombination and are conserved. The first RecA analog was found in budding yeasts (Aboussekra *et al.*, 1992; Shinohara *et al.*, 1992) and was designated as Rad51.

Eukaryotes possess a family of genes homologous to *RecA/Rad51*. Homology is restricted to a region similar to the Walker consensus nucleotide

sequence. The proteins encoded by these genes are Rad51 paralogs. These are Rad55 and Rad57 in *S. cerevisiae* and Rad51B, Rad51C, Rad51D, Xrcc2, and Xrcc3 in human. One of the function of these paralogs is to promote the landing of Rad51 on ssDNA (Sung *et al.*, 2003; Symington, 2002). A fraction containing the paralogs contains Holliday junctions (Liu *et al.*, 2004), which are recombination intermediates. In addition to Rad51, its meiosis-specific homolog Dmc1 was found in *S. cerevisiae* and other eukaryotes (Bishop *et al.*, 1992). Both Rad51 and Dmc1 proved to function during meiosis (Bishop, 1994), but Dmc1 functions only in meiosis and plays no role in DNA repair in somatic cells.

1. Rad51 and Dmc1 Proteins

Rad51 is required for meiotic and mitotic recombination and for DNA repair in somatic cells (Sonoda *et al.*, 1998). This protein is evolutionarily conserved: its primary structure has 50% identity in yeast and human (Shinohara *et al.*, 1993). Like RecA, Rad51 cooperatively interacts with ssDNA to form a right-hand helical filament. This process depends on ATP and is required for ssDNA transfer during recombination (Egelman, 2001; Ogawa *et al.*, 1993). Other proteins of the complex (RPA)—Rad52, Rad55–Rad57, and Rad54—continue recombination initiated by the interaction of Rad51 with ssDNA (Symington, 2002).

Dmc1 is expressed only during meiosis. This protein is also conserved and has 50% identity to Rad51 (Bishop *et al.*, 1992; Habu *et al.*, 1996). Dmc1 forms octameric structures and binds to DNA in the form of a ring. In yeast and human, Dmc1 expedites the formation of a D-loop in double-strand DNA and, then, ssDNA assimilation by the D-loop and renaturation with one of the D-loop single strands (Gupta *et al.*, 2001; Hong *et al.*, 2001; Masson *et al.*, 1999). It is surprising that Dmc1 is absent from ascomycetes *Neurospora* and *Sordaria*, nematode *C. elegans*, and fly *Drosophila*. According to Shinohara and Shinohara (2004), a possible explanation is that yeast Rad51 is less efficient in transferring ssDNA than bacterial RecA and, consequently, needs the assistance of Dmc1 in organisms with large chromosomes such as mammals and flowering plants, whereas Rad51 of *Neurospora*, nematode and fly does not need such assistance. Experiments with the *dmc1* and *rad51* mutants suggest that Dmc1 is required for transferring ssDNA through a distance greater than usual between sister chromatids of eukaryotic chromosomes containing more DNA than in *Neurospora*, *C. elegans*, and *Drosophila*, because the *dmc1* mutant lack single-strand invasion (SEI) into the D loop with the formation of joint molecules (DNA molecules with double Holliday junctions), while SEI between sister chromatids is preserved. Dmc1 expedites homologous recombination (Bishop *et al.*, 1999; Schwacha and Kleckner, 1997). Ample experimental evidence obtained with the single

and double *dmc1* and *rad51* mutants testifies that Rad51 is indispensable to eukaryotic recombination, whereas mutations associated with a loss or a weakening of the Dmc1 function are less detrimental to recombination and the recombination-dependent development of meiosis (Shinohara and Shinohara, 2004).

Foci of fluorescent antibodies against Rad51 and Dmc1 were observed on zygotene meiotic chromosomes of *S. cerevisiae*, *Lilium longiflorum*, and mouse (Bishop, 1994; Tarsounas *et al.*, 1999; Terasawa *et al.*, 1995). Immuno-gold antibodies for RecA-like proteins were localized on early meiotic nodules of *L. longiflorum* SCs (Anderson *et al.*, 1997). This is a cytological demonstration that Rad51 and Dmc1 are early recombination proteins. The presence of Rad51 in zygotene chromosomes is a prerequisite to the subsequent appearance of Dmc1, whereas the appearance of Rad51 foci on chromosomes does not depend on the preliminary binding of Dmc1. This conclusion is based on results obtained with the *rad51* and *dmc1* mutants of yeasts (Bishop, 1994; Shinohara *et al.*, 1997) and with knockout mice (Pittman *et al.*, 1998). Immunocytochemical detection with EM showed that Rad51 and Dmc1 are colocalized in RNs of the mouse SC (Tarsounas *et al.*, 1999). These proteins do not produce heterodimers in the two-hybrid system (Dresser *et al.*, 1997) and, presumably, do not form heterodimeric filaments on DNA (Zickler and Kleckner, 1999). High-resolution analysis with specific antibodies suggests that, although close together, Rad51 and Dmc1 each form an independent SC-associated filament on DNA (Shinohara *et al.*, 2000).

There is a model postulating that Rad51 and Dmc1 interact with different free ends of ssDNA in the DSB region and form independent filaments on these ends (Shinohara *et al.*, 2000). On experimental evidence, only the ssDNA end that carries the Rad51 filament is involved in SEI (Hunter and Kleckner, 2001). Thus, Rad51 is essential for the landing of Dmc1 on DNA during meiotic zygotene, but the mechanism of this interaction is still unclear (Shinohara and Shinohara, 2004). Studies with the two-hybrid system revealed a weak interaction of Dmc1 with the transversal-filament protein SCP1 (Tarsounas *et al.*, 1999); immunoprecipitation yielded a complex of Dmc1 with the meiosis-specific cohesin Rec8. Moreover, the *rec8* mutant of *S. cerevisiae* is dramatically defective in recombination (Klein *et al.*, 1999). This is not surprising, because Rec8 provides a basis for the SC lateral elements (Eijpe *et al.*, 2003). There are other findings closely associating the normal function of Dmc1 with the normal development of the SC in cell nuclei.

2. Evolution of RecA-Rad51 Family Proteins

The *recA* gene was isolated from more than 65 eubacteria (Eisen, 1995) and three archaebacteria (Sandler *et al.*, 1996). In *S. cerevisiae*, Rad51 has 49% identity with Dmc1 and only 31% and 17% identity with Rad55 and Rad57,

respectively. Archaeabacterial RecA displays 42–46% similarity to *S. cerevisiae* Rad51 and Dmc1; in the case of eubacterial RecA, the similarity is 22% and 26%, respectively.

Phylogenetic analysis showed that eukaryotic *recA*-like genes have originated from duplications occurring early in evolution and involving archaeabacteria (Stassen *et al.*, 1997). The duplications gave rise to two putative monophyletic groups of *recA*-like genes. One comprises 11 orthologs of *S. cerevisiae rad51* and includes *rad51* of ascomycetes *Schizosaccharomyces pombe* and *Neurospora crassa*, basidiomycete *Coprinus cinereus*, tomato *Lycopersicon esculentum*, fly *D. melanogaster*, frog *Xenopus laevis*, chicken *Gallus gallus*, and mammals *Mus musculus* and human. The other group includes seven orthologs of *S. cerevisiae DMC1*. Sequence and phylogenetic analyses revealed vast lineage- and gene-specific differences in evolution rate for the proteins encoded by the genes of this group. Dmc1 evolved more rapidly compared with Rad51, and both proteins of fungi (especially yeasts) evolved more rapidly than their vertebrate homologs. *Drosophila* Rad51 quickly and considerably diverged from the other proteins of the group.

V. Proteins of the SMC Family

Condensation of mitotic and meiotic chromosomes is an important event in the cell cycle and is essential for preparing chromosomes for being transferred into daughter cells in anaphase regardless of the division type. Two separate processes take place. One is association (cohesion) of sister chromatids. Cohesion is a result of replication. The other process is chromosome condensation, which transforms the chromatids into physically tough rod-like structures. The resulting chromosome prepared for division consists of tightly paired, condensed chromatids. Genetic and biochemical studies have shown that protein complexes of two types, cohesins and condensins, are responsible for these processes. The core of these complexes is formed by proteins of the structural maintenance of chromosomes (SMC) family. Other SMC protein complexes are involved in dosage compensation and recombinational repair. SMC proteins are chromosomal ATPases and are conserved both among eukaryotes and among prokaryotes.

Molecules of SMC proteins consist of 1000–1500 amino-acid residues (110–170 kDa) and reach 100 nm in length. Their molecular organization is similar: the N-terminal globular domain with the Wolker A nucleotide-binding motif and the C-terminal globular domain ending with the DA box (Wolker B) have a conserved primary structure; the central joint domain is moderately conserved and is flanked by nonconserved helical domains. Most eukaryotes examined each have many SMC proteins, which group into four

major subtypes, SMC1–SMC4. SMC proteins are functionally active only as dimers. Prokaryotic proteins are homodimers, whereas eukaryotes have heterodimers of two types: SMC1–SMC3 (the core component of cohesin) and SMC2–SMC4 (the core component of condensin). In addition, two other proteins, SMC5 and SMC6, have been found to form a heterodimeric core of a DNA repair complex. Dimers interact with non-SMC proteins to form active complexes varying in function (Haering *et al.*, 2002; Hirano, 2002; Hirano and Mitchison, 1994).

Heterodimers are formed in two different ways. In the case of SMC1–SMC3, the helical domains of the SMC monomer interact intramolecularly to form a common coiled coil, whereas the N and C domains form a common globular head domain. The joint domains of the resulting intricate monomers interact to yield a heterodimer. Thus, all domains other than the joint domain are homodimeric. In the case of SMC2–SMC4, the coiled-coil and globular domains result from intermolecular interactions between the SMC2 and SMC4 monomers and the five domains are all heterodimeric (Cobbe and Heck, 2004).

The cohesin complex differs in behavior between meiosis and mitosis. The difference is that the complex is not disrupted in metaphase I to ensure the segregation of sister chromatids in meiosis I. Disruption (programmed hydrolysis) of the complex in the pericentric region does not take place until meiosis II. In prophase I, proteins of the cohesin core interact with the recombination machinery and facilitate homologous chromosome synapsis along with specific SC proteins (Eijpe *et al.*, 2000, 2003; Klein *et al.*, 1999; Pelttari *et al.*, 2001). SMC1 β , a meiosis-specific analog of SMC1, has been found in mammalian testes (Revenkova *et al.*, 2001). In addition, cohesion of mammalian meiotic chromosomes involves stromalin (STAG3), which has been isolated and is homologous to the yeast cohesin Rec11. The two proteins each replace somatic Scc3 in meiosis (Pezzi *et al.*, 2000).

SMC family proteins have a wide phylogenetic distribution from prokaryotes to eukaryotes, the latter possessing even tissue-specific forms (e.g., meiotic SMC1 β). These proteins form different complex structures (homodimers, heterodimers of two proteins), play different molecular roles, and interact differently with DNA and other proteins. However, all SMC proteins are surprisingly similar. The similarity concerns not only the primary structure of the C, N, and central (joint) domains, but also the secondary (coiled-coil) structure of the intercalating domains, which is of special importance in the context of this article. Along with the secondary structure, even the size of the domains (240–350 residues in the left domain and 280–380 residues for the right one) is conserved (Pavlova and Zakiyan, 2003). The cause of this similarity lies probably in the fundamental properties of the DNA double helix, because it is DNA that is utilized as a substrate by all proteins of the SMC family.

Analysis of the phylogenetic relationships on the basis of primary structure similarity (Cobbe and Heck, 2004; Jones and Sgouros, 2001) did not reveal any strict line with some SMC proteins originating from others, suggesting rather a simultaneous origin of all forms from a common ancestor. This finding may have nothing to do with phylogeny, demonstrating that the structure of SMC proteins is determined by their function. It is this fact that is probably reflected by the phylogenetic tree in this case.

A. SMC and Cohesin Proteins in Meiosis

In yeasts, the SMC1–SMC3 heterodimer is required for sister chromatid cohesion and DNA recombination. Mammals possess SMC1 β , a specific meiotic SMC protein. The main DNA-binding C-terminal motif of SMC1 β is highly homologous to SMC1. The N-terminal region (residues 1–150) differs from that of SMC1 by more than 50%. SMC1 β is expressed specifically in the testes and is coprecipitated with SMC3 from a nuclear extract of testicular cells. SMC1 β has been localized immunocytochemically along the axial cores and lateral elements of the SC in meiotic prophase I. In late pachytene-diplotene, SMC1 β dissociates from chromosome arms throughout the chromosome length apart from the pericentric region, where SMC1 β persists until metaphase II (Revenkova *et al.*, 2001). SMC1 β -deficient mice (both females and males) are sterile. Meiosis is blocked in pachytene in males and is highly error-prone until metaphase II in females. Yet the axial cores are shorter in prophase I, sister chromatid cohesion is weak, and recombination centers are absent (Revenkova *et al.*, 2004).

The SC formation is preceded by the formation of pro-axial elements (axial cores) with the involvement of the meiotic cohesin Rec8. Then, the meiotic cohesin SMC1 β , cohesin SMC3, and the axial-element proteins SCP2 and SCP3 form a normal axial element. In metaphase I, SMC1 β , SMC3, SCP2, and SCP3 become undetectable on chromosome arms and cluster in pericentric regions, where they persist until anaphase II. In contrast, Rec8 is located along the chromosome arms until anaphase I to ensure sister chromatid cohesion and remains detectable close to the centromeres until anaphase II. It is thought that Rec8 provides a basis for the formation of both the axial elements and recombination complexes (Eijpe *et al.*, 2003). SMC1 β has been found in all vertebrates examined (Table IV). This correlates with the presence of SCP3 in these organisms (see Table III). Moreover, SMC1 β and SCP3 colocalize on meiotic chromosomes and synchronously become detectable and undetectable through the meiotic phases (Eijpe *et al.*, 2003). Thus, the presence of SMC1 β and SCP3 in the SC lateral elements probably reflects the specifics of SC formation in vertebrates.

TABLE IV

Homologs of Specific Meiotic Cohesin SMC1 β in Different Species

Species	SMC1 β homolog
<i>Danio rerio</i>	XP_688375 (similar to SMC1 β)
<i>Oryzias latipes</i>	SMC1 β (Iwai <i>et al.</i> , 2004)
<i>Gallus gallus</i>	XP_416467 (similar to SMC1 β)
<i>Mus musculus</i>	mSMC1 β (Revenkova <i>et al.</i> , 2001)
<i>H. sapiens</i>	hSMC1 β (Revenkova <i>et al.</i> , 2001)

Data for *D. rerio* and *O. latipes* are obtained by Bogdanov *et al.* specifically for this chapter.

It should be noted that meiotic cohesins coexist with mitotic cohesins in the same cell during meiosis, rather than replacing them as believed previously. The SMC1 β + SMC3 complex is tightly associated with the SC lateral elements, whereas the SMC1 β + SMC3 complex is localized in chromatin loops and forms only single foci in the lateral elements (Prieto *et al.*, 2002). The same is true for the cohesins REC8/Rad21 (Revenkova and Jessberger, 2005). Different cohesin complexes are formed along the meiotic chromosome length. For instance, a complex of Rec8 and Rec11 is in chromosome arms and a complex of Rec8 and Psc3 is in the centromeric region in yeast *S. pombe* (Kitajima *et al.*, 2003). The preceding suggests that meiotic cohesins are synthesized to provide a specific association of the cohesin complex with SC proteins, first and foremost, with proteins of the SC lateral elements.

It appears that cohesins are responsible not only for association of sister chromatids and serve the role of axial chord for the SC lateral elements. Together with SCP3, the cohesins Rad21/Rec8 are involved in monopolar attachment of sister kinetochores during metaphase I and anaphase I (Parra *et al.*, 2003). Immunocytochemical and EM study in mouse meiosis conducted by these authors was summarized as follows: "...both proteins (Rec21 and SCP3) colocalize and are partially released from chromosome arms during late prophase I stages, although they persist at the interchromatid domain of metaphase I bivalents. ...During late prophase I SCP3 and Rad21 accumulate at centromeres, and together with the chromosomal passenger proteins INCENP and aurora-B kinase, show a complex 'double cornet'-like distribution at the inner domain of metaphase I centromeres beneath the associated sister kinetochores." Furthermore, these authors observed that Rad21 and SCP3 are displaced from centromeres during telophase I when sister kinetochores separate, and are not present at metaphase II centromeres. "Thus, we hypothesize that Rad21, and the superimposed SCP3 and SCP2, are involved in the monopolar attachment of sister

kinetochores during meiosis I, and are not responsible for the maintenance of sister-chromatid centromere cohesion during meiosis II as previously suggested," they conclude (Parra *et al.*, 2003).

Cohesins are quite conserved, although high similarity is restricted to the Rec8/Rad21 domain. For instance, *C. elegans* REC-8 and *S. cerevisiae* Rec8p have only 41.6% similarity (17.3% identity) (Pasierbek *et al.*, 2001). Analysis of the domain structure has revealed a near identical organization of the Rad21/Rec8 family proteins, which all contain the same cohesin domain. This makes it possible to assume that the difference between Rad21 and Rec8 of one organism is lower than between the analogous proteins of different organisms. To verify, we examined *in silico* the following proteins of the Rec8 family: yeast Rec8, the mouse Rec8-like protein, human REC8L1 (which was selected from the homologs found for the mouse protein by the BLAST program), *C. elegans* W02A2.6p (which is homologous to the Rad21/Rec8 family proteins and has been termed REC-8 by Pasierbek *et al.* [2001]), and variant 1 of *A. thaliana* Syn1/Dif1 (Caryl *et al.*, 2003). In addition, we searched the fish *Danio rerio* proteome for homologs of mouse Rec8 and found eight different proteins. Of these, we selected one that has been annotated as meiosis-specific cohesin. All these proteins are designated as Rec8 in the figures for convenience. For comparison, we used proteins of the Rad21 family: the well-known mouse and yeast proteins, the human Rad21-like protein, *A. thaliana* Rad21-1 variant 1 (which was chosen from several proteins annotated as Rad21 homologs), the *D. rerio* protein annotated as Rad21, and the hypothetical *C. elegans* protein containing the Rad21/Rec8 domain. At the first step, we used the TreeTop-Phylogenetic Tree Prediction program from the GeneBee package (Institute of Physico-Chemical Biology, Moscow State University; http://www2.genebee.msu.su/services/phtree_reduced.html) and analyzed the amino-acid sequence alignment for each set of proteins. The highest similarity was observed for the N-terminal region of about 80 residues and the C-terminal region of a smaller size. Interestingly, Rad21 proved to be conserved to a greater extent: several common motifs were found. Such motifs were not detected in the case of Rec8. The CDART program confirmed the results obtained for Rad21, because two Rad21/Rec8 domains were identified: a larger one at the N end of the protein molecule and a smaller one at the C end. The *A. thaliana* and *D. rerio* proteins selected from the database were fully similar in domain organization to the other proteins of the set. In the Rec8 set, all proteins also had the same two domains with the exception of the *C. elegans* and *D. rerio* proteins, each containing only the first, large Rad21/Rec8 domain. Note again that the *D. rerio* protein is annotated as a meiosis-specific cohesin in the NCBI database, whereas the *C. elegans* protein has been selected from four similar proteins on the basis of experimental findings (Pasierbek *et al.*, 2001).

We searched the *C. elegans* proteome for a homolog of yeast Rec8 with the BLAST program, but did not find any candidate.

Then, the TreeTop program was used to construct a phylogenetic tree for the full-size Rec8 and Rad21 (tree 1; Fig. 13), their N-terminal regions (200 a.a.), (tree 2, not shown), and the rest of the molecule (tree 3, not shown). On tree 1 (Fig. 13), all Rec8 proteins are clustered together, including the questionable *D. rerio* protein. All Rad21 proteins similarly formed one cluster with the exception of the *A. thaliana* protein, which was close to *C. elegans* Rec8. Tree 2 showed that homology of the N-terminal domains is greater than that of full-size proteins, because even *A. thaliana* Rad21 grouped with its homologs. The C-terminal regions proved to be more divergent because of *A. thaliana* Rad21 difference. Thus, the Rad21 and Rec8 proteins form two separate subfamilies, differing both in the main domain and in the rest of the molecule. We think that the difference is indicative of a considerable functional dissimilarity of the two proteins.

To identify the specific features of meiotic cohesins compared with their mitotic analogs, we used the MEME program (Multiple EM for Motif Elicitation, <http://meme.sdsc.edu/meme/website/intro.html>, which searches

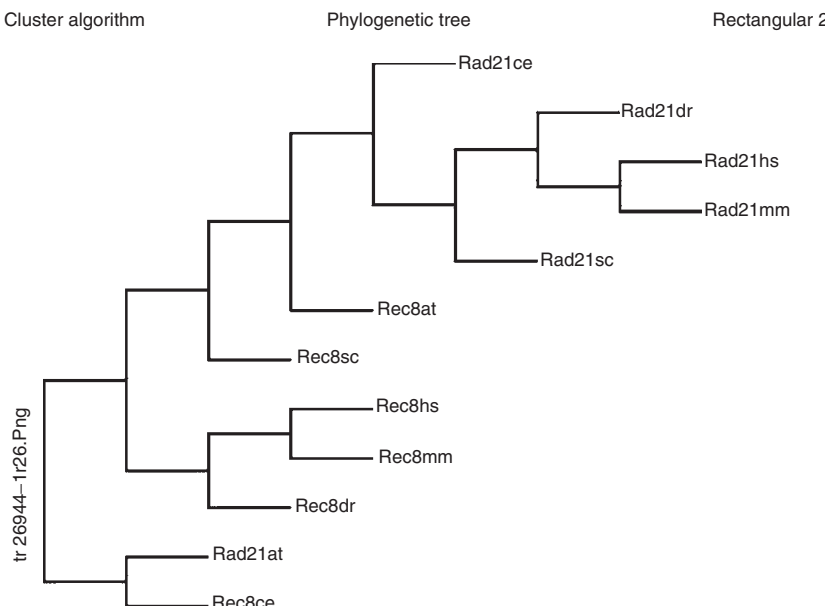


FIG. 13 Phylogenetic tree built for cohesins Rec8 and Rad21 in the following species: sc, *Saccharomyces cerevisiae*; ce, *Caenorhabditis elegans*; at, *Arabidopsis thaliana*; dr, *Danio rerio*; hs, *Homo sapiens*; mm, *Mus musculus*. For details see the text.

for consensus sequences) to analyze the detailed structure of the Rad21/Rec8 domain in these proteins. The results are shown in Fig. 14. The structure of the Rad21/Rec8 domain was near identical in all Rad21 proteins. A far greater diversity was observed in the Rec8 set. Motif 1 was obligatorily present in all of these proteins. The difference between the Rad21 and Rec8 cohesins was that the latter did not show the strict order of motifs 2, 3, and 1.

Phylogenetic trees were also constructed with the addition of *Drosophila* C(2)M, which has been assigned to the α -kleisin superfamily, which harbors Rec8 (Heidmann *et al.*, 2004). It has been noted, however, that C(2)M is a highly divergent kleisin and, according to a number of its features, acts as an SC component rather than as a cohesin. Our findings support this assumption, because C(2)M proved to lack the known conserved domains and grouped with none of the Rad21/Rec8-family proteins on the phylogenetic trees.

We analyzed the secondary structure of Rec8 and Rad21 from organisms representing different taxonomic groups. The result was quite unexpected. In general, the secondary structure, in particular, the α -helical configuration of individual regions of the protein molecule, varied greatly among different organisms. In one organism, Rec8 and Rad21 differed in structure in some cases (*A. thaliana*, *D. rerio*) and were quite similar in some others (mammals, *C. elegans*, yeasts), suggesting a multifunctional character for the two proteins. The efficient functioning of a protein needs not only a functional domain, which is responsible for the interaction with the substrate, but also

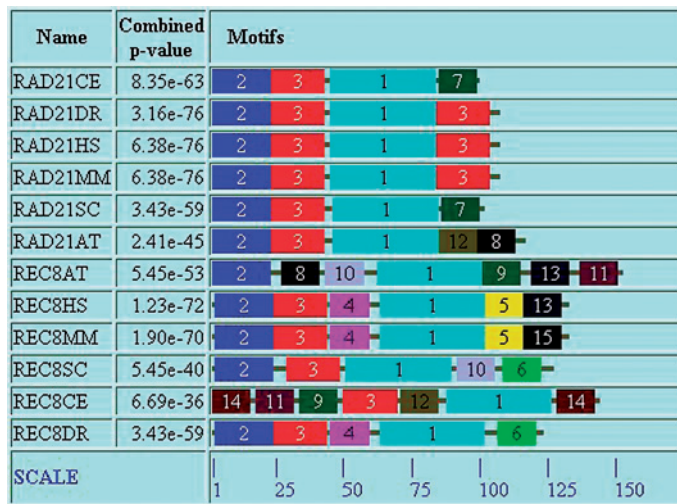


FIG. 14 Conserved motifs of the Rec8/Rad21 domain in studied species. Designations as in Fig. 13.

regions responsible for the interactions with other proteins. This role can be played (directly or indirectly) by α -helical regions. This feature is characteristic of multifunctional proteins involved in multiprotein complexes, such as the cohesin complex.

B. Protein Shugoshin Ensures Sister Chromatid Nondisjunction in Meiosis I

Members of the shugoshin protein family have been found to play the major role in preventing hydrolysis of the cohesion proteins located close to the centromere in meiotic metaphase I in fission and budding yeasts, *Z. mays*, and *Drosophila* (Hamant *et al.*, 2005; Katis *et al.*, 2004; Kerrebrock *et al.*, 1995; Kitajima *et al.*, 2004; Marston *et al.*, 2004; Rabitsch *et al.*, 2004). Shugoshins are localized only in the centromeric and pericentric regions of chromosomes and only in metaphase I and are absent from chromosomes during mitosis. Mutations inactivating the shugoshin genes cause a premature loss of cohesion and premature segregation of sister chromatids during meiosis I. As the earlier studies have revealed, such mutations include *sgo1* in yeasts, *zmsgol-1* in *Z. mays*, and classical *mei-S332* in *D. melanogaster*.

As is the case with other genes known to be meiosis-specific, expression of the shugoshin genes is not restricted to meiosis. However, the *zmsgol1* phenotype is expressed only during meiosis owing to the coordination of molecular processes in the cell nucleus. In maize, ZmSGO1 is in centromeric and pericentric regions of chromosomes: this protein colocalizes with the cohesin Rec8 and prevents its hydrolysis during metaphase I (Hamant *et al.*, 2005). In *Z. mays*, protein AFD1 is a REC8 homolog, and ZmSGO1 loading is AFD1/ZmREC8 dependent (i.e. ZmSGO1 recruitment to chromosomes requires REC8-regulated sister chromatid cohesion). In *afdl-3*, a weak *afdl* allele, in which AFD1 protein level is very low but not null, immunolocalization experiments showed that ZmSGO1 foci were visible, although their intensity was reduced compared to that of wild-type meiocytes (Hamant *et al.*, 2005). These results strongly suggest that SGO1 localization in maize is dependent on REC8. In contrast, Shugoshin recruitment has been shown to be REC8 independent in yeast and *Drosophila*, and MEI-S332 in *Drosophila* assembles even onto unreplicated chromatids (Kitajima *et al.*, 2004; Lee *et al.*, 2004).

REC8 is present all along the arms from leptotene, but at metaphase I ZmSGO1 localizes only at pericentromeric regions of chromosomes. It could mean that ZmSGO1 recruitment at the centromere does not rely on AFD1/ZmREC8 only and could depend also on centromeric- and pericentromeric-specific proteins (Kitajima *et al.*, 2003). The presence of conserved regions within the Shugoshin family has been previously proposed to be required for Shugoshin centromere localization (Lee *et al.*, 2004). Although ZmSGO1

contains both conserved regions, the recruitment of ZmSGO1 to the centromeres is different than for other Shugoshins, suggesting that regulation of Shugoshin's recruitment to chromosomes does not rely only on these regions.

The coincidence of functions with a lack of primary structure homology has been observed for the yeast and *Drosophila* and maize genes responsible for suppression of cohesin hydrolysis in the pericentric region during metaphase I (Hamant *et al.*, 2005; Katis *et al.*, 2004; Kitajima *et al.*, 2004; Marston *et al.*, 2004; Rabitsch *et al.*, 2004). Thus, functional similarity of specific meiotic shugoshins in taxonomically distant organisms is due not to their amino-acid sequence similarity, but depends on one or two domains, protecting REC8-family cohesins from hydrolysis at metaphase I, and the precise temporal regulation of this protection remains to be investigated. Kitajima *et al.* (2006) have found a specific subtype of serine/threonine protein phosphatase 2A (PP2A) associated with human shugoshin. PP2A colocalizes with shugoshin at centromeres and is required for centromeric protection. Purified shugoshin complex has an ability to reverse the phosphorylation of cohesin *in vitro*, suggesting that dephosphorylation of cohesin is the mechanism of protection at centromeres. Meiotic shugoshin of fission yeast also associates with PP2A, with both proteins collaboratively protecting Rec8-containing cohesin at centromeres. Thus, these researchers have revealed a conserved mechanism of centromeric protection of eukaryotic chromosomes in mitosis and meiosis.

VI. Importance of Secondary Protein Structure for Ultrastructure Morphogenesis

The previous data allowed us to conclude that, in some cases, proteins differing in primary structure and yet having functionally important domains similar in secondary structure play the same structural role in functionally similar cells of organisms located far apart on the evolutionary ladder: ascomycetes, nematodes, insects, flowering plants, and mammals. In particular, this is the case with germ line cells dividing via meiosis, as the earlier examples demonstrate. The question is whether the same regularity is characteristic of somatic cells and is thereby universal.

Two examples best illustrate the lack of conservation of the primary structure (its neutrality) in proteins of functionally similar organelles and the important role of their secondary structure and domain organization. One is the interaction of structural proteins with DNA (proteins of the SC lateral elements) and the other is the protein–protein interaction between molecules connecting cell ultrastructures at nanometer distances (proteins of the SC central space). The latter case is of particular interest because two

surfaces, the inner surfaces of the SC lateral elements, are connected at nanometer distances, comparable to protein dimensions. Hence, we decided initially to analyze the proteins of cell structures meeting such requirements and chose the kinetochore proteins (protein-DNA interactions) and gap junctions in cell-to-cell contacts.

A. Kinetochore Proteins

Among the 40 kinetochore proteins identified in mammals and fungi, only a few can be considered evolutionarily conserved and essential for the functioning of kinetochores (Cheo, 1997). One of them is the mammalian protein CENPC, which forms the inner kinetochore surface exposed to chromatin. The protein Mif2p is its yeast homolog. These proteins are very similar, but their similarity is restricted to two small blocks of amino-acid residues (Brown, 1995; Meluh and Koshland, 1995). Region I of Mif2p consists of 52 residues and is similar by 43% to the corresponding region of human CENPC. A temperature-sensitive mutation *mif* is known for each region, suggesting that the conserved area serves as a functional domain (Brown, 1995). Both CENPC and Mif2p have characteristics essential for binding to DNA, although no absolutely specific DNA-binding area has been found. The homology of the two proteins and their genes is most evident from the phenotypes determined by the *cenpc* and *mif2* mutations. Each mutation leads to aberrant segregation of chromosomes (Fukagawa and Brown, 1997; Kalitsis *et al.*, 1998). Taking into account these and the preceding findings, it can be concluded that human CENPC and yeast Mif2p are homologous in the Vavilovian sense, because their mutational variation leads to similar cell phenotypes. This phenomenon proved to be even more significant when a similar protein of the inner surface of kinetochores was found in maize *Z. mays* L. Five variants of this protein all have region I of 23 amino acids at the C end, which shows 61% and 74% homology to the corresponding region of yeast Mif2p and human CENPC, respectively (Dawe *et al.*, 1999). No homology was found in region II. One of the five variants, CenpC, was isolated from anthers at synchronous prophase I of meiosis. CenpC is homologous by 78–95% to the other four variants, isolated from 13-day embryos, germinating seeds, young shoots, and young (2 week) leaves, and can be considered meiosis-specific. The specificity for meiosis is insignificant in this case; it is more important that the DNA-binding regions of all these proteins in yeasts, maize, and human have a high degree of homology. It is important that, in the course of biological evolution, nature selected only one protein variant capable of binding to the centromeric DNA, which markedly differs in primary structure between yeasts and mammals.

B. Connexins and Innexins (Pannexins)

Examples of functional and topological similarity of proteins differing in primary structure (amino-acid sequence) can be found beyond meiosis. One is provided by gap junction proteins, which occur in a wide range of multicellular organisms and ensure cell-to-cell contacts by forming transport channels.

Intercellular gap contacts are similar in structure and function among vertebrates and invertebrates; yet they are formed by proteins belonging to different families. The proteins have no primary structure homology, and their genes differ in nucleotide sequence (Phelan and Starich, 2001; Stebbins *et al.*, 2000). The structure and dimensions of channels are strongly uniform owing to a similar domain organization of the corresponding proteins, connexins (in vertebrates) and innexins (in invertebrates). Orthologs of connexins have not been found in invertebrates (Stebbins *et al.*, 2000), whereas innexins are similar to several vertebrate proteins and the whole family is known as pannexins (Pestova, 2005).

More than 40 connexins and more than 30 innexins are known today; the number of the corresponding genes (homologs and orthologs) has reached 245 (Pestova, 2005). Genes coding for the gap junction proteins substantially vary in size. For instance, the human pannexin genes range from 8799 to 48,230 bp (Pestova, 2005). The size variation is determined by different sizes of the gene region coding for the C-terminal domain and the sizes of introns. In addition, the genes vary in organization, each including 2–5 exons. Notwithstanding the great differences in size and structure of their genes, the gap junction proteins differ in size to a far lesser extent. The protein size varies from 392 to 697 amino-acid residues in mouse and human. *Drosophila* innexins are similar in size to the mouse and human proteins: Inx2 and Inx3 consist of 367 and 395 residues, respectively (Pestova, 2005; Stebbins *et al.*, 2000).

Innexins/pannexins and connexins are similar in the distribution of hydrophobic amino acid residues and in topology: each has four transmembrane domains (TMDs), two extracellular loops, and one cytoplasmic loop (Fig. 15). The TMDs cross the plasma membrane four times. The two terminal domains are embedded into the cytoplasm. The C-terminal domain and the intracellular loop are the most variable regions of the deduced gap junction protein. In contrast, the N-terminal and central domains are conserved to the greatest extent (Phelan and Starich, 2001; Shibata *et al.*, 2001; Stebbins *et al.*, 2000; von Maltzahn *et al.*, 2004). For instance, human PANX1 and mouse Panx1 have nearly identical N-terminal domains and different C-terminal domains. All four TMDs and the loops between them belong to a C-terminal region of ~300 amino-acid residues (Pestova, 2005). It is characteristic of the gap junction proteins that the second extracellular loop

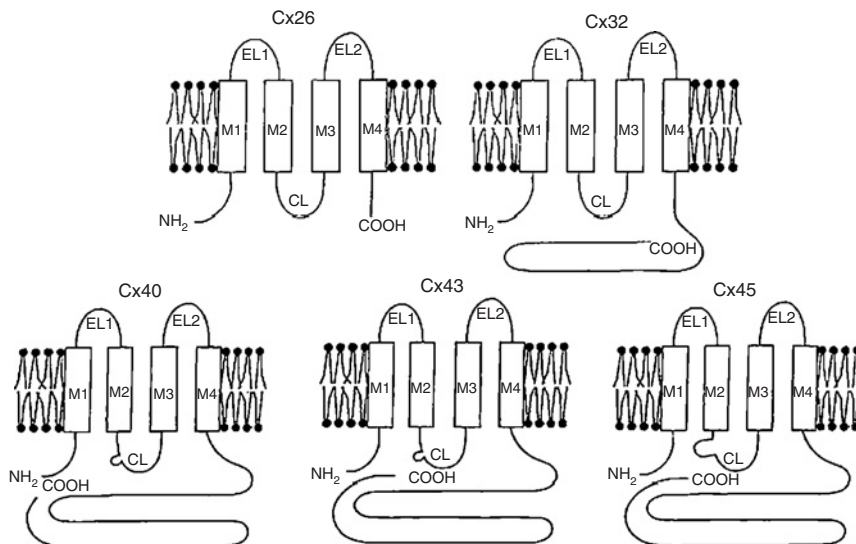


FIG. 15 Schematic drawing of molecular configurations of connexin proteins. The alpha group (Cx43 and Cx40) contains larger cytoplasmic loops than the beta group (Cx32 and Cx26), but smaller loops than Cx45. (From Shibata *et al.*, 2001, with permission from the Japanese Society for Clinical Molecular Morphology.)

harbors two conserved cysteines and the second TMD has a conserved proline (Foote *et al.*, 1998; Pestova, 2005; Suchyna *et al.*, 1993). The greatest similarity has been observed for the two first TMDs and the region between them (Pestova, 2005).

In addition, gap junction proteins possess several functionally important short motifs. The key determinant regulating the transfer of connexin to the membrane to assemble a transport channel is in the first TMD (Martin *et al.*, 2001). The third TMD and the C-terminal domain (amino-acid residues 207–219) are necessary for integration of connexins into the membrane and for their correct assembly (oligomerization). The C-terminal domain contains a cytoplasmic calmodulin-binding site, which is important for the assembly of hetero-oligomers (Ahmad *et al.*, 2001; Martin *et al.*, 2000).

As mentioned previously, connexins and innexins (pannexins) are non-homologous in amino-acid sequence. Although considerably varying in extent, homology exists within each family. Innexins vary in amino-acid sequence to a greater extent compared with connexins. Only a few amino acid residues of the conserved region are invariant in innexins (Hua *et al.*, 2003). Yet *Drosophila* innexins have orthologs, for instance, in the *C. elegans*, silkworm *Bombyx mori*, and grasshopper *Schistocerca americana* proteomes. *Drosophila* innexins have 29–47% homology to each other, Inx2 has 76% homology to Sa-Inx(2) of *S. americana*, and its N end has 84% homology to the corresponding

region of *B. mori* Bm-Inx2. In addition, Bm-Inx(2) shows 86% homology to the N-terminal region of Sa-Inx(2) (Stebbins *et al.*, 2000). Likewise, human and mouse connexins are similar to each other (mouse mCx39 and human hCx40.1 have 60% homology), although only some members of the family have orthologs in the other genome (von Maltzahn *et al.*, 2004; Willecke *et al.*, 2002).

Pannexins have been found in insects, worms, and mollusks. As for vertebrates, only human and mouse pannexins are known (PANX1-PANX3 and Panx1-Panx3, respectively) (Baranova *et al.*, 2004). All pannexins are quite conserved. For instance, the mouse PANX2 gene has six orthologs in the *C. elegans* genome (Pestova, 2005). Human pannexins display about 50% homology to each other, although homology between particular human pannexins and their mouse counterparts reaches 94% (Pestova, 2005).

Gap junctions play a role in embryo development, homeostasis, and synchronous muscle contractions. Channels provide for metabolic and electric communication between cells by transporting low-molecular-weight compounds of no more than 1 kDa: inorganic salts, ions, and metabolites (Shibata *et al.*, 2001; Stebbins *et al.*, 2000; Willecke *et al.*, 2002). The gap between the membranes of adjacent cells is 3 nm. Two adjacent cells assembly a transport channel toward each other. The resulting halves are then joined as a lock and a key. One half consists of six monomers, either identical (homomeric channels) or different (heteromeric channels) (Stebbins *et al.*, 2000). When an organ contains several gap junction proteins, their distribution is specific for particular cells, depending on the substances transported (Shibata *et al.*, 2001).

What are the causes of the high similarity of secondary and tertiary structures among dozens of gap junction proteins from evolutionarily distant organisms? Two causes are obvious: the specific function and the arrangement of channels in the cell membrane. The cell needs transport channels for a narrow range of small metabolites, which imposes limitations on the number and dimensions of the TMDs of channel components. On the other hand, the cell membrane itself is similar in structure and dimensions in different multicellular organisms, which can well determine the similarity of transport channels incorporated in the membrane. The intercellular space width, which is 3 nm in the gap junction region, is probably optimal for the exact joining of two half-channels produced by two adjacent cells.

C. Nuclear Pore Proteins

The nuclear pore provides another example of the correspondence between the secondary structure of proteins to the size and functions of the cell organelle formed by them. Nuclear pores go across the nuclear membrane

and connect the nucleoplasm with the cytoplasm, providing for passive transport of small metabolites, export of proteins into the nucleus, and import of mRNAs from the nucleus. The maximal size of transportable macromolecules is 25 nm (10 nm in amoebae) (Allen *et al.*, 2000). Several hundreds of nuclear pores constitute the nuclear pore complex (NPC) of the cell. The nuclear pore is a highly regular and symmetrical structure. The NPC consists of several groups of protein nucleoporins (Nups) (Fig. 16), existing in a nuclear pore complex in 8–32 copies (Cronshaw *et al.*, 2002; Rout *et al.*, 2000). Proteins of different groups playing different functions considerably differ from each other in structure, while proteins of one group are organized similarly.

The core structures of yeast and vertebrate NPCs are similar at the electron-microscopic level, but the amino-acid sequence similarity of the relevant Nups is only 25–30% on average (Allen *et al.*, 2000; Ryan and Wente, 2000). About

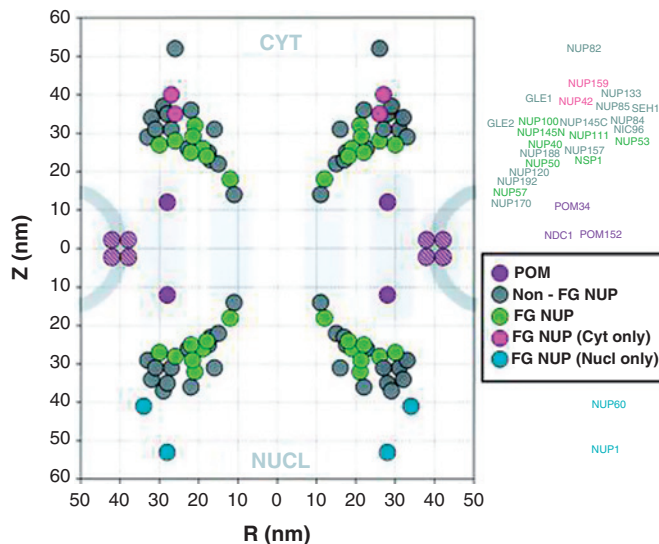


FIG. 16 Plot of the position of nucleoporins in the NPC. Statistical analysis of the distribution of the gold particles in each montage allows determination of the position of the proteins relative to the NPC cylindrical axis (R) and mirror plane of pseudosymmetry (Z). The plotted circle size was arbitrarily chosen for the sake of clarity. A mask for a cross-section of the yeast NPC and pore membrane is shown schematically to scale in light gray. We have highlighted the FG nups, the majority of which were found on both sides of the NPC (green), and a few that were found toward the periphery and exclusively on the nuclear side (blue) or the cytoplasmic side of the NPC (red). Most of the non-FG nups (dark gray) were found on both sides. The integral membrane protein Pom34p (purple) was close to the membrane, as were the inferred positions of Pom152p and Ndc1p (purple stripes). (From Rout *et al.*, 2000, with permission from the authors.)

two thirds of all Nups are conserved in structure and function. Because of their larger sizes and complexity, some vertebrate NPC proteins lack orthologs in the yeast proteome. For instance, this is the case with Nup37, Nup43, Nup358, gp210, POM121, and ALADIN (Cronshaw *et al.*, 2002). Some mammalian Nups each have several yeast orthologs. For instance, Nup98 contains domains specific for yeast Nup145p and Nup116p (Ryan and Wente, 2000), however Nup155 is similar to Nup157p/Nup170p (Cronshaw *et al.*, 2002). Notwithstanding these differences, conservation involves not only the symmetrical core structure of the NPC, but also complexes of peripheral Nups. Speaking more exactly, it is the structure and function of particular domains and their position in the NPC that are conserved among various organisms (Rout and Aitchison, 2001).

Let us consider the most interesting groups of NPC proteins. Nups, which often contact several partners, harbor various functional domains. Most Nups contain repeats (for more detail, see Table IV of Cronshaw *et al.*, 2002). Of these, the FG repeats are best studied. The FG repeats have been found in half of NPC proteins, including eight major. The repeat unit contains from two, phenylalanine and glycine (FG), to five (FXFG, FGXN, GLFG, KPXFS/TFG) amino-acid residues. FG-Nups occur throughout the NPC and are especially abundant in peripheral filaments. These proteins interact specifically with many transport factors. Many FG-Nups display low similarity to several proteins of the same proteome and several representatives of other proteomes. The similarity of FG-Nups is restricted to the repeat-containing region. It is possible that the unique domains have developed more recently and are responsible for the functional difference between the corresponding yeast and vertebrate proteins (Davis, 1995).

Nup145p is of particular interest. Its C-terminal domain shows homology to vertebrate Nup96 and Nups of *Schizosaccharomyces pombe* and *C. elegans* (Ryan and Wente, 2000). The N-terminal domain contains the GLFG repeats and an RNA-binding motif and is homologous to yeast Nup100p and Nup116p, rat and human Nup98, and the same Nups of *S. pombe* and *C. elegans* that have homology to the C-terminal domain. A region of 190 a.a. has 78% similarity between Nup100p and Nup116p and 55% with Nup145p. This region harbors a conserved octapeptide that resembles the consensus characteristic of single-stranded nucleic acid-binding proteins (Davis, 1995).

Another interesting group of NPC proteins includes pore membrane proteins (POMs). Only a few POMs are known (Davis, 1995). Vertebrate gp210 lacks yeast orthologs; its N-terminal domain is in the lumen of the nuclear envelope (NE). Of the two hydrophobic segments present in this region, only one serves as a transmembrane domain. The other possibly interacts with the NE lipid bilayer or other similar proteins to form the pore membrane. Likewise, POM121 have been found only in vertebrates. This protein has

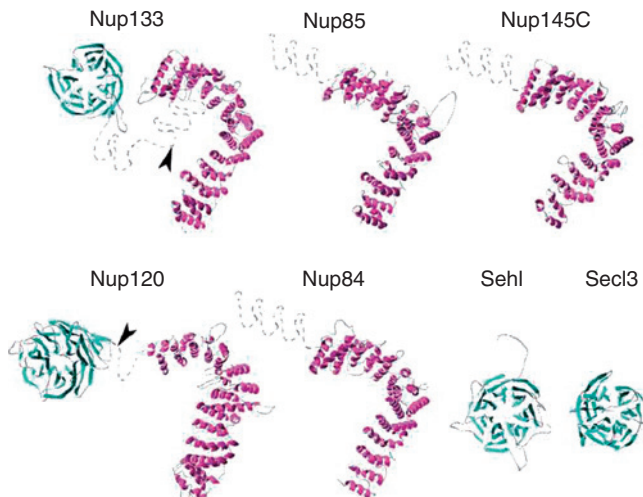


FIG. 17 Ribbon representation of Nup models. β -sheets (β -propellers) are colored cyan and α -helices (α -solenoids) are colored magenta. Gray dashed lines indicate regions that were not modeled. Arrowheads indicate the positions of high proteolytic susceptibility. (From Devos *et al.*, 2004, with permission from the authors.)

one transmembrane domain, while its major part, including the XFXFG repeats, is a component of the NPC core.

Three proteins of this group are known in yeasts: Pom34p, Ndc1p, and Pom152p, the last two forming a complex. Pom152p has one transmembrane domain; part of the protein is in the NE lumen (Davis, 1995). Again, though absolutely lacking similarity in amino-acid sequence, pore membrane proteins are similar in organization, location, and function. The *y*Nup84/*v*Nup107–160 subcomplex (of yeasts and vertebrates, respectively), which is a component of the NPC core, is of interest in three respects. First, all seven components of the yeast subcomplex have vertebrate homologs. Second, proteins of this subcomplex are highly similar in organization to membrane proteins of cytoplasmic-coated vesicles. Coated vesicles ensure endocytosis and vesicular traffic between the Golgi complex, lysosomes, and ER. Sec13p and Seh1p occur both in the NPC, and in coated vesicles. Third, these proteins have domains that form a β -propeller, an α -solenoid, or a combination of both (Fig. 17). The propeller is formed of several blades arranged around the central axis. Each blade consists of four-strand antiparallel β -sheets. In the α -solenoid, many pairs of antiparallel α -helices are stacked to produce a rigid structure. Nup85p exemplifies a combination of the two structures, consisting of α -helices to about 50%, loops to 23%, and turns to 5%; the rest is represented by β -sheets (Devos *et al.*, 2004).

The proteins ySec13 and ySeh1 are single-domain β -propellers of six and seven blades, respectively. These proteins represent the class of WD-repeat proteins (tryptophan-aspartic acid). Vertebrate Sec13L is related to yeast Sec13p and Seh1p (30% and 34% identity and 47% and 54% similarity, respectively). Human Sec13R is homologous to Sec13p both in amino acid sequence (50% and 66%) and in function (Cronshaw *et al.*, 2002). The structure of the protein components of the yNup84 complex is conserved not only among yeasts and vertebrates, but in *A. thaliana*, although the amino-acid sequence homology is low (Devos *et al.*, 2004). Thus, the NPC is a highly organized structure whose components, though differing in organization, are quite conserved at the level of domain structure and function among all eukaryotes examined from yeasts to human.

VII. Conclusion: Organelle Morphology as Dependent on the Protein Structure

The cytological mechanism of meiosis is highly conserved among all eukaryotes. Some meiosis-specific structural proteins of yeasts, plant *A. thaliana*, nematode *C. elegans*, *Drosophila*, and mammals play the same roles during meiosis, but do not have primary structure (amino-acid sequence) homology. However, such proteins are similar in domain organization and conformation. Yeast and plant enzymes involved in meiotic recombination possess similar epitopes. These findings testify that the similarity of higher-order organization allows specific meiotic proteins to form analogous subcellular structures, produce similar cytological patterns of meiosis, and determine similar functions of the corresponding subcellular structures. All these factors lead eventually to conservation of the scheme of meiosis among evolutionarily distant eukaryotes.

The gap between homologous chromosomes rendered parallel in meiotic prophase I was observed long ago under a microscope and was termed synaptic space, or synaptic gap, in cytology. It was unclear what factors maintain chromosomes at a certain distance from each other, with the gap preserved. This problem was resolved by the discovery of the well-structured SC. We have attempted to explain the molecular nature of the structural uniformity (i.e., evolutionary conservation) of the SC central space, that is, a gap within the SC, in evolutionarily distant eukaryotes. This and other examples allowed us to conclude that the structural and functional similarity of the same organelle in evolutionarily distant organisms is due to conformational similarity of the important structural and functional proteins of these organelles. These and other examples demonstrate that structural and functional similarity of the same organelles in evolutionarily distant organisms is

due to conformational similarity of structurally and functionally important domains of the proteins forming these organelles. Three-dimensional (3D) subcellular structures are formed necessarily by 3D proteins, which are ordered in supramolecular complexes in nanometer spaces. Principles of self-assembly of macromolecules into large complexes by a simple aggregation of macromolecules with predefined, rigid complementary structures as well as by domain rearrangements were reviewed by Namba (2001). Different types of self-assembling protein associations and a generalized theory of physical mechanisms of self-assembly were reviewed and discussed by Kentsis and Borden (2004).

Supramolecular structures—such as enzyme complexes, ribosomes, protein fibers, viruses, and membranes—are not synthesized as whole giant molecules linked covalently; they are rather assembled as a result of non-covalent aggregation of macromolecular subunits. A review by Rajagopal and Schneider (2004) presents a number of examples of noncovalent associations of peptides and proteins that make supramolecular architectures, such as ribbons, nanotubules, monolayers with nanoscale order, as well as varieties of lateral and facial assembly of unfolded peptides that lead to fibril growth, etc.

In the case of meiosis, some of these models can be used to explain assembly of the rodlike domains of fibrillar SCP1 in the structured space of the “synaptic gap” between homologous chromosomes, and assembly of protein globules into the crystal-like lattice composing SC lateral elements shown in Fig. 4B. The use of protein subunits for assembling large structures has several advantages. First, a lower amount of genetic information is needed for repetitive small subunits. Second, the assembly and dissociation of subunits is easily controllable, because subunits are linked together by many relatively weak (noncovalent) bonds. This allows a correction mechanism, which is capable of removing damaged subunits during assembly.

The experience of cell biologists provide, at least, two evidences of self-assembly of SC elements into SC-like polycomplexes. The first one was found by Bogdanov (1977) in *Ascaris* males meiosis as well as by Fiil *et al.* (1977) in *Ascaris* female meiosis when they found polymerization of SC material into polycomplexes shed from chromatin and located in cytoplasm of leptotene cells. It meant that DNA or chromatin did not promote the assembling of these polycomplexes and “polymerization” went spontaneously in cytoplasm prior to synapsis of chromosomes within the nuclei. The second example was described by Ollinger *et al.* (2005). They experimentally expressed SCP1 in a heterologous system (i.e., in COS-7 cells that normally do not express SC proteins). It was demonstrated that under these experimental conditions SCP1 is able to form structures that closely resemble SCs (i.e., polycomplexes). Moreover, it was shown that mutations modifying the length of the central α -helical domain of SCP1 influence the width of polycomplexes.

Finally, Ollinger *et al.* demonstrate that deletions of the nonhelical N- or C-termini both affect polycomplex assembly, although in a different manner. The conclusion was made that SCP1 is a primary determinant of SC assembly that plays a key role in synapsis of homologous chromosomes (Ollinger *et al.*, 2005).

Mentioning these fundamental concepts supported by experimental evidences, we emphasize that they can well explain the conservation of meiosis among eukaryotes. The scheme of meiosis is based on the properties of particular proteins and nucleoprotein complexes. Moreover, self-assembling structures can consist of different protein subunits and nucleic acids, as demonstrated long ago for viruses and, more recently, ribosomes. Here we call attention to the fact that protein domains similar in dimensions and spatial organization (conformation) can serve as components of the same subcellular structures in phylogenetically distant organisms even when the primary structures of these domains greatly differ.

We specifically tried to apply the aforementioned principles to different subcellular structures, such as cell gap contacts and nuclear pore complexes, trying to demonstrate that these principles are “working” not only within the frame of meiosis, but may have much more broad application in cell biology.

There is a special issue of *Chromosoma* (2006) volume 115, # 3 devoted to the 50-year anniversary of the discovery of synaptonemal complex. Some problems discussed here are described therein and discussed from different points of view. The issue opens with an article by Moses (2006) describing the history of the discovery of the synaptonemal complex in 1956 and adaptation of synaptonemal complex as a tool for cytogenetics.

REFERENCES

Abussekhra, A., Chanet, R., Adjiri, A., and Fabre, F. (1992). Semidominant suppressors of Srs2 helicase mutations of *Saccharomyces cerevisiae* map in the *RAD51* gene, whose sequence predicts a protein with similarities to prokaryotic RecA proteins. *Mol. Cell. Biol.* **12**, 3224–3234.

Ahmad, S., Martin, P. E., and Evans, W. H. (2001). Assembly of gap junction channels: Mechanism, effects of calmodulin antagonists and identification of connexin oligomerization. *Eur. J. Biochem.* **268**, 4544–4552.

Allen, T. D., Cronshaw, J. M., Bagley, S., Kiseleva, E., and Goldberg, M. W. (2000). The nuclear pore complex: Mediator of translocation between nucleus and cytoplasm. *J. Cell Sci.* **113**, 1651–1659.

Anderson, L. K., Doyle, G. G., Brigham, B., Carter, J., Hooker, K. D., Lai, A., Rice, M., and Stack, S. M. (2003). High-resolution crossover maps for each bivalent of *Zea mays* using recombination nodules. *Genetics* **165**, 849–865.

Anderson, L. K., Offenberg, H. H., Verkuijlen, W. M. H. C., and Heyting, C. (1997). RecA-like proteins are components of the meiotic nodules in lily. *Proc. Natl. Acad. Sci. USA* **94**, 6868–6873.

Anderson, L. K., Royer, S. M., Page, S. L., McKim, K. S., Lai, A., Lilly, M. A., and Hawley, R. S. (2005). Juxtaposition of C(2)M and the transverse filament protein C(3)G within the central region of *Drosophila* synaptonemal complex. *Proc. Natl. Acad. Sci. USA* **102**, 4482–4487.

Anuradha, S., and Muniyappa, K. (2004). *Saccharomyces cerevisiae* Hop1 zinc finger motif is the minimal region required for its function *in vitro*. *J. Biol. Chem.* **279**, 28961–28969.

Anuradha, S., and Muniyappa, K. (2005). Molecular aspects of meiotic chromosome synapsis and recombination. *Prog. Nucleic Acid Res. Mol. Biol.* **79**, 49–132.

Armstrong, S. J., Caryl, A. P., Jones, G. H., and Franklin, F. C. H. (2002). Asy1, a protein required for meiotic chromosome synapsis, localizes to axis-associated chromatin in *Arabidopsis* and *Brassica*. *J. Cell Sci.* **115**, 3645–3655.

Baranova, A., Ivanov, D., Petrash, N., Pestova, A., Skoblov, M., Kelmanson, I., Shagin, D., Nazarenko, S., Geraymovych, E., Litvin, O., Tiunova, A., Born, T. L., et al. (2004). The mammalian pannexin family is homologous to the invertebrate innexin gap junction proteins. *Genomics* **83**, 706–716.

Bishop, D. K. (1994). RecA homologs Dmc1 and rad51 interact to form multiple nuclear complexes prior to meiotic chromosome synapsis. *Cell* **79**, 1081–1092.

Bishop, D. K., Park, D., Xu, L., and Kleckner, N. (1992). *DMC1*: A meiosis-specific yeast homolog of *E. coli recA* required for recombination, synaptonemal complex formation, and cell-cycle progression. *Cell* **69**, 439–456.

Bishop, D. K., Nikolski, Y., Oshiro, J., Chon, J., Shinohara, M., and Chen, X. (1999). High copy number suppression of the meiotic arrest caused by a *dmc1* mutation: *REC114* imposes an early recombination block and *RAD54* promotes a *DMC1*-independent DSB repair pathway. *Genes Cells* **4**, 425–444.

Bogdanov, Yu. F. (1977). Formation of cytoplasmic synaptonemal-like polycomplexes at leptotene and normal synaptonemal complexes at zygotene in *Ascaris suum* male meiosis. *Chromosoma* **61**, 1–21.

Bogdanov, Yu. F. (2003). Variation and evolution of meiosis. *Rus. J. Genet.* **39**, 363–381.

Bogdanov, Yu. F., Dadashev, S. Ya., and Grishaeva, T. M. (2002b). Comparative genomics and proteomics of *Drosophila*, Brenner's Nematode, and *Arabidopsis*. Identification of functionally similar genes and proteins of synapsis of meiotic chromosomes. *Rus. J. Genet.* **38**, 908–917.

Bogdanov, Yu. F., Dadashev, S. Ya., and Grishaeva, T. M. (2003). *In silico* search for functionally similar proteins involved in meiosis and recombination in evolutionarily distant organisms. *In Silico Biol.* **3**, 173–185.

Bogdanov, Yu. F., Grishaeva, T. M., and Dadashev, S. Ya. (2002a). Gene *CG17604* of *Drosophila melanogaster* may be a functional homolog of yeast gene *ZIP1* and mammal gene *Sep1* (*SYCP1*) encoding proteins of the synaptonemal complex. *Rus. J. Genet.* **38**, 108–112.

Botelho, R. J., DiNicolo, L., Tsao, N., Karaiskakis, A., Tarsounas, M., Moens, P. B., and Pearlman, R. E. (2001). The genomic structure of *SYCP3*, a meiosis-specific gene encoding a protein of the chromosome core. *Biochim. Biophys. Acta* **1518**, 294–299.

Brown, M. T. (1995). Sequence similarity between the yeast chromosomal segregation protein Mif2 and the mammalian centromere protein CENP-C. *Gene* **160**, 111–116.

Carlton, P. M., and Cande, W. Z. (2002). Telomeres act autonomously in maize to organize the meiotic bouquet from a semipolarized chromosome orientation. *J. Cell Biol.* **157**, 231–242.

Carpenter, A. T. C. (1988). Thoughts on recombination nodules, meiotic recombination, and chiasmata. In “Genetic recombination” (R. Kucherlapati and G. R. Smith, Eds.), pp. 549–574. American Society for Microbiology, Washington, DC.

Carpenter, A. T. C. (1994). The recombination nodule story—seeing what you are looking at. *BioAssays* **16**, 69–74.

Caryl, A. P., Jones, G. H., and Franklin, F. C. H. (2003). Dissecting plant meiosis using *Arabidopsis thaliana* mutants. *J. Exp. Bot.* **54**, 25–38.

Chen, Y.-T., Venditti, C. A., Theiler, G., Stevenson, B. J., Iseli, C., Gure, A. O., Jongeneel, C. V., Old, L. J., and Simpson, A. J. G. (2005). Identification of CT46/HORMAD1, an immunogenic cancer/testis antigen encoding a putative meiosis-related protein. *Cancer Immun.* **5**, 1–8.

Cheo, K. H. A. (1997). “The centromere.” Oxford University Press, New York.

Chervitz, S. A., Aravind, L., Sherlock, G., Ball, C. A., Koonin, E. V., Dwight, S. S., Harris, M. A., Dolinski, K., Mohr, S., Smith, T., Weng, S., Cherry, J. M., et al. (1998). Comparison of the complete protein sets of worm and yeast: Orthology and divergence. *Science* **282**, 2022–2028.

Chua, P. R., and Roeder, G. S. (1998). Zip2, a meiosis-specific protein required for the initiation of chromosome synapsis. *Cell* **93**, 349–359.

Cobbe, N., and Heck, M. M. (2004). The evolution of SMC proteins: Phylogenetic analysis and structural implications. *Mol. Biol. Evol.* **21**, 332–347.

Cronshaw, J. M., Krutchinsky, A. N., Zhang, W., Chait, B. T., and Matunis, M. J. (2002). Proteomic analysis of the mammalian nuclear pore complex. *J. Cell Biol.* **158**, 915–927.

Davis, L. I. (1995). The nuclear pore complex. *Ann. Rev. Biochem.* **64**, 865–896.

Dawe, R. K., Reed, L. M., Yu, H.-G., Muszynski, M. G., and Hiatt, E. N. (1999). A maize homolog of mammalian CENPC is a conservative component of the inner kinetochore. *Plant Cell* **11**, 1227–1238.

Dernburg, A. F., McDonald, K., Moulder, G., Barstead, R., Dresser, M., and Villeneuve, A. M. (1998). Meiotic recombination in *C. elegans* initiates by a conserved mechanism and is dispensable for homologous chromosome synapsis. *Cell* **94**, 387–398.

Devos, D., Dokudovskaya, S., Alber, F., Williams, R., Chait, B. T., Sali, A., and Rout, M. P. (2004). Components of coated vesicles and nuclear pore complexes share a common molecular architecture. *PLoS Biol.* **2**, e380.

Dobson, M. J., Pearlman, R. E., Karaiskakis, A., Spyropoulos, B., and Moens, P. B. (1994). Synaptonemal complex proteins: Occurrence, epitope mapping and chromosome disjunction. *J. Cell Sci.* **107**, 2749–2760.

Dong, H., and Roeder, G. S. (2000). Organization of the yeast Zip1 protein within the central region of the synaptonemal complex. *J. Cell Biol.* **148**, 417–426.

Dresser, M. E., Ewing, D. J., Conrad, M. M., Dominguez, A. M., Barstead, R., Jiang, H., and Kodadek, T. (1997). *DMC1* functions in a *Saccharomyces cerevisiae* meiotic pathway that is largely independent of the *RAD51* pathway. *Genetics* **147**, 533–544.

Egelman, E. H. (2001). Does a stretched DNA structure dictate the helical geometry of RecA-like filaments? *J. Mol. Biol.* **309**, 539–542.

Eijpe, M., Heyting, C., Gross, B., and Jessberger, R. (2000). Association of mammalian SMC1 and SMC3 proteins with meiosis chromosomes and synaptonemal complexes. *J. Cell Sci.* **113**, 673–682.

Eijpe, M., Offenberg, H., Jessberger, R., Revenkova, E., and Heyting, C. (2003). Meiotic cohesin REC8 marks the axial elements of rat synaptonemal complexes before cohesins SMC1 and SMC3. *J. Cell Biol.* **160**, 657–670.

Eisen, J. A. (1995). The RecA protein as a model molecule for molecular systematic studies of bacteria: Comparison of trees of RecAs and 16S rRNAs from the same species. *J. Mol. Evol.* **41**, 1105–1123.

Fedotova, Yu. S., Bogdanov, Yu. F., Gadzhieva, S. A., Sosnikhina, S. A., Smirnov, V. G., and Mikhailova, E. I. (1994). Meiotic mutants of rye, *Secale cereale* L. II. The nonhomologous synapsis in desynaptic mutants *sy7* and *sy10*. *Theor. Appl. Genet.* **88**, 1029–1036.

Fiil, A., Goldstein, P., and Moens, P. B. (1977). Precocious formation of synaptonemal-like polycomplexes and their subsequent fate in female *Ascaris lumbricoides* var. *suum*. *Chromosoma* **65**, 21–36.

Foote, C. I., Zhou, L., Zhu, X., and Nicholson, B. J. (1998). The pattern of disulfide linkages in the extracellular loop regions of connexin 32 suggests a model for the docking interface of gap junctions. *J. Cell Biol.* **140**, 1187–1197.

Fukagawa, T., and Brown, T. (1997). Efficient conditional mutation of the vertebrate CENPC gene. *Hum. Mol. Genet.* **6**, 2301–2308.

Golubovskaya, I. N., Harper, L. C., Pawlowski, W. P., Schichnes, D., and Cande, W. Z. (2002). The *pam1* gene is required for meiotic bouquet formation and efficient homologous synapsis in maize (*Zea mays* L.). *Genetics* **162**, 1979–1993.

Gorach, G. G., Safronov, V. V., Kolomiets, O. L., and Bogdanov, Yu. F. (1985). Biochemical and ultrastructural analyses of synaptonemal complex in mammalian spermatocytes. *Tsitolgya (Leningrad)* **27**, 1347–1352.

Grishaeva, T. M., Dadashev, S. Y., and Bogdanov, Yu. F. (2001). Gene *CG17604* of *Drosophila melanogaster* predicted *in silico* may be the *c(3)G* gene. *Drosophila Info. Serv.* **84**, 84–88.

Grishaeva, T. M., Dadashev, S. Ya., and Bogdanov, Yu. F. (2004). Computer search and analysis of synaptonemal complex proteins in the Nematode *Caenorhabditis elegans*. *Biomeditsinskaya Khimiya (Moscow)* **50**, 3–10.

Gupta, R. C., Golub, E., Bi, B., and Radding, C. M. (2001). The synaptic activity of HsDmc1, a human recombination protein specific to meiosis. *Proc. Natl. Acad. Sci. USA* **98**, 8433–8439.

Habu, T., Taki, T., West, A., Nishimune, Y., and Morita, T. (1996). The mouse and human homologs of *DMC1*, the yeast meiosis-specific homologous recombination gene, have a common unique form of exon-skipped transcript in meiosis. *Nucleic Acids Res.* **24**, 470–477.

Haering, C. H., Lowe, J., Hochwagen, A., and Nasmyth, K. (2002). Molecular architecture of SMC proteins and the yeast cohesion complex. *Mol. Cell.* **9**, 773–788.

Hamant, O., Golubovskaya, I., Meeley, R., Fiume, E., Timofejeva, L., Schleiffer, A., Nasmyth, K., and Cande, W. Z. (2005). A Rec8-dependent shugoshin is required for maintenance of centromeric cohesion during meiosis and has no mitotic functions. *Curr. Biol.* **15**, 948–954.

Havekes, F. W. J., de Jong, J. H., Heyting, C., and Ramanna, M. S. (1994). Synapsis and chiasma formation in four meiotic mutants of tomato (*Lycopersicon esculentum*). *Chrom. Res.* **2**, 315–325.

Hawley, R. S., McKim, K. S., and Arbel, T. (1993). Meiotic segregation in *Drosophila melanogaster* females: Molecules, mechanisms, and myths. *Annu. Rev. Genet.* **27**, 281–317.

Heidmann, D., Horn, S., Heidmann, S., Schleiffer, A., Nasmyth, K., and Lehner, C. F. (2004). The *Drosophila* meiotic kleisin C(2)M functions before the meiotic divisions. *Chromosoma* **113**, 177–187.

Heyting, C. (1996). Synaptonemal complex: Structure and function. *Curr. Opin. Cell Biol.* **8**, 389–396.

Higgins, J. D., Sanchez-Moran, E., Armstrong, S. J., Jones, G. H., and Franklin, F. C. H. (2005). The *Arabidopsis* synaptonemal complex protein ZYP1 is required for chromosome synapsis and normal fidelity of crossing over. *Genes Dev.* **19**, 2488–2500.

Hirano, T. (2002). The ABCs of SMC proteins: Two-armed ATPases for chromosome condensation, cohesion and repair. *Genes Dev.* **16**, 399–414.

Hirano, T., and Mitchison, T. J. (1994). A heterodimeric coiled-coil protein required for mitotic chromosome condensation *in vitro*. *Cell* **79**, 449–458.

Hollingsworth, N. M., Goetsch, L., and Byers, B. (1990). The *HOP1* gene encodes a meiosis-specific component of yeast chromosomes. *Cell* **61**, 73–84.

Hong, E. L., Shinohara, A., and Bishop, D. K. (2001). *Saccharomyces cerevisiae* Dmc1 protein promotes renaturation of single-strand DNA (ssDNA) and assimilation of ssDNA into homologous super-coiled duplex DNA. *J. Biol. Chem.* **276**, 41906–41912.

Hua, V. B., Chang, A. B., Tchieu, J. H., Kumar, N. M., Nielsen, P. A., and Saier, M. H. Jr. (2003). Sequence and phylogenetic analyses of 4 TMS junctional proteins of animals: Connexins, innexins, claudins and occludins. *J. Membr. Biol.* **194**, 59–76.

Hunter, N., and Kleckner, N. (2001). The single-end invasion: An asymmetric intermediate at the double-strand break to double-holliday junction transition of meiotic recombination. *Cell* **106**, 59–70.

Iwai, T., Lee, J., Yoshii, A., Yokota, T., Mita, K., and Yamashita, M. (2004). Changes in the expression and localization of cohesin subunits during meiosis in a non-mammalian vertebrate, the medaka fish. *Gene Expr.* **4**, 495–504.

Jenkins, G., and Okumus, A. (1992). Indiscriminate synapsis in achiasmate *Allium fistulosum* L. (Liliaceae). *J. Cell Sci.* **103**, 415–422.

Jones, S., and Sgouros, J. (2001). The cohesin complex: Sequence homologies, interaction networks and shared motifs. *Genome Biol.* **2**, research 0009.1–0009.12. Online since March 6, 2001.

Jones, G. H., Armstrong, S. J., Caryl, A. P., and Franklin, F. C. H. (2003). Meiotic chromosome synapsis and recombination in *Arabidopsis thaliana*; an integration of cytological and molecular approaches. *Chrom. Res.* **11**, 205–215.

Kalitsis, P., Fowler, K. J., Earle, E., Hill, J., and Choo, K. H. (1998). Target disruption of mouse centromere protein C gene leads to mitotic dissaray and early embryo death. *Proc. Natl. Acad. Sci. USA* **95**, 1136–1141.

Katis, V. L., Galova, M., Rabitsch, K. P., Gregan, J., and Nasmyth, K. (2004). Maintenance of cohesin at centromeres after meiosis I in budding yeast requires a kinetochore-associated protein related to MEI-S332. *Curr. Biol.* **14**, 560–572.

Katis, V. L., Matos, J., Mori, S., Shirahige, K., Zachariae, W., and Nasmyth, K. (2004). Spo13 facilitates monopolin recruitment to kinetochores and regulates maintenance of centromeric cohesion during yeast meiosis. *Curr. Biol.* **14**, 2183–2196.

Kentsis, A., and Borden, K. L. (2004). Physical mechanisms and biological significance of supramolecular protein self-assembly. *Curr. Protein Pept. Sci.* **5**, 125–134.

Kerrebrock, A. W., Moore, D.R., Wu, J. S., and Orr-Weaver, T. L. (1995). Mei-S332, a *Drosophila* protein required for sister-chromatid cohesion, can localize to meiotic centromere regions. *Cell* **83**, 247–256.

Kihara, H. (1927). Über das Verhalten der “end to end” gebundenen Chromosomen von *Rumex acetosella* und *Oenothera biennis* während der heterotypischen Kernteilung. *Jahrb. Wiss. Bot.* **66**, 429–460.

Kitajima, T. S., Kawashima, S. A., and Watanabe, Y. (2004). The conserved kinetochore protein shugoshin protects centromeric cohesion during meiosis. *Nature* **427**, 510–517.

Kitajima, T. S., Sakuno, T., Ishiguro, K., Shunichiro, I. S., Natsume, T., Shigehiro, A., Kawashima, A., and Watanabe, Y. (2006). Shugoshin collaborates with protein phosphatase 2A to protect cohesin. *Nature* advance online publication 15 March 2006 doi:10.1038/nature04663.

Kitajima, T. S., Yokobayashi, S., Yamamoto, M., and Watanabe, Y. (2003). Distinct cohesin complexes organize meiotic chromosome domains. *Science* **300**, 1152–1155.

Kleckner, N., Storlazzi, A., and Zickler, D. (2003). Coordinate variation in meiotic pachytene SC length and total crossover/chiasma frequency under conditions of constant DNA length. *Trends Genet.* **19**, 623–628.

Klein, F., Mahr, P., Galova, M., Buonomo, S. B. C., Michaelis, C., Nairz, K., and Nasmyth, K. (1999). A central role for cohesins in sister chromatid cohesion, formation of axial elements, and recombination during yeast meiosis. *Cell* **98**, 91–103.

La Cour, L. F., and Wells, B. (1970). Meiotic prophase in anthers of asynaptic wheat. A light and electron microscopic study. *Chromosoma* **29**, 419–427.

Lammers, J. H., Offenberg, H. H., van Aalderen, M., Vink, A. C., Dietrich, A. J., and Heyting, C. (1994). The gene encoding a major component of the lateral elements of synaptonemal complexes of the rat is related to X-linked lymphocyte-regulated genes. *Mol. Cell. Biol.* **14**, 1137–1146.

Lee, J., Iwai, T., Yokota, T., and Yamashita, M. (2003). Temporally and spatially selective loss of Rec8 protein from meiotic chromosomes during mammalian meiosis. *J. Cell Sci.* **116**, 2781–2790.

Lee, J. Y., Dej, K. J., Lopez, J. M., and Orr-Weaver, T. L. (2004). Control of centromere localization of the MEI-S332 cohesion protection protein. *Curr. Biol.* **14**, 1277–1283.

Liu, J. G., Yuan, L., Brundell, E., Bjorkroth, B., Daneholt, B., and Hoog, C. (1996). Localization of the N-terminus of SCP1 to the central element of the synaptonemal complex and evidence for direct interactions between the N-termini of SCP1 molecules organized head-to-head. *Exp. Cell Res.* **226**, 11–19.

Liu, Y., Masson, J. Y., Shah, R., O'Regan, P., and West, S. C. (2004). RAD51C is required for Holliday junction processing in mammalian cells. *Science* **303**, 243–246.

Lorenz, A., Wells, J. L., Pryce, D. W., Novatchkova, M., Eisenhaber, F., McFarlane, R. J., and Loidl, J. (2004). *S. pombe* meiotic linear elements contain proteins related to synaptonemal complex components. *J. Cell Sci.* **117**, 3343–3351.

MacQueen, A. J., Colaiacovo, M. P., McDonald, K., and Villeneuve, A. M. (2002). Synapsis-dependent and -independent mechanisms stabilize homolog pairing during meiotic prophase in *C. elegans*. *Genes Dev.* **16**, 2428–2442.

Maguire, M. P., and Riess, R. W. (1996). Synaptic defects of *asynaptic* homozygotes in maize at the electron microscopic level. *Genome* **39**, 1194–1198.

Manheim, E. A., and McKim, K. S. (2003). The synaptonemal complex component C(2)M regulate meiotic crossing over in *Drosophila*. *Curr. Biol.* **13**, 276–285.

Marston, A. L., Tham, W. H., Shah, H., and Amon, A. (2004). A genome-wide screen identifies genes required for centromeric cohesion. *Science* **303**, 1367–1370.

Martin, P. E., Steggles, J., Wilson, C., Ahmad, S., and Evans, W. H. (2000). Targeting motifs and functional parameters governing the assembly of connexins into gap junctions. *Biochem. J.* **349**, 281–287.

Martin, P. E., Blundell, G., Ahmad, S., Errington, R. G., and Evans, W. H. (2001). Multiple pathways in the trafficking and assembly of connexin 26, 32 and 43 into gap junction intercellular communication channels. *J. Cell Sci.* **114**, 3845–3855.

Martinez-Garay, I., Jablonka, S., Sutajova, M., Steuernagel, P., Gal, A., and Kutsche, K. (2002). A new gene family (FAM9) of low-copy repeats in Xp22.3 expressed exclusively in testis: Implications for recombinations in this region. *Genomics* **80**, 259–267.

Martinez-Perez, E., Shaw, P., Reader, S., Aragon-Alcaide, L., Miller, T., and Moore, G. (1999). Homologous chromosome pairing in wheat. *J. Cell Sci.* **112**, 1761–1769.

Masson, J. Y., Davies, A. A., Hajibagheri, N., Van Dyck, E., Benson, F. E., Stasiak, A. Z., Stasiak, A., and West, S. C. (1999). The meiosis-specific recombinase hDmcl forms ring structures and interacts with hRad51. *EMBO J.* **18**, 6552–6560.

Meluh, P. B., and Koshland, D. (1995). Evidence that the *Mif2* gene of *Saccharomyces cerevisiae* encodes a centromere protein with homology to the mammalian centromere protein CENP-C. *Mol. Biol. Cell.* **6**, 793–807.

Meuwissen, R. L. J., Meerts, I., Hoovers, J. M. N., Leschot, J., and Heyting, C. (1997). Human synaptonemal complex protein 1 (SCP1): Isolation and characterization of the cDNA and chromosomal localization of the gene. *Genomics* **39**, 377–384.

Meuwissen, R. L. J., Offenberg, H. H., Dietrich, A. J. J., Riesewijk, A., van Iersel, M., and Heyting, C. (1992). A coiled-coil related protein specific for the synapsed regions of meiotic prophase chromosomes. *EMBO J.* **11**, 5091–5100.

Mikhailova, E. I., Sosnikhina, S. P., Kirillova, G. A., Tikhonov, O. A., Smirnov, V. G., Jones, R. N., and Jenkins, G. (2001). Nuclear dispositions of subtelomeric and pericentromeric chromosomal domains during meiosis in *asynaptic* mutants of rye. *J. Cell Sci.* **114**, 1875–1882.

Moens, P. B., Kolas, N. K., Tarsounas, M., Marcon, E., Cohen, P. E., and Spyropoulos, B. (2002). The time course and chromosomal localization of recombination-related proteins at meiosis in the mouse are compatible with models that can resolve the early DNA-DNA interactions without reciprocal recombination. *J. Cell Sci.* **115**, 1611–1622.

Moh, C. C., and Nilan, R. A. (1954). “Short” chromosome—a mutant in barley induced by atomic bomb irradiation. *Cytologia (Tokyo)* **19**, 48–53.

Moses, M. J. (2006). A new chromosome structure is revealed. *Chromosoma* **115**, 152–154.

Namba, K. (2001). Roles of partly unfolded conformations in macromolecular self-assembly. *Genes Cells* **6**, 1–12.

Nonomura, K. I., Nakano, M., Murata, K., Miyoshi, K., Eiguchi, M., Miyao, A., Hirochika, H., and Kurata, N. (2004). An insertional mutation in the rice *PAIR2* gene, the ortholog of *Arabidopsis ASY1*, results in a defect in homologous chromosome pairing during meiosis. *Mol. Gen. Genom.* **271**, 121–129.

Offenberg, H. H., Schalk, J. A., Meuwissen, R. L., van Aalderen, M., Kester, H. A., Dietrich, A. J., and Heyting, C. (1998). SCP2: A major protein component of the axial elements of synaptonemal complexes of the rat. *Nucleic Acids Res.* **26**, 2572–2579.

Ogawa, T., Yu, X., Shinohara, A., and Egelman, E. H. (1993). Similarity of the yeast RAD51 filament to the bacterial RecA filament. *Science* **259**, 1896–1899.

Ollinger, R., Alsheimer, M., and Benavente, R. (2005). Mammalian protein SCP1 forms synaptonemal complex-like structures in the absence of meiotic chromosomes. *Mol. Biol. Cell* **16**, 212–217.

Page, S. L., and Hawley, R. S. (2001). *c(3)G* encodes a *Drosophila* synaptonemal complex protein. *Genes Devel.* **15**, 3130–3143.

Page, S. L., and Hawley, R. S. (2004). The genetics and molecular biology of the synaptonemal complex. *Annu. Rev. Cell Dev. Biol.* **20**, 525–558.

Parra, M. T., Viera, A., Gomez, R., Page, J., Carmena, M., Earnshaw, W. C., Rufas, J. S., and Suja, J. A. (2003). Dynamic relocalization of the chromosomal passenger complex proteins inner centromere protein (INCENP) and aurora-B kinase during male mouse meiosis. *J. Cell Sci.* **116**, 961–974.

Pasierbek, P., Jantsch, M., Melcher, M., Schleiffer, A., Schweizer, D., and Loidl, J. (2001). Meiotic chromosome pairing and disjunction cohesion protein with functions in *Caenorhabditis elegans*. *Genes Dev.* **15**, 1349–1360.

Pavlova, S. V., and Zakiyan, S. M. (2003). Structural protein of the SMC family (Structural Maintenance of Chromosomes) and their role in reorganization of chromatin. *Rus. J. Genet.* **39**, 1301–1316.

Pawlowski, W. P., Golubovskaya, I. N., Timofeejeva, L., Meeley, R. B., Sheridan, W. F., and Cande, W. Z. (2004). Coordination of meiotic recombination, pairing, and synapsis by PHS1. *Science* **303**, 89–92.

Pelttari, J., Hoja, M.-R., Yuan, L., Liu, J.-G., Brundell, E., Moens, P., Santucci-Darmanin, S., Jessberger, R., Barbero, J. L., Heyting, C., and Höög, C. (2001). A meiotic chromosomal core consisting of cohesin complex proteins recruits DNA recombination proteins and promotes synapsis in the absence of an axial element in Mammalian meiotic cells. *Mol. Cell. Biol.* **21**, 5667–5677.

Penkina, M. V., Karpova, O. I., and Bogdanov, Yu. F. (2002). Synaptonemal complex proteins are specific proteins of meiotic chromosomes. *Mol. Biol. (Moscow)* **36**, 397–407.

Pestova, A. A. (2005). Structural and functional characteristics of genes coding transmembrane proteins—pannexins in human and mouse. Postgraduate Thesis (in Russian). Vavilov Inst. Gen. Genet., Russ. Acad. Sci. Moscow.

Pezzi, N., Prieto, I., Kremer, L., Jurado, L. A. P., Valero, C., del Mazo, J., Martinez-A., C., and Barbero, J. L. (2000). STAG3, a novel gene encoding a protein involved in meiotic

chromosome pairing and location of STAG3-related genes flanking the Williams-Beuren syndrome deletion. *FASEB J.* **14**, 581–592.

Phelan, P., and Starich, T. A. (2001). Innexins get into the gap. *BioEssays*. **23**, 388–396.

Pigozzi, M. I., and Solari, A. J. (1999). Recombination nodule mapping and chiasma distribution in spermatocytes of the pigeon, *Columba livia*. *Genome* **42**, 308–314.

Pittman, D. E., Cobb, J., Schimenti, K. J., Wilson, E. A., Cooper, D. M., Brignull, E., Handel, M. A., and Schimenti, J. C. (1998). Meiotic prophase arrest with failure of chromosome synapsis in mice deficient for Dmcl, a germ-line-specific RecA homolog. *Mol. Cell.* **1**, 697–705.

Prieto, I., Pezzi, N., Buesa, J. M., Kremer, L., Barthelemy, I., Carreiro, C., Roncal, F., Martinez, A., Gomez, L., Fernandez, R., Martinez-A., C., and Barbero, J. L. (2002). STAG2 and Rad21 mammalian mitotic cohesins are implicated in meiosis. *EMBO Reports* **3**, 543–550.

Priming, M., Williams, R. M., Winzeler, E. A., Tevzadze, G. G., Conway, A. R., Hwang, S. Y., Davis, R. W., and Esposito, R. E. (2000). The core meiotic transcriptome of budding yeast. *Nature Genet.* **26**, 415–423.

Rabitsch, K. P., Gregan, J., Schleiffer, A., Javerzat, J. R., Eisenhaber, R., and Nasmyth, K. (2004). Two fission yeast homologs of *Drosophila* Mei-S332 are required for chromosome segregation during meiosis I and II. *Curr. Biol.* **14**, 287–301.

Rajagopal, K., and Schneider, J. P. (2004). Self-assembling peptides and proteins for nanotechnological applications. *Curr. Opin. Struct. Biol.* **14**, 480–486.

Rasmussen, S. W., and Holm, P. B. (1981). Chromosome pairing and synaptonemal complex formation. In “Molec. Bases Genet. Proc. Proc. 14th Int. Congr. Genet. 1978.” Vol. 3, Book 2. Mir Publisher, Moscow, pp. 331–342.

Revenkova, E., Eijpe, M., Heyting, C., Gross, B., and Jessberger, R. (2001). Novel meiosis-specific isoform of mammalian SMC1. *Mol. Cell. Biol.* **21**, 6984–6998.

Revenkova, E., Eijpe, M., Heyting, C., Hodges, C. A., Hunt, P. A., Liebe, B., Scherthan, H., and Jessberger, R. (2004). Cohesin SMC1 beta is required for meiotic chromosome dynamics, sister chromatid cohesion and DNA recombination. *Nat. Cell Biol.* **6**, 555–562.

Revenkova, E., and Jessberger, R. (2005). Keeping sister chromatids together: Cohesins in meiosis. *Reproduction* **130**, 783–790.

Rhoades, M. M. (1961). Meiosis. In “The Cell” (J. Brachet and A. E. Mirsky, Eds.), pp. 3–75. Academic Press, New York.

Roca, A. I., and Cox, M. M. (1997). RecA protein: Structure, function, and role in recombinational DNA repair. *Prog. Nucleic Acid Res. Mol. Bio.* **56**, 129–223.

Roeder, G. S. (1997). Meiotic chromosomes: It takes two to tango. *Genes Dev.* **11**, 2600–2621.

Rout, M. P., and Aitchison, J. D. (2001). The nuclear pore complex as a transport machine. *J. Biol. Chem.* **276**, 16593–16596.

Rout, M. P., Aitchison, J. D., Suprapto, A., Hjertaas, K., Zhao, Y., and Chait, B. T. (2000). The yeast nuclear pore complex: Composition, architecture, and transport mechanism. *J. Cell Biol.* **148**, 635–651.

Rubin, M. G., Yandell, M. D., Wortman, J. R., Gabor Miklos, G. L., Nelson, C. R., Hariharan, I. K., Fortini, M. E., Li, P. W., Apweiler, R., Fleischmann, W., Cherry, J. M., Henikoff, S., et al. (2000). Comparative genomics of the eukaryotes. *Science* **287**, 2204–2215.

Ryan, K. J., and Wente, S. R. (2000). The nuclear pore complex: A protein machine bringing the nucleus and cytoplasm. *Curr. Opin. Cell Biol.* **12**, 361–371.

Sandler, S. J., Satin, L. H., Samra, H. S., and Clark, A. J. (1996). *recA*-like genes from three archean species with putative protein products similar to Rad51 and Dmcl proteins of the yeast *Saccharomyces cerevisiae*. *Nucleic Acids Res.* **24**, 2125–2132.

Schalk, J. A. C. (1999). SCP-2, a major protein component of the axial element of synaptonemal complexes. PhD Thesis. Wageningen Agricultural University, Wageningen, The Netherlands.

Schmekel, K., and Daneholt, B. (1995). The central region of the synaptonemal complex revealed in three dimensions. *Trends Cell Biol.* **5**, 239–242.

Schmekel, K., Meuwissen, R. L., Dietrich, A. J. J., Vink, A. C. G., van Marle, J., Van Veen, H., and Heyting, C. (1996). Organization of SCP1 protein molecules within synaptonemal complex of the rat. *Exptl. Cell Res.* **226**, 20–30.

Schmekel, K., Skoglund, U., and Daneholt, B. (1993a). The three-dimensional structure of the central region in a synaptonemal complex: A comparison between rat and two insect species, *Drosophila melanogaster* and *Blaps cibrosa*. *Chromosoma* **102**, 682–692.

Schmekel, K., Wahrmann, J., Skoglund, U., and Daneholt, B. (1993b). The central region of the synaptonemal complex in *Blaps cibrosa* studied by electron microscope tomography. *Chromosoma* **102**, 669–681.

Schwacha, A., and Kleckner, N. (1997). Interhomolog bias during meiotic recombination: meiotic functions promote a highly differentiated interhomolog-only pathway. *Cell* **90**, 1123–1135.

Schwarzacher, T. (2003). Meiosis, recombination and chromosomes: a review of gene isolation and fluorescent *in situ* hybridization data in plants. *J. Exper. Bot.* **54**, 11–23.

Sherman, J. D., and Stack, S. M. (1995). Two-dimensional spreads of synaptonemal complexes from solanaceous plants. VI. High-resolution recombination nodule map for tomato (*Lycopersicon esculentum*). *Genetics* **141**, 683–708.

Shibata, Y., Kumai, M., Nishii, K., and Nakamura, K. (2001). Diversity and molecular anatomy of gap junctions. *Med. Electron Microsc.* **34**, 153–159.

Shinohara, A., and Shinohara, M. (2004). Roles of *RecA* homologues *Rad51* and *Dmc1* during meiotic recombination. *Cytogenet. Genome Res.* **107**, 201–207.

Shinohara, A., Ogawa, H., and Ogawa, T. (1992). Rad21 protein involved in repair and recombination in *S. cerevisiae* is a *RecA*-like protein. *Cell* **69**, 457–470.

Shinohara, A., Ogawa, H., Matsuda, Y., Ushio, N., Ikeo, K., and Ogawa, T. (1993). Cloning of human, mouse and fission yeast recombination genes homologous to *RAD51* and *recA*. *Nat. Genet.* **4**, 239–243.

Shinohara, A., Gasior, S., Ogawa, T., Kleckner, N., and Bishop, D. K. (1997). *Saccharomyces cerevisiae* *recA* homologues *RAD51* and *DMC1* have both distinct and overlapping roles in meiotic recombination. *Genes Cells* **2**, 615–629.

Shinohara, M., Gasior, S. L., Bishop, D. K., and Shinohara, A. (2000). Tid1/Rdh54 promotes colocalization of *rad51* and *dmc1* during meiotic recombination. *Proc. Natl. Acad. Sci. USA* **97**, 10814–10819.

Shoeman, R. L., and Traub, P. (1993). Assembly of intermediate filaments. *BioEssays* **15**, 605–611.

Smith, A. V., and Roeder, G. S. (1997). The yeast Red1 protein localizes to the cores of meiotic chromosomes. *J. Cell Biol.* **136**, 957–967.

Smith, A. V., and Roeder, G. S. (2000). Cloning and characterization of the *Kluyveromyces lactis* homologs of the *Saccharomyces cerevisiae* *RED1* and *HOP1* genes. *Chromosoma* **109**, 50–61.

Smith, P. A., and King, R. C. (1968). Genetic control of synaptonemal complexes in *Drosophila melanogaster*. *Genetics* **60**, 335–351.

Solari, A. J. (1998). Structural analysis of meiotic chromosomes and synaptonemal complexes in higher vertebrates. *Methods Cell. Biol.* **53**, 235–256.

Sonoda, E., Sasaki, M. S., Buerstedde, J. M., Bezzubova, O., Shinohara, A., Ogawa, H., Takata, M., Yamaguchi-Iwai, Y., and Takeda, S. (1998). Rad51-deficient vertebrate cells accumulate chromosomal breaks prior to cell death. *EMBO J.* **17**, 598–608.

Sosnikhina, S. P., Fedotova, Yu. S., Smirnov, V. G., Mikhailova, E. I., Kolomiets, O. L., and Bogdanov, Yu. F. (1992). Meiotic mutants in rye *Secale cereale* L. I. Synaptic mutant *sy1*. *Theor. Appl. Genet.* **84**, 979–984.

Sosnikhina, S. P., Mikhailova, E. I., Tikholiz, O. A., Priyatina, S. N., Smirnov, V. G., Dadashev, S. Y., Kolomiets, O. L., and Bogdanov, Y. F. (2005). Meiotic mutations in rye *Secale cereale* L. *Cytogenet. Genome Res.* **109**, 215–220.

Stack, S. M., and Anderson, L. K. (2001). A model for chromosome structure during the mitotic and meiotic cell cycles. *Chromosome Res.* **9**, 175–198.

Stassen, N. Y., Logsdon, Jr. J. M., Vora, G. J., Offenberg, H. H., Palmer, J. D., and Zolan, M. E. (1997). Isolation and characterization of *rad51* orthologs from *Coprinus cinereus* and *Lycopersicon esculentum*, and phylogenetic analysis of eukaryotic *recA* homologs. *Curr. Genet.* **31**, 144–157.

Stebbins, L. A., Todman, M. G., Phillips, R., Greer, C. E., Tam, J., Phelan, P., Jacobs, K., Bacon, J. P., and Davies, J. A. (2000). Gap junctions in *Drosophila*: Developmental expression of the entire innexin gene family. *Mol. Biol. Cell* **11**, 2459–2470.

Steinert, P. M. (1990). The two-chain coiled-coil molecule of native epidermal keratin intermediate filaments is a type I-type II heterodimer. *J. Biol. Chem.* **265**, 8766–8774.

Stewart, M. (1993). Intermediate filament structure and assembly. *Curr. Opin. Cell Biol.* **5**, 3–11.

Suchyna, T. M., Xu, L. X., Gao, F., Fourtner, C. R., and Nicholson, B. J. (1993). Identification of a proline residue as a transduction element involved in voltage gating of gap junctions. *Nature* **365**, 847–849.

Sung, P., Krejci, L., Van Komen, S., and Sehorn, M. G. (2003). Rad51 recombinase and recombination mediators. *J. Biol. Chem.* **278**, 42729–42732.

Suzuki, M., and Yagi, N. (1991). Structure of the SPXX motif. *Proc. Biol. Sci.* **246**, 231–235.

Swanson, C. P. (1960). “Cytology and cytogenetics.” Macmillan, London.

Sym, M., and Roeder, G. S. (1995). Zip1-induced changes in synaptonemal complex structure and polycomplex assembly. *J. Cell Biol.* **128**, 455–466.

Sym, M., Engebrecht, J., and Roeder, G. S. (1993). ZIP1 is a synaptonemal complex protein required for meiotic chromosome synapsis. *Cell* **72**, 365–378.

Symington, L. S. (2002). Role of *RAD52* epistasis group genes in homologous recombination and double-strand break repair. *Microbiol. Mol. Biol. Rev.* **66**, 630–670.

Tarsounas, M., Morita, T., Pearlman, R. E., and Moens, P. B. (1999). RAD51 and DMC1 form mixed complexes associated with mouse meiotic chromosome cores and synaptonemal complexes. *J. Cell Biol.* **147**, 207–220.

Terasawa, M., Shinohara, A., Hotta, Y., Ogawa, H., and Ogawa, T. (1995). Localization of RecA-like recombination proteins on chromosomes of the lily at various meiotic stages. *Genes Dev.* **9**, 925–934.

Timofeeva, L. P., and Golubovskaya, I. N. (1991). A new type of desynaptic gene in maize identified by microscopy of synaptonemal complexes. *Tsitolgiya (Leningrad)* **33**, 3–8.

Trelles-Sticken, E., Dresser, M. E., and Scherthan, H. (2000). Meiotic telomere protein Ndj1p is required for meiosis-specific telomere distribution, bouquet formation, and efficient homologue pairing. *J. Cell Biol.* **151**, 95–106.

Tung, K. S., and Roeder, G. S. (1998). Meiotic chromosome morphology and behavior in *zip1* mutants of *Saccharomyces cerevisiae*. *Genetics* **149**, 817–832.

Vavilov, N. I. (1987). Zakon gomologicheskikh ryadov v nasledstvennoi izmenchivosti (The law of homological series in hereditary variation). Nauka, Leningrad.

von Maltzahn, J., Euwens, C., Willecke, K., and Sohl, G. (2004). The novel mouse connexin39 gene is expressed in developing striated muscle fibers. *J. Cell Sci.* **117**, 5381–5392.

von Wettstein, D., Rasmussen, S. W., and Holm, P. B. (1984). The synaptonemal complex in genetic segregation. *Annu. Rev. Genet.* **18**, 331–413.

Willecke, K., Eiberger, J., Degen, J., Eckardt, D., Romualdi, A., Guldenagel, M., Deutsch, U., and Sohl, G. (2002). Structural and functional diversity of connexin genes in the mouse and human genome. *Biol. Chem.* **383**, 725–737.

Woltering, D., Baumgartner, B., Bagchi, S., Larkin, B., Loidl, J., De Los Santos, T., and Hollingsworth, N. M. (2000). Meiotic segregation, synapsis, and recombination checkpoint functions require physical interaction between the chromosomal proteins Red1p and Hop1p. *Mol. Cell. Biol.* **20**, 6646–6658.

Zetka, M. C., Kawasaki, I., Strome, S., and Müller, F. (1999). Synapsis and chiasma formation in *Caenorhabditis elegans* require HIM-3, a meiotic chromosome core component that functions in chromosome segregation. *Genes Dev.* **13**, 2258–2270.

Zickler, D. (1973). Fine structure of chromosome pairing in ten Ascomycetes meiotic and premeiotic (mitotic) synaptonemal complexes. *Chromosoma* **40**, 401–416.

Zickler, D. (2006). From early homologue recognition to synaptonemal complex formation. *Chromosoma*. DOI 10.1007/s00412-006-0048-6.

Zickler, D., and Kleckner, N. (1998). The leptotene to zygotene transition of meiosis. *Ann. Rev. Genet.* **32**, 619–697.

Zickler, D., and Kleckner, N. (1999). Meiotic chromosomes: Integrating structure and function. *Ann. Rev. Genet.* **33**, 603–754.

Fibroblast Differentiation in Wound Healing and Fibrosis

Ian A. Darby* and Tim D. Hewitson†

*School of Medical Sciences, RMIT University, Melbourne, Australia

†Department of Nephrology, The Royal Melbourne Hospital;

Department of Medicine, University of Melbourne, Melbourne, Australia

The contraction of granulation tissue from skin wounds was first described in the 1960s. Later it was discovered that during tissue repair, fibroblasts undergo a change in phenotype from their normal relatively quiescent state in which they are involved in slow turnover of the extracellular matrix, to a proliferative and contractile phenotype termed myofibroblasts. These cells show some of the phenotypic characteristics of smooth muscle cells and have been shown to contract *in vitro*. In the 1990s, a number of researchers in different fields showed that myofibroblasts are present during tissue repair or response to injury in a variety of other tissues, including the liver, kidney, and lung. During normal repair processes, the myofibroblastic cells are lost as repair resolves to form a scar. This cell loss is via apoptosis. In pathological fibroses, myofibroblasts persist in the tissue and are responsible for fibrosis via increased matrix synthesis and for contraction of the tissue. In many cases this expansion of the extracellular matrix impedes normal function of the organ. For this reason much interest has centered on the derivation of myofibroblasts and the factors that influence their differentiation, proliferation, extracellular matrix synthesis, and survival. Further understanding of how fibroblast differentiation and myofibroblast phenotype is controlled may provide valuable insights into future therapies that can control fibrosis and scarring.

KEY WORDS: Fibroblast, Myofibroblast, Wound healing, Fibrosis, Actin, Apoptosis, Collagen. © 2007 Elsevier Inc.

I. Introduction

Fibroblasts are present in many tissues in the body, normally in a relatively quiescent state and are mainly responsible for the production and turnover of extracellular matrix (ECM) molecules. It has been approximately 35 years since it was first reported that fibroblasts are also capable of changing during tissue repair processes to a contractile phenotype involved both in increased extracellular matrix production and contraction during the repair process. Since that time, much interest has centered on the control of this cell and, in particular, the factors that control fibroblast phenotype, proliferation, extracellular matrix production, and their disappearance as tissue repair resolves. It is now apparent that the fibroblast and the differentiated cell it gives rise to, the myofibroblast, is involved in tissue repair or the response to injury in many tissues in the body and is also an important cell in numerous pathological settings, particularly pathological fibrosis and scarring in a number of organs and in the stromal response around tumors. In this review we will discuss the various roles of the myofibroblast, its derivation, control of its phenotype, and its disappearance during scar resolution.

II. Inflammation and Wound Healing

A. Inflammation

Tissue repair in all organs begins with inflammation, which represents the defining biological response to trauma in adults. Inflammatory reactions are triggered by a diverse range of events including, among others, physical injury, infection, and exposure to toxins. In the case of physical trauma, platelet aggregation forms a hemostatic plug and blood coagulation forms the provisional matrix. Platelets release growth factors and adhesive proteins that stimulate the inflammatory response and induce cell migration via chemotaxis into the wound environment. Likewise, in immunological and toxic injuries, the immune response triggers the recruitment of inflammatory cells.

Important cells involved in the process include hematogenous cells, and associated resident macrophages and lymphocytes. In the early stages of acute inflammation, polymorphonuclear granulocytes (polymorphs) are the predominant infiltrating leucocytes. If the tissue is infected by pus-producing bacteria, there is sustained and enhanced polymorph infiltration. If the bacteria survive long enough, abscess formation may result. The resulting pus consists of polymorphs, cell debris, and exudate (Ryan and Majno, 1977).

Subsequently the intensity of the inflammatory response subsides and the polymorph infiltration is replaced by monocyte infiltration. Polymorphous

clear cells are lost during this phase by apoptosis. When the monocyte reaches the extravascular tissue it undergoes transformation into the larger phagocytic macrophage, which is then involved in removal of debris. Following activation, macrophages also secrete a wide range of biologically active mediators that are involved in tissue destruction (proteases, oxygen-derived free radicals), chemotaxis (cytokines, chemokines), vascular hemodynamics (thromboxane A₂, prostaglandins), and fibrogenesis (growth factors, “remodeling” matrix metalloproteinases [MMPs] including collagenases and elastase) (Robbins and Cotran, 2004). However, heterogeneity exists among macrophage populations, with different stimuli producing different activation states. Kupffer cells in the liver are resident macrophages with a similar role in liver inflammation through release of reactive oxygen species and cytokines (Bataller and Brenner, 2005). In chronic inflammation, macrophage accumulation persists with their numbers supplemented by local proliferation (Ren *et al.*, 1991) and recirculation (Lan *et al.*, 1993).

B. Wound Healing

Wound healing is the universal response to the inflammation that follows injury. It consists of a series of consecutive but overlapping events: these include cell proliferation, migration, extracellular matrix deposition (collectively known as fibrogenesis), resolution, and remodeling (Fig. 1).

The provisional fibrin–fibronectin matrix acts as a scaffold for cell adhesion and migration. In cutaneous wounds, keratinocytes start migrating to fill the wound defect within hours. Local proliferation of these cells is important in larger wounds where migration of cells alone is insufficient to close the defect. In addition, keratinocytes are a major source of growth factors that stimulate fibrogenesis and angiogenesis in the tissue below; these include transforming growth factor-beta (TGF β), vascular endothelial growth factor (VEGF), epidermal growth factor (EGF), and keratinocyte growth factor (KGF). The induction of these factors is driven at least in part by factors such as the hypoxia caused by the loss of vascular perfusion in this area, and subsequent induction of hypoxia-inducible transcription factors. Fibroblasts quickly move into the provisional matrix, and are the principal basis of fibrogenesis. Their rapid proliferation is an important early event in response to injury, mitogenesis exponentially increasing at the site of injury within days in a renal model of injury (Hewitson *et al.*, 1995), and also in skin wounds. Fibroblasts are the main source of the ECM proteins, mostly collagen and fibronectin, that constitutes the newly formed granulation tissue thereby providing structural integrity to the wound, while specialized fibroblasts, called myofibroblasts, provide the force for wound contraction, an efficient and important part of wound closure. Importantly, fibrogenesis continues as long as these cells persist in the wound;

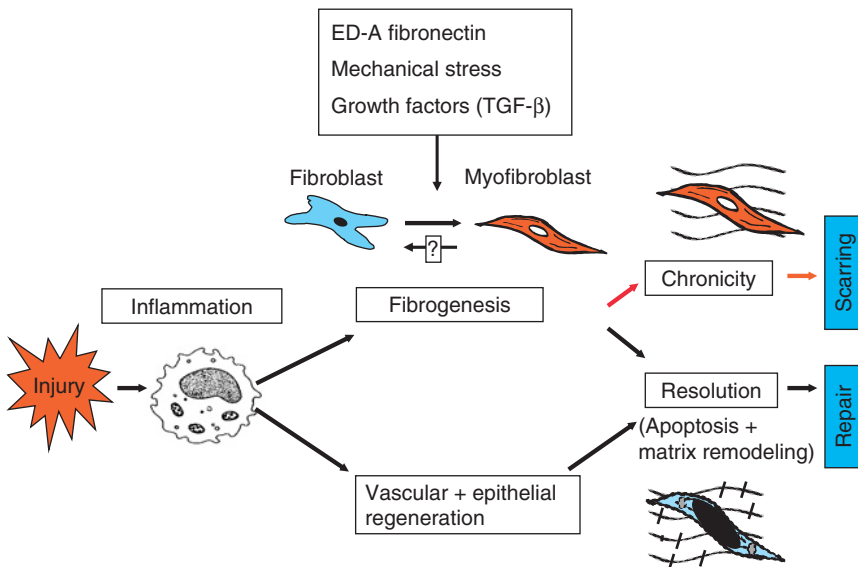


FIG. 1 Generalized model of wound healing and scarring versus pathological fibrosis.

their removal or loss by apoptosis being part of the transition between granulation tissue and healing or scar formation (Darby *et al.*, 1990; Desmouliere *et al.*, 1995).

Providing adequate blood supply to the newly formed granulation tissue is an important part of healing. Again a number of proangiogenic growth factors are released at the injury site, in an attempt to provide renewed vascularization (Li *et al.*, 2003). These include transforming growth factor-beta-1 (TGF β 1), basic fibroblast growth factor (FGF-2), angiopoietin, platelet-derived growth factor (PDGF), and VEGF and directly and indirectly contribute to revascularization by promoting the formation of new capillaries and stimulating proliferation of endothelial cells, migration, and tube formation (organization) through the growth factor receptors expressed on endothelial cells and pericytes.

Finally, it is now accepted that the matrix is subject to remodeling by collagenous and noncollagenous proteinases, including metalloproteinases and plasmin/plasminogen family. Although the functional significance of these proteases is poorly understood, it is accepted that the balance between collagen synthesis and degradation is an important factor in determining the extent of ECM accumulation (Li *et al.*, 2003; Yaguchi *et al.*, 1998).

Although the type and size and depth of injury are important (e.g., scalpel incisions causing less injury than burns or excisional wounds), the body's response is surprisingly consistent, not only for the different types of trauma

but also the response in different organs in general. The response of internal organs to parenchymal injury is therefore much the same as that which occurs in skin wound healing.

C. Healing versus Scarring

The wound healing response is an attempt to repair injury and restore tissue function. However, whereas acute wounds go through this linear series of events, chronic nonhealing wounds do not. Some areas of chronic wounds are in different phases at the same time, and progression to the next phase does not occur in the same coordinated manner. The end result of this is the failure of wound healing and accumulation of excess matrix, called scarring. The most obvious example of this is in the skin in hypertrophic and keloid scarring in which healing fails to resolve. However, internal organs also show analogous scarring with the liver, lung, and kidney being obvious examples in which pathologies induce fibrosis and scarring that may or may not resolve over time.

D. Distinction Between Healing and Scarring

Although the biology of healing and scarring remain similar, ultimately it is the extent and nature of inflammation that distinguishes the two processes.

Although this process in many respects resembles a recapitulation of embryogenesis, there is an important distinction. Fetuses may heal and do not scar or show only limited scarring. Fetal wound healing therefore represents the pinnacle of wound biology—restoration of tissue function without the formation of significant amounts of scar tissue. Conversely, complete regeneration of complex tissue and organs in adults is usually precluded by fibrotic reactions that lead to scarring (Harty *et al.*, 2003). The distinction between wound healing in the fetus and the adult has not surprisingly been the subject of much attention.

Originally it was thought the sterile environment of the amniotic fluid accounted for the observed difference in fetal healing. However the observation that marsupials heal without scarring in the mother's pouch suggested otherwise. Ultimately it has been a serendipitous finding in the immunologically abnormal MRL mouse that has provided the greatest insight (Heber-Katz *et al.*, 2004). MRL mice have a major defect in immune regulation, which results in a number of autoimmune defects. When ear hole punches are used to identify mice in laboratory colonies, the holes heal without scarring with a regeneration of the cartilage that forms the structural basis of the ear. Furthermore these exciting findings have been duplicated in a model of cardiac fibrosis (Leferovich *et al.*, 2001), suggesting that inflammation, or perhaps more correctly, the nature of the inflammation determines the balance between

restoration, healing, and scarring. Other tissues may show apparently reduced scarring with the oral cavity being an obvious example. It has been suggested that local fibroblasts in the oral cavity behave more like fetal fibroblasts in showing less contractile properties and greater motility, though this is somewhat controversial (Shannon *et al.*, 2006).

E. Cellular Basis of Healing and Scarring

Important cells involved in the process include hematogenous cells and connective tissue cells such as fibroblasts and associated resident macrophages and lymphocytes. Monoclonal antibodies have been used by a number of groups to phenotype the infiltrating hematogenous cells in various forms of inflammation. In renal disease (Alexopoulos *et al.*, 1989; Hooke *et al.*, 1987; Sabadini *et al.*, 1988), the interstitial infiltrate is similar in nearly all forms of tubulointerstitial injury secondary to glomerulonephritis and resembles that seen in primary tubulointerstitial nephropathies and allograft rejection (Cameron, 1992). T lymphocytes form the majority of hematogenous cells present, with monocytes, B cells, natural killer and plasma cells making up the remainder. Within the T-lymphocyte population there is variability in the relative proportion of T-cell subsets (Cameron, 1992). Patients with idiopathic pulmonary fibrosis generally demonstrate a neutrophil predominant alveolitis. Likewise in the lung, the specific pattern of T lymphocytes is related to the etiology. Increased CD4+ lymphocytes are often found in the alveolar space in patients with pulmonary sarcoidosis, whereas individuals with hypersensitivity pneumonitis may have increased numbers of CD8+ cells. (Paine and Ward, 1999).

The paucity of specific markers for fibroblasts, however, has meant that their enumeration has been largely neglected. The fibroblast is central to both wound healing and the pathogenesis of organ fibrosis. For instance, selective deletion of fibroblasts by transfection with a gene that results in cell death, herpes virus thymidine kinase, is sufficient to prevent renal interstitial fibrosis after injury (Iwano *et al.*, 2001).

III. Fibroblasts and Myofibroblasts

A. Fibroblasts

The fibroblasts present in various connective tissues represent a heterogeneous population of cells. Other than the myofibroblast, first described by Gabbiani (Gabbiani *et al.*, 1971; Majno *et al.*, 1971), there is no formal

nomenclature to define fibroblast subphenotypes (Trelstad and Birk, 1985). An important question is therefore, what is a fibroblast?

Ultrastructurally, fibroblasts are identified on the basis of their stellate appearance with elongated, branching processes (Takahashi-Iwanaga, 1994). They have prominent rough endoplasmic reticulum (ER) and Golgi apparatus, characteristic of cells with a high biosynthetic activity (Sappino *et al.*, 1990). Even though fibroblasts have been extensively studied *in vitro*, information concerning their *in vivo* differentiation is limited (Sappino *et al.*, 1990). Several groups have attempted to identify fibroblasts on the basis of immunohistochemical staining, with limited success (Table I). These attempts have been largely unsuccessful due to the poor antigenicity of fibroblasts and the nonspecific nature of the antigen used. For instance, many of the commonly used antibodies for macrophages overlap in specificity with fibroblast markers (Inoue *et al.*, 2005) and markers based on the fibroblast role in extracellular matrix (collagen) production and assembly such as prolyl hydroxylase are only partially specific given that other cell types can deposit extracellular matrix molecules and stain for this marker. The isolation of the fibroblast specific protein, FSP-1, and generation of antisera to it, has therefore been a substantial step in elucidating the role of renal fibroblasts (Strutz *et al.*, 1995), at least in the mouse.

B. Myofibroblasts

1. Myofibroblasts in Tissue Repair

Early in normal tissue repair the fibroblasts that invade the wound resemble active but undifferentiated fibroblasts with abundant rough ER, as would be expected for extracellular matrix-producing cells (Darby *et al.*, 1990). As healing and the repair process progresses, myofibroblasts begin to appear (Figs. 2 and 3). Myofibroblasts are mesenchymal cells with features of both fibroblasts and smooth muscle cells (Sappino *et al.*, 1990). Ultrastructurally these cells are characterized by features of both fibroblasts; including spindle shape, prominent cytoplasmic projections, abundant rough ER, and features of smooth muscle cells—longitudinal cytoplasmic bundles of microfilaments and multiple nuclear membrane folds (Sappino *et al.*, 1990). Myofibroblasts also display a “fibronexus” that connects the intracellular microfilaments both to other myofibroblasts and surrounding extracellular matrix (Eyden, 1993). The fibronexus may thus mediate continuity between contractile filaments and matrix proteins (Eyden, 1993). Expression of the protein smoothelin may reliably distinguish smooth muscle cells from myofibroblasts, with a number of reports suggesting that smoothelin is found exclusively in smooth muscle cells (Miller and Marshall, 1980; van der Loop *et al.*, 1996).

TABLE I
Fibroblast "Specific" Antisera

Clone	Immunogen	Specificity	Reference
ER-TR7	Fibroblasts	Fibroblasts, reticulin	(Van Vliet <i>et al.</i> , 1986)
1B10	Thymic fibroblasts	Fibroblasts, macrophages	(Ronnov-Jessen <i>et al.</i> , 1992)
5B5	Prolyl hydroxylase	Fibroblasts and other collagen producing cells	(Wilkinson <i>et al.</i> , 1992)
Rabbit polyclonal	Ecto-5'-Nucleotidase	Fibroblasts, macrophages	(Bachmann <i>et al.</i> , 1993)
1A4	α -smooth muscle actin	Smooth muscle cells, myofibroblasts	(Darby <i>et al.</i> , 1990)
FSP-1		Murine fibroblasts	(Strutz <i>et al.</i> , 1995)

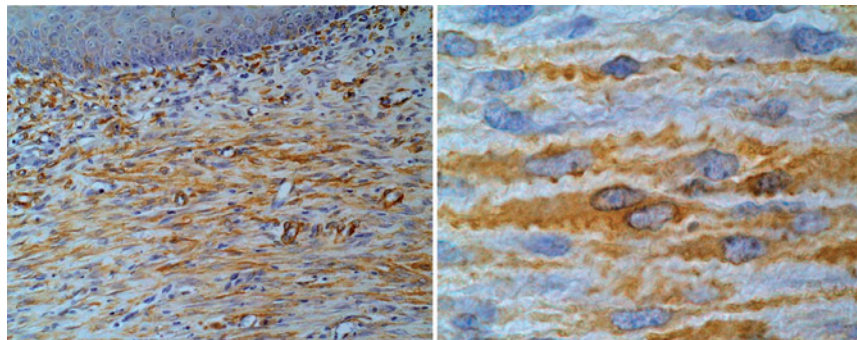


FIG. 2 Myofibroblasts take up an orientation that lines up with mechanical tension across the wound and parallel to the epidermis. The cells also show signs of contraction with rippling of both the cytoplasm and nucleus. Staining is with anti- α -smooth muscle actin antibody.

2. Differentiation Markers

Cytoskeletal protein differentiation markers have been used as a marker of mesenchymal phenotype (Sappino *et al.*, 1990). Microfilaments, intermediate filaments, and microtubules are the three components of the eukaryotic cell cytoskeleton. Microfilaments consist mainly of actin, intermediate filaments are usually a mixture of vimentin and/or desmin, and the microtubules are predominantly tubulin (Desmoulière and Gabbiani, 1992).

Expression of the smooth muscle specific protein α -smooth muscle actin (α -SMA) is often used as a marker of myofibroblast phenotype. α -SMA is one of six different actin isoforms (Vandekerckhove and Weber, 1978) that are present in all eukaryotic cells. β and γ actins are present in all cells,

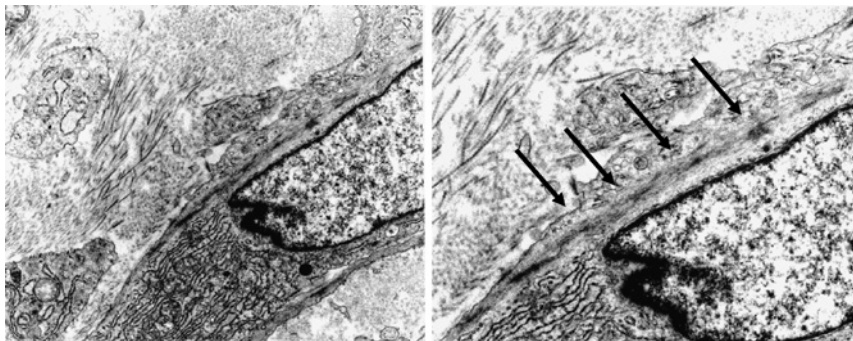


FIG. 3 Myofibroblasts have prominent cortical microfilament bundles with dense bodies. These are not observed in normal connective tissue fibroblasts. (Reproduced with permission from Darby *et al.* (1990).

whereas the distribution of α -cardiac, α -skeletal, and α -smooth muscle isoforms are tissue-specific (Desmouliere and Gabbiani, 1992).

Myofibroblasts may however differ in the smooth muscle proteins expressed. Expression of the cytoskeletal protein α -SMA is used as an almost universal marker of myofibroblast phenotype; the same cannot be said for desmin and smooth muscle myosin. Four different myofibroblast phenotypes have been identified in skin wounds, based on morphology and the distribution of tissue-specific cytoskeletal proteins. Type V myofibroblasts express vimentin only, type VA express vimentin and α -SMA, VAD are positive for vimentin, α -SMA and desmin, while VD are positive for vimentin and desmin only (Gabbiani, 1992; Sappino *et al.*, 1990; Skalli *et al.*, 1989). Desmin-containing myofibroblasts are usually only found in hypertrophic scars and fibromatoses (Skalli *et al.*, 1989). To date, myofibroblast expression of smooth muscle myosin has not been described (Gabbiani, 1992).

3. Myofibroblasts in Organ Fibrosis

Myofibroblasts have been observed in practically all fibrotic conditions involving retraction and reorganization of connective tissue and have been the subject of several reviews (Desmoulière *et al.*, 1992, 2003; Sappino *et al.*, 1990; Schmitt-Graff *et al.*, 1994). In addition to their involvement in skin wound healing (Gabbiani *et al.*, 1971; Hebda *et al.*, 1993; Majno *et al.*, 1971), myofibroblasts are most commonly found, and well-characterized in pulmonary fibrosis (Kuhn and McDonald, 1991; Vyalov *et al.*, 1993), hepatic fibrosis (Schmitt-Graff *et al.*, 1993), cardiac fibrosis (Leslie *et al.*, 1991), and numerous carcinomas associated with an inflammatory response (Takahashi *et al.*, 1994), such as breast (Ronnov-Jessen and Petersen, 1993), pancreas, and

TABLE II

Principal Pathologic Situations in Which Myofibroblasts Have Been Identified

Pathology	References
Skin wound healing	(Darby <i>et al.</i> , 1990; Hebda <i>et al.</i> , 1993; Majno <i>et al.</i> , 1971; Pattison <i>et al.</i> , 1994)
Pulmonary fibrosis	(Blum, 1994; Kuhn and McDonald, 1991; Vyalov <i>et al.</i> , 1993; Zhang <i>et al.</i> , 1994)
Hepatic fibrosis	(Bhathal, 1972; Schmitt-Graff <i>et al.</i> , 1993; Tanaka <i>et al.</i> , 1991)
Tumors	(Hewitt <i>et al.</i> , 1993; Ronnov-Jessen and Petersen, 1993; Takahashi <i>et al.</i> , 1994)
Cardiac overload	(Leslie <i>et al.</i> , 1991)
Renal fibrosis	(Alpers <i>et al.</i> , 1994; Essawy <i>et al.</i> , 1997; Goumenos <i>et al.</i> , 1994; Hewitson <i>et al.</i> , 1995; Pedagogos <i>et al.</i> , 1997; Vangelista <i>et al.</i> , 1989)

bowel (Hewitt *et al.*, 1993; Takahashi *et al.*, 1994) (Table II). The role of myofibroblasts has been extensively studied in skin wound healing where they are thought to be responsible for wound contraction (Grinnell, 1994; Majno *et al.*, 1971). Studies quantifying myofibroblasts in granulation tissue have shown that the number of myofibroblasts is proportional to the rate of wound contraction (Rungger-Brandle and Gabbiani, 1983). Nagle *et al.* described interstitial fibroblasts with smooth muscle characteristics in a rabbit model of renal obstruction some 30 years ago (Nagle *et al.*, 1973). More recently, we and others have described interstitial cells with the ultrastructural features of myofibroblasts in renal biopsies with various nephropathies (Alpers *et al.*, 1994; Essawy *et al.*, 1997; Goumenos *et al.*, 1994; Hewitson and Becker, 1995; Pedagogos *et al.*, 1997; Vangelista *et al.*, 1989). Spindle-shaped interstitial cells in the fibrotic interstitium, which stain for the smooth muscle-specific actin isoform (α -smooth muscle actin) (Figs. 4 and 5) are thus well-studied in both experimental models of disease and in human disease, consistent with their important role in scar formation.

4. Cancer-Associated Stromal Myofibroblasts

Another area of research that has gained momentum is the presence of myofibroblasts in the stroma around tumors and their role in tumor progression. It is now established that myofibroblasts are present in the stroma around a number of different cancers and that these may play an important role in signaling the tumor cells, both to increase tumor progression and to promote tumor invasion (Kalluri and Zeisberg, 2006). Local fibroblasts in the connective tissue, likely give rise to many of the myofibroblasts present in the stromal reaction; however, it has also been found that bone marrow-derived

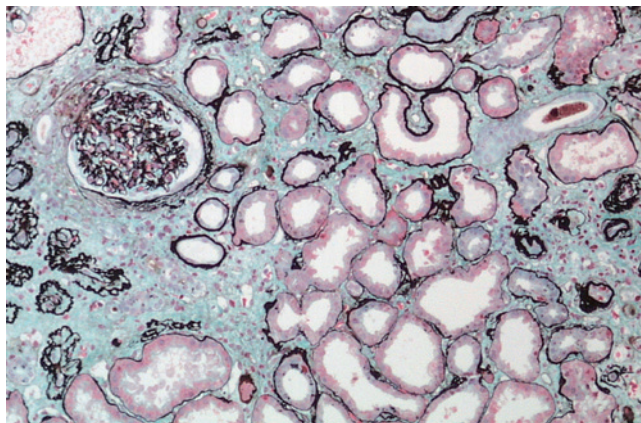


FIG. 4 An example of pathological fibrosis in an organ. This renal biopsy, stained with silver Masson's, shows the expansion of the interstitium caused by fibroblast activation and increased extracellular matrix synthesis.

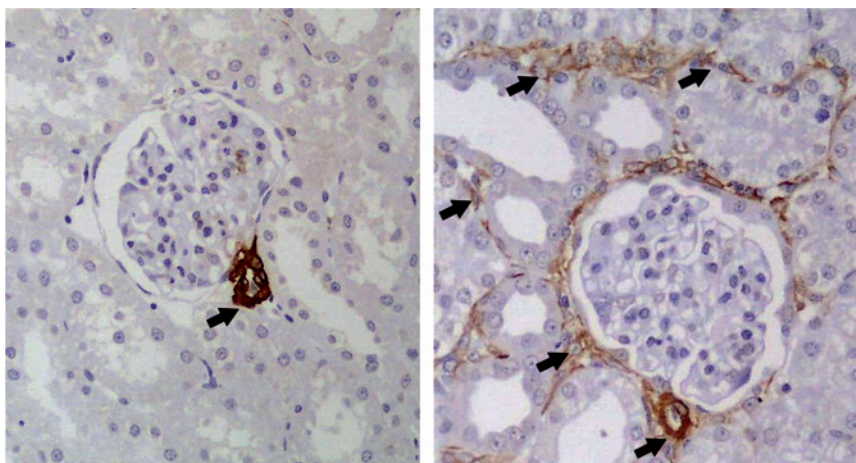


FIG. 5 Staining for the myofibroblast marker, α -smooth muscle actin shows that in the normal kidney biopsy (left) only the arteriole adjacent to the glomerulus is positive, whereas in the biopsy from a fibrotic kidney (right), there are numerous α -smooth muscle actin-positive myofibroblasts present in the interstitium.

myofibroblasts are present (Direkze *et al.*, 2003; Ishii *et al.*, 2003). The presence of myofibroblasts in the tumor stroma may provide a source of growth factors that signal tumor cells, but also could be involved in connective tissue remodeling allowing expansion and invasion. Indeed many myofibroblasts have been found to be present at the front of invasion in malignant tumors (De Wever

and Mareel, 2003). It has also been suggested that the tumor cells may induce changes in the myofibroblast population in the stroma by paracrine mechanisms, resulting in selection for a subpopulation of highly proliferative myofibroblasts that lack p53, the cell cycle checkpoint control (Hill *et al.*, 2005).

C. Origin of the Fibroblast

It has been assumed that pluripotential mesenchymal stem cells can give rise to various differentiated mesenchymal cells including smooth muscle cells, pericytes, and fibroblasts (Jimenez and Martinez, 1992). For many years it has been postulated that the fibroblast cell system, at least *in vitro*, is a terminally differentiating cell system. In studies using skin fibroblasts, Bayreuther *et al.* proposed that fibroblasts differentiate along a terminal lineage in the same way as hemopoietic cells (Bayreuther *et al.*, 1988, 1991). Similarly in studies using rabbit renal fibroblasts Müller *et al.* identified three mitotically active progenitor fibroblasts (cell types MF I, MF II, MF III) and three postmitotic fibroblast cell types (PMF IV, PMF V, and PMF VI) (Müller *et al.*, 1992; Rodemann *et al.*, 1991). Cell type PMF VI has been shown by biochemical analysis to have the highest biosynthetic activity for various fibroblast-specific components and secreted proteins (i.e., collagen and other ECM proteins) (Müller *et al.*, 1992).

More recently however, we recognize the plasticity of cell phenotypes. Fibroblasts may be recruited from resident cell populations, circulating precursors, and transforming epithelial cells.

1. Resident Fibroblasts

Electron microscopy studies have consistently shown that in many organs there are resident populations of fibroblastlike cells that proliferate rapidly in response to injury. Local proliferation and migration from adjacent tissues, in particular the perivascular region, have generally been accepted as the mechanisms by which tissue fibroblast numbers may increase (Wiggins *et al.*, 1993). In skin wounds, strong staining near the wound margins for proliferation markers such as bromodeoxyuridine (BrdU) (Fig. 6) and for MMP-13 (collagenase) (Fig. 7) is suggestive of fibroblast proliferation and migration from surrounding unwounded connective tissue (Darby *et al.*, 1997; Desmoulière *et al.*, 2003).

2. Circulating Precursors

Bucala *et al.* (1994) were able to isolate a population of so-called fibrocytes, cells in healing skin wounds that expressed both the hematogenous cell marker CD34+ and procollagen I. In circumstances of sex-mismatched bone marrow transplants, they were able to show mismatched DNA in

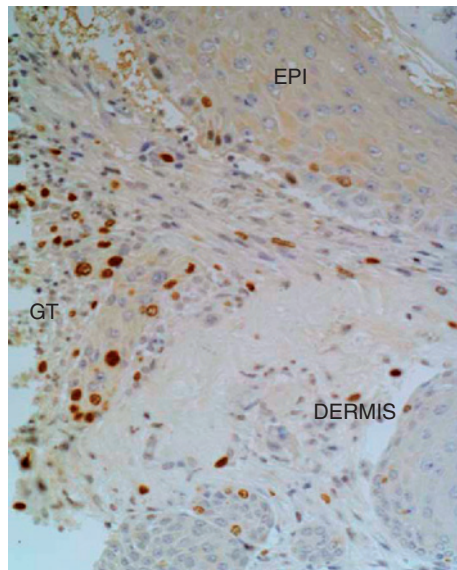


FIG. 6 The concentration of BrdU-positive cells (brown nuclei) at the wound margin shows evidence of cell recruitment from surrounding unwounded dermis.

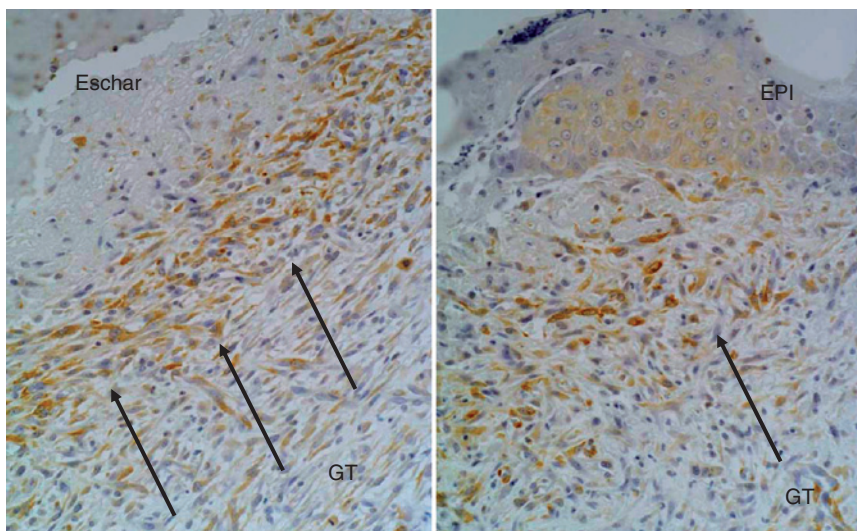


FIG. 7 MMP13 (collagenase) staining suggests that myofibroblasts are not only migrating and dissecting off the eschar (left), but also invading from surrounding unwounded dermis (right) where they are seen staining strongly at the wound margin.

these cells, confirming that they were of donor origin. Likewise, there are now also reports that bone marrow-derived fibrocytes traffic to areas of renal (Grimm *et al.*, 2001) and pulmonary (Phillips *et al.*, 2004; Schmidt *et al.*, 2003) fibrosis.

3. Epithelial–Mesenchymal Transition

Epithelial–mesenchymal transition (EMT), is the process that facilitates the derivation of a multitude of functionally specialized cells, tissues, and organs in the developing embryo (Khew-Goodall and Wadham, 2005). Consistent with the recapitulation of developmental programs during “wound healing,” a reverse process occurs in response to tissue injury, where epithelial cells acquire features of mesenchymal cells. During EMT, epithelial cells lose polarity and cell–cell contacts and undergo dramatic cytoskeletal remodeling. Concurrent with the loss of epithelial cell adhesion and cytoskeletal components, cells undergoing EMT acquire mesenchymal cell expression profiles and migratory phenotype. EMT is therefore in essence, a process of reverse embryogenesis.

Renal tubular EMT, by definition, is a process in which renal tubular cells lose their epithelial phenotype and acquire features characteristic of mesenchymal cells (Liu, 2004a). The process of EMT has been found to be particularly significant in the pathogenesis of tubulointerstitial fibrosis that accompanies all progressive renal disease (Liu, 2004a). Pioneering work from Strutz *et al.* (1995) indicated that renal tubular epithelial cells can express fibroblast markers in disease states, suggesting that epithelial-to-mesenchymal transition is a potential source of cells in pathological kidneys. Likewise TGF β 1 can induce alveolar EMT in human lung epithelia cells; a process inhibited by Smad2 gene silencing, but not by MEK inhibitors (Kasai *et al.*, 2005).

Elegant renal experiments in a murine model of unilateral ureteric obstruction have attempted to address the relative importance of the various potential sources of fibroblasts (Iwano *et al.*, 2002). Using bone marrow chimeras and transgenic reporter mice, the authors were able to estimate that resident fibroblasts, EMT and circulating precursors contributed 52%, 38%, and 9% of the fibroblast burden, respectively (Iwano *et al.*, 2002). In the kidney, it remains unclear whether myofibroblasts can be derived directly from EMT, or only indirectly via a prior transition into fibroblasts.

D. Origin of the Myofibroblast

The derivation of the myofibroblast phenotype is also complex. Its close association with fibroblasts in parenchymal wound healing systems (Clark, 1989) suggests that it may modulate from fibroblasts. Much of the rationale

for this hypothesis is derived from *in vitro* studies in which quiescent fibroblasts express α -smooth muscle actin upon stimulation (Ronnov-Jessen and Petersen, 1993).

Ultrastructural studies in sequential skin wounds also suggest that myofibroblasts are derived from resting fibroblasts in the wound margin (Bouissou *et al.*, 1988; Darby *et al.*, 1990). Bayreuther *et al.* believe that the myofibroblast corresponds to the postmitotic fibroblast PMF IV (Bayreuther *et al.*, 1991). However, other possibilities include a pericyte origin (Nehls and Drenckhahn, 1993) and even a macrophage derivation has been postulated (Bhawan and Majno, 1989). At least in some specialized fibrogenic systems, myofibroblast-like cells may be derived from a specialized cell type, as in renal glomerulosclerosis in which myofibroblasts represent activated mesangial cells (Alpers *et al.*, 1992). Likewise in hepatic fibrosis, myofibroblasts are derived from both vitamin A-storing hepatic stellate cells and activated perisinusoidal cells (Hines *et al.*, 1993). The relative importance of these two cell types may depend on the origin of the liver injury (Bataller and Brenner, 2005). In experimental models of hepatic fibrosis induced by carbon tetrachloride, it is mainly the hepatic stellate cells that are activated and subsequently differentiate into myofibroblasts, whereas in models using cholestasis (bile duct ligation) the perisinusoidal and connective tissue fibroblasts present in portal regions become activated and participate in the fibrotic response, expressing myofibroblast markers in the process.

IV. Fibrogenic Mediators

A. Fibrogenic Mediators

The activity of fibroblasts and their subsequent differentiation into myofibroblasts is dependent on a combination of the action of growth factors and other soluble mediators, extracellular matrix components, and mechanical stress.

1. Profibrotic Cytokines and Growth Factors

A long list of cytokines (including polypeptide growth factors) is likely to play a role in fibrogenesis. Growth factors and other cytokines may be produced by both resident and infiltrating inflammatory cells. A hierarchy is likely to exist among the many cytokines considered to be putative mediators of injury (Atkins, 1995).

The macrophage is a central figure in chronic inflammation because of the great number of biologically active products it can produce (Vangelista

et al., 1991). Growth factors the macrophage is known to synthesize and secrete include PDGF (Zhuo *et al.*, 1998), FGF-2 (Baird *et al.*, 1985), and TGF β 1 (Associan *et al.*, 1987). Compelling evidence for the role of macrophages as mediators of injury has been provided by renal studies in which macrophage infiltration was reduced by X-ray irradiation (Diamond and Pesek-Diamond, 1991) and antimacrophage serum (Matsumoto and Hatane, 1989). Such treatments resulted in a concomitant decrease in severity of injury. Although these studies establish a role for macrophage-mediated injury, they do not specifically establish a direct role in upregulation of fibrogenesis.

Importantly fibroblasts express receptors for a number of cytokines including PDGF (Alpers *et al.*, 1993, 1994), TGF β 1 (Noronha *et al.*, 1995), and tumor necrosis factor- α (TNF α) (Noronha *et al.*, 1995). These factors may mediate their recruitment and activation during injury. Alvarez *et al.* described heterogeneity in the paracrine response of fibroblasts derived from different anatomical locations, once again highlighting the heterogeneous nature of the fibroblast phenotype (Alvarez *et al.*, 1992).

Although primarily thought to be a producer of extracellular matrix, fibroblasts are also capable of producing prostaglandins (Korn, 1985), erythropoietin (Bachmann *et al.*, 1993), and cytokines (Noronha *et al.*, 1995). Fibroblasts are therefore capable of both autocrine and paracrine responses, further amplifying the fibrogenic response.

Several authors have now consistently shown that the acquisition of myofibroblast features in skin (Desmoulière *et al.*, 1993), renal (Masterson *et al.*, 2004), and lung fibroblasts (Evans *et al.*, 2003) is TGF β 1-mediated. A role for TGF β 1 in fibrogenesis has been hypothesized on the basis of observations that TGF β 1-neutralizing antibodies (Border *et al.*, 1990) and the natural TGF β 1-binding glycoprotein, decorin (Border *et al.*, 1992), abrogate renal fibrogenesis.

In some cases, TGF β 1 activities are mediated by downstream activation of connective tissue growth factor (CTGF). An immediate early response gene, CTGF is a potent stimulus for myofibroblast differentiation and matrix synthesis in a variety of tissues (Leask and Abraham, 2004). Overexpression of CTGF is a consistent feature of fibrotic lesions, and the combination of TGF β 1 and CTGF promotes ongoing fibrosis (Leask and Abraham, 2004).

Local subcutaneous application of granulocyte macrophage-colony stimulating factor (GM-CSF), a growth factor known for its hemopoietic effects, induces the accumulation of myofibroblasts (Rubbia-Brandt *et al.*, 1991); however, it has been postulated that this occurs through macrophage activation and subsequent secretion of macrophage-derived factors such as TGF β 1 because GM-CSF applied directly to fibroblasts *in vitro* has no effect on α -SMA expression.

Cytokines and growth factors act in a synergistic paracrine fashion to stimulate tissue formation (Clark, 1989). Although the effect of these agonists on the quantity of collagen produced has been studied extensively by cell culture methods, results are difficult to apply to *in vivo* situations because of complicated fibroblast inflammatory cell and cytokine interactions (Larjava *et al.*, 1990).

2. Other Soluble Profibrotic Factors

A variety of mesenchymal cells, including fibroblasts, express receptors for the vasoactive mediators endothelin-1 and angiotensin II. Both have profibrotic effects in cultured gingival fibroblasts (Ohuchi *et al.*, 2002).

3. Extracellular Matrix

ECM is not only generated by fibroblasts but also acts as a potent regulator of fibroblast function. Changes in the composition of ECM can therefore directly stimulate fibrogenesis. In most cases these effects are mediated through interaction with integrins (Geiger *et al.*, 2001; Paine and Ward, 1999). Both fibroblast proliferation and collagen synthesis are influenced by adhesion to extracellular matrix. The more firmly lung fibroblasts are anchored, the more they proliferate and synthesize collagen (Paine and Ward, 1999). However, this does not seem to hold true for fibroblasts isolated from fibrotic lungs, which continue to proliferate on a soft substrate, in an anchorage-independent manner (Torry *et al.*, 1994), suggesting that fibroblast responses to ECM signals are critical components that restrict fibroblast activity in the normal homeostasis (Paine and Ward, 1999).

Cytokine effects may also be enhanced by the ability of ECM to bind soluble mediators. For example, collagen IV and chondroitin sulphate proteoglycan binds TGF β 1, whereas heparan sulfate proteoglycan binds FGF-2 and TGF β 1 (Schlondorff, 1993). ECM may thus act as a so-called “reservoir” of growth factors (Li *et al.*, 2003; Schlondorff, 1993).

Nonenzymatic glycation is a ubiquitous reaction between reducing sugars and polypeptides that ultimately generates irreversibly advanced glycated end products (AGEs). This occurs during normal aging, but to a greater degree in diabetes, where interaction between AGEs and their binding proteins lead to the activation of a range of cytokines. Specifically, AGEs have been shown to promote EMT (Oldfield *et al.*, 2001), ostensibly through generation of TGF β 1.

Fibronectin is a multifunctional protein found as both a soluble plasma form and insoluble constituent of ECM, with a number of splice variants further contributing to fibronectin polymorphism. The human ED-A variant (and EIIIA homologue in rats) is abundantly expressed during embryogenesis

and wound healing/fibrosis where its expression closely parallels α SMA expression. Molecular studies have shown that the ED-A isoform is a critical cofactor required for TGF β 1 induction of myofibroblast differentiation (Serini *et al.*, 1999).

4. Mechanical Tension

Mechanical stress is an important mediator of fibroblast differentiation in those of tissues in which mechanical tension and transmission of force occurs, such as the skin. It is thought that the presence of ED-A fibronectin splice variant, mechanical tension, and TGF β 1 are required to obtain the full differentiation to the myofibroblast phenotype (Tomasek *et al.*, 2002), although the presence of mechanical tension may on its own produce a partial phenotype where cells possess stress fibers but lack α -smooth muscle actin positive immunostaining. Studies have shown that externally applied mechanical loads can lead to rapid induction of changes in the extracellular matrix composition, suggesting adaptation of the matrix to mechanical loading (Chiquet *et al.*, 2003) and a putative stretch responsive promoter has been found in genes which respond to mechanical tension or stretch, such as tenascin and collagen XII (Chiquet, 1999). Signaling through this pathway may also account for the differences observed between stressed fibroblast-populated collagen lattices and those that are free floating *in vitro*. Floating collagen lattices are remodeled and “contract” over time, while stressed lattices express greater levels of α -smooth muscle actin and are thus more capable of true contraction.

5. Naturally Occurring Inhibitors of Fibrogenesis

Increasingly we recognize that not only are fibroblasts regulated by a number of profibrotic factors, but also that there are a number of endogenous factors that downregulate fibroblast function. The most studied of these, hepatocyte growth factor (HGF) (Liu, 2004b), bone morphogenic factor-7 (BMP-7) (Zeisberg *et al.*, 2004), and the hormone relaxin (Samuel and Hewitson, 2006), maintain tissue integrity by antagonizing TGF β 1 activity and signaling. After injury, reduced levels of these endogenous factors can accelerate fibrosis (Eddy, 2005).

B. Signal Transduction in Fibroblasts

The microenvironment following tissue injury therefore represents a complex mixture of inflammatory, fibrogenic, and antifibrogenic mediators. How do fibroblasts recognize and make sense of often-conflicting signals? As with

other inflammatory circumstances in general, growth factors and cytokines signal through the numerous well-described signal transduction pathways.

1. Receptor Binding

Receptors acting at the membrane level transduce extracellular signals into a cytosolic one, where subsequent communication of signals involves translocation of intracellular signaling components. These membrane receptors take various forms. Arguably the most important fibrogenic factors, TGF β ₁ and PDGF, signal through a receptor serine/threonine kinase and tyrosine kinase, respectively.

TGF β ₁ belongs to a superfamily of structurally related regulatory proteins that include three mammalian TGF isoforms (TGF β ₁ - β ₂, - β ₃), activin/inhibin, and bone morphogenic proteins. Signaling through functional cooperation of the Smad proteins, the TGF- β receptor phosphorylates receptor-regulated Smads (Smad2, Smad3), a pathway that is strictly regulated at various levels, including inhibition by Smad7, which complexes with Smad2 and Smad3 to prevent phosphorylation (Schnaper *et al.*, 2002).

PDGF is secreted as a homodimer, composed of two A-, B-, C-, or D-chains or a heterodimer composed of an A- and B-chain, which complex variously with α or β receptor subunits. The PDGF B chain, as part of either PDGF-BB or PDGF-AB, is a potent mesenchymal cell mitogen (Floege, 2002), while various PDGF-BB isoforms mediate chemotaxis, contraction, and the activity of other factors (Johnson *et al.*, 1993). Induction of PDGF-B type receptors on smooth muscle cells is seen in atherosclerosis and renal allograft rejection has long been recognized (Fellstrom *et al.*, 1989).

Likewise, the janus tyrosine kinase family is important for cytokine signaling, whereas G-protein transmembrane receptors signal through associated effector enzymes such as Ras GTPases, a convergent point in signal cascades for many mitogens (Khwaja *et al.*, 2000).

Finally, integrins have a particularly important role in fibrogenesis, mediating the interaction between mesenchymal cells and ECM. Expressed on both leukocytes and parenchymal cells, they bind to extracellular matrix proteins and, in the case of leukocytes, to ligands on other cells. Integrin proteins are heterodimers that consist of paired α and β chains. At least 14 α subunits and eight β subunits have been characterized thus far, with the pairing of a subunit determining specificity (Paine and Ward, 1999). Integrins containing the $\beta 1$ chain or the αv chain are particularly important for their role in binding to matrix proteins. The multiple integrin heterodimers allow fine control both of the matrix components to which the cell can adhere, and the signals transduced (Geiger *et al.*, 2001). In many cases effects are mediated by activation of focal adhesion kinase, a member of the tyrosine kinase family (Yasuda *et al.*, 2002).

2. Nonreceptor Mediated Signaling

In addition to receptor signal transduction, nonreceptor mediated signaling (e.g., by nitric oxide) is an important means of influencing fibroblast function (Hewitson *et al.*, 2002).

3. Second Messenger Pathways

The activation and translocation of kinases from the cytoplasm to the nucleus provide the link between extracellular signals and gene expression. Again these pathways take many forms and include, among others, the mitogen-activated protein kinase, phosphatidylinositol 3-kinase, and protein kinase C cascades. In each case the end result is the phosphorylation and activation of nuclear transcription factors, with gene transcription being controlled by the interaction of transcription factors with specific DNA sequences known as promoter or enhancer motifs (Mann and Smart, 2002).

Various transcription factor families have established roles in fibrosis. Nuclear factor- κ B (NF- κ B), perhaps the best known of the nuclear transcription families, promotes the upregulation of cytokines involved in inflammation (Guizarro and Egido, 2001). Mesenchymal cell differentiation is under the control of NF- κ B (Klahr and Morrissey, 2000) and MyoD, a member of the basic helix-loop-helix family (Mayer and Leinwand, 1997), while various members of the Kruppel-like transcription factor family regulate collagen transcription in hepatic stellate cells (Mann and Smart, 2002). Conversely, peroxisome proliferator activated receptor γ (PPAR γ) is active in quiescent mesenchymal cells (Mann and Smart, 2002), suggesting that it may block fibrogenesis.

C. Fibroblast Responses

The fibroblast response to this microenvironment includes differentiation, migration, proliferation, and increased ECM synthetic activity.

1. Differentiation

Molecular regulation of (myo)fibroblast differentiation remains poorly understood. TGF β 1 seem to play a central role, having been shown consistently to upregulate α SMA expression in a diverse range of fibroblasts (Desmoulière *et al.*, 1993; Evans *et al.*, 2003; Masterson *et al.*, 2004). However, although the importance of TGF β 1 is well recognized, TGF β 1 upregulates only a subset of smooth muscle differentiation markers in non-smooth muscle cells (Hautmann *et al.*, 1999). How these override the repressor

activity that normally suppresses expression of α SMA is unclear (Hautmann *et al.*, 1999).

In fibrocytes, the TGF β 1-induced increases in α SMA expression are paralleled by a loss of CD34 expression (Abe *et al.*, 2001; Schmidt *et al.*, 2003). The ED-A isoform of fibronectin is required for TGF β 1-mediated acquisition of myofibroblast features by human subcutaneous fibroblasts (Serini *et al.*, 1999). The collagenase MMP-2 is necessary and sufficient to stimulate myofibroblast transition (Cheng and Lovett, 2003).

Renal mesangial cells isolated from C/EBP δ null mice express much less α SMA than their wild-type counterparts, suggesting the involvement of the transcription factor C/EBP δ in myofibroblast differentiation (Takeji *et al.*, 2004). Another regulator of myofibroblast differentiation that may be involved in phenotypic change from fibroblast to myofibroblast is the clotting enzyme, thrombin. Thrombin has, in addition to its clotting activity, a cell surface receptor that is activated by cleavage of the receptor N-terminus (extracellular domain). Proteinase-activated receptors exist that are activated by thrombin cleavage; specifically proteinase-activated receptor-1 (PAR-1). PAR-1 activation has been shown to stimulate myofibroblast differentiation in lung fibroblasts (Bogatkevich *et al.*, 2001) and in renal fibroblasts, at least *in vitro* (Hewitson *et al.*, 2005).

2. Migration

Leucocytes and mesenchymal cells such as fibroblasts, are attracted to the site of injury by various chemotactic factors including TGF- β . Indeed TGF- β is chemotactic for monocytes and fibroblasts; fibroblast chemotaxis being signaled through Smad3. Interestingly, TGF- β stimulation of the myofibroblast phenotype in fibroblasts is not dependent on Smad3 (Flanders *et al.*, 2003). In many cases these cells are in turn activated to produce further proinflammatory cytokines, thus initiating a cascade of events that can lead to fibrosis (Kovacs and DiPietro, 1994).

Migration is dependent upon interaction between cells and surrounding ECM. For fibroblasts to move from place to place, cells must form and release the adjacent ECM. Several studies indicate that the profile of integrin expression in motile fibroblasts differs from that in resting fibroblasts (Clark, 1993; Paine and Ward, 1999). Fibroblasts therefore display a phenotypic switch in their integrin expression, which may in part explain the temporal distinction in the various phases of wound healing.

In a rabbit model of crescentic glomerulonephritis, Wiggins *et al.* (1993) demonstrated that fibroblast-like cells migrated from a perivascular location into the interstitium, accumulating in a periglomerular distribution. Such migration may be in response to chemotactic substances produced by the inflamed glomerulus (Wiggins *et al.*, 1993). Very similar findings have been

found in a combined model of periarterial fibrosis and proliferative glomerulonephritis (Faulkner *et al.*, 2005). Evidence suggests that activated fibroblasts also secrete stromelysin and collagenases, which assist with their interstitial migration by dissolving the surrounding interstitial matrix (Kuncio *et al.*, 1991).

3. Mitogenesis

Fibroblasts derived from fibrotic lesions continue to exhibit a hyperproliferative growth pattern when compared to kidneys isolated from normal kidneys (Rodemann and Müller, 1990). Cytokines are mitogenic through not only direct effects but also indirectly by stimulating the release of other cytokines (Kovacs and DiPietro, 1994). The most important function of PDGF is to stimulate proliferation of mesenchymal cells including fibroblasts and smooth muscle cells. These cells not only respond to PDGF in a paracrine fashion, but also have an autocrine pathway available through peptide production (Noronha *et al.*, 1995).

TGF β 1 may act as both an inhibitor and promoter of cell proliferation. TGF β 1 has a biphasic response on mesenchymal cells in culture, inhibiting proliferation at high concentrations, while being mitogenic in low concentrations. These paradoxical effects are thought to be the result of interaction with other growth factors (Kovacs and DiPietro, 1994). Likewise GM-CSF stimulates *in vitro* proliferation of not just hemopoietic cells, but also of a number of mesenchymal cells including fibroblasts (Denhar *et al.*, 1988).

4. Matrix Synthesis

The extracellular material once only described as reticulin is now known to consist of a complex matrix of collagen, proteoglycans, and glycoproteins (Lemley and Kriz, 1991). The distribution and composition of the extracellular matrix is surprisingly similar across various organs, at least before injury. The interstitium in the lung, liver, and kidney is principally composed of the triple helical fibrillar collagens (type I and III), elastin, proteoglycans, and fibronectin, whereas lung and alveolar basement membranes consist mainly of type IV and laminin (Paine and Ward, 1999). Type I collagen is the major collagen in adult dermis (Kirsner and Eaglstein, 1993). Fibrosis is associated with major alterations in both the type and quantity of matrix synthesis.

In advanced stages of disease the liver contains approximately six times more ECM than normal (Bataller and Brenner, 2005). Increased synthesis of fibronectin by fibroblasts is thought to be an early event in both wound healing and fibrosis (Goyal and Wiggins, 1991), with the fibronectin matrix

providing a scaffold on which subsequent interstitial collagen is fixed (Clark, 1989; Goyal and Wiggins, 1991). Fibronectin is involved in adhesion of cells to substrate and other cells, and as such probably represents a primer in organization of fibrotic tissue before the appearance of collagenous protein (Hynes and Yamada, 1982). Furthermore, as described earlier, synthesis of the fibronectin splice variant EDA, and its rat ortholog EIIIA, have important profibrotic effects including promoting EMT.

Our work in renal disease suggests that upregulation of the various collagen isotypes is temporally distinct with increased accumulation of interstitial collagen I and IV occurring well before increases in collagen III (unpublished observations). Conversely, although Type III collagen is a minority component of normal adult skin, aberrant synthesis occurs within 48 hours of skin wound healing (Kirsner and Eaglstein, 1993).

Most commonly recognized for their collagen-producing ability, fibroblastlike cells are the intrinsic collagen-producing cells in most organs. However, they are not the only cells capable of collagen production with collagen-producing cells in the renal cortex known to include glomerular (Kreisberg and Karnovsky, 1983; Scheinman *et al.*, 1992) and tubular (Creely *et al.*, 1988; Scheinman *et al.*, 1992) epithelial cells, mesangial cells (Scheinman *et al.*, 1992), and interstitial fibroblasts (Rodemann and Müller, 1991). Fibroblasts cannot be grown from isolated cortical glomeruli, which suggests that they are not necessary for matrix production, at least in glomerulosclerosis (Alvarez *et al.*, 1992).

5. Contraction

Wound contraction has long been recognized as a feature of skin wound healing. Contraction was originally thought to result from the polymerization of collagen fibrils, due therefore to the tensile strength of collagen (Botsford, 1941; Howes *et al.*, 1929). Abercrombie *et al.* described the dissociation of collagen formation and contraction at late stages of wound healing, suggesting other factors may be involved (Abercrombie *et al.*, 1954). This group was also able to demonstrate that wounds in ascorbic acid-deficient animals can close independently of collagen formation (Abercrombie *et al.*, 1956). Although these studies did not contradict the role of physiochemical contraction, they cast doubt on the notion that collagen polymerization alone was sufficient to account for wound contraction.

The observation that fibroblasts acquire prominent cytoplasmic microfilaments therefore suggested that they perform a contractile function in wound healing (Gabbiani *et al.*, 1972; Majno *et al.*, 1971). Indeed, strips of granulation tissue have been shown to have the ability to contract *ex vivo* in response to various compounds that stimulate smooth muscle cell contraction (Higton and James, 1964; Majno *et al.*, 1971).

Not surprisingly then, studies quantifying myofibroblasts in granulation tissue have shown that the number of myofibroblasts is proportional to the rate of wound contraction (Rungger-Brandle and Gabbiani, 1983). Elegant experiments from Hinz *et al.* (2001) demonstrated that cultures of lung myofibroblasts, but not fibroblasts, are able to deform silicon sheets when used as *in vitro* substrates for fibroblast attachment. The myofibroblast fibronexus connects the intracellular microfilaments both to other myofibroblasts and surrounding extracellular matrix (Eyden, 1993) thereby mediating contraction.

However, it is worth remembering that wound contraction may be due not only to the contractile properties of specialized mesenchymal cells but also indirectly through cell migration. Ehrlich *et al.* propose that fibroblast locomotion (or traction) is sufficient to reorganize extracellular matrix (Ehrlich, 1988). This postulate is based on the observation that collagen gel lattices populated with growing fibroblasts are able to contract in the absence of stress fiber formation. Contraction of the gel occurred during cell migration, ceasing once cells were no longer motile (Ehrlich, 1988).

Contraction in the myofibroblast is mediated by α -smooth muscle actin and by nonmuscle myosin as myofibroblasts do not or only rarely express smooth muscle myosin. The pathway for contractile signaling involves Rho kinase activation (Grinnell *et al.*, 1999) and blockers of Rho kinase inhibit PDGF-stimulated lattice contraction (Abe *et al.*, 2003; Lee *et al.*, 2003).

V. Regulation of Fibrogenesis

A. Resolution or Progression

Resolution of inflammation represents an important step in limiting the chronicity of inflammation (Kuncio *et al.*, 1991). Fibrogenesis continues as long as permissive conditions exist. The persistent accumulation of inflammatory cells is associated with the continued destruction of renal tissue and deposition of scar tissue. If unchecked this leads to progression of scarring and ultimately in the case of internal organs, organ failure. Abscess formation is an extreme example of uncontrolled inflammation, where disintegrating neutrophils not only degrade tissue but also amplify the immune response (Ryan and Majno, 1977).

Ideally inflammation will resolve efficiently, resulting in complete restoration of tissue structure and function. This occurs frequently in skin wounding, and can occur in the renal context, as with poststreptococcus glomerulonephritis (Vogl *et al.*, 1986) and ischemic acute renal failure (Forbes *et al.*, 2000).

Such resolution of inflammation may ultimately be the factor that distinguishes between “healing” and “scarring.”

For resolution of inflammation to occur, the following events must take place: (1) removal of stimulus, (2) dissipation of mediators, (3) cessation of cell infiltration, and finally (4) clearance of inflammatory cells (Haslett, 1992).

In particular, how inflammatory cells are removed remains controversial, with exmigration, phenotypic modulation, and cell death all possible mechanisms.

Ultrastructural studies in skin wound healing suggest that the prevalence of α SMA-negative fibroblastic cells increases at the completion of healing, consistent with phenotypic modulation or dedifferentiation of wound myofibroblasts (Darby *et al.*, 1990). However, *in vitro* studies suggest that the myofibroblast is a part of a terminally differentiating cell lineage, therefore arguing against dedifferentiation (Bayreuther *et al.*, 1991). The demonstration of lymphatic macrophage drainage and trafficking in experimental glomerulonephritis (Lan *et al.*, 1993) implicates some role for exmigration in resolution of tubulointerstitial inflammation.

Increasing evidence suggests that apoptosis is the major mechanism of decreasing cellularity during the various stages of “wound healing.” Apoptosis is a form of cell death that does not lead to an inflammatory response and may therefore be important in resolution of inflammation and fibrogenesis (Darby *et al.*, 1990; Desmouliere *et al.*, 1995; Greenhalgh, 1998). It is characterized by endonuclease activation resulting in rapid DNA degradation, with engulfment of the membrane-bound cellular fragments (apoptotic bodies) without release of cell contents (including inflammatory mediators) (Lu *et al.*, 2005). Importantly, apoptosis leads to the safe removal of cells by phagocytosis, whereas in contrast, necrosis provokes tissue injury and inflammation (Greenhalgh, 1998; Lu *et al.*, 2005). Qualitative and quantitative studies in skin wound healing (Darby *et al.*, 1990; Desmouliere *et al.*, 1995) have repeatedly shown that fibroblastic cells are removed by apoptosis at the completion of wound healing (Fig. 8).

It seems likely that regulation of myofibroblast apoptosis may be involved in both impairment of tissue repair; in cases where apoptosis is increased inappropriately or prematurely, such as that seen in skin wound healing in diabetes mellitus (Darby *et al.*, 1997). Further evidence for this comes from studies showing that the presence of advanced glycosylation end products in the skin may result in fibroblast apoptosis and that this can be mimicked by treatment with AGE-modified collagen (carboxy methyl lysine [CML]-collagen) (Alikhani *et al.*, 2005). AGE-modified matrix *in vitro* can inhibit attachment, spreading, and proliferation and induce apoptosis of fibroblasts (Alikhani *et al.*, 2005; Darby *et al.*, 2006). Conversely, it has been speculated that delayed or absent induction of apoptosis in myofibroblasts

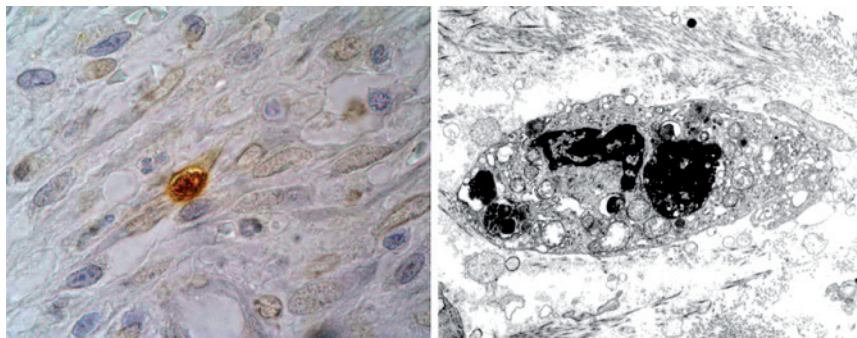


FIG. 8 Myofibroblasts are deleted during granulation tissue resolution by apoptosis. Visible here in granulation tissue, apoptotic cells have TUNEL-positive nuclei (left) and in electron micrographs have classical apoptotic nuclear morphology (right). (Electron micrograph reproduced with permission from Darby *et al.*, 1990.)

may result in increased scarring, such as that seen in hypertrophic scars or keloids.

B. Remodeling

Following deposition of extracellular matrix, mechanisms exist whereby this immature matrix may be remodeled as part of scarring. These include the action of proteinases (Jones *et al.*, 1991) and scar contraction (Rudolph *et al.*, 1992). This serves to highlight tubulointerstitial scarring may be a product of several factors other than matrix synthesis *per se*.

Degradation of the ECM involves proteolytic digestion by two families of enzymes, the metalloproteinases and plasminogen activator/plasmin (Alexander and Werb, 1989). The identification of collagenases and their inhibitor proteins in a number of organs indicates that ECM accumulation may be a result of either increased synthesis or decreased degradation (Eddy, 2005; Yaguchi *et al.*, 1998).

The metalloproteinase family includes a number of members with various and partly overlapping specificities (Alexander and Werb, 1989). This family of proteinases is divided into three groups: collagenases which degrade interstitial collagens Type I, II, and III, type IV collagenases/gelatinases which degrade basement membrane collagen and gelatins, and stromelysins which degrade a broad range of substrates including proteoglycans, laminin, gelatins, and fibronectin (Martrisian, 1990).

The production of these enzymes by endothelial cells, fibroblasts, and macrophages can be induced by a wide variety of stimuli (Jones *et al.*, 1991).

Matrix metalloproteinases are also regulated by control of activation and the presence of specific inhibitors known as tissue inhibitors of metalloproteinases (TIMP) (Martrisian, 1990). The serine protease plasmin is active in degradation of laminin and to some extent gelatin, fibronectin and collagen type III, IV, and V (Alexander and Werb, 1989). Much of the degradative effect of the plasmin/plasminogen system is achieved through activation of the matrix metalloproteinases (Jones *et al.*, 1995).

The remodeling of the matrix may play an important role in regulating the survival of myofibroblasts. In granulation tissue, the application of a skin flap over a wound results in the rapid remodeling of the granulation tissue, accomplished by an induction of apoptosis in fibroblasts and other cell types such as vascular endothelium (Garbin *et al.*, 1996). This was subsequently shown to correlate with increased MMP expression and reduced expression of TIMP (Darby *et al.*, 2002). In a similar vein, changes in the levels of MMPs and TIMPs has been shown in fibrotic liver to be able to regulate loss of myofibroblasts in fibrotic regions, with exogenous TIMP or MMP inhibitor being able to block the induction of apoptosis (Murphy *et al.*, 2002).

C. Therapies Aimed at Downregulating Fibroblast Function

Excess fibrosis or scarring can be disfiguring and in the case of internal organs, life-threatening. Not surprisingly then, considerable effort has been devoted to developing rational treatment strategies for fibrocontractive diseases. Given the central role of the fibroblast in this process, much of this attention has focused on downregulation of fibroblast function, with cell culture studies in particular providing pharmacological insights.

Ostensibly by increasing intracellular cAMP and cGMP concentrations, phosphodiesterase inhibitors reduce proliferation and collagen synthesis by renal and hepatic myofibroblasts (Hewitson *et al.*, 2000; Preaux *et al.*, 1997). Other potential antagonists include the HMG coenzyme A inhibitors, called statins (Kelynack *et al.*, 2002), and pirfenidone (Hewitson *et al.*, 2001). Although highly toxic, lysyl oxidase and prolyl hydroxylase inhibitors have at least established the proof of principle of targeting inhibition of collagen assembly (Franklin, 1997). As mentioned previously, we now recognize that a number of endogenous autocoids may moderate fibroblast function. Several studies highlight the ability of HGF (Matsumoto and Nakamura, 2001), BMP-7 (Zeisberg *et al.*, 2004), and relaxin (Samuel, 2005) to downregulate collagen synthesis. In the case of relaxin, benefits are at least in part due to increased generation of collagenases in renal (Masterson *et al.*, 2004) and lung (Unemori *et al.*, 2000) fibroblasts.

VI. Concluding Remarks

In many respects, the pathologic process of fibrosis in internal organs resembles disordered wound healing in the skin. If we define fibrosis by the presence of an increased density of interstitial collagenous matrix (especially collagens type I and III), the histological picture of fibrosis could be produced by increased production and/or reduced breakdown of collagen, or by the loss of normal cellular content leaving behind the interstitial reticulin (Gonzalez-Avila *et al.*, 1988; Hewitson *et al.*, 1998; Jones, 1996). In each case fibroblasts are central to the process—proliferating and migrating to the site of injury, synthesizing ECM, and increasing the density of matrix through contraction.

REFERENCES

Abe, M., Ho, C. H., Kamm, K. E., and Grinnell, F. (2003). Different molecular motors mediate platelet-derived growth factor and lysophosphatidic acid-stimulated floating collagen matrix contraction. *J. Biol. Chem.* **278**, 47707–47712.

Abe, R., Donnelly, S. C., Peng, T., Bucala, R., and Metz, C. N. (2001). Peripheral blood fibrocytes: Differentiation pathway and migration to wound sites. *J. Immunol.* **166**, 7556–7562.

Abercrombie, M., Flint, M. H., and James, D. W. (1954). Collagen formation and wound contraction during repair of small excised wounds in the skin of rats. *J. Embryol. Exp. Morphol.* **2**, 264–274.

Abercrombie, M., Flint, M. H., and James, D. W. (1956). Wound contraction in relation to collagen formation in scorbutic guinea pigs. *J. Embryol. Exp. Morphol.* **4**, 167–175.

Alexander, C. M., and Werb, Z. (1989). Proteinases and extracellular matrix remodeling. *Curr. Opin. Cell Biol.* **1**, 974–982.

Alexopoulos, E., Seron, D., Hartley, R. B., Nolasco, F., and Cameron, J. S. (1989). The role of interstitial infiltrates in IgA nephropathy: A study with monoclonal antibodies. *Nephrol. Dial. Transplant.* **4**, 187–195.

Alikhani, Z., Alikhani, M., Boyd, C. M., Nagao, K., Trackman, P. C., and Graves, D. T. (2005). Advanced glycation end products enhance expression of pro-apoptotic genes and stimulate fibroblast apoptosis through cytoplasmic and mitochondrial pathways. *J. Biol. Chem.* **280**, 12087–12095.

Alpers, C. E., Hudkins, K. L., Floege, J., and Johnson, R. J. (1994). Human renal cortical interstitial cells with some features of smooth muscle cells participate in tubulointerstitial and crescentic glomerular injury. *J. Am. Soc. Nephrol.* **5**, 201–210.

Alpers, C. E., Hudkins, K. L., Gown, A. M., and Johnson, R. J. (1992). Enhanced expression of “muscle-specific” actin in glomerulonephritis. *Kidney Int.* **41**, 1134–1142.

Alpers, C. E., Seifert, R. A., Hudkins, K. L., Johnson, R. J., and Bowen-Pope, D. F. (1993). PDGF-receptor localizes to mesangial, parietal epithelial and interstitial cells in human and primate kidneys. *Kidney Int.* **43**, 286–294.

Alvarez, R. J., Sun, M. J., Haverty, T. P., Iozzo, R. V., Myers, J. C., and Neilson, E. G. (1992). Biosynthetic and proliferative characteristics of tubulointerstitial fibroblasts probed with paracrine cytokines. *Kidney Int.* **41**, 14–23.

Associan, R. K., Fleurdelys, B. E., Stevenson, H. C., Miller, P. J., Madtes, D. K., Raines, E. W., Ross, R., and Sporn, M. B. (1987). Expression and secretion of type beta transforming growth factor by activated human macrophages. *Proc. Natl. Acad. Sci. USA* **84**, 6020–6024.

Atkins, R. C. (1995). Interleukin-1 in crescentic glomerulonephritis. *Kidney Int.* **48**, 576–586.

Bachmann, S., Le Hir, M., and Eckardt, K.-U. (1993). Co-localization of erythropoietin mRNA and ecto-5'-nucleotidase immunoreactivity in peritubular cells of rat renal cortex indicates that fibroblasts produce erythropoietin. *J. Histochem. Cytochem.* **41**, 335–341.

Baird, A., Mormede, P., and Bohlen, P. (1985). Immunoreactive fibroblast growth factor in cells of peritoneal exudate suggests its identity with macrophage derived growth factor. *Biochem. Biophys. Res. Commun.* **126**, 358–364.

Bataller, R., and Brenner, D. A. (2005). Liver fibrosis. *J. Clin. Invest.* **115**, 209–218.

Bayreuther, K., Franz, P. I., Gogol, J., Hapke, C., Maier, M., and Meinrath, H. G. (1991). Differentiation of primary and secondary fibroblasts in cell culture systems. *Mut. Res.* **1991**, 233–242.

Bayreuther, K., Rodemann, H. P., Hommel, R., Dittman, K., Albiez, M., and Franz, P. I. (1988). Human skin fibroblasts *in vitro* differentiate along a terminal cell lineage. *Proc. Natl. Acad. Sci. USA* **85**, 5112–5116.

Bhathal, P. S. (1972). Presence of modified fibroblasts in cirrhotic livers in man. *Pathology* **4**, 139–144.

Bhawan, J., and Majno, G. (1989). The myofibroblast. Possible derivation from macrophages in xanthogranuloma. *Am. J. Dermatopathol.* **11**, 255–258.

Blum, C. B. (1994). Comparison of properties of four inhibitors of 3-hydroxy-3-methylglutaryl-coenzyme A reductase. *Am. J. Cardiol.* **73**, 3D–11D.

Bogatkevich, G. S., Tourkina, E., Silver, R. M., and Ludwicka-Bradley, A. (2001). Thrombin differentiates normal lung fibroblasts to a myofibroblast phenotype via the proteolytically activated receptor-1 and a protein kinase C-dependent pathway. *J. Biol. Chem.* **276**, 45184–45192.

Border, W. A., Noble, N. A., Yamamoto, T., Harper, J. R., Yamaguchi, U., Pierschbacher, M. D., and Ruoslahti, E. (1992). Natural inhibitor of transforming growth factor- β protects against scarring in experimental kidney disease. *Nature* **360**, 361–364.

Border, W. A., Okuda, S., Languino, L. R., Sporn, M. B., and Ruoslahti, E. (1990). Suppression of experimental glomerulonephritis by antiserum against transforming growth factor β 1. *Nature* **346**, 371–374.

Botsford, T. W. (1941). The tensile strength of sutured skin wounds during healing. *Surg. Gynaec. Obstet.* **72**, 690–697.

Bouissou, H., Pieraggi, M., Julian, M., Uhart, D., and Kokolo, J. (1988). Fibroblasts in dermal tissue repair. *Int. J. Dermatol.* **27**, 564–570.

Bucala, R., Spiegel, L. A., Chesney, J., Hogan, M., and Cerami, A. (1994). Circulating fibrocytes define a new leukocyte subpopulation that mediates tissue repair. *Mol. Med.* **1**, 71–81.

Cameron, J. S. (1992). Tubular and interstitial factors in the progression of glomerulonephritis. *Pediatr. Nephrol.* **6**, 292–303.

Cheng, S., and Lovett, D. H. (2003). Gelatinase A (MMP-2) is necessary and sufficient for renal tubular cell epithelial-mesenchymal transformation. *Am. J. Pathol.* **162**, 1937–1949.

Chiquet, M. (1999). Regulation of extracellular matrix gene expression by mechanical stress. *Matrix Biol.* **18**, 417–426.

Chiquet, M., Renedo, A. S., Huber, F., and Fluck, M. (2003). How do fibroblasts translate mechanical signals into changes in extracellular matrix production? *Matrix Biol.* **22**, 73–80.

Clark, R. A. F. (1989). Wound repair. *Curr. Opin. Cell Biol.* **1**, 1000–1008.

Clark, R. A. F. (1993). Regulation of fibroplasia in cutaneous wound repair. *Am. J. Med. Sci.* **306**, 42–48.

Creely, J., Commers, P., and Haralson, M. (1988). Synthesis of type III collagen by cultured kidney epithelial cells. *Connect. Tissue Res.* **18**, 107–122.

Darby, I., Skalli, O., and Gabbiani, G. (1990). Alpha-Smooth muscle actin is transiently expressed by myofibroblasts during experimental wound healing. *Lab. Invest.* **63**, 21–29.

Darby, I. A., Bisucci, T., Hewitson, T. D., and MacLellan, D. G. (1997). Apoptosis is increased in a model of diabetes-impaired wound healing in genetically diabetic mice. *Int. J. Biochem. Cell Biol.* **29**, 191–200.

Darby, I. A., Bisucci, T., Pittet, B., Garbin, S., Gabbiani, G., and Desmouliere, A. (2002). Skin flap-induced regression of granulation tissue correlates with reduced growth factor and increased metalloproteinase expression. *J. Pathol.* **197**, 117–127.

Darby, I. A., Coulomb, B., and Desmoulière, A. (2006). Fibroblast/myofibroblast differentiation, proliferation and apoptosis: Role of extracellular matrix glycosylation. In “Biological Mechanisms of Tooth Eruption, Resorption and Movement” (Z. Davidovitch, J. Mah, and S. Suthanarak, Eds.), pp. 109–117. UCLA Press, Los Angeles.

De Wever, O., and Mareel, M. (2003). Role of tissue stroma in cancer cell invasion. *J. Pathol.* **200**, 429–447.

Denhar, S., Gaboury, L., Galloway, P., and Eaves, C. (1988). Human granulocyte-macrophage colony-stimulating factor is a growth factor active on a variety of cell types of nonhemopoietic origin. *Proc. Natl. Acad. Sci. USA* **85**, 9253–9257.

Desmouliere, A., Darby, I. A., and Gabbiani, G. (2003). Normal and pathologic soft tissue remodeling: Role of the myofibroblast, with special emphasis on liver and kidney fibrosis. *Lab. Invest.* **83**, 1689–1707.

Desmouliere, A., and Gabbiani, G. (1992). The cytoskeleton of arterial smooth muscle cells during human and experimental atheromatosis. *Kidney Int.* **41**(Suppl. 37), S87–S89.

Desmoulière, A., Geinoz, A., Gabbiani, F., and Gabbiani, G. (1993). Transforming growth factor beta induces alpha smooth muscle actin expression in granulation tissue myofibroblasts and in quiescent and growing cultured fibroblasts. *J. Cell Biol.* **123**, 104–111.

Desmoulière, A., Redard, M., Darby, I., and Gabbiani, G. (1995). Apoptosis mediates the decrease in cellularity during the transition between granulation tissue and scar. *Am. J. Pathol.* **146**, 56–66.

Desmoulière, A., Rubbia-Brandt, L., Grau, G., and Gabbiani, G. (1992). Heparin induces alpha-smooth muscle actin expression in cultured fibroblasts and in granulation tissue myofibroblasts. *Lab. Invest.* **67**, 716–726.

Diamond, J. R., and Pesek-Diamond, I. (1991). Sublethal X-irradiation during puromycin nephrosis prevents late renal injury. *Am. J. Physiol.* **260**, F779–F786.

Direkze, N. C., Forbes, S. J., Brittan, M., Hunt, T., Jeffery, R., Preston, S. L., Poulsom, R., Hodivala-Dilke, K., Alison, M. R., and Wright, N. A. (2003). Multiple organ engraftment by bone-marrow-derived myofibroblasts and fibroblasts in bone-marrow-transplanted mice. *Stem Cells* **21**, 514–520.

Eddy, A. A. (2005). Progression in chronic kidney disease. *Adv. Chronic Kidney Dis.* **12**, 353–365.

Ehrlich, H. P. (1988). Wound closure: Evidence of cooperation between fibroblasts and collagen matrix. *Eye* **2**, 149–157.

Essawy, M., Soylemezoglu, O., Muchaneta-Kubara, E. C., Shortland, J., Brown, C. B., and El Nahas, A. M. (1997). Myofibroblasts and the progression of diabetic nephropathy. *Nephrol. Dial. Transplant.* **12**, 12–43.

Evans, R. A., Tian, Y. C., Steadman, R., and Phillips, A. O. (2003). TGF-beta1-mediated fibroblast-myofibroblast terminal differentiation—the role of Smad proteins. *Exp. Cell Res.* **282**, 90–100.

Eyden, B. P. (1993). Brief review of the fibronexus and its significance for myofibroblastic differentiation and tumour diagnosis. *Ultrastruct. Pathol.* **17**, 611–622.

Faulkner, J. L., Szczykalski, L. M., Springer, F., and Barnes, J. L. (2005). Origin of interstitial fibroblasts in an accelerated model of angiotensin II-induced renal fibrosis. *Am. J. Pathol.* **167**, 1193–1205.

Fellstrom, B., Klareskog, L., Hedin, C. H., Larsson, E., Ronnstrand, L., Terracio, L., Tufveson, G., Wahlberg, J., and Rubin, K. (1989). Platelet-derived growth factor receptors in the kidney—upregulated expression in inflammation. *Kidney Int.* **36**, 1099–1102.

Flanders, K. C., Major, C. D., Arabshahi, A., Aburime, E. E., Okada, M. H., Fujii, M., Blalock, T. D., Schultz, G. S., Sowers, A., Anzano, M. A., Mitchell, J. B., Russo, A., et al. (2003). Interference with transforming growth factor-beta/Smad3 signaling results in accelerated healing of wounds in previously irradiated skin. *Am. J. Pathol.* **163**, 2247–2257.

Floege, J. (2002). Glomerular remodelling: Novel therapeutic approaches derived from the apparently chaotic growth factor network. *Nephron* **91**, 582–587.

Forbes, J. M., Hewitson, T. D., Becker, G. J., and Jones, C. L. (2000). Ischemic acute renal failure: Long-term histology of cell and matrix changes in the rat. *Kidney Int.* **57**, 2375–2385.

Franklin, T. J. (1997). Therapeutic approaches to organ fibrosis. *Int. J. Biochem. Cell Biol.* **29**, 79–89.

Gabbiani, G. (1992). The biology of the myofibroblast. *Kidney Int.* **41**, 530–532.

Gabbiani, G., Hirschel, B. J., Ryan, G. B., Statkov, P. R., and Manjno, G. (1972). Granulation tissue as a contractile organ. *J. Exp. Med.* **135**, 719–735.

Gabbiani, G., Ryan, G. B., and Majno, G. (1971). Presence of modified fibroblasts in granulation tissue and their possible role in wound contraction. *Experientia* **27**, 549–550.

Garbin, S., Pittet, B., Montandon, D., Gabbiani, G., and Desmoulière, A. (1996). Covering by a flap induces apoptosis of granulation tissue myofibroblasts and vascular cells. *Wound Repair Regen.* **4**, 244–251.

Geiger, B., Bershadsky, A., Pankov, R., and Yamada, K. M. (2001). Transmembrane crosstalk between the extracellular matrix—cytoskeleton crosstalk. *Nat. Rev. Mol. Cell Biol.* **2**, 793–805.

Gonzalez-Avila, G., Vadillo-Ortega, F., and Perez-Taamayo, R. (1988). Experimental diffuse interstitial fibrosis: A biochemical approach. *Lab. Invest.* **59**, 245–252.

Goumenos, D. S., Brown, C. B., Shortland, J., and El Nahas, A. M. (1994). Myofibroblasts, predictors of progression of mesangial IgA nephropathy? *Nephrol. Dial. Transplant* **9**, 1418–1425.

Goyal, M., and Wiggins, R. (1991). Fibronectin mRNA and protein accumulation, distribution and breakdown in rabbit antiglomerular basement membrane disease. *J. Am. Soc. Nephrol.* **1**, 1334–1341.

Greenhalgh, D. G. (1998). The role of apoptosis in wound healing. *Int. J. Biochem. Cell Biol.* **30**, 1019–1030.

Grimm, P. C., Nickerson, P., Jeffery, J., Savani, R. C., Gough, J., McKenna, R. M., Stern, E., and Rush, D. N. (2001). Neointimal and tubulointerstitial infiltration by recipient mesenchymal cells in chronic renal-allograft rejection. *N. Engl. J. Med.* **345**, 93–97.

Grinnell, F. (1994). Fibroblasts, myofibroblasts, and wound contraction. *J. Cell Biol.* **124**, 401–404.

Grinnell, F., Ho, C. H., Lin, Y. C., and Skuta, G. (1999). Differences in the regulation of fibroblast contraction of floating versus stressed collagen matrices. *J. Biol. Chem.* **274**, 918–923.

Guijarro, C., and Egido, J. (2001). Transcription factor-kB (NF-kB) and renal disease. *Kidney Int.* **59**, 415–424.

Harty, M., Neff, A. W., King, M. W., and Mescher, A. L. (2003). Regeneration or scarring: An immunologic perspective. *Dev. Dyn.* **226**, 268–279.

Haslett, C. (1992). Resolution of acute inflammation and the role of apoptosis in the tissue fate of granulocytes. *Clin. Sci.* **83**, 639–648.

Hautmann, M. B., Adam, P. J., and Owens, G. K. (1999). Similarities and differences in smooth muscle alpha-actin induction by TGF-beta in smooth muscle versus non-smooth muscle cells. *Arterioscler. Thromb. Vasc. Biol.* **19**, 2049–2058.

Hebda, P. A., Collins, M. A., and Tharp, M. D. (1993). Mast cell and myofibroblast in wound healing. *Dermatol. Clin.* **11**, 685–696.

Heber-Katz, E., Leferovich, J., Bedelbaeva, K., Gourevitch, D., and Clark, L. (2004). The scarless heart and the MRL mouse. *Philos. Trans. R. Soc. Lond. B Biol. Sci.* **359**, 785–793.

Hewitson, T. D., and Becker, G. J. (1995). Interstitial myofibroblasts in IgA glomerulonephritis. *Am. J. Nephrol.* **15**, 111–117.

Hewitson, T. D., Darby, I. A., Bisucci, T., Jones, C. L., and Becker, G. J. (1998). Evolution of tubulointerstitial fibrosis in experimental renal infection and scarring. *J. Am. Soc. Nephrol.* **9**, 632–642.

Hewitson, T. D., Kelynack, K. J., Tait, M., Martic, M., Jones, C. L., Margolin, S. B., and Becker, G. J. (2001). Pirfenidone reduces *in vitro* rat renal fibroblast activation and mitogenesis. *J. Nephrol.* **14**, 453–460.

Hewitson, T. D., Martic, M., Kelynack, K. J., Pedagogos, E., and Becker, G. J. (2000). Pentoxifylline reduces *in vitro* renal myofibroblast proliferation and collagen secretion. *Am. J. Nephrol.* **20**, 82–88.

Hewitson, T. D., Martic, M., Kelynack, K., Pagel, C. N., Mackie, E. J., and Becker, G. J. (2005). Thrombin is a pro-fibrotic factor for rat renal fibroblasts *in vitro*. *Nephron Exp. Nephrol.* **101**, e42–e49.

Hewitson, T. D., Tait, M. G., Martic, M., Kelynack, K. J., and Becker, G. J. (2002). Dipyridamole inhibits *in vitro* renal myofibroblast proliferation and collagen synthesis. *J. Lab. Clin. Med.* **140**, 199–208.

Hewitson, T. D., Wu, H., and Becker, G. J. (1995). Interstitial myofibroblasts in experimental renal infection and scarring. *Am. J. Nephrol.* **15**, 411–417.

Hewitt, R. E., Powe, D. G., Carter, I., and Turner, D. R. (1993). Desmoplasia and its relevance to colorectal tumour invasion. *Int. J. Cancer* **53**, 62–69.

Higton, D. J., and James, D. W. (1964). The force of contraction of full thickness wounds of rabbit skin. *Br. J. Surg.* **51**, 462–466.

Hill, R., Song, Y., Cardiff, R. D., and Van Dyke, T. (2005). Selective evolution of stromal mesenchyme with p53 loss in response to epithelial tumorigenesis. *Cell* **123**, 1001–1011.

Hines, J. E., Johnson, S. J., and Burt, A. D. (1993). *In vivo* responses of macrophages and perisinusoidal cells to cholestatic liver injury. *Am. J. Pathol.* **142**, 511–518.

Hinz, B., Celetta, G., Tomasek, J. J., Gabbiani, G., and Chaponnier, C. (2001). Alpha-smooth muscle actin expression upregulates fibroblast contractile activity. *Mol. Biol. Cell* **12**, 2730–2741.

Hooke, D. H., Gee, D. C., and Atkins, R. C. (1987). Leukocyte analysis using monoclonal antibodies in human glomerulonephritis. *Kidney Int.* **31**, 964–972.

Howes, E. L., Sooy, J. W., and Harvey, S. C. (1929). The healing of wounds as determined by their tensile strength. *JAMA* **92**, 42–45.

Hynes, R. O., and Yamada, K. M. (1982). Fibronectins: Multifunctional modular glycoproteins. *J. Cell Biol.* **95**, 369–377.

Inoue, T., Plieth, D., Venkov, C. D., Xu, C., and Neilson, E. G. (2005). Antibodies against macrophages that overlap in specificity with fibroblasts. *Kidney Int.* **67**, 2488–2493.

Ishii, G., Sangai, T., Oda, T., Aoyagi, Y., Hasebe, T., Kanomata, N., Endoh, Y., Okumura, C., Okuhara, Y., Magae, J., Emura, M., Ochiya, T., *et al.* (2003). Bone-marrow-derived myofibroblasts contribute to the cancer-induced stromal reaction. *Biochem. Biophys. Res. Commun.* **309**, 232–240.

Iwano, M., Fischer, A., Okada, H., Plieth, D., Xue, C., Danoff, T. M., and Neilson, E. G. (2001). Conditional abatement of tissue fibrosis using nucleoside analogs to selectively corrupt DNA replication in transgenic fibroblasts. *Mol. Ther.* **3**, 149–159.

Iwano, M., Plieth, D., Danoff, T. M., Xue, C., Okada, H., and Neilson, E. G. (2002). Evidence that fibroblasts derive from epithelium during tissue fibrosis. *J. Clin. Invest.* **110**, 341–350.

Jimenez, S. A., and Martinez, A. (1992). Fibroblasts. In “Encyclopedia of Immunology” (I. M. Roitt and P. J. Delves, Eds.), pp. 562–567. Academic Press, London.

Johnson, R. J., Floege, J., Couser, W. G., and Alpers, C. E. (1993). Role of platelet-derived growth factor in glomerular disease. *J. Am. Soc. Nephrol.* **4**, 119–128.

Jones, C. L. (1996). Matrix degradation in renal disease. *Nephrology* **2**, 13–23.

Jones, C. L., Buch, S., Post, M., McCulloch, L., Liu, E., and Eddy, A. A. (1991). Pathogenesis of interstitial fibrosis in chronic purine aminonucleoside nephrosis. *Kidney Int.* **40**, 1020–1031.

Jones, C. L., Fecondo, J., Kelynack, K., Forbes, J., Walker, R., and Becker, G. J. (1995). Tissue inhibitor of the metalloproteinases and renal extracellular matrix accumulation. *Exp. Nephrol.* **3**, 80–86.

Kalluri, R., and Zeisberg, M. (2006). Fibroblasts in cancer. *Nat. Rev. Cancer* **6**, 392–401.

Kasai, H., Allen, J. T., Mason, R. M., Kamimura, T., and Zhang, Z. (2005). TGF- β 1 induces human alveolar epithelial to mesenchymal cell transition (EMT). *Respir. Res.* **6**, 56.

Kelynack, K. J., Hewitson, T. D., Martic, M., McTaggart, S., and Becker, G. J. (2002). Lovastatin downregulates renal myofibroblast function *in vitro*. *Nephron* **91**, 701–709.

Khew-Goodall, Y., and Wadham, C. (2005). A perspective on regulation of cell-cell adhesion and epithelial-mesenchymal transition: Known and novel. *Cells Tissues Organs* **179**, 81–86.

Khwaja, A., Connolly, J. O., and Hendry, B. M. (2000). Prenylation inhibitors in renal disease. *Lancet* **355**, 741–744.

Kirsner, R. S., and Eaglstein, W. H. (1993). The wound healing process. *Dermatol. Clin.* **11**, 629–640.

Klahr, S., and Morrissey, J. J. (2000). The role of vasoactive compounds, growth factors and cytokines in the progression of renal disease. *Kidney Int.* **75**(Suppl.), S7–S14.

Korn, J. H. (1985). Substrain heterogeneity in prostaglandin E2 synthesis of human dermal fibroblasts. *Arthritis. Rheum.* **28**, 315–322.

Kovacs, E. J., and DiPietro, L. A. (1994). Fibrogenic cytokines and connective tissue production. *FASEB J.* **8**, 854–861.

Kreisberg, J. I., and Karnovsky, M. J. (1983). Glomerular cells in culture. *Kidney Int.* **23**, 439–447.

Kuhn, C., and McDonald, J. A. (1991). The roles of the myofibroblast in idiopathic pulmonary fibrosis. *Am. J. Pathol.* **138**, 1257–1265.

Kuncio, G. S., Neilson, E. G., and Haverty, T. (1991). Mechanisms of tubulointerstitial fibrosis. *Kidney Int.* **39**, 550–556.

Lan, H. Y., Nikolic-Paterson, D. J., and Atkins, R. C. (1993). Trafficking of inflammatory macrophages from the kidney to draining lymph nodes during experimental glomerulonephritis. *Clin. Exp. Immunol.* **92**, 336–341.

Larjava, H., Sandberg, M., Happonen, R.-P., and Vuorio, E. (1990). Differential localization of type I and type III procollagen messenger ribonucleic acids in inflamed periodontal and periapical connective tissues by *in situ* hybridization. *Lab. Invest.* **62**, 96–103.

Leask, A., and Abraham, D. J. (2004). TGF- β signaling and the fibrotic response. *FASEB J.* **18**, 816–827.

Lee, D. J., Ho, C. H., and Grinnell, F. (2003). LPA-stimulated fibroblast contraction of floating collagen matrices does not require Rho kinase activity or retraction of fibroblast extensions. *Exp. Cell Res.* **289**, 86–94.

Leferovich, J. M., Bedelbaeva, K., Samulewicz, S., Zhang, X. M., Zwas, D., Lankford, E. B., and Heber-Katz, E. (2001). Heart regeneration in adult MRL mice. *Proc. Natl. Acad. Sci. USA* **98**, 9830–9835.

Lemley, K. V., and Kriz, W. (1991). Anatomy of the renal interstitium. *Kidney Int.* **39**, 370–381.

Leslie, K. O., Taatjes, D. J., Schwarz, J., vonTurkovich, M., and Low, R. B. (1991). Cardiac myofibroblasts express alpha smooth muscle actin during right ventricular pressure overload in the rabbit. *Am. J. Pathol.* **139**, 207–216.

Li, J., Zhang, Y. P., and Kirsner, R. S. (2003). Angiogenesis in wound repair: Angiogenic growth factors and the extracellular matrix. *Microsc. Res. Tech.* **60**, 107–114.

Liu, Y. (2004a). Epithelial to mesenchymal transition in renal fibrogenesis: Pathologic significance, molecular mechanism, and therapeutic intervention. *J. Am. Soc. Nephrol.* **15**, 1–12.

Liu, Y. (2004b). Hepatocyte growth factor in kidney fibrosis: Therapeutic potential and mechanisms of action. *Am. J. Physiol. Renal Physiol.* **287**, F7–F16.

Lu, Q., Harrington, E. O., and Rounds, S. (2005). Apoptosis and lung injury. *Keio J. Med.* **54**, 184–189.

Majno, G., Gabbiani, G., Hirschel, B., Ryan, G. B., and Statkov, P. R. (1971). Contraction of granulation tissue *in vitro*: Similarity to smooth muscle. *Science* **173**, 548–550.

Mann, D. A., and Smart, D. E. (2002). Transcriptional regulation of hepatic cell activation. *Gut* **50**, 891–896.

Martrisian, L. M. (1990). Metalloproteinases and their inhibitors in matrix remodelling. *Trends Genet.* **6**, 121–125.

Masterson, R., Hewitson, T. D., Kelynack, K. J., Martic, M., Parry, L., Bathgate, R. A., Darby, I. A., and Becker, G. J. (2004). Relaxin downregulates renal fibroblast function and stimulates matrix remodelling *in vitro*. *Nephrol. Dial. Transplant.* **19**, 544–552.

Matsumoto, K., and Hatane, M. (1989). Effect of anti-macrophage serum on the proliferation of glomerular cells in nephrotic serum nephritis in the rat. *J. Clin. Lab. Immunol.* **28**, 39–44.

Matsumoto, K., and Nakamura, T. (2001). Hepatocyte growth factor: Renotropic role and potential therapeutics for renal diseases. *Kidney Int.* **59**, 2023–2038.

Mayer, D. C., and Leinwand, L. A. (1997). Sarcomeric gene expression and contractility in myofibroblasts. *J. Cell Biol.* **139**, 1477–1484.

Miller, T., and Marshall, E. (1980). Suppressor cell regulation of cell-mediated immune responses in renal infection. *J. Clin. Invest.* **66**, 621–628.

Müller, G. A., Markovic-Lipkovski, J., Frank, J., and Rodemann, H. P. (1992). The role of interstitial cells in the progression of renal diseases. *J. Am. Soc. Nephrol.* **2**(Suppl.), S198–S205.

Murphy, F. R., Issa, R., Zhou, X., Ratnarajah, S., Nagase, H., Arthur, M. J., Benyon, C., and Iredale, J. P. (2002). Inhibition of apoptosis of activated hepatic stellate cells by tissue inhibitor of metalloproteinase-1 is mediated via effects on matrix metalloproteinase inhibition: Implications for reversibility of liver fibrosis. *J. Biol. Chem.* **277**, 11069–11076.

Nagle, R. B., Kneiser, M. R., Bulger, R. E., and Benditt, E. P. (1973). Induction of smooth muscle characteristics in renal interstitial fibroblasts during obstructive nephropathy. *Lab. Invest.* **29** No.4., 422–427.

Nehls, V., and Drenckhahn, D. (1993). The versatility of microvascular pericytes: From mesenchyme to smooth muscle? *Histochemistry* **99**, 1–12.

Noronha, I. L., Niemir, Z., Stein, H., and Waldherr, R. (1995). Cytokines and growth factors in renal disease. *Nephrol. Dial. Transplant.* **10**, 775–786.

Ohuchi, N., Koike, K., Sano, M., Kusama, T., Kizawa, Y., Hayashi, K., Taniguchi, Y., Ohsawa, M., Iwamoto, K., and Murakami, H. (2002). Proliferative effects of angiotensin II and endothelin-1 on guinea pig gingival fibroblast cells in culture. *Comp Biochem. Physiol C. Toxicol. Pharmacol.* **132**, 451–460.

Oldfield, M. D., Bach, L. A., Forbes, J. M., Nikolic-Paterson, D., McRobert, A., Hallas, V., Atkins, R. C., Osicka, T., Jerums, G., and Cooper, M. E. (2001). Advanced glycation end products cause epithelial-myofibroblast transdifferentiation via the receptor for advanced glycation end products (RAGE). *J. Clin. Invest.* **108**, 1853–1863.

Paine, R., III, and Ward, P. A. (1999). Cell adhesion molecules and pulmonary fibrosis. *Am. J. Med.* **107**, 268–279.

Pattison, J., Nelson, P. J., Huie, P., Von Leuttichau, I., Farshid, G., Sibley, R. K., and Krensky, A. M. (1994). RANTES chemokine expression in cell-mediated transplant rejection of the kidney. *Lancet* **343**, 209–211.

Pedagogos, E., Hewitson, T. D., Nicholls, K. M., and Becker, G. J. (1997). The myofibroblast in chronic transplant rejection. *Transplantation* **64**, 1192–1197.

Phillips, R. J., Burdick, M. D., Hong, K., Lutz, M. A., Murray, L. A., Xue, Y. Y., Belperio, J. A., Keane, M. P., and Strieter, R. M. (2004). Circulating fibrocytes traffic to the lungs in response to CXCL12 and mediate fibrosis. *J. Clin. Invest.* **114**, 438–446.

Preaux, A. M., Mallat, A., Rosenbaum, J., Zafrani, E. S., and Mavier, P. (1997). Pentoxyfylline inhibits growth and collagen synthesis of cultured human hepatic myofibroblast-like cells. *Hepatology* **26**, 315–322.

Ren, K., Brentjens, J., Chen, Y., Brodkin, M., and Noble, B. (1991). Glomerular macrophage proliferation in experimental immune complex nephritis. *Clin Immunol. Immunopathol.* **60**, 384–398.

Robbins, S., and Cotran, R. S. (2004). Acute and chronic inflammation. In “Pathologic Basis of Disease” (V. Kumar, A. K. Abbas, and N. Fausto, Eds.), 7th ed., pp. 47–86. Saunders, Philadelphia.

Rodemann, H. P., and Müller, G. A. (1990). Abnormal growth and clonal proliferation of fibroblasts derived from kidneys with interstitial fibrosis. *Proc. Soc. Exp. Biol. Med.* **195**, 57–63.

Rodemann, H. P., and Müller, G. A. (1991). Characterization of human renal fibroblasts in health and disease: II. *In vitro* growth, differentiation, and collagen synthesis of fibroblasts from kidneys with interstitial fibrosis. *Am. J. Kidney Dis.* **17**, 684–686.

Rodemann, H. P., Müller, G. A., Knecht, A., Norman, J. T., and Fine, L. G. (1991). Fibroblasts of rabbit kidney in culture I. Characterization and identification of cell-specific markers. *Am. J. Physiol.* **261**, F283–F291.

Ronnov-Jessen, L., Celis, J. E., Van Deurs, B., and Petersen, O. W. (1992). A fibroblast-associated antigen: Characterisation in fibroblasts and immunoreactivity in smooth muscle differentiated stromal cells. *J. Histochem. Cytochem.* **40**, 475–486.

Ronnov-Jessen, L., and Petersen, O. W. (1993). Induction of a-smooth muscle actin by transforming growth factor- β 1 in quiescent human breast gland fibroblasts. *Lab. Invest.* **68**, 696–707.

Rubbia-Brandt, L., Sappino, A. P., and Gabbiani, G. (1991). Locally applied GM-CSF induces the accumulation of alpha-smooth muscle actin containing myofibroblasts. *Virchows Arch. [B]* **60**, 73–82.

Rudolph, R., Vande Berg, J., and Ehrlich, H. P. (1992). Wound contraction and scar contracture. In “Wound Healing: Biochemical and Clinical Aspects” (I. K. Cohen, R. F. Diegelman, and W. J. Lindbald, Eds.), pp. 96–114. Saunders, Philadelphia.

Rungger-Brandle, E., and Gabbiani, G. (1983). The role of the cytoskeletal and cytocontractile elements in pathologic processes. *Am. J. Pathol.* **110**, 361–385.

Ryan, G. B., and Majno, G. (1977). “Inflammation,” 1st ed, Upjohn, Kalamazoo.

Sabadini, E., Castiglione, A., Colasanti, G., Ferrario, F., Civardi, R., Fellin, G., and D’Amico, G. (1988). Characterization of interstitial infiltrating cells in Berger’s disease. *Am. J. Kidney Dis.* **12**, 307–315.

Samuel, C. S. (2005). Relaxin: Antifibrotic properties and effects in models of disease. *Clin. Med. Res.* **3**, 241–249.

Samuel, C. S., and Hewitson, T. D. (2006). Relaxin in cardiovascular and renal disease. *Kidney Int.* **69**, 1498–1502.

Sappino, A., Schurch, W., and Gabbiani, G. (1990). Differentiation repertoire of fibroblastic cells: Expression of cytoskeletal proteins as a marker of phenotypic modulations. *Lab. Invest.* **63**, 144–161.

Scheinman, J. I., Tanaka, H., Haralson, M., Wang, S.-L., and Brown, O. (1992). Specialized collagen mRNA and secreted collagens in human glomerular epithelial, mesangial, and tubular cells. *J. Am. Soc. Nephrol.* **2**, 1475–1483.

Schlondorff, D. (1993). Renal complications of nonsteroidal anti-inflammatory drugs. *Kidney Int.* **44**, 643–653.

Schmidt, M., Sun, G., Stacey, M. A., Mori, L., and Mattoli, S. (2003). Identification of circulating fibrocytes as precursors of bronchial myofibroblasts in asthma. *J. Immunol.* **171**, 380–389.

Schmitt-Graff, A., Chakroun, G., and Gabbiani, G. (1993). Modulation of perisinusoidal cell cytoskeletal features during experimental hepatic fibrosis. *Virchows Archiv. A Pathol. Anat.* **422**, 99–107.

Schmitt-Graff, A., Desmoulière, A., and Gabbiani, G. (1994). Heterogeneity of myofibroblast phenotypic features: An example of fibroblastic cell plasticity. *Virchows Arch.* **425**, 3–24.

Schnaper, H. W., Hayashida, T., and Poncelet, A.-C. (2002). It's a Smad World: Regulation of TGF- β signaling in the kidney. *J. Am. Soc. Nephrol.* **13**, 1126–1128.

Serini, G., Bochaton-Piallet, M., Ropraz, P., Geinoz, A., Borsi, L., Zardi, L., and Gabbiani, G. (1999). The fibronectin domain ED-A is crucial for myofibroblastic phenotype induction by transforming growth factor-beta1. *J. Cell Biol.* **142**, 873–881.

Shannon, D. B., McKeown, S. T., Lundy, F. T., and Irwin, C. R. (2006). Phenotypic differences between oral and skin fibroblasts in wound contraction and growth factor expression. *Wound. Repair Regen.* **14**, 172–178.

Skalli, O., Schurch, W., Seemayer, T. A., Lagace, R., Montandon, D., Pittet, B., and Gabbiani, G. (1989). Myofibroblasts from diverse pathological settings are heterogeneous in their content of actin isoforms and intermediate filament proteins. *Lab. Invest.* **60**, 275–285.

Strutz, F., Okada, H., Lo, C. W., Danoff, T., Carone, R. L., Tomaszewski, J., and Neilson, E. G. (1995). Identification and characterisation of a fibroblast marker—FSP1. *J. Cell Biol.* **130**, 393–405.

Takahashi, K., Totsune, K., and Mouri, T. (1994). Endothelin in chronic renal failure. *Nephron.* **66**, 373–379.

Takahashi-Iwanaga, H. (1994). The three-dimensional cytoarchitecture of the interstitial tissue in the rat kidney. *Cell Tissue Res.* **264**, 269–281.

Takeji, M., Kawada, N., Moriyama, T., Nagatoya, K., Oseto, S., Akira, S., Hori, M., Imai, E., and Miwa, T. (2004). CCAAT/Enhancer-binding protein delta contributes to myofibroblast transdifferentiation and renal disease progression. *J. Am. Soc. Nephrol.* **15**, 2383–2390.

Tanaka, Y., Nouchi, T., Yamane, M., Irie, T., Miyakawa, H., Sato, C., and Marumo, F. (1991). Phenotypic modulation in lipocytes in experimental liver fibrosis. *J. Pathol.* **164**, 273–278.

Tomasek, J. J., Gabbiani, G., Hinz, B., Chaponnier, C., and Brown, R. A. (2002). Myofibroblasts and mechano-regulation of connective tissue remodelling. *Nat. Rev. Mol. Cell Biol.* **3**, 349–363.

Torry, D. J., Richards, C. D., Podor, T. J., and Gauldie, J. (1994). Anchorage-independent colony growth of pulmonary fibroblasts derived from fibrotic human lung tissue. *J. Clin. Invest.* **93**, 1525–1532.

Trelstad, R. L., and Birk, D. E. (1985). The fibroblast in morphogenesis and fibrosis: Cell topography and surface-related functions. *CIBA Found. Symp.* **114**, 4–19.

Unemori, E. N., Pickford, L. B., Salles, A. L., Piercy, C. E., Grove, B. H., Erikson, M. E., and Amento, E. P. (2000). Relaxin induces an extracellular matrix-degrading phenotype in human lung fibroblasts *in vitro* and inhibits lung fibrosis in a murine model *in vivo*. *J. Clin. Invest.* **98**, 2739–2745.

van der Loop, F. T., Schaart, G., Timmer, E. D., Ramaekers, F. C., and van Eys, G. J. (1996). Smoothelin, a novel cytoskeletal protein specific for smooth muscle cells. *J. Cell Biol.* **134**, 401–411.

Van Vliet, E., Melis, M., Foidart, J. M., and Van Ewijk, W. (1986). Reticular fibroblasts in peripheral lymphoid organs identified by a monoclonal antibody. *J. Histochem. Cytochem.* **34**, 883–890.

Vandekerckhove, J., and Weber, K. (1978). At least six different actins are expressed in higher mammals: An analysis based on the amino-acid sequences of the amino-terminal tryptic peptides. *J. Mol. Biol.* **126**, 783–802.

Vangelista, A., Frasca, G. M., Severi, B., and Bonomini, V. (1989). The role of myofibroblasts in renal interstitial fibrosis and their relationship with fibronectin and type IV collagen. *Contrib. Nephrol.* **70**, 135–141.

Vangelista, A., Frasca, G. M., Severi, B., and Bonomini, V. (1991). Clinical Factors in Progressive Renal Damage: The Role of Interstitial Fibrosis. *Am. J. Kidney Dis.* **17**, 62–64.

Vogl, W., Renke, M., Mayer-Eichberger, D., Schmitt, H., and Bohle, A. (1986). Long-term prognosis for endocapillary glomerulonephritis of poststreptococcal type in children and adults. *Nephron* **44**, 58–65.

Vyalov, S. L., Gabbiani, G., and Kapanci, Y. (1993). Rat alveolar myofibroblasts acquire smooth muscle actin expression during bleomycin-induced pulmonary fibrosis. *Am. J. Pathol.* **143**, 1754–1765.

Wiggins, R., Goyal, M., Merritt, S., and Killen, P. D. (1993). Vascular adventitial cell expression of collagen I messenger ribonucleic acid in anti-glomerular basement membrane antibody induced crescentic nephritis in the rabbit. A cellular source for interstitial collagen synthesis in inflammatory renal disease. *Lab. Invest.* **68**, 557–565.

Wilkinson, L. S., Pitsillides, A. A., Worrall, J. G., and Edwards, J. C. W. (1992). Light microscopic characterisation of the fibroblast-like synovial intimal cell (Synoviocyte). *Arthritis. Rheum.* **35**, 1179–1184.

Yaguchi, T., Fukuda, Y., Ishizaki, M., and Yamanaka, N. (1998). Immunohistochemical and gelatin zymography studies for matrix metalloproteinases in bleomycin-induced pulmonary fibrosis. *Pathol. Int.* **48**, 954–963.

Yasuda, T., Kondo, S., Owada, M., Ishida, M., and Harris, R. C. (2002). Integrins and the cytoskeleton: Focal adhesion kinase and paxillin. *Nephrol. Dial. Transplant.* **14**, 58–60.

Zeisberg, M., Muller, G. A., and Kalluri, R. (2004). Are there endogenous molecules that protect kidneys from injury? The case for bone morphogenic protein-7 (BMP-7). *Nephrol. Dial. Transplant.* **19**, 759–761.

Zhang, K., Rekhter, M. D., Gordon, D., and Phan, S. H. (1994). Myofibroblasts and their role in lung collagen gene expression during pulmonary fibrosis. A combined immunohistochemical and *in situ* hybridization study. *Am. J. Pathol.* **145**, 114–125.

Zhuo, J., Dean, R., Maric, C., Aldred, P. G., Harris, P., Alcorn, D., and Mendelsohn, F. A. O. (1998). Localization and interactions of vasoactive peptide receptors in renomedullary interstitial cells of the kidney. *Kidney Int.* **54**, S22–S28.

This page intentionally left blank

Tumor Hypoxia and Targeted Gene Therapy

Olga Greco* and Simon Scott†

*Tumour Microcirculation Group, University of Sheffield, Royal Hallamshire Hospital, Sheffield, United Kingdom

†Medway School of Pharmacy, The University of Kent, Kent, United Kingdom

Hypoxia is an integral characteristic of the tumor microenvironment, primarily due to the microvascular defects that accompany the accelerated neoplastic growth. The presence of tumor hypoxic areas correlates with negative outcome after radiotherapy, chemotherapy, and surgery, as hypoxia not only provides an environment directly facilitating chemo- and radio-resistance, but also encourages the evolution of phenotypic changes inducing permanent resistance to treatment and metastatic spread. Therefore, successful treatment of hypoxic cells has the potential to not only improve local control but also impact overall patient survival. Specific and selective targeting of hypoxic tumor areas can be achieved at all three steps of a gene therapy treatment: delivery of the therapeutic gene to the tumor, regulation of gene expression, and therapeutic efficacy. In this review the latest developments and innovations in hypoxia-targeted gene therapy are discussed. In particular, approaches such as hypoxia-conditionally replicating viruses, cellular vehicles, and gene therapy means to disrupt the hypoxia-inducible factor (HIF) signaling are outlined.

KEY WORDS: HIF, HRE, Radiation, Chemotherapy, Bioreductive drugs, CArG elements, Suicide gene therapy, Cre/loxP. © 2007 Elsevier Inc.

I. Introduction

A. Tumor Hypoxia

The majority of solid tumors, regardless of their origin, location, or genetic alterations, show areas at reduced oxygen partial pressure (pO₂). Hypoxia is an integral characteristic of the tumor microenvironment, primarily due to

the microvascular defects that accompany the accelerated neoplastic growth. The inadequate vascular geometry relative to the volume of oxygen-consuming tumor cells creates diffusion-limited O₂ delivery (chronic hypoxia) (Thomlinson and Gray, 1955). Moreover, the dynamic changes in microregional blood flow in tumors have been related to the formation of areas of perfusion-limited O₂ delivery (acute or transient hypoxia) (Brown, 1979; Chaplin *et al.*, 1987; Kimura *et al.*, 1996). Chronic and transient hypoxia have been detected in animal tumor models as well as in human cancers (Brizel *et al.*, 1997; Hill *et al.*, 1996; Raleigh *et al.*, 1998; Vaupel and Hockel, 1998). Measurements of solid tumors pO₂, obtained by polarographic needle electrodes, have indicated a decrease in median pO₂ levels compared with their normal tissues of origin. For example, measurements carried out in normal breast revealed a median pO₂ of 65 mmHg (8.6% O₂), whereas in breast carcinomas of stages pT1-4 the median pO₂ was 28 mmHg (3.9% O₂) (Vaupel and Hockel, 1998). More than 30% of the breast cancers investigated exhibited pO₂ values between 0 and 2.5 mmHg (0.3% O₂). In contrast, values <12.5 mmHg (1.6% O₂) could not be detected in the normal breast. Hypoxia is also present in metastatic lesions, and in metastases of carcinomas of the head and neck, breast, and rectal cancers lower median pO₂ values and higher hypoxic fractions were recorded, compared not only with the normal surrounding tissue, but also the primary tumors (Becker *et al.*, 1998; Vaupel and Hockel, 1998).

It has long been known that the presence of tumor hypoxic areas correlates with negative outcome after radiotherapy, chemotherapy, and surgery. Hypoxia not only provides an environment directly facilitating chemo- and radio-resistance (reduction of radiation-generated, DNA-damaging reactive oxygen intermediates; impaired delivery of drugs), but also encourages the evolution of phenotypic changes inducing permanent resistance to treatment and metastatic spread (Greco *et al.*, 2003). An association between primary tumor oxygenation and the likelihood of distant metastasis has been reported in clinical studies involving patients with high-grade soft tissue sarcoma (Brizel *et al.*, 1996) and advanced squamous cell carcinoma of the uterine cervix (Fyles *et al.*, 2002; Pitson *et al.*, 2001; Sundfor *et al.*, 1998). Also, a positive correlation has been observed between tumor lactate concentration and the presence of metastatic deposits in cervix and head and neck squamous cell carcinomas (Brizel *et al.*, 2001; Rofstad *et al.*, 2000). Therefore, successful treatment of hypoxic cells has the potential to not only improve local control but also impact overall patient survival.

B. Cellular Signaling in Response to Hypoxia

Approximately 1% of the genome of mammalian cells is transcriptionally induced by the hypoxic stress (Le *et al.*, 2004). More than 60 of these genes are regulated by the transcription factor hypoxia-inducible factor (HIF)-1 (Semenza, 2003), a heterodimer consisting of two basic-helix-loop-helix

proteins from the Per-aryl hydrocarbon receptor nuclear translocator (ARNT)-Sim (PAS) family of transcription factors: HIF-1 α (120 kDa) and HIF-1 β (91–94 kDa) (Wang *et al.*, 1995). The endothelial PAS domain protein (EPAS)-1 has been reported to show close sequence homology and similar properties to HIF-1 α , and therefore has been renamed HIF-2 α or HIF-1 α -like factor (HLF) (Wenger and Gassmann, 1997). Originally believed to be expressed predominantly in endothelial cells, HIF-2 α has been detected in a number of different cell and tissue types *in vitro* and *in vivo* (Talks *et al.*, 2000; Wiesener *et al.*, 1998). A third HIF α subunit, HIF-3 α , shares sequence identity with that of HIF-1 α and HIF-2 α (57 and 53% identity at the N-terminal basic helix-loop-helix [bHLH]/PER-ARNT-SIM [PAS] domains, respectively) (Gu *et al.*, 1998). Of the α and β subunits, HIF α is oxygen-sensitive and regulated mainly at posttranslational levels (Pugh *et al.*, 1997). HIF α protein levels increase during hypoxia and the protein is degraded within 3–5 minutes during reoxygenation (Huang *et al.*, 1996), by targeting it to the ubiquitin-proteasome degradation pathway. This process is mediated by the von Hippel-Lindau (VHL) protein, which binds to HIF-1 α after hydroxylation of two HIF-1 α proline residues (402 and 564) in its C-terminal oxygen-dependent degradation domain (ODDD) (Fig. 1) and targets it for destruction by the proteasome (Ivan *et al.*, 2001; Jaakkola *et al.*, 2001). HIF-1 α hydroxylation is strictly dependent on the presence of oxygen as a cosubstrate and iron as a cofactor. On the other hand, under hypoxia, hydroxylation does not occur, HIF-1 α remains stable, and complexes with the β subunit to form the functional transcription factor. Asparagine residue 803 of HIF-1 α is also hydroxylated in an oxygen-dependent manner by factor inhibiting HIF-1 (FIH-1), blocking the HIF interaction with the coactivators p300 and CBP (Lando *et al.*, 2002; Mahon *et al.*, 2001). Furthermore, acetylation of lysine 532 in the HIF-1 α ODDD by ARD1 increases its interaction with the VHL protein and consequent degradation (Jeong *et al.*, 2002). However, studies indicate that ARD1 may not have a central role in HIF-1 α posttranslational regulation (Arnesen *et al.*, 2005; Bilton *et al.*, 2005; Fisher *et al.*, 2005), whereas small ubiquitin-related modifier (SUMO) 1 appears to stabilize HIF-1 α and enhance its transcriptional activity (Bae *et al.*, 2004; Mazure *et al.*, 2004).

To modulate gene expression, the HIF heterodimer interacts with the p300/CBP and SRC-1 family of coactivators (Arany *et al.*, 1996; Carrero *et al.*, 2000; Kung *et al.*, 2000), and binds to enhancer sequences named hypoxia responsive elements (HREs), containing the core sequence 5'-RCGTG-3'. HREs have been found at varying distances from and orientations to the coding sequence region of hypoxia-regulated genes, and can be utilized as a means to control therapeutic gene expression in hypoxic tumor areas.

Although HIF is regulated mainly by oxygen, other factors can modulate its synthesis and stability. Growth factor stimulation induces HIF transcriptional activity in tumor cells via a signal pathway leading from receptor tyrosine kinases such as the human epidermal growth factor receptor (HER)-2 to

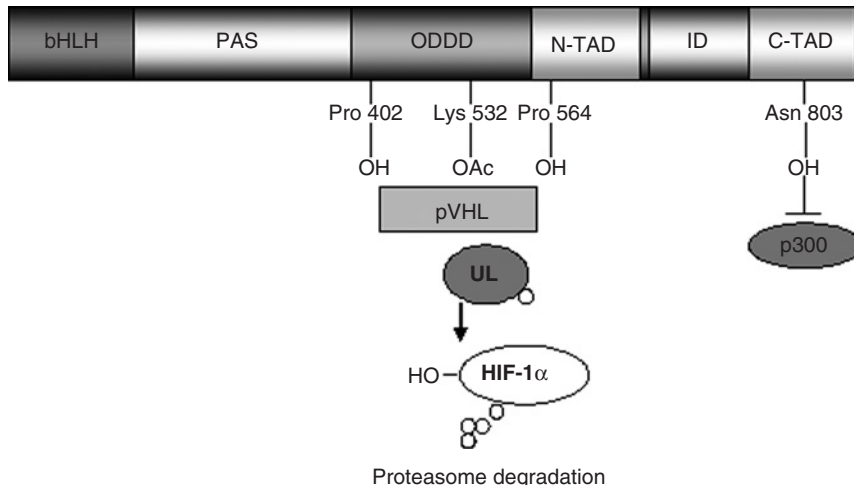


FIG. 1 Domain structure of HIF-1 α . HIF-1 α presents basic helix-loop-helix (bHLH) and PER-ARNT-SIM (PAS) domains, which are involved in the dimerization with HIF-1 β and DNA binding. HIF-1 α also contains two independent transactivation domains (N-TAD and C-TAD), the N-TAD within the oxygen-dependent degradation domain (ODDD). In oxygenated cells, the proline residues 402 and 564 are oxidatively modified by a prolyl hydroxylase. This iron-dependent process is necessary for binding of HIF-1 α to the von Hippel-Lindau (VHL) protein, followed by the activation of the ubiquitin-E3 ligase (UL) and HIF-1 α proteasome degradation. Asparagine residue 803 is also hydroxylated in an oxygen-dependent manner by factor inhibiting HIF-1 (FIH-1), blocking the HIF interaction with the coactivator p300. Acetylation of lysine 532 increases HIF-1 α interaction with the VHL protein and consequent degradation. Under hypoxia, HIF-1 α complexes with HIF-1 β to form the functional transcription factor.

phosphatidylinositol-3-kinase (PI3K), Akt, and FRAP (Laughner *et al.*, 2001) (Fig. 2). In particular, Akt can phosphorylate HIF-1 β , enhance its ability to bind to HIF-1 α , and therefore increase HIF-1 transcription stability (Li *et al.*, 2005a). This pathway is negatively regulated by the tumor suppressor protein PTEN, by dephosphorylating the products of the PI3K reactions (Fig. 2) (Zhong *et al.*, 2000). Other genetic alterations, such as overexpression of the v-src oncogene (Jiang *et al.*, 1997) or inactivation of tumor suppressor genes such as p53 (Ravi *et al.*, 2000), also result in enhanced transcriptional activity of HIF.

II. Hypoxia-Targeted Gene Therapy

Although a significant adverse factor for cancer prognosis, severe hypoxia does not occur in normal tissues and thus can be exploited for selective cancer treatment. In particular, tumor cells at reduced oxygen concentration can be

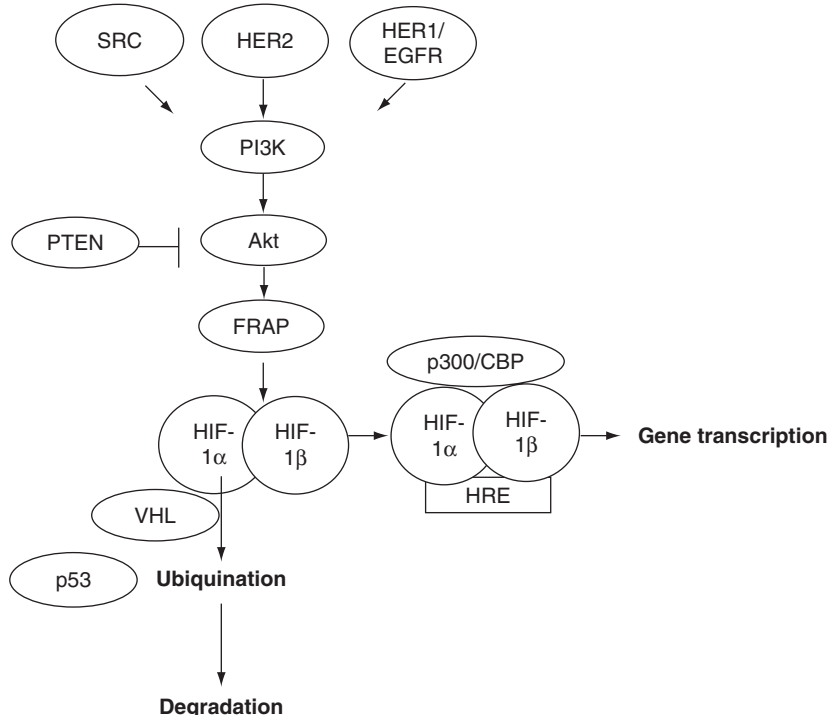


FIG. 2 Regulation of HIF-1 synthesis and activity. Tyrosine kinases, such as SRC, the human epidermal growth factor receptor (HER)-2 and HER-1/epidermal growth factor receptor (EGFR), activate the phosphatidylinositol-3-kinase (PI3K)/Akt/FRAP pathway. Akt can phosphorylate HIF-1 β and enhance its ability to bind to HIF-1 α , therefore increasing HIF-1 transcription stability via hypoxia responsive elements (HREs). This pathway is negatively regulated by the tumor suppressor protein PTEN. Binding of p53 to HIF-1 α increase its targeting to ubiquination and degradation.

specifically targeted via gene therapy approaches. Hypoxia-specificity can be achieved at all three steps of a gene therapy treatment: delivery of the therapeutic gene to the tumor, regulation of gene expression, and therapeutic efficacy (Greco *et al.*, 2000, 2003; Scott and Greco, 2004). Novel approaches to hypoxia-targeted cancer gene therapy will be outlined in this review.

A. Therapeutic Modification of the Hypoxic Signaling

HIF is common to all mammalian cells, human tissues, and organs tested to date (Maxwell *et al.*, 1993; Wiener *et al.*, 1996) and has an important pathophysiological role within solid tumors. Compared with the wild-type

tumors, mouse Hepa-1 hepatomas from HIF-1 β -deficient cells presented reduced hypoxia-mediated gene expression, vascularity, and growth rate (Maxwell *et al.*, 1997). Analogously, *HIF-1 β* ^{-/-} knockout embryonic stem (ES) cells failed to activate hypoxia-responsive genes and to respond to a decrease in glucose concentration (Maltepe *et al.*, 1997). *HIF-1 β* ^{-/-} embryos were not viable past embryonic day 10.5 and showed defective angiogenesis of the yolk sac and branchial arches, stunted development, and embryo wasting. Similar effects were seen in HIF-1 α -deficient embryos (Ryan *et al.*, 1998). In subcutaneously implanted *HIF-1 α* ^{-/-} ES cells, vessel perfusion, oxygenation, vascular endothelial growth factor receptor (*VEGF*) expression, and growth were significantly reduced (Carmeliet *et al.*, 1998; Ryan *et al.*, 1998, 2000).

HIF α overexpression in solid tumors, compared with normal tissues (Talks *et al.*, 2000), is a consequence of both intratumoral hypoxia and genetic alterations, the latter being active in some tumor cells only. HIF has been linked to a more aggressive disease and has been indicated as a prognostic marker for a number of tumor sites. Increased levels of HIF-1 α protein in human prostate cancer cell lines correlated with enhanced metastatic potential (Zhong *et al.*, 1998). More importantly, the HIF-1 α subunit was overexpressed in 68% of different neoplastic lesions but not in nonmalignant tumors such as breast fibroadenoma and uterine leiomyoma (Zhong *et al.*, 1999). In patients undergoing chemotherapy, radiotherapy, and/or surgery, HIF-1 α production was a strong independent prognostic marker in cancer of the oropharynx (Aebersold *et al.*, 2001), of the esophagus (Koukourakis *et al.*, 2001) and head and neck (Koukourakis *et al.*, 2002), in breast cancer (Schindl *et al.*, 2002), lung cancer (Swinson *et al.*, 2004), transitional cell carcinoma of the upper urinary tract (Nakanishi *et al.*, 2005), early stage (Birner *et al.*, 2000) but not locally advanced cervical carcinoma (Haugland *et al.*, 2002), nor in patients with ovarian cancer (Birner *et al.*, 2001). However, a significant reduction in overall survival after platinum-based chemotherapy was observed in ovarian cancer patients with overexpression of both *p53* and *HIF-1 α* (Birner *et al.*, 2001). By comparison, in early operable non-small-cell lung cancer, HIF-2 α but not HIF-1 α protein levels were significantly associated with poor prognosis (5-year survival) (Giatromanolaki *et al.*, 2001).

Hence, inhibition of HIF activity represents an interesting approach to specifically target tumors with a potentially negative prognosis. To this end, gene therapy systems have been tested to silence components of the HIF pathway, by using antisense phosphorothioate oligodeoxynucleotides (ODN) and small interfering RNA (siRNA) technology. Indeed, administration of an antisense HIF-1 α ODN to glioblastoma cells, as well as to normal astrocytes and fibroblasts, induced a dose-dependent inhibition of HRE-mediated reporter expression, which was mirrored by a depletion in HIF-1 α mRNA and protein

levels (Dai *et al.*, 2003). Besides its role in the adaptation to the hypoxic stress, HIF can modulate the apoptotic response, although its role remains controversial. Some reports suggest that HIF-1 α is a mediator of hypoxia-induced apoptosis, by activating the transcription of proapoptotic genes such as *NIX* and *NIP3* (Sowter *et al.*, 2001), others indicate that HIF-1 α can prevent tumor cell death (Akakura *et al.*, 2001), by upregulating antiapoptotic proteins such Bcl-2 and Bcl-X_L (Park *et al.*, 2002). Indeed, inhibition of HIF-1 α transactivation by transfection with antisense ODN or siRNA induced a significant increase in apoptosis in human tongue squamous cell carcinoma, glioblastoma hepatobiliary, and pancreatic cancer cells *in vitro*, under both normoxic and hypoxic conditions (Dai *et al.*, 2003; Mizuno *et al.*, 2005; Zhang *et al.*, 2004). Furthermore, HIF-1 α antisense ODN treatment attenuated the synthesis of antiapoptotic proteins such as Bcl-2 and IAP-2 and increased levels of caspase-3 activity, while p53 was not involved in the induced cell death (Dai *et al.*, 2003; Zhang *et al.*, 2004). Interestingly, this decrease in viability could not be observed in human hepatoma HepG2 cells, characterized by undetectable levels of HIF-1 α under normoxia, indicating that depletion of HIF-1 α expression preferably induces apoptosis in cells harboring a constitutive level of HIF-1 α (Zhang *et al.*, 2004). Delivery of a plasmid vector containing an HIF-1 α antisense ODN induced rapid regression of small tumor xenografts from EL-4 thymic lymphoma cells, although it could only slow the growth of large (>0.4 cm in diameter) tumors, even at high doses of DNA (Sun *et al.*, 2001, 2003). Similar results were observed after delivery of the *VHL* gene. However, large tumors that were refractory to these single therapies showed significant VEGF loss, inhibition of angiogenesis, apoptosis, and growth arrest after combined, synergistic, antisense HIF and sense *VHL* gene therapy (Sun *et al.*, 2003) or antisense HIF and T-cell costimulator B7-1 immuno-gene therapy (Sun *et al.*, 2001). Additionally, antitumor efficacy of HIF-1 α antisense combined with *VHL* overexpression has also been confirmed in a glioma model (Sun *et al.*, 2006).

One of the effects of HIF posttranslational stabilization is the activation of the transforming growth factor α (TGF- α)/epidermal growth factor receptor (EGFR) pathway (Gunaratnam *et al.*, 2003). In particular, HIF-2 α mediates constitutive EGFR activation driving tumorigenesis in *VHL*-deficient renal cell carcinoma (Smith *et al.*, 2005). This process could be inhibited by RNA interference to EGFR, which prevented autonomous growth of *VHL*^{-/-} renal cell carcinoma cell lines in culture, their ability to form spheroids and *in vivo* tumor growth (Smith *et al.*, 2005).

Heterodimerization of HIF α with ARNT/HIF-1 β is crucial for binding to HREs. ARNT is a common binding partner for several bHLH-PAS proteins and, compared with HIF α , is relatively abundant in cells. On the other hand, transcriptional coactivators such as p300 and CBP are limiting factors because of competition among interacting proteins for binding to their overlapping

interacting domains. Therefore, disruption of the interaction between HIF α with p300/CBP has the potential to result in efficient inhibition of the activation of a plethora of hypoxia-responsive genes. Retroviral overexpression of polypeptides corresponding to the HIF-1 α C-terminal transactivation (C-TAD) domain or the p300 CH1 domain blocked HIF-p300/CBP interaction and attenuated hypoxia-inducible gene expression (Kung *et al.*, 2000). The C-TAD polypeptide was particularly efficient in inhibiting hypoxia-activated reporter expression (80–90% attenuation compared with an empty vector) and *in vivo* growth of tumor xenografts established from retrovirally transduced human HCT116 colon and MDA-MB435 breast carcinoma cells expression (Kung *et al.*, 2000).

B. Hypoxia-Regulated Therapeutic Gene Expression

The high frequency of HIF-1 expression across human tumors of diverse origin has also been extensively exploited for HRE-directed gene therapy of the hypoxic environment. Hypoxia-controlled apoptosis was obtained in human glioblastoma cells expressing the *Bax* gene under the control of nine copies of the HRE from the erythropoietin (*Epo*) gene (Ozawa *et al.*, 2005). *Bax* is a death-promoting member of the *Bcl2* family of genes, and translocation of BAX homodimer to the mitochondria can activate the caspase pathway, causing apoptotic death of mammalian cells (Hanahan and Weinberg, 2000). HRE-Bax-transfected U-251 cells showed a significant increase in apoptosis under anoxia in culture, and when implanted as mouse flank tumor xenografts (Ozawa *et al.*, 2005).

Survivin, a protein involved in apoptosis, is expressed in 60–70% of common tumor types, but not in normal tissue (Altieri, 2003). Survivin is transcriptionally upregulated in cancer, but not in normal cells, and its promoter was activated by hypoxia (Yang *et al.*, 2004). Hypoxic targeting of a survivin-based gene therapy vector containing an autocatalytic caspase 3 gene, was further increased by the addition of six VEGF HREs upstream of the survivin core promoter. Effective induction of apoptosis was observed in hypoxic tumor cells, without loss of selectivity of either promoter components (Yang *et al.*, 2004).

“Suicide” gene therapy, or gene-directed enzyme/prodrug therapy (GDEPT), consists of delivering to the tumor cells a gene encoding an enzyme which is nontoxic per se, but is able to convert a prodrug into a potent cytotoxin (Greco and Dachs, 2001; Patterson *et al.*, 2003). HRE-controlled GDEPT has shown potential *in vitro* and *in vivo* (Binley *et al.*, 2003; Greco *et al.*, 2002; Patterson *et al.*, 2002). HREs have been successfully used to control the expression of the HSV thymidine kinase (HSVtk) and the cytosine deaminase (CD) genes, able to selectively convert the prodrugs ganciclovir (GCV) and

5-fluorocytosine (5-FC), respectively into cytotoxic agents (Ingram and Porter, 2005; Ogura *et al.*, 2005; Wang *et al.*, 2005).

Most solid tumors depend on an intact, albeit abnormal, vasculature supply for their survival. Selective disruption of the tumor blood vessels causes malignant cells to starve of oxygen and nutrients, leading to secondary tumor necrosis. Disrupting the tumor vasculature presents a number of advantages over standard cytotoxic approaches, such as direct access to the target, simplified agent delivery, and the lack in endothelial cells of drug resistance characteristic of neoplastic cells. VEGF, one of the most studied hypoxia-regulated genes, is considered the main regulator of tumor angiogenesis and the most potent endothelial cell mitogen (Ferrara *et al.*, 2003). VEGF binding to its receptors (VEGFRs), VEGFR-1 (Flt-1) and -2 (Flk-1), results in endothelial cell differentiation, survival, capillary tube formation, and vascular permeability. Inhibition of the interaction of VEGF with its receptors, and therefore the downstream intracellular pathway, stunted angiogenesis, and tumor growth (Millauer *et al.*, 1994; Ogawa *et al.*, 2002). Hypoxia-targeted interference with the VEGF/VEGFR pathway has been obtained by engineering a replication defective HSV amplicon containing a soluble Flk-1, lacking its membrane spanning domain, controlled by VEGF HREs (Pin *et al.*, 2004a). Conditioned medium from human SK-HEP-1 hepatocellular carcinoma cells transduced with the HRE-Flk-1 HSV inhibited *in vitro* tube formation in human umbilical vein endothelial cells (HUEVCs). Furthermore, a single HSV injection (10^6 plaque forming units, pfu) resulted in significant growth delay of SK-HEP-1 tumor xenografts (Pin *et al.*, 2004a). Such high efficacy of a single virus inoculation could be due to some sort of positive feedback mechanism whereby tumor hypoxia activates the HREs in the virus, leading to soluble Flk-1 expression, inhibition of angiogenesis, and induction of further hypoxia. This positive feedback could overcome limitations of amplicon-mediated gene delivery, such as reduced transduction efficiency and transient gene expression.

C. Hypoxia-Targeted Gene Therapy Vectors

1. Hypoxia-Activated Oncolytic Viruses

Lytic viruses can infect, replicate in, and lyse mammalian cells. By targeting virus replication to tumor cells, it is possible to achieve potent cytotoxicity, because the local replication amplifies the input dose through secondary infection and creates a high concentration of therapeutic agent at the tumor site. Furthermore, oncolytic viruses can be armed with therapeutic genes for increased tumor toxicity, without any loss in terms of patient safety (Freytag *et al.*, 2002, 2003). There are several strategies to achieve tumor-selectivity of replication-competent viruses, for example by exploiting viruses' inherent

tumor tropism (e.g., Newcastle disease virus) (Lorenz *et al.*, 2003), by deleting viral genes that are crucial for replication in normal tissues but are dispensable on tumor cells with defects in specific pathways (attenuation; e.g., the adenovirus Onyx-015 replicating in p53 mutated cells) (McCormick, 2003), by restricting replication gene expression to tumor cells using tissue- or condition-specific promoters, such as hypoxia-responsive promoters. Oncolytic viruses, such as vesicular stomatitis viruses and adenoviruses, have potential to be used for hypoxia-targeted gene therapy, as they have been shown to be able to infect and replicate under hypoxic conditions *in vitro* and *in vivo* (Connor *et al.*, 2004; Post *et al.*, 2004a). However, a reduction in adenovirus replication and cytolytic activity has been observed in normal and cancer cells transduced *in vitro* with replication-competent viruses (Pipiya *et al.*, 2005; Shen and Hermiston, 2005), due to posttranslational degradation of the adenoviral early 1 (E1A) protein, essential for adenovirus replication (Shen and Hermiston, 2005).

Post and Van Meir (2003) developed an oncolytic virus that can specifically conditionally replicate in hypoxic cells. This adenovirus contains a hypoxia responsive promoter, with six VEGF HREs, controlling the expression of the E1A gene. Normal human fibroblasts and human malignant glioma cells infected with the virus (multiplicity of infection, MOI = 1–100) showed a significant increase in cytopathic effects and virus replication under hypoxia (1% O₂), *in vitro* (Post and Van Meir, 2003; Post *et al.*, 2004a). Some cytopathic effects and E1A expression could also be observed under normoxia, especially at the higher doses of virus. However, in LN229 glioma xenografts treated for 5 days with intratumor injections of 10⁸ pfu/day, virus replication was restricted to the hypoxic tumor regions, resulting in tumor growth inhibition and even regression (Post *et al.*, 2004a). Normoxic E1A expression in normal and tumor cells infected with a VEGF HRE-regulated oncolytic adenovirus was also observed *in vitro* by Cho and colleagues (Cho *et al.*, 2004). This promoter “leakiness” could be eliminated by the insertion of a “stuffer” sequence between the adenoviral packaging signal and the HRE expression system. Furthermore, to restrict replication to the tumor, the adenovirus was also attenuated by deletion of the E1B55 gene, which counteracts the function of p53 (Yew and Berk, 1992). Indeed, *in vitro* cytopathic effects after hypoxic stimulus *in vitro* could be detected at virus MOIs as low as 0.1 in tumor cells, whereas an MOI of 50 was required in normal cells. *In vivo*, the HRE-regulated virus could replicate and decrease tumor growth, without affecting the body weight of the injected mice (Cho *et al.*, 2004).

In a similar approach, Cuevas and colleagues (2003) constructed an attenuated adenovirus with the E1A gene under the control of nine VEGF HREs, and the E4 gene regulated by an E2F-1 responsive promoter. Besides requiring HIF activation, this virus could selectively replicate in tumor cells,

because the E2F-1 transcription factor, required for cell cycle progression, is upregulated in pRb-mutated cancer cells. Indeed, under normoxic conditions virus replication, amplification, and cytotoxicity could be selectively observed in *VHL*-defective renal cell carcinoma lines, which were shown to overproduce HIF-1 α (Cuevas *et al.*, 2003). Hypoxic activation and *in vivo* antitumor activity of the virus were also demonstrated in cells with functional HIF regulatory pathways (Cuevas *et al.*, 2003).

One of the advantages of artificial hybrid promoters for gene therapy is their flexibility, because several elements of different origin can be arranged in various orders, numbers, and relative orientation, to optimize gene regulation. Dual-specific promoters have been described containing HREs in combination with estrogen-responsive promoters (Hernandez-Alcoceba *et al.*, 2001), cytokine-inducible enhancers (Modlich *et al.*, 2000), and hepatoma-associated enhancers (Ido *et al.*, 2001). To restrict virus replication to hypoxic, estrogen receptor-positive breast cancer cells, an adenovirus has been constructed whereby the promoter controlling the E1A gene contained three HREs from the phosphoglycerate kinase (*PGK*) 1 gene followed by five estrogen responsive elements (Hernandez-Alcoceba *et al.*, 2002). The composite promoter maintained its properties of low basal activity and high inducibility within the adenoviral context, partially due to the presence of an “insulator sequence” inserted between the overlapping E1A enhancer/packaging signals and the E1A promoter (Hernandez-Alcoceba *et al.*, 2002). Exposure to estradiol and/or hypoxia (1% O₂) selectively induced virus replication and cytotoxicity in estrogen receptor-positive MCF-7 and BT-474 breast cancer cells, whereas hypoxia was strictly required for lysis in estrogen receptor-negative HeLa cervical cancer cells. As an added level of safety, in this virus the *E4* gene was placed under the control of either the human telomerase reverse transcriptase promoter (hTERT) or the E2F-1 promoter, both selectively active in tumor cells. Four repeated injections of the resulting virus induced a significant reduction in the volume of tumor xenografts established from BT-474 cells, and no side effects were observed in the animals (Hernandez-Alcoceba *et al.*, 2002).

Herpes simplex virus (HSV) strains have also been successfully engineered for selective replication within tumors (Post *et al.*, 2004b). In particular, attenuated HSVs with a defective UL39 gene encoding the large subunit of ribonucleotide reductase, the main rate-limiting enzyme for viral DNA synthesis and replication, exclusively replicate in rapidly dividing cancer cells that provide high levels of ribonucleotide reductase (Mineta *et al.*, 1994). By transfecting human MCF-7 mammary and murine CT26 colorectal carcinoma cells with a plasmid containing the UL39 gene under the control of ten VEGF HREs prior to virus infection, Fong and colleagues observed an increase in cytolysis under hypoxia *in vitro* (Pin *et al.*, 2004b; Reinblatt *et al.*, 2004). When CT26 cells were injected into the spleen of syngeneic

Balb/C mice to create an *in vivo* model of liver metastasis, virus infection resulted in a ~65% decrease in tumor weight and nodule counts in cells transfected with the HRE-UL39 construct, compared with mock transfected cells (Reinblatt *et al.*, 2004).

2. Eukaryotic Delivery Vehicles

Interest in the possibility of using human cells for the delivery of gene therapy to tumors has been increasing. This approach may have the advantage of both systemic delivery and reduced toxicity compared with other delivery systems (e.g., viruses), especially via adverse immunogenic reactions. In the case of cellular delivery, it is envisaged that gene therapy vectors would be carried as “Trojan horses” inside cells, only being activated on reaching a specific target tissue or microenvironment. In practice this would first mean the isolation, purification and, if possible, expansion of a specific cell type from a patient. These cells would be genetically modified *ex vivo* to carry a therapeutic gene, under the appropriate regulatory control (e.g., a hypoxia-responsive gene promoter), and reintroduced into the patient. Depending on the cell type, this would be either into the general circulation, relying on the cells’ natural “homing” abilities to reach the malignant tissue, or by direct administration. Once within the tumor, therapeutic gene expression would occur, either constitutively or under the control of a conditional gene promoter. The subsequent destruction of the tumor would rely on a potent bystander effect, whereby the therapeutic gene product in the vector-bearing cells would bring about the death of neighboring tumor cells, either by direct transfer or by conversion of a prodrug to a diffusible cytotoxin.

Candidates for such cellular delivery vehicles include macrophages (Burke, 2003) and endothelial progenitor cells (Wei *et al.*, 2004). Circulating monocytes extravasate from blood vessels supplying tumors and infiltrate malignant tissues, such as breast (Kelly *et al.*, 1988; Leek *et al.*, 1996; Lewis *et al.*, 2000), prostate (Burton *et al.*, 2000; Lissbrant *et al.*, 2000), and ovarian (Negus *et al.*, 1997) carcinomas, in large numbers while differentiating into macrophages. In addition, large numbers of macrophages have also been safely infused into cancer patients, resulting in efficient local tumor infiltration (Andreesen *et al.*, 1998). Macrophage recruitment into tumors is believed to be due, at least in part, to the production of monocyte chemotactic protein 1 (MCP1) (Ueno *et al.*, 2000), macrophage colony stimulating factor (MCSF) (Tang *et al.*, 1992), and VEGF (Lewis *et al.*, 2000) within the tumor. Furthermore, preferential accumulation of macrophages in hypoxic areas has also been observed (Burton *et al.*, 2000; Leek *et al.*, 1999; Negus *et al.*, 1998), possibly due to upregulation of VEGF (Lewis *et al.*, 2000) or endothelin-2 (Grimshaw *et al.*, 2002) by hypoxic tumor cells. Under hypoxic conditions macrophages are known to upregulate HIF-1 (Burke *et al.*, 2002), suggesting

that HIF-1-regulated constructs could be employed for hypoxia-activated gene therapy via macrophage delivery. Indeed, such a system has been used for experimental gene therapy *in vitro* using adenovirus-transduced macrophages and a tumor spheroid model (Griffiths *et al.*, 2000). In this study, an adenovirus vector carried the cytochrome P450 (CYP2B6) gene under the control of an HRE promoter. Macrophage infiltration of hypoxic tumor spheroids led to significant tumor cell death via CYP2B6 conversion of cyclophosphamide to its toxic metabolite. This study illustrates the potential for using macrophages for therapeutic gene delivery to target hypoxic tumor cells. Furthermore, as macrophages can survive for several months in the body, this approach may result in long-term therapeutic gene expression. Finally, systemic circulation of macrophages raises the possibility for targeting metastases as well as primary tumors. Indeed, breast cancer metastases have been shown to be at least as hypoxic as the primaries from which they derived (Fuller *et al.*, 1994). Thus, HIF1-activated gene therapy should also be applicable for metastatic targeting.

Transfection of macrophages with genetic constructs has been attempted using several methods. High transfer efficiencies have been reported for adenoviruses (De *et al.*, 1998; Haddada *et al.*, 1993; Schneider *et al.*, 1997). Although wild-type retroviruses are ineffective at infecting nonproliferating cells such as monocytes and macrophages, the C-type spleen necrosis virus has been modified by the addition of a nuclear localization signal to its matrix protein, permitting high-level macrophage infection (Parveen *et al.*, 2000). Lentiviruses have also been shown to efficiently infect, and integrate into the genome of, macrophages (Miyake *et al.*, 1998; Schroers *et al.*, 2000). A macrophage-derived cell line has been engineered to produce retroviruses within experimental tumors, resulting in retroviral marker gene delivery and expression in host T lymphocytes (Pastorino *et al.*, 2001). Monocytes have been transfected using adeno-associated virus (Liu *et al.*, 2000) and a strain of vaccinia poxvirus (Paul *et al.*, 2000). Nonviral agents, such as lipoplexes, have also been used for macrophage transfection (Simoes *et al.*, 1999). Transduction of macrophages by electroporation, using Amaxa Biosystems Nucleofector system, lead to DNA transfer to 60–70% cells, but significant cell death over the next 72 h (Scott, unpublished data).

In cancer patients, frantic angiogenesis is restricted to growing tumor masses, regardless of their genetic make-up. Endothelial progenitor cells home mainly to the sites of active neovasculogenesis. Wei and colleagues (2004) transfected mouse embryonic endothelial progenitor cells (eEPCs) using the lipid-based reagent Lipofect (Stratagene), with a plasmid containing a suicide gene composed of the yeast CD fused to uracil phosphoribosyl transferase, the latter introduced to shortcut rate-limiting enzymatic steps. Following intravenous (i.v.) injection, the eEPCs were seen to home to primary and metastatic Lewis lung tumors in syngeneic and nonsyngeneic mice, where they were incorporated into sprouting tumor vessels for at least

10 days after injection. In particular, the eEPC carriers were preferentially found in hypoperfused and hypovascularized metastases, accumulating around hypoxic areas (Wei *et al.*, 2004). When the prodrug 5-FC was concurrently given to mice alongside the gene therapy vector-modified eEPCs, a significant increase in animal survival was observed. The 5-FC was converted into 5-FU within the eEPCs and, via its pronounced bystander effect, killed not only the carrier cells but also the surrounding tumor cells, especially within the hypoxic areas (Wei *et al.*, 2004). However, prolongation of survival was moderate and no cures were achieved, suggesting that for successful tumor eradication an eEPC-sparing suicide system or combination with a conventional treatment may be required (see section III). As for macrophages, adenovirus transfection has also been successful for eEPCs (Choo *et al.*, 2005).

Rigorous criteria will need to be applied for developing cell-based vehicles, such as simple harvesting and purification procedures, tolerance to *ex vivo* expansion, high level of gene transfer, adequate tissue tropism upon systemic introduction, and low risk of untoward cell proliferation or differentiation in patients. Another potential problem of cell-based therapeutic approaches is the potential, due to the relatively long life of such cell types, for the eliciting of neutralizing antibodies after several months of exposure to therapeutic proteins. This may reduce the long-term effectiveness of this approach.

3. Prokaryotic Delivery Vehicles

The ability of anaerobic bacteria to selectively germinate and replicate in necrotic and hypoxic regions of solid tumors makes them a promising tumor-selective vehicle for hypoxia-targeted gene therapeutics. In the 1950s and 1960s, wild-type anaerobic bacteria were administered to cancer patients with little or no associated toxicity, but also no therapeutic gain (Carey *et al.*, 1967; Malmgren and Flanigan, 1955). However, because of their large genome size, bacteria can be genetically engineered to express multiple therapeutic transgenes. Bacteria are also very motile and, if necessary, their spread can be controlled with antibiotics (Theys *et al.*, 2001a). Examples of prokaryotic vectors include anaerobic bacteria of the genera *Clostridium*, *Bifidobacterium*, and tumor-invasive *Salmonella* auxotroph.

Clostridia have been engineered to express suicide genes, such as the *Escherichia coli* nitroreductase (NTR; Fox *et al.*, 1996; Lemmon *et al.*, 1997) and CD (Liu *et al.*, 2002; Theys *et al.*, 2001b), the cytokines tumor necrosis factor (TNF)- α (Nuyts *et al.*, 2001a) and interleukin-2 (Barbe *et al.*, 2005). Spores of *C. beijerinckii* bearing the NTR gene were injected i.v. into tumor-bearing mice, and NTR protein was detected in all tumors tested but not in normal tissues (Lemmon *et al.*, 1997). *In vitro* conversion of the

prodrug CB1954 into a cytotoxic agent was also demonstrated using this vector (Fox *et al.*, 1996; Lemmon *et al.*, 1997). The *in vivo*, i.v. injection of spores of CD-modified *C. sporogens*, followed by systemic administration of the prodrug 5-FC, induced significant antitumor activity (Liu *et al.*, 2002). To further increase tumor hypoxia, the vascular disrupting agent combretastatin-A-4 phosphate (CA-4-P), shown to selectively induce dramatic shutdown of tumor blood vessels (Tozer *et al.*, 2005), was injected to rhabdomyosarcoma bearing rats following administration with CD-expressing *C. acetobutylicum* (Theys *et al.*, 2001b). The combined treatment resulted in enhanced bacterial colonization and higher levels of active CD, especially in small tumors ($<3\text{ cm}^3$) (Theys *et al.*, 2001b). Further tumor selectivity could be achieved by utilizing the radiation-responsive prokaryotic promoter from the *recA* gene to control TNF- α expression (Nuyts *et al.*, 2001b). After two Gy γ -rays, recombinant *C. acetobutylicum* produced levels of TNF- α 44% higher than unirradiated bacteria, and a further 42% increase was observed after a repeated two Gy exposure (Nuyts *et al.*, 2001b).

Attenuated hyperinvasive auxotrophic mutants of *Salmonella typhimurium* can selectively target tumor tissues and amplify in necrotic spaces to levels in excess of 10^9 bacteria per gram of tissue (Pawelek *et al.*, 1997). When these auxotrophs were inoculated intraperitoneally into melanoma-bearing mice, they suppressed tumor growth and prolonged average survival to twice that of untreated mice. Moreover, when the animals were inoculated with *S. typhimurium* expressing HSVtk, GCV-mediated, dose-dependent suppression of tumor growth was measured (Pawelek *et al.*, 1997). Similarly, conversion of 5-FC into 5-FU was observed in tumors colonized by CD-expressing *S. typhimurium* but not in the normal tissues of the inoculated rats (Mei *et al.*, 2002). In a small pilot trial, attenuated CD-expressing *Salmonella* was administered intratumorally to refractory cancer patients (Nemunaitis *et al.*, 2003). No significant adverse events were observed, and two of the three patients presented intratumor bacterial colonization and conversion of 5-FC to 5-FU.

Bifidobacteria are Gram-positive nonpathogenic anaerobes, found in the gastrointestinal tract. Compared to *Clostridia* and *Salmonella*, the lack of pathogenesis of *Bifidobacterium*, used in the preparation of fermented milk products, might be advantageous if used in human therapeutic treatment. Immediately after i.v. inoculation of *B. longum* to tumor-bearing mice and rats, viable bacilli could be detected throughout the animal body, but following 4–7 days the bacteria proliferation was restricted to the tumor mass (Yazawa *et al.*, 2000, 2001). Strains of *B. longum* and *B. adolescentis* were also modified to express the antiangiogenic agent endostatin (O'Reilly *et al.*, 1997). Tail vein and oral delivery of the modified bacteria to tumor-bearing mice resulted in selective tumor colonization and significant inhibition of tumor angiogenesis and growth (Fu *et al.*, 2005; Li *et al.*, 2003).

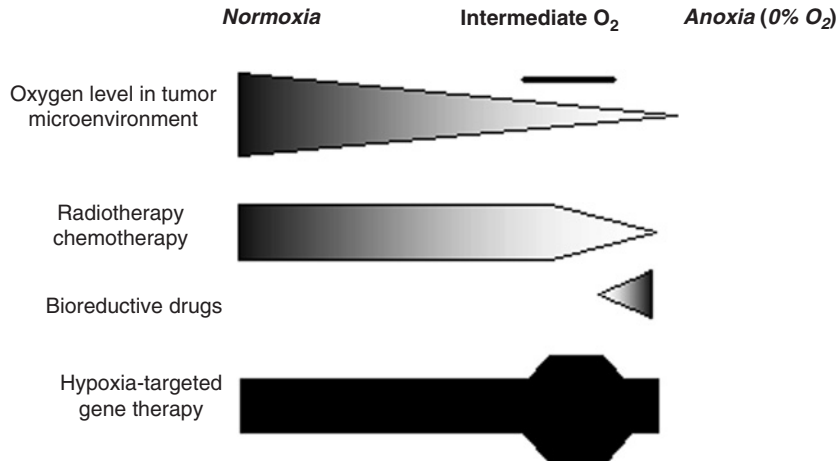


FIG. 3 Efficacy of various treatment modalities under different tumor oxygenation conditions. The schematic illustrates the principle of combining hypoxia-targeted gene therapy (effective against tumor cells at intermediate oxygen levels; 0.1–3% O₂) with conventional treatments, mainly toxic toward well-oxygenated cells. On the other hand, bioreductive drugs are optimally activated at very-low oxygen concentrations (<0.1% O₂).

III. Combination of Hypoxia Gene Therapy with Conventional Treatments

To target hypoxic cells, a number of bioreductive drugs have been developed to be optimally activated at very low oxygen concentrations (<0.1% O₂; Stratford and Workman, 1998). However, Wouters and Brown (1997) concluded the tumor response is highly dependent on cells existing at intermediate oxygen levels (0.5–20 mmHg, ~0.1–3% O₂), and that effective therapeutic agents will need to specifically target this population (Fig. 3). Thus, new therapies need to be developed to target tumor cytotoxicity in these areas. Hypoxia-targeted gene therapy approaches have been developed to function effectively in hypoxic areas of tumors, but also crucially in areas of intermediate oxygen tension. Using combined gene therapy and chemo/radiotherapy protocols, it may be possible to increase tumor cell kill per dose of conventional treatment, without increasing toxicity to normal tissues.

A. Hypoxia Gene Therapy and Radiotherapy

The data just outlined support HIF-1 as a therapeutic target in the treatment of solid tumors. However, Höpfl *et al.* (2002) have shown that mixing wild-type

and HIF-1-deficient cells (lacking either HIF-1 α or HIF-1 β) in the same tumor at a ratio as low as 1:100 can restore the growth of the mixed tumors to match the wild-type tumors. Therefore, any therapy targeting HIF-1 only will need to be either extremely effective or combined with another therapeutic strategy. HIF-1 β -deficient mouse hepatoma Hepa-1 cells showed increased sensitivity to radiation compared with their wild-type counterpart, and this responsiveness was maintained even in mixed tumors (Williams *et al.*, 2005). Interestingly, this change in radiosensitivity was not due to a difference in tumor oxygenation, but likely to be linked to a survival signal activated by HIF-1 β following irradiation. Indeed tumor reoxygenation following radiation can enhance HIF-1 production, initiating a cytokine cascade aimed to protect endothelial cells from apoptosis (Moeller *et al.*, 2004).

Replication deficient adenoviruses can efficiently deliver HIF-1 α -targeting siRNAs to cancer cells in culture to induce a significant increase in apoptosis under hypoxic conditions (Zhang *et al.*, 2004). Although tumor growth delay was observed in tumor xenografts established from preinfected HeLa and HCT116 cells, no antitumor effect was observed when the tumors of 0.7–0.8 cm in diameter were infected with the siRNA adenovector. This disappointing lack of effectiveness is unlikely to be due to low infection efficiency (5–15%) only, as even xenografts established from stable lines transfected with a doxycycline-inducible HIF-1 α siRNA could not be completely eradicated by HIF-1 inhibition alone (Li *et al.*, 2005b). However, when HIF-1 α siRNA adenovirus delivery was combined with a 3 \times 6 Gy radiation schedule, the gene therapy and radiotherapy could induce a small but significant increase in tumor growth delay, compared with radiation alone (Zhang *et al.*, 2004). In combining HIF-1 inhibition with radiotherapy, tumor response appears to be highly dependent on treatment sequencing (Moeller *et al.*, 2005). HIF-1 blockade via retroviral delivery of siRNA was found to protect tumor cells irradiated under hypoxia by promoting cell cycle arrest. This effect is dependent on the p53 status of the cells and on the tumor microenvironment, as HIF is involved in maintaining glucose metabolism and ATP production in tumor cells (Moeller *et al.*, 2005). On the other hand, HIF-1 inhibition significantly enhanced the radiation damage to the tumor vasculature, by decreasing endothelial cell viability (Moeller *et al.*, 2004, 2005). Because vascular effects of HIF-1 blockade are independent of sequencing with radiation, although the effects on tumor cell apoptosis, metabolism, and proliferation require HIF-1 blockade before radiation treatment, maximum tumor response was achieved when radiation was administered before siRNA activation (Moeller *et al.*, 2005). This effect was particularly marked in cells expressing wild-type p53.

For bioreductive drugs to be activated, the cells need to be hypoxic and to produce the appropriate set of reductase enzymes. By contrast, bioactivation is restricted by the presence of oxygen in normal tissue. The lead compound in this area is tirapazamine (TPZ), which exhibits a high specificity for

hypoxic cells over a broad range of oxygen partial pressure, at clinically relevant levels (Koch, 1993). In clinical trials, the combination of TPZ, cisplatin, and radiotherapy resulted in acceptable levels of toxicity (Craighead *et al.*, 2000) and remarkably good and durable clinical responses in patients with advanced head and neck cancers (Rischin *et al.*, 2001). The redox-sensitive flavoprotein NADPH:cytochrome P450 reductase (P450R) plays a central role in the bioactivation of TPZ. P450R overexpression in human fibrosarcoma (HT1080) or breast cancer (MDA231) cells conferred increased sensitivity to TPZ and RSU1069 (1-(3-aziridinyl-2-hydroxypropyl-2-nitroimidazole) (Patterson *et al.*, 1997; Saunders *et al.*, 2000). In HT1080 cells transfected with the P450R coding sequence under the control of a murine *PGK-1* HRE trimer upstream of the SV40 minimal promoter, 18-h anoxic incubation produced a 30-fold enhancement of *in vitro* hypoxic cytotoxicity of RSU1069 (Patterson *et al.*, 2002). P450R-HT1080 tumor xenografts treated with a combination of a single 10 Gy X-ray dose and RB6145 (250 mg/kg), a precursor of RSU1069, displayed a 50% cure rate 100 days after therapy (Patterson *et al.*, 2002). By contrast, hypoxia-inducible GFP control tumors were refractory to 10 Gy, RB6145 alone, or the combination, with 100% mortality at 100 days. In another study by the same group, a replication-defective adenovirus was constructed containing an HRE trimer from the lactate dehydrogenase (*LDH*) A gene controlling the expression of P250R (Cowen *et al.*, 2004). Infection of HT1080 cells *in vitro* caused selective hypoxic sensitization to TPZ, and combined administration of the virus, TPZ, and 10 Gy resulted in complete regression of 85% of the tumors *in vivo* (Cowen *et al.*, 2004).

To combine hypoxia-mediated gene therapy with radiotherapy and to maximize the activation of the vectors within the tumor mass, we have constructed gene therapy vectors consisting of HREs from the *Epo*, *PGK-1*, and *VEGF* genes and radiation-responsive CArG elements from the early growth response (*Egr*) 1 gene, linked to the cytomegalovirus immediate early (CMV IE) basal promoter (Greco *et al.*, 2002). Using a GFP reporter assay, induction of these promoters following 5 Gy irradiation, 0.1% O₂, or dual treatments was compared with the activation of the independent responsive elements and the CMV IE promoter, in MCF-7 breast and T24 bladder carcinoma cells. As expected, isolated CArGs and HREs responded to radiation and hypoxia respectively, with some cross-reactivity also noted. In particular promoter comprising five HREs from the *Epo* gene and nine CArG elements (denoted Epo/E9) produced the most selective and robust initiation of gene expression, across all treatments and tumor cell types, and could effectively drive experimental suicide gene therapy *in vitro* (Greco *et al.*, 2002). The Epo/E9 enhancer maintained its selective hypoxia and radiation responsiveness when inserted in a retroviral vector, in the context of the mammary-specific whey acid promoter (WAP) (Lipnik *et al.*, 2006). Expression analysis *in vitro* showed widely preserved mammary-specific promoter

activity, which *in vivo* was restricted to the hypoxic tumor areas (Lipnik *et al.*, 2006). No reductions in responsiveness and some cooperative effect between HREs from *Epo*, *PGK-1*, *LDH*, and *Egr-1* enhancers was also noted in the context of the SV40 minimal promoter, in a panel of tumor cell lines (Chadderton *et al.*, 2005). Radiation was found to induce HIF-1 α expression in all cell lines tested, whereas HIF-2 α was activated by radiation in one cell line only. However, combined radiation and hypoxia treatment did not result in further increases in HIF-1 α or HIF-2 α expression (Chadderton *et al.*, 2005).

Inducible promoters offer the potential to selectively control therapeutic gene expression in the tumor while minimizing normal tissue toxicity. Nevertheless, when activated, these promoters often result in lower activity compared with strong constitutive promoters, and transgene expression is limited to the period of stimulation, returning to basal levels following withdrawal of the induction trigger. We have devised a “molecular switch” vector system based on *Cre/loxP* recombination, which allows long-term, high-level expression following activation by hypoxia and/or radiation (Greco *et al.*, 2006). In this system, a primary inducible promoter controls the expression of *Cre* recombinase (derived from bacteriophage P1), which in turn recognizes specific DNA sequences (*loxP* sites), causing intramolecular recombination (Fig. 4). Unidirectional *loxP* sites flank (or “*flox*”), a transcriptional silencing “Stop” cassette that prevents expression of a transgene from an upstream constitutive secondary promoter (Fig. 4). In U87 and MCF-7 cells exposed to hypoxia and/or radiation, the HRE/CArG promoter rapidly activated *Cre* recombinase expression leading to selective and sustained HSVtk synthesis (Greco *et al.*, 2006). Killing of transfected tumor cells was measured after incubation with GCV. *In vitro*, higher and more selective GCV-mediated toxicity was achieved with the switch vectors, when compared with the same inducible promoters driving *HSVtk* expression directly. In tumor xenografts implanted in nude mice, the HRE/CArG-switch induced significant growth delay and tumor eradication (Greco *et al.*, 2006).

B. Hypoxia Gene Therapy and Chemotherapy

Hypoxia-induced resistance has been shown for several chemotherapeutic agents both *in vitro* and *in vivo* (Chaplin *et al.*, 1989; Grau and Overgaard, 1988; Teicher *et al.*, 1981). Several factors may be involved. First, hypoxic cells slow down or even arrest their rate of progression through the cell division cycle (Durand and Raleigh, 1998), resulting in a loss of efficacy of most anticancer agents, which are primarily effective against rapidly dividing cells. Second, because of drug metabolism by the cells in the intermediate tumor layers, the limited penetration of plasma-borne agents leads to a

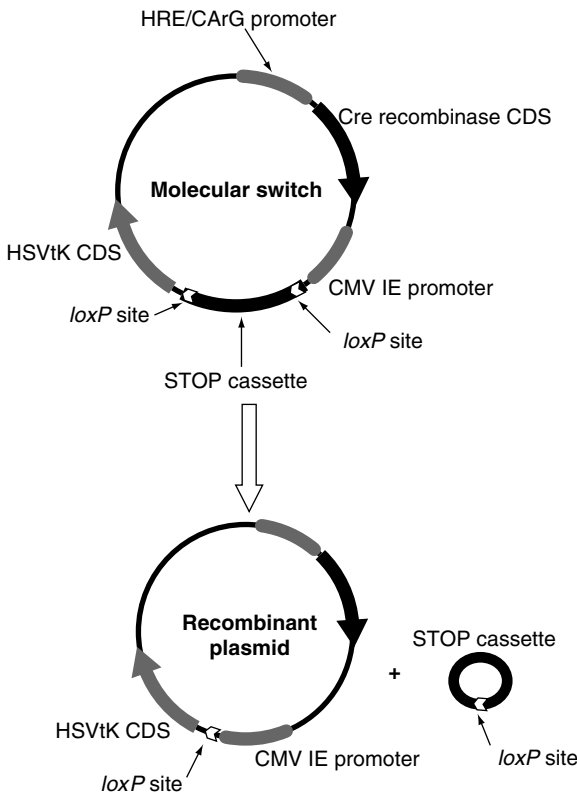


FIG. 4 Molecular switch vector and activation mechanism. In the hypoxia- and radiation-responsive switch vector, hypoxia and/or radiation cause the activation of the inducible promoter containing five HREs from the *Epo* gene and nine CArG elements (E9) from the *Egr 1* gene, inducing *Cre* expression. *Cre* recombinase then recognizes the *loxP* sequences flanking the transcriptional Stop cassette. *Cre/loxP* recombination excises Stop, leading to the juxtaposition of the strong, constitutive CMV IE gene promoter with the *HSVtk* gene, permitting a high-level of suicide gene expression.

reduction in the dose of drug reaching the hypoxic population. Also, the extracellular pH is lower in hypoxic than in well-oxygenated areas, while the intracellular pH is kept constant (Griffiths, 1991). This leads to the uptake and activity of weak acids such as chlorambucil being increased, while those of weak bases like vinblastine are decreased (Chaplin *et al.*, 1998). Finally, hypoxia can induce the production of stress proteins responsible for resistance to doxorubicin, etoposide, and methotrexate (Hughes *et al.*, 1989; Sanna and Rofstad, 1994; Shen *et al.*, 1987) and studies have highlighted the direct role of HIF in the response to chemotherapeutic agents. For instance, mouse embryo fibroblasts lacking HIF-1 α were more

sensitive to carboplatin and etoposide than their wild-type counterpart (Unruh *et al.*, 2003). Conversely, HIF targeting using an adenovirus containing a dominant negative HIF-1 α with the ODDD removed increased the anaerobic efficacy of etoposide in HT1080 and HCT116 cells *in vitro* (Brown *et al.*, 2005). This was re conducted to a decrease in hypoxic downregulation of the proapoptotic protein Bid, shown to be involved in the resistance of hypoxic cells to etoposide (Erler *et al.*, 2004).

IV. Concluding Remarks

Gene therapy of the hypoxic tumor environment presents a number of promising developments and applications in oncology. In particular, the combination of hypoxia-targeted gene therapy with conventional treatments such as radiotherapy represents an exciting approach to overcome and exploit the inherent resistance of tumor cells. It is anticipated that such molecular therapeutics will in the near future transform the way we treat most solid tumors.

REFERENCES

Aebersold, D. M., Burri, P., Beer, K. T., Laissue, J., Djonov, V., Greiner, R. H., and Semenza, G. L. (2001). Expression of hypoxia-inducible factor-1alpha: A novel predictive and prognostic parameter in the radiotherapy of oropharyngeal cancer. *Cancer Res.* **61**, 2911–2916.

Akakura, N., Kobayashi, M., Horiuchi, I., Suzuki, A., Wang, J., Chen, J., Niizeki, H., Kawamura, K., Hosokawa, M., and Asaka, M. (2001). Constitutive expression of hypoxia-inducible factor-1alpha renders pancreatic cancer cells resistant to apoptosis induced by hypoxia and nutrient deprivation. *Cancer Res.* **61**, 6548–6554.

Altieri, D. C. (2003). Validating survivin as a cancer therapeutic target. *Nat. Rev. Cancer* **3**, 46–54.

Andreesen, R., Henneman, B., and Krause, S. W. (1998). Adoptive immunotherapy of cancer using monocyte-derived macrophages: Rationale, current status, and perspectives. *J. Leukoc. Biol.* **64**, 419–426.

Arany, Z., Huang, L. E., Eckner, R., Bhattacharya, S., Jiang, C., Goldberg, M. A., Bunn, H. F., and Livingston, D. M. (1996). An essential role for p300/CBP in the cellular response to hypoxia. *Proc. Natl. Acad. Sci. USA* **93**, 12969–12973.

Arnesen, T., Anderson, D., Baldersheim, C., Lanotte, M., Varhaug, J. E., and Lillehaug, J. R. (2005). Identification and characterization of the human ARD1-NATH protein acetyltransferase complex. *Biochem. J.* **386**, 433–443.

Bae, S. H., Jeong, J. W., Park, J. A., Kim, S. H., Bae, M. K., Choi, S. J., and Kim, K. W. (2004). Sumoylation increases HIF-1alpha stability and its transcriptional activity. *Biochem. Biophys. Res. Commun.* **324**, 394–400.

Barbe, S., Van Mellaert, L., Theys, J., Geukens, N., Lammertyn, E., Lambin, P., and Anne, J. (2005). Secretory production of biologically active rat interleukin-2 by Clostridium acetobutylicum DSM792 as a tool for anti-tumor treatment. *FEMS Microbiol. Lett.* **246**, 67–73.

Becker, A., Hansgen, G., Bloching, M., Weigel, C., Lautenschlager, C., and Dunst, J. (1998). Oxygenation of squamous cell carcinoma of the head and neck: Comparison of primary tumors, neck node metastases, and normal tissue. *Int. J. Radiat. Oncol. Biol. Phys.* **42**, 35–41.

Bilton, R., Mazure, N., Trottier, E., Hattab, M., Dery, M. A., Richard, D. E., Pouyssegur, J., and Brahimi-Horn, M. C. (2005). Arrest-defective-1 protein, an acetyltransferase, does not alter stability of hypoxia-inducible factor (HIF)-1alpha and is not induced by hypoxia or HIF. *J. Biol. Chem.* **280**, 31132–31140.

Binley, K., Askham, Z., Martin, L., Spearman, H., Day, D., Kingsman, S., and Naylor, S. (2003). Hypoxia-mediated tumour targeting. *Gene Ther.* **10**, 540–549.

Birner, P., Gatterbauer, B., Oberhuber, G., Schindl, M., Rossler, K., Prodinger, A., Budka, H., and Hainfellner, J. A. (2001). Expression of hypoxia-inducible factor-1 alpha in oligodendroglomas: Its impact on prognosis and on neoangiogenesis. *Cancer* **92**, 165–171.

Birner, P., Schindl, M., Obermair, A., Plank, C., Breitenecker, G., and Oberhuber, G. (2000). Overexpression of hypoxia-inducible factor 1alpha is a marker for an unfavorable prognosis in early-stage invasive cervical cancer. *Cancer Res.* **60**, 4693–4696.

Brizel, D. M., Schroeder, T., Scher, R. L., Walenta, S., Clough, R. W., Dewhirst, M. W., and Mueller-Klieser, W. (2001). Elevated tumor lactate concentrations predict for an increased risk of metastases in head-and-neck cancer. *Int. J. Radiat. Oncol. Biol. Phys.* **51**, 349–353.

Brizel, D. M., Scully, S. P., Harrelson, J. M., Layfield, L. J., Bean, J. M., Prosnitz, L. R., and Dewhirst, M. W. (1996). Tumor oxygenation predicts for the likelihood of distant metastases in human soft tissue sarcoma. *Cancer Res.* **56**, 941–943.

Brizel, D. M., Sibley, G. S., Prosnitz, L. R., Scher, R. L., and Dewhirst, M. W. (1997). Tumor hypoxia adversely affects the prognosis of carcinoma of the head and neck. *Int. J. Radiat. Oncol. Biol. Phys.* **38**, 285–289.

Brown, J. M. (1979). Evidence for acutely hypoxic cells in mouse tumours and a possible mechanism of reoxygenation. *Br. J. Radiol.* **52**, 650–656.

Brown, L. M., Cowen, R. L., Debray, C., Eustace, A., Erler, J. T., Sheppard, F. C., Parker, C. A., Stratford, I. J., and Williams, K. J. (2005). Reversing Hypoxic Cell Chemoresistance *In Vitro* Using Genetic And Small Molecule Approaches Targeting Hypoxia Inducible Factor-1. *Mol. Pharmacol.* **69**, 411–418.

Burke, B. (2003). Macrophages as novel cellular vehicles for gene therapy. *Expert Opin. Biol. Ther.* **3**, 919–924.

Burke, B., Tang, N., Corke, K. P., Tazzyman, D., Ameri, K., Wells, M., and Lewis, C. E. (2002). Expression of HIF-1 α by human macrophages: Implications for the use of macrophages in hypoxia-regulated cancer gene therapy. *J. Pathol.* **196**, 204–212.

Burton, J. L., Wells, J. M., Corke, K. P., Maitland, N., Hambdy, F. C., and Lewis, C. E. (2000). Macrophages accumulate in avascular, hypoxic areas of prostate tumours: Implications for the targeted therapeutic gene delivery to such sites. *J. Pathol.* **192**, 8A.

Carey, R. W., Holland, J. F., Whang, H. Y., Neter, E., and Bryant, B. (1967). Clostridial oncolysis in man. *Eur. J. Cancer* **3**, 37–46.

Carmeliet, P., Dor, Y., Herbert, J. M., Fukumura, D., Brusselmans, K., Dewerchin, M., Neeman, M., Bono, F., Abramovitch, R., Maxwell, P., Koch, C. J., and Ratcliffe, P., et al. (1998). Role of HIF-1alpha in hypoxia-mediated apoptosis, cell proliferation and tumour angiogenesis. *Nature* **394**, 485–490.

Carrero, P., Okamoto, K., Coumailleau, P., O'Brien, S., Tanaka, H., and Poellinger, L. (2000). Redox-regulated recruitment of the transcriptional coactivators CREB-binding protein and SRC-1 to hypoxia-inducible factor 1alpha. *Mol. Cell. Biol.* **20**, 402–415.

Chadderton, N., Cowen, R. L., Sheppard, F. C., Robinson, S., Greco, O., Scott, S. D., Stratford, I. J., Patterson, A. V., and Williams, K. J. (2005). Dual responsive promoters to target therapeutic gene expression to radiation-resistant hypoxic tumor cells. *Int. J. Radiat. Oncol. Biol. Phys.* **62**, 213–222.

Chaplin, D. J., Acker, B., and Olive, P. L. (1989). Potentiation of the tumor cytotoxicity of melphalan by vasodilating drugs. *Int. J. Radiat. Oncol. Biol. Phys.* **16**, 1131–1135.

Chaplin, D. J., Horsman, M. R., Trotter, M. J., and Siemann, D. W. (1998). Therapeutic significance of microenvironmental factors. In “Therapeutic significance of microenvironmental factors” (M. Molls and P. Vaupel, Eds.), pp. 133–143. Springer-Verlag, Berlin.

Chaplin, D. J., Olive, P. L., and Durand, R. E. (1987). Intermittent blood flow in a murine tumor: Radiobiological effects. *Cancer Res.* **47**, 597–601.

Cho, W. K., Seong, Y. R., Lee, Y. H., Kim, M. J., Hwang, K. S., Yoo, J., Choi, S., Jung, C. R., and Im, D. S. (2004). Oncolytic effects of adenovirus mutant capable of replicating in hypoxic and normoxic regions of solid tumor. *Mol. Ther.* **10**, 938–949.

Choo, H.-J., Youn, S.-W., Cheon, S.-I., Kim, T.-Y., Hur, J., Zhang, S.-Y., Lee, S. P., Park, K.-W., Lee, M.-M., Choi, Y.-S., Park, Y.-B., and Kim, H.-S. (2005). Regulation of endothelial cell and endothelial progenitor cell survival and vasculogenesis by integrin-linked kinase. *Arterioscler. Thromb. Vasc. Biol.* **25**, 1154–1160.

Connor, J. H., Naczki, C., Koumenis, C., and Lyles, D. S. (2004). Replication and cytopathic effect of oncolytic vesicular stomatitis virus in hypoxic tumor cells *in vitro* and *in vivo*. *J. Virol.* **78**, 8960–8970.

Cowen, R. L., Williams, K. J., Chinje, E. C., Jaffar, M., Sheppard, F. C., Telfer, B. A., Wind, N. S., and Stratford, I. J. (2004). Hypoxia targeted gene therapy to increase the efficacy of tirapazamine as an adjuvant to radiotherapy: Reversing tumor radioresistance and effecting cure. *Cancer Res.* **64**, 1396–1402.

Craighead, P. S., Pearcey, R., and Stuart, G. (2000). A phase I/II evaluation of tirapazamine administered intravenously concurrent with cisplatin and radiotherapy in women with locally advanced cervical cancer. *Int. J. Radiat. Oncol. Biol. Phys.* **48**, 791–795.

Cuevas, Y., Hernandez-Alcoceba, R., Aragones, J., Naranjo-Suarez, S., Castellanos, M. C., Esteban, M. A., Martin-Puig, S., Landazuri, M. O., and del Peso, L. (2003). Specific oncolytic effect of a new hypoxia-inducible factor-dependent replicative adenovirus on von Hippel-Lindau-defective renal cell carcinomas. *Cancer Res.* **63**, 6877–6884.

Dai, S., Huang, M. L., Hsu, C. Y., and Chao, K. S. (2003). Inhibition of hypoxia inducible factor 1alpha causes oxygen-independent cytotoxicity and induces p53 independent apoptosis in glioblastoma cells. *Int. J. Radiat. Oncol. Biol. Phys.* **55**, 1027–1036.

De, S. K., Venkateshan, C. N., Seth, P., Gadjusek, D. C., and Gibbs, C. J. (1998). Adenovirus-mediated human immunodeficiency virus-1 Nef expression in human monocytes/macrophages and effect of Nef on down-modulation of Fc gamma receptors and expression of monokines. *Blood* **91**, 2108–2117.

Durand, R. E., and Raleigh, J. A. (1998). Identification of nonproliferating but viable hypoxic tumor cells *in vivo*. *Cancer Res.* **58**, 3547–3550.

Erler, J. T., Cawthorne, C. J., Williams, K. J., Koritzinsky, M., Wouters, B. G., Wilson, C., Miller, C., Demonacos, C., Stratford, I. J., and Dive, C. (2004). Hypoxia-mediated down-regulation of Bid and Bax in tumors occurs via hypoxia-inducible factor 1-dependent and -independent mechanisms and contributes to drug resistance. *Mol. Cell. Biol.* **24**, 2875–2889.

Ferrara, N., Gerber, H. P., and LeCouter, J. (2003). The biology of VEGF and its receptors. *Nat. Med.* **9**, 669–676.

Fisher, T. S., Etages, S. D., Hayes, L., Crimin, K., and Li, B. (2005). Analysis of ARD1 function in hypoxia response using retroviral RNA interference. *J. Biol. Chem.* **280**, 17749–17757.

Fox, M. E., Lemmon, M. J., Mauchline, M. L., Davis, T. O., Giaccia, A. J., Minton, N. P., and Brown, J. M. (1996). Anaerobic bacteria as a delivery system for cancer gene therapy: *In vitro* activation of 5-fluorocytosine by genetically engineered clostridia. *Gene Ther.* **3**, 173–178.

Freytag, S. O., Khil, M., Stricker, H., Peabody, J., Menon, M., DePeralta-Venturina, M., Nafziger, D., Pegg, J., Paielli, D., Brown, S., Barton, K., Lu, M., *et al.* (2002). Phase I study of replication-competent adenovirus-mediated double suicide gene therapy for the treatment of locally recurrent prostate cancer. *Cancer Res.* **62**, 4968–4976.

Freytag, S. O., Stricker, H., Pegg, J., Paielli, D., Pradhan, D. G., Peabody, J., DePeralta-Venturina, M., Xia, X., Brown, S., Lu, M., and Kim, J. H. (2003). Phase I study of replication-competent adenovirus-mediated double-suicide gene therapy in combination with conventional-dose three-dimensional conformal radiation therapy for the treatment of newly diagnosed, intermediate- to high-risk prostate cancer. *Cancer Res.* **63**, 7497–7506.

Fu, G. F., Li, X., Hou, Y. Y., Fan, Y. R., Liu, W. H., and Xu, G. X. (2005). Bifidobacterium longum as an oral delivery system of endostatin for gene therapy on solid liver cancer. *Cancer Gene Ther.* **12**, 133–140.

Fuller, J., Feldmann, H. J., Molls, M., and Sack, H. (1994). Studies on oxygen partial pressure in tumor tissue under radiotherapy and thermoradiotherapy. *Strahlenther. Onkol.* **170**, 453–460.

Fyles, A., Milosevic, M., Hedley, D., Pintilie, M., Levin, W., Manchul, L., and Hill, R. P. (2002). Tumor hypoxia has independent predictor impact only in patients with node-negative cervix cancer. *J. Clin. Oncol.* **20**, 680–687.

Giatromanolaki, A., Koukourakis, M. I., Sivridis, E., Pastorek, J., Wykoff, C. C., Gatter, K. C., and Harris, A. L. (2001). Expression of hypoxia-inducible carbonic anhydrase-9 relates to angiogenic pathways and independently to poor outcome in non-small cell lung cancer. *Cancer Res.* **61**, 7992–7998.

Grau, C., and Overgaard, J. (1988). Effect of cancer chemotherapy on the hypoxic fraction of a solid tumor measured using a local tumor control assay. *Radiother. Oncol.* **13**, 301–309.

Greco, O., and Dachs, G. U. (2001). Gene directed enzyme/prodrug therapy of cancer: Historical appraisal and future prospectives. *J. Cell. Physiol.* **187**, 22–36.

Greco, O., Marples, B., Dachs, G. U., Williams, K. J., Patterson, A. V., and Scott, S. D. (2002). Novel chimeric gene promoters responsive to hypoxia and ionizing radiation. *Gene Ther.* **9**, 1403–1411.

Greco, O., Marples, B., Joiner, M. C., and Scott, S. D. (2003). How to overcome (and exploit) tumor hypoxia for targeted gene therapy. *J. Cell. Physiol.* **197**, 312–325.

Greco, O., Patterson, A. V., and Dachs, G. U. (2000). Can gene therapy overcome the problem of hypoxia in radiotherapy? *J. Radiat. Res. (Tokyo)* **41**, 201–212.

Greco, O., Joiner, M. C., Doleh, A., Powell, A. D., Hillman, G. G., and Scott, S. D. (2006). Hypoxia- and radiation-activated Cre/loxP “molecular switch” vectors for gene therapy of cancer. *Gene Ther.* **13**, 206–215.

Griffiths, J. R. (1991). Are cancer cells acidic? *Br. J. Cancer* **64**, 425–427.

Griffiths, L., Binley, K., Iqball, S., Kan, O., Maxwell, P., Ratcliffe, P., Lewis, C., Harris, A., Kingsman, S., and Naylor, S. (2000). The macrophage—a novel system to deliver gene therapy to pathological hypoxia. *Gene Ther.* **7**, 255–262.

Grimshaw, M. J., Wilson, J. L., and Balkwill, F. R. (2002). Endothelin-2 is a macrophage chemoattractant: Implications for macrophage distribution in tumors. *Eur. J. Immunol.* **32**, 2393–2400.

Gu, Y. Z., Moran, S. M., Hogenesch, J. B., Wartman, L., and Bradfield, C. A. (1998). Molecular characterization and chromosomal localization of a third alpha-class hypoxia inducible factor subunit, HIF3alpha. *Gene Expr.* **7**, 205–213.

Gunaratnam, L., Morley, M., Franovic, A., de Paulsen, N., Mekhail, K., Parolin, D. A., Nakamura, E., Lorimer, I. A., and Lee, S. (2003). Hypoxia inducible factor activates the

transforming growth factor-alpha/epidermal growth factor receptor growth stimulatory pathway in VHL(−/−) renal cell carcinoma cells. *J. Biol. Chem.* **278**, 44966–44974.

Haddada, H., Lopez, M., Martinache, C., Ragot, T., Abina, M. A., and Perricaudet, M. (1993). Efficient adenovirus-mediated gene transfer into human blood monocyte-derived macrophages. *Biochem. Biophys. Res. Commun.* **195**, 1174–1183.

Hanahan, D., and Weinberg, R. A. (2000). The hallmarks of cancer. *Cell* **100**, 57–70.

Haugland, H. K., Vukovic, V., Pintilie, M., Fyles, A. W., Milosevic, M., Hill, R. P., and Hedley, D. W. (2002). Expression of hypoxia-inducible factor-1alpha in cervical carcinomas: Correlation with tumor oxygenation. *Int. J. Radiat. Oncol. Biol. Phys.* **53**, 854–861.

Hernandez-Alcoceba, R., Pihalja, M., Nunez, G., and Clarke, M. F. (2001). Evaluation of a new dual-specificity promoter for selective induction of apoptosis in breast cancer cells. *Cancer Gene Ther.* **8**, 298–307.

Hernandez-Alcoceba, R., Pihalja, M., Qian, D., and Clarke, M. F. (2002). New oncolytic adenoviruses with hypoxia- and estrogen receptor-regulated replication. *Hum. Gene Ther.* **13**, 1737–1750.

Hill, S. A., Pigott, K. H., Saunders, M. I., Powell, M. E., Arnold, S., Obeid, A., Ward, G., Leahy, M., Hoskin, P. J., and Chaplin, D. J. (1996). Microregional blood flow in murine and human tumours assessed using laser Doppler microprobe. *Br. J. Cancer Suppl.* **27**, S260–S263.

Höpfel, G., Wenger, R. H., Ziegler, U., Stallmach, T., Gardelle, O., Achermann, R., Wergin, M., Kaser-Hotz, B., Saunders, H. M., Williams, K. J., Stratford, I. J., Gassmann, M., et al. (2002). Rescue of hypoxia-inducible factor-1alpha-deficient tumor growth by wild-type cells is independent of vascular endothelial growth factor. *Cancer Res.* **62**, 2962–2970.

Huang, L. E., Arany, Z., Livingston, D. M., and Bunn, H. F. (1996). Activation of hypoxia-inducible transcription factor depends primarily upon redox-sensitive stabilization of its alpha subunit. *J. Biol. Chem.* **271**, 32253–32259.

Hughes, C. S., Shen, J. W., and Subjeck, J. R. (1989). Resistance to etoposide induced by three glucose-regulated stresses in Chinese hamster ovary cells. *Cancer Res.* **49**, 4452–4454.

Ido, A., Uto, H., Moriuchi, A., Nagata, K., Onaga, Y., Onaga, M., Hori, T., Hirono, S., Hayashi, K., Tamaoki, T., and Tsubouchi, H. (2001). Gene therapy targeting for hepatocellular carcinoma: Selective and enhanced suicide gene expression regulated by a hypoxia-inducible enhancer linked to a human alpha-fetoprotein promoter. *Cancer Res.* **61**, 3016–3021.

Ingram, N., and Porter, C. D. (2005). Transcriptional targeting of acute hypoxia in the tumour stroma is a novel and viable strategy for cancer gene therapy. *Gene Ther.* **12**, 1058–1069.

Ivan, M., Kondo, K., Yang, H., Kim, W., Valiando, J., Ohh, M., Salic, A., Asara, J. M., Lane, W. S., and Kaelin, W. G., Jr. (2001). HIFalpha targeted for VHL-mediated destruction by proline hydroxylation: Implications for O2 sensing. *Science* **292**, 464–468.

Jaakkola, P., Mole, D. R., Tian, Y. M., Wilson, M. I., Gielbert, J., Gaskell, S. J., Kriegsheim, A., Hebestreit, H. F., Mukherji, M., Schofield, C. J., Maxwell, P. H., Pugh, C. W., et al. (2001). Targeting of HIF-alpha to the von Hippel-Lindau ubiquitylation complex by O2-regulated prolyl hydroxylation. *Science* **292**, 468–472.

Jeong, J. W., Bae, M. K., Ahn, M. Y., Kim, S. H., Sohn, T. K., Bae, M. H., Yoo, M. A., Song, E. J., Lee, K. J., and Kim, K. W. (2002). Regulation and destabilization of HIF-1alpha by ARD1-mediated acetylation. *Cell* **111**, 709–720.

Jiang, B. H., Agani, F., Passaniti, A., and Semenza, G. L. (1997). V-SRC induces expression of hypoxia-inducible factor 1 (HIF-1) and transcription of genes encoding vascular endothelial growth factor and enolase 1: Involvement of HIF-1 in tumor progression. *Cancer Res.* **57**, 5328–5335.

Kelly, P. M., Davison, R. S., Bliss, E., and McGee, J. O. (1988). Macrophages in human breast disease: A quantitative immunohistochemical study. *Br. J. Cancer* **57**, 174–177.

Kimura, H., Braun, R. D., Ong, E. T., Hsu, R., Secomb, T. W., Papahadjopoulos, D., Hong, K., and Dewhirst, M. W. (1996). Fluctuations in red cell flux in tumor microvessels can lead to transient hypoxia and reoxygenation in tumor parenchyma. *Cancer Res.* **56**, 5522–5528.

Koch, C. J. (1993). Unusual oxygen concentration dependence of toxicity of SR-4233, a hypoxic cell toxin. *Cancer Res.* **53**, 3992–3997.

Koukourakis, M. I., Giatromanolaki, A., Sivridis, E., Simopoulos, C., Turley, H., Talks, K., Gatter, K. C., and Harris, A. L. (2002). Hypoxia-inducible factor (HIF1A and HIF2A), angiogenesis, and chemoradiotherapy outcome of squamous cell head-and-neck cancer. *Int. J. Radiat. Oncol. Biol. Phys.* **53**, 1192–1202.

Koukourakis, M. I., Giatromanolaki, A., Skarlatos, J., Corti, L., Blandamura, S., Piazza, M., Gatter, K. C., and Harris, A. L. (2001). Hypoxia inducible factor (HIF-1a and HIF-2a) expression in early esophageal cancer and response to photodynamic therapy and radiotherapy. *Cancer Res.* **61**, 1830–1832.

Kung, A. L., Wang, S., Klco, J. M., Kaelin, W. G., and Livingston, D. M. (2000). Suppression of tumor growth through disruption of hypoxia-inducible transcription. *Nat. Med.* **6**, 1335–1340.

Lando, D., Peet, D. J., Whelan, D. A., Gorman, J. J., and Whitelaw, M. L. (2002). Asparagine hydroxylation of the HIF transactivation domain a hypoxic switch. *Science* **295**, 858–861.

Laughner, E., Taghavi, P., Chiles, K., Mahon, P. C., and Semenza, G. L. (2001). HER2 (neu) signaling increases the rate of hypoxia-inducible factor 1alpha (HIF-1alpha) synthesis: Novel mechanism for HIF-1-mediated vascular endothelial growth factor expression. *Mol. Cell. Biol.* **21**, 3995–4004.

Le, Q. T., Denko, N. C., and Giaccia, A. J. (2004). Hypoxic gene expression and metastasis. *Cancer Metastasis Rev.* **23**, 293–310.

Leek, R. D., Lewis, C. E., Whitehouse, R., Greenall, M., Clarke, J., and Harris, A. L. (1996). Association of macrophage infiltration with angiogenesis and prognosis in invasive breast carcinoma. *Cancer Res.* **56**, 4625–4629.

Leek, R. D., Landers, R. J., Underwood, J. C., Harris, A. L., and Lewis, C. E. (1999). Necrosis correlates with high vascular density and focal macrophage infiltration in invasive carcinoma of the breast. *Br. J. Cancer* **79**, 991–995.

Lemmon, M. J., van Zijl, P., Fox, M. E., Mauchline, M. L., Giaccia, A. J., Minton, N. P., and Brown, J. M. (1997). Anaerobic bacteria as a gene delivery system that is controlled by the tumor microenvironment. *Gene Ther.* **4**, 791–796.

Lewis, J. S., Landers, R. J., Underwood, J. C., Harris, A. L., and Lewis, C. E. (2000). Expression of vascular endothelial growth factor by macrophages is up-regulated in poorly vascularized areas of breast carcinomas. *J. Pathol.* **192**, 150–158.

Li, L., Lin, X., Staver, M., Shoemaker, A., Semizarov, D., Fesik, S. W., and Shen, Y. (2005a). Evaluating hypoxia-inducible factor-1alpha as a cancer therapeutic target via inducible RNA interference *in vivo*. *Cancer Res.* **65**, 7249–7258.

Li, X., Fu, G. F., Fan, Y. R., Liu, W. H., Liu, X. J., Wang, J. J., and Xu, G. X. (2003). Bifidobacterium adolescentis as a delivery system of endostatin for cancer gene therapy: Selective inhibitor of angiogenesis and hypoxic tumor growth. *Cancer Gene Ther.* **10**, 105–111.

Li, Y. M., Zhou, B. P., Deng, J., Pan, Y., Hay, N., and Hung, M. C. (2005b). A hypoxia-independent hypoxia-inducible factor-1 activation pathway induced by phosphatidylinositol-3 kinase/Akt in HER2 overexpressing cells. *Cancer Res.* **65**, 3257–3263.

Lipnik, K., Greco, O., Scott, S., Knappm, E., Mayrhofer, E., Rosenfellner, D., Gunzburg, W. H., Salmons, B., and Hohenadl, C. (2006). Hypoxia- and radiation-inducible, breast cell-specific targeting of retroviral vectors. *Virology* **349**, 121–133.

Lissbrant, I. F., Stattin, P., Wikstrom, P., Damber, J. E., Egevad, L., and Bergh, A. (2000). Tumour associated macrophages in human prostate cancer: Relation to clinicopathological variables and survival. *Int. J. Oncol.* **17**, 445–451.

Liu, S. C., Minton, N. P., Giaccia, A. J., and Brown, J. M. (2002). Anticancer efficacy of systemically delivered anaerobic bacteria as gene therapy vectors targeting tumor hypoxia/necrosis. *Gene Ther.* **9**, 291–296.

Liu, Y., Santin, A. D., Mane, M., Chiriva-Internati, M., Parham, G. P., Ravaggi, A., and Hermonat, P. L. (2000). Transduction and utility of the granulocyte macrophage colony stimulating factor gene into monocytes and dendritic cells by adeno-associated virus. *J. Interferon Cytokine Res.* **20**, 21–30.

Lorenz, R. M., Pecora, A. L., Major, P. P., Hotte, S. J., Laurie, S. A., Roberts, M. S., Groene, W. S., and Bamat, M. K. (2003). Overview of phase I studies of intravenous administration of PV701, an oncolytic virus. *Curr. Opin. Mol. Ther.* **5**, 618–624.

Mahon, P. C., Hirota, K., and Semenza, G. L. (2001). FIH-1: A novel protein that interacts with HIF-1alpha and VHL to mediate repression of HIF-1 transcriptional activity. *Genes Dev.* **15**, 2675–2686.

Malmgren, R. A., and Flanigan, C. C. (1955). Localization of the vegetative form of Clostridium tetani in mouse tumours following intravenous spore administration. *Cancer Res.* **15**, 473–478.

Maltepe, E., Schmidt, J. V., Baunoch, D., Bradfield, C. A., and Simon, M. C. (1997). Abnormal angiogenesis and responses to glucose and oxygen deprivation in mice lacking the protein ARNT. *Nature* **386**, 403–407.

Maxwell, P. H., Dachs, G. U., Gleadle, J. M., Nicholls, L. G., Harris, A. L., Stratford, I. J., Hankinson, O., Pugh, C. W., and Ratcliffe, P. J. (1997). Hypoxia-inducible factor-1 modulates gene expression in solid tumors and influences both angiogenesis and tumor growth. *Proc. Natl. Acad. Sci. USA* **94**, 8104–8109.

Maxwell, P. H., Pugh, C. W., and Ratcliffe, P. J. (1993). Inducible operation of the erythropoietin 3' enhancer in multiple cell lines: Evidence for a widespread oxygen-sensing mechanism. *Proc. Natl. Acad. Sci. USA* **90**, 2423–2427.

Mazure, N. M., Brahim-Horn, M. C., Berta, M. A., Benizri, E., Bilton, R. L., Dayan, F., Ginouves, A., Berra, E., and Pouyssegur, J. (2004). HIF-1: Master and commander of the hypoxic world. A pharmacological approach to its regulation by siRNAs. *Biochem. Pharmacol.* **68**, 971–980.

McCormick, F. (2003). Cancer-specific viruses and the development of ONYX-015. *Cancer Biol. Ther.* **2**, S157–S160.

Mei, S., Theys, J., Landuyt, W., Anne, J., and Lambin, P. (2002). Optimization of tumor-targeted gene delivery by engineered attenuated *Salmonella typhimurium*. *Anticancer Res.* **22**, 3261–3266.

Millauer, B., Shawver, L. K., Plate, K. H., Risau, W., and Ullrich, A. (1994). Glioblastoma growth inhibited *in vivo* by a dominant-negative Flk-1 mutant. *Nature* **367**, 576–579.

Mineta, T., Rabkin, S. D., and Martuza, R. L. (1994). Treatment of malignant gliomas using ganciclovir-hypersensitive, ribonucleotide reductase-deficient herpes simplex viral mutant. *Cancer Res.* **54**, 3963–3966.

Miyake, K., Suzuki, N., Matsuoka, H., Tohyama, T., and Shimada, T. (1998). Stable integration of human immunodeficiency virus-based retroviral vectors into the chromosomes of nondividing cells. *Hum. Gene Ther.* **9**, 467–475.

Mizuno, T., Nagao, M., Yamada, Y., Narikiyo, M., Ueno, M., Miyagishi, M., Taira, K., and Nakajima, Y. (2005). Small interfering RNA expression vector targeting hypoxia-inducible factor 1 alpha inhibits tumor growth in hepatobiliary and pancreatic cancers. *Cancer Gene Ther.* **13**, 131–140.

Modlich, U., Pugh, C. W., and Bicknell, R. (2000). Increasing endothelial cell specific expression by the use of heterologous hypoxic and cytokine-inducible enhancers. *Gene Ther.* **7**, 896–902.

Moeller, B. J., Cao, Y., Li, C. Y., and Dewhirst, M. W. (2004). Radiation activates HIF-1 to regulate vascular radiosensitivity in tumors: Role of reoxygenation, free radicals, and stress granules. *Cancer Cell* **5**, 429–441.

Moeller, B. J., Dreher, M. R., Rabbani, Z. N., Schroeder, T., Cao, Y., Li, C. Y., and Dewhirst, M. W. (2005). Pleiotropic effects of HIF-1 blockade on tumor radiosensitivity. *Cancer Cell* **8**, 99–110.

Nakanishi, K., Hiroi, S., Tominaga, S., Aida, S., Kasamatsu, H., Matsuyama, S., Matsuyama, T., and Kawai, T. (2005). Expression of hypoxia-inducible factor-1alpha protein predicts survival in patients with transitional cell carcinoma of the upper urinary tract. *Clin. Cancer Res.* **11**, 2583–2590.

Negus, R. P., Stamp, G. W., Hadley, J., and Balkwill, F. R. (1997). Quantitative assessment of the leukocyte infiltrate in ovarian cancer and its relationship to the expression of C-C chemokines. *Am. J. Pathol.* **150**, 1723–1734.

Negus, R. P., Turner, L., Burke, F., and Balkwill, F. R. (1998). Hypoxia down-regulates MCP-1 expression: Implications for macrophage distribution in tumours. *J. Leukoc. Biol.* **63**, 758–765.

Nemunaitis, J., Cunningham, C., Senzer, N., Kuhn, J., Cramm, J., Litz, C., Cavagnolo, R., Cahill, A., Clairmont, C., and Sznol, M. (2003). Pilot trial of genetically modified, attenuated *Salmonella* expressing the *E. coli* cytosine deaminase gene in refractory cancer patients. *Cancer Gene Ther.* **10**, 737–744.

Nuyts, S., Theys, J., Landuyt, W., van Mellaert, L., Lambin, P., and Anne, J. (2001a). Increasing specificity of anti-tumor therapy: Cytotoxic protein delivery by non-pathogenic clostridia under regulation of radio-induced promoters. *Anticancer Res.* **21**, 857–861.

Nuyts, S., Van Mellaert, L., Theys, J., Landuyt, W., Bosmans, E., Anne, J., and Lambin, P. (2001b). Radio-responsive recA promoter significantly increases TNF α production in recombinant clostridia after 2 Gy irradiation. *Gene Ther.* **8**, 1197–1201.

O'Reilly, M. S., Boehm, T., Shing, Y., Fukai, N., Vasios, G., Lane, W. S., Flynn, E., Birkhead, J. R., Olsen, B. R., and Folkman, J. (1997). Endostatin: An endogenous inhibitor of angiogenesis and tumor growth. *Cell* **88**, 277–285.

Ogawa, T., Takayama, K., Takakura, N., Kitano, S., and Ueno, H. (2002). Anti-tumor angiogenesis therapy using soluble receptors: Enhanced inhibition of tumor growth when soluble fibroblast growth factor receptor-1 is used with soluble vascular endothelial growth factor receptor. *Cancer Gene Ther.* **9**, 633–640.

Ogura, M., Shibata, T., Yi, J., Liu, J., Qu, R., Harada, H., and Hiraoka, M. (2005). A tumor-specific gene therapy strategy targeting dysregulation of the VHL/HIF pathway in renal cell carcinomas. *Cancer Sci.* **96**, 288–294.

Ozawa, T., Hu, J. L., Hu, L. J., Kong, E. L., Bollen, A. W., Lamborn, K. R., and Deen, D. F. (2005). Functionality of hypoxia-induced BAX expression in a human glioblastoma xenograft model. *Cancer Gene Ther.* **12**, 449–455.

Park, S. Y., Billiar, T. R., and Seol, D. W. (2002). Hypoxia inhibition of apoptosis induced by tumor necrosis factor-related apoptosis-inducing ligand (TRAIL). *Biochem. Biophys. Res. Commun.* **291**, 150–153.

Parveen, Z., Krupetsky, A., Engelstadter, M., Cichutek, K., Pomeranitz, R. J., and Dornburg, R. (2000). Spleen necrosis virus-derived C-type retroviral vectors for gene transfer to quiescent cells. *Nat. Biotechnol.* **18**, 623–629.

Pastorino, S., Massazza, S., Cilli, M., Varesio, L., and Bosco, M. C. (2001). Generation of high-titer retroviral vector-producing macrophages as vehicles for *in vivo* gene transfer. *Gene Ther.* **8**, 431–441.

Patterson, A. V., Saunders, M. P., Chinje, E. C., Talbot, D. C., Harris, A. L., and Strafford, I. (1997). Overexpression of human NADPH: Cytochrome c (P450) reductase confers enhanced sensitivity to both tirapazamine (SR 4233) and RSU 1069. *Br. J. Cancer* **76**, 1338–1347.

Patterson, A. V., Saunders, M. P., and Greco, O. (2003). Prodrugs in genetic chemoradiotherapy. *Curr. Pharm. Des.* **9**, 2131–2154.

Patterson, A. V., Williams, K. J., Cowen, R. L., Jaffar, M., Telfer, B. A., Saunders, M., Airley, R., Honess, D., van der Kogel, A. J., Wolf, C. R., and Stratford, I. J. (2002). Oxygen-sensitive enzyme-prodrug gene therapy for the eradication of radiation-resistant solid tumours. *Gene Ther.* **9**, 946–954.

Paul, S., Snary, D., Hoebecke, J., Allen, D., Balloul, J. M., Bizouarne, N., Dott, K., Geist, M., Hilgers, J., Kieny, M. P., Burchell, J., Taylor-Papadimitriou, J., *et al.* (2000). Targeted macrophage toxicity using a nonreplicative live vector expressing a tumor-specific single-chain variable region fragment. *Hum. Gene Ther.* **11**, 1417–1428.

Pawelek, J. M., Low, K. B., and Bermudes, D. (1997). Tumor-targeted Salmonella as a novel anticancer vector. *Cancer Res.* **57**, 4537–4544.

Pin, R. H., Reinblatt, M., Bowers, W. J., Federoff, H. J., and Fong, Y. (2004a). Herpes simplex virus amplicon delivery of a hypoxia-inducible angiogenic inhibitor blocks capillary formation in hepatocellular carcinoma. *J. Gastrointest. Surg.* **8**, 812–822; discussion 822–823.

Pin, R. H., Reinblatt, M., and Fong, Y. (2004b). Employing tumor hypoxia to enhance oncolytic viral therapy in breast cancer. *Surgery* **136**, 199–204.

Pipiya, T., Sauthoff, H., Huang, Y. Q., Chang, B., Cheng, J., Heitner, S., Chen, S., Rom, W. N., and Hay, J. G. (2005). Hypoxia reduces adenoviral replication in cancer cells by downregulation of viral protein expression. *Gene Ther.* **12**, 911–917.

Pitson, G., Fyles, A., Milosevic, M., Wylie, J., Pintilie, M., and Hill, R. (2001). Tumor size and oxygenation are independent predictors of nodal diseases in patients with cervix cancer. *Int. J. Radiat. Oncol. Biol. Phys.* **51**, 699–703.

Post, D. E., and Van Meir, E. G. (2003). A novel hypoxia-inducible factor (HIF) activated oncolytic adenovirus for cancer therapy. *Oncogene* **22**, 2065–2072.

Post, D. E., Devi, N. S., Li, Z., Brat, D. J., Kaur, B., Nicholson, A., Olson, J. J., Zhang, Z., and Van Meir, E. G. (2004a). Cancer therapy with a replicating oncolytic adenovirus targeting the hypoxic microenvironment of tumors. *Clin. Cancer Res.* **10**, 8603–8612.

Post, D. E., Fulci, G., Chiocca, E. A., and Van Meir, E. G. (2004b). Replicative oncolytic herpes simplex viruses in combination cancer therapies. *Curr. Gene Ther.* **4**, 41–51.

Pugh, C. W., O'Rourke, J. F., Nagao, M., Gleadle, J. M., and Ratcliffe, P. J. (1997). Activation of hypoxia-inducible factor-1; definition of regulatory domains within the alpha subunit. *J. Biol. Chem.* **272**, 11205–11214.

Raleigh, J. A., Calkins-Adams, D. P., Rinker, L. H., Ballenger, C. A., Weissler, M. C., Fowler, W. C., Jr., Novotny, D. B., and Varia, M. A. (1998). Hypoxia and vascular endothelial growth factor expression in human squamous cell carcinomas using pimonidazole as a hypoxia marker. *Cancer Res.* **58**, 3765–3768.

Ravi, R., Mookerjee, B., Bhujwalla, Z. M., Sutter, C. H., Artemov, D., Zeng, Q., Dillehay, L. E., Madan, A., Semenza, G. L., and Bedi, A. (2000). Regulation of tumor angiogenesis by p53-induced degradation of hypoxia-inducible factor 1alpha. *Genes Dev.* **14**, 34–44.

Reinblatt, M., Pin, R. H., Federoff, H. J., and Fong, Y. (2004). Utilizing tumor hypoxia to enhance oncolytic viral therapy in colorectal metastases. *Ann. Surg.* **239**, 892–899; discussion 899–902.

Rischin, D., Peters, L., Hicks, R., Hughes, P., Fisher, R., Hart, R., Sexton, M., D'Costa, I., and von Roemeling, R. (2001). Phase I trial of concurrent tirapazamine, cisplatin, and radiotherapy in patients with advanced head and neck cancer. *J. Clin. Oncol.* **19**, 535–542.

Rofstad, E. K., Sundfor, K., Lyng, H., and Trope, C. G. (2000). Hypoxia-induced treatment failure in advanced squamous cell carcinoma of the uterine cervix is primarily due to hypoxia-induced radiation resistance rather than hypoxia-induced metastasis. *Br. J. Cancer* **83**, 354–359.

Ryan, H. E., Lo, J., and Johnson, R. S. (1998). HIF-1 alpha is required for solid tumor formation and embryonic vascularization. *EMBO J.* **17**, 3005–3015.

Ryan, H. E., Poloni, M., McNulty, W., Elson, D., Gassmann, M., Arbeit, J. M., and Johnson, R. S. (2000). Hypoxia-inducible factor-1alpha is a positive factor in solid tumor growth. *Cancer Res.* **60**, 4010–4015.

Sanna, K., and Rofstad, E. K. (1994). Hypoxia-induced resistance to doxorubicin and methotrexate in human melanoma cell lines *in vitro*. *Int. J. Cancer* **58**, 258–262.

Saunders, M. P., Patterson, A. V., Chinje, E. C., Harris, A. L., and Stratford, I. J. (2000). NADPH: Cytochrome c (P450) reductase activates tirapazamine (SR4233) to restore hypoxic and oxic cytotoxicity in an aerobic resistant derivative of the A549 lung cancer cell line. *Br. J. Cancer* **82**, 651–656.

Schindl, M., Schoppmann, S. F., Samonigg, H., Hausmaninger, H., Kwasny, W., Gnant, M., Jakesz, R., Kubista, E., Birner, P., and Oberhuber, G. (2002). Overexpression of hypoxia-inducible factor 1alpha is associated with an unfavorable prognosis in lymph node-positive breast cancer. *Clin. Cancer Res.* **8**, 1831–1837.

Schneider, S. D., Rusconi, S., Seger, R. A., and Josle, J. P. (1997). Adenovirus-mediated gene transfer into monocyte-derived macrophages of patients with X-linked chronic granulomatous disease: *Ex vivo* correction of deficient respiratory burst. *Gene Ther.* **4**, 524–532.

Schroers, R., Sinha, I., Segall, H., Schmidt-Wolf, I. G., Rooney, C. M., Brenner, M. K., Sutton, R. E., and Chen, S. Y. (2000). Transduction of human PBMC-derived dendritic cells and macrophages by an HIV-1-based lentiviral vector system. *Mol. Ther.* **1**, 171–179.

Scott, S. D., and Greco, O. (2004). Radiation and hypoxia inducible gene therapy systems. *Cancer Metast. Rev.* **23**, 269–276.

Semenza, G. L. (2003). Targeting HIF-1 for cancer therapy. *Nat. Rev. Cancer* **3**, 721–732.

Shen, B. H., and Hermiston, T. W. (2005). Effect of hypoxia on Ad5 infection, transgene expression and replication. *Gene Ther.* **12**, 902–910.

Shen, J., Hughes, C., Chao, C., Cai, J., Bartels, C., Gessner, T., and Subjeck, J. (1987). Coinduction of glucose-regulated proteins and doxorubicin resistance in Chinese hamster cells. *Proc. Natl. Acad. Sci. USA* **84**, 3278–3282.

Simoes, S., Slepushkin, V., Pretzer, E., Dazin, P., Gaspar, R., Pedroso de Lima, M. C., and Duzgunes, N. (1999). Transfection of human macrophages by lipoplexes via the combined use of transferrin and pH-sensitive peptides. *J. Leukoc. Biol.* **65**, 270–279.

Smith, K., Gunaratnam, L., Morley, M., Franovic, A., Mekhail, K., and Lee, S. (2005). Silencing of epidermal growth factor receptor suppresses hypoxia-inducible factor-2-driven VHL^{−/−} renal cancer. *Cancer Res.* **65**, 5221–5230.

Sowter, H. M., Ratcliffe, P. J., Watson, P., Greenberg, A. H., and Harris, A. L. (2001). HIF-1-dependent regulation of hypoxic induction of the cell death factors BNIP3 and NIX in human tumors. *Cancer Res.* **61**, 6669–6673.

Stratford, I. J., and Workman, P. (1998). Bioreductive drugs into the next millennium. *Anticancer Drug Des.* **13**, 519–528.

Sun, X., Kanwar, J. R., Leung, E., Lehnert, K., Wang, D., and Krissansen, G. W. (2001). Gene transfer of antisense hypoxia inducible factor-1 alpha enhances the therapeutic efficacy of cancer immunotherapy. *Gene Ther.* **8**, 638–645.

Sun, X., Kanwar, J. R., Leung, E., Vale, M., and Krissansen, G. W. (2003). Regression of solid tumors by engineered overexpression of von Hippel-Lindau tumor suppressor protein and antisense hypoxia-inducible factor-1alpha. *Gene Ther.* **10**, 2081–2089.

Sun, X., Liu, M., Wei, Y., Liu, F., Zhi, X., Xu, R., and Krissansen, G. W. (2006). Overexpression of von Hippel-Lindau tumor suppressor protein and antisense HIF-1alpha eradicates gliomas. *Cancer Gene Ther.* **13**, 428–435.

Sundfor, K., Lyng, H., and Rofstad, E. K. (1998). Tumour hypoxia and vascular density as predictors of metastasis in squamous cell carcinoma of the uterine cervix. *Br. J. Cancer* **78**, 822–827.

Swinson, D. E., Jones, J. L., Cox, G., Richardson, D., Harris, A. L., and O'Byrne, K. J. (2004). Hypoxia-inducible factor-1 alpha in non small cell lung cancer: Relation to growth factor, protease and apoptosis pathways. *Int. J. Cancer* **111**, 43–50.

Talks, K. L., Turley, H., Gatter, K. C., Maxwell, P. H., Pugh, C. W., Ratcliffe, P. J., and Harris, A. L. (2000). The expression and distribution of the hypoxia-inducible factors HIF-1alpha and HIF-2alpha in normal human tissues, cancers, and tumor-associated macrophages. *Am. J. Pathol.* **157**, 411–421.

Tang, R., Beuvon, F., Ojeda, M., Mosseri, V., Pouillart, P., and Scholl, S. (1992). M-CSF (monocyte colony stimulating factor) and M-CSF receptor expression by breast tumour cells: M-CSF mediated recruitment of tumour infiltrating monocytes? *J. Cell. Biochem.* **50**, 350–356.

Teicher, B. A., Lazo, J. S., and Sartorelli, A. C. (1981). Classification of antineoplastic agents by their selective toxicities toward oxygenated and hypoxic tumor cells. *Cancer Res.* **41**, 73–81.

Theys, J., Landuyt, W., Nuyts, S., Van Mellaert, L., Bosmans, E., Rijnders, A., Van Den Bogaert, W., van Oosterom, A., Anne, J., and Lambin, P. (2001a). Improvement of Clostridium tumour targeting vectors evaluated in rat rhabdomyosarcomas. *FEMS Immunol. Med. Microbiol.* **30**, 37–41.

Theys, J., Landuyt, W., Nuyts, S., Van Mellaert, L., van Oosterom, A., Lambin, P., and Anne, J. (2001b). Specific targeting of cytosine deaminase to solid tumors by engineered Clostridium acetobutylicum. *Cancer Gene Ther.* **8**, 294–297.

Thomlinson, R. H., and Gray, L. H. (1955). The histological structure of some human lung cancers and the possible implications for radiotherapy. *Br. J. Cancer* **9**, 539–549.

Tozer, G. M., Kanthou, C., and Baguley, B. C. (2005). Disrupting tumour blood vessels. *Nat. Rev. Cancer* **5**, 423–435.

Ueno, T., Toi, M., Saji, H., Muta, M., Bando, H., Kuroi, K., Koike, M., Inadera, H., and Matsushima, K. (2000). Significance of macrophage chemoattractant protein-1 in macrophage recruitment, angiogenesis, and survival in human breast cancer. *Clin. Cancer Res.* **6**, 3282–3289.

Unruh, A., Ressel, A., Mohamed, H. G., Johnson, R. S., Nadrowitz, R., Richter, E., Katschinski, D. M., and Wenger, R. H. (2003). The hypoxia-inducible factor-1 alpha is a negative factor for tumor therapy. *Oncogene* **22**, 3213–3220.

Vaupel, P., and Hockel, M. (1998). Oxygenation of human tumours. In "Therapeutic Significance of Microenvironmental Factors" (M. Molls and P. Vaupel, Eds.), pp. 133–143. Springer-Verlag, Berlin.

Wang, D., Ruan, H., Hu, L., Lamborn, K. R., Kong, E. L., Rehemtulla, A., and Deen, D. F. (2005). Development of a hypoxia-inducible cytosine deaminase expression vector for gene-directed prodrug cancer therapy. *Cancer Gene Ther.* **12**, 276–283.

Wang, G. L., Jiang, B. H., Rue, E. A., and Semenza, G. L. (1995). Hypoxia-inducible factor 1 is a basic-helix-loop-helix-PAS heterodimer regulated by cellular O₂ tension. *Proc. Natl. Acad. Sci. USA* **92**, 5510–5514.

Wei, J., Blum, S., Unger, M., Jarmy, G., Lamarter, M., Geishauser, A., Vlastos, G. A., Chan, G., Fischer, K. D., Rattat, D., Debatin, K. M., Hatzopoulos, A. K., *et al.* (2004). Embryonic endothelial progenitor cells armed with a suicide gene target hypoxic lung metastases after intravenous delivery. *Cancer Cell* **5**, 477–488.

Wenger, R. H., and Gassmann, M. (1997). Oxygen(es) and the hypoxia-inducible factor-1. *Biol. Chem.* **378**, 609–616.

Wiener, C. M., Booth, G., and Semenza, G. L. (1996). *In vivo* expression of mRNAs encoding hypoxia-inducible factor 1. *Biochem. Biophys. Res. Commun.* **225**, 485–488.

Wiesener, M. S., Turley, H., Allen, W. E., Willam, C., Eckardt, K. U., Talks, K. L., Wood, S. M., Gatter, K. C., Harris, A. L., Pugh, C. W., Ratcliffe, P. J., and Maxwell, P. H. (1998).

Induction of endothelial PAS domain protein-1 by hypoxia: Characterization and comparison with hypoxia-inducible factor-1alpha. *Blood* **92**, 2260–2268.

Williams, K. J., Telfer, B. A., Xenaki, D., Sheridan, M. R., Desbaillets, I., Peters, H. J., Honess, D., Harris, A. L., Dachs, G. U., van der Kogel, A., and Stratford, I. J. (2005). Enhanced response to radiotherapy in tumors deficient in the function of hypoxia-inducible factor-1. *Radiother. Oncol.* **75**, 89–98.

Wouters, B. G., and Brown, J. M. (1997). Cells at intermediate oxygen levels can be more important than the “hypoxic fraction” in determining tumor response to fractionated radiotherapy. *Radiat. Res.* **147**, 541–550.

Yang, L., Cao, Z., Li, F., Post, D. E., Van Meir, E. G., Zhong, H., and Wood, W. C. (2004). Tumor-specific gene expression using the survivin promoter is further increased by hypoxia. *Gene Ther.* **11**, 1215–1223.

Yazawa, K., Fujimori, M., Amano, J., Kano, Y., and Taniguchi, S. (2000). Bifidobacterium longum as a delivery system for cancer gene therapy: Selective localization and growth in hypoxic tumors. *Cancer Gene Ther.* **7**, 269–274.

Yazawa, K., Fujimori, M., Nakamura, T., Sasaki, T., Amano, J., Kano, Y., and Taniguchi, S. (2001). Bifidobacterium longum as a delivery system for gene therapy of chemically induced rat mammary tumors. *Breast Cancer Res. Treat.* **66**, 165–170.

Yew, P. R., and Berk, A. J. (1992). Inhibition of p53 transactivation required for transformation by adenovirus early 1B protein. *Nature* **357**, 82–85.

Zhang, X., Kon, T., Wang, H., Li, F., Huang, Q., Rabbani, Z. N., Kirkpatrick, J. P., Vujaskovic, Z., Dewhirst, M. W., and Li, C. Y. (2004). Enhancement of hypoxia-induced tumor cell death *in vitro* and radiation therapy *in vivo* by use of small interfering RNA targeted to hypoxia-inducible factor-1alpha. *Cancer Res.* **64**, 8139–8142.

Zhong, H., Agani, F., Baccala, A. A., Laughner, E., Riobello-Camacho, N., Isaacs, W. B., Simons, J. W., and Semenza, G. L. (1998). Increased expression of hypoxia inducible factor-1alpha in rat and human prostate cancer. *Cancer Res.* **58**, 5280–5284.

Zhong, H., Chiles, K., Feldser, D., Laughner, E., Hanrahan, C., Georgescu, M. M., Simons, J. W., and Semenza, G. L. (2000). Modulation of hypoxia-inducible factor 1alpha expression by the epidermal growth factor/phosphatidylinositol 3-kinase/PTEN/AKT/FRAP pathway in human prostate cancer cells: Implications for tumor angiogenesis and therapeutics. *Cancer Res.* **60**, 1541–1545.

Zhong, H., De Marzo, A. M., Laughner, E., Lim, M., Hilton, D. A., Zagzag, D., Buechler, P., Isaacs, W. B., Semenza, G. L., and Simons, J. W. (1999). Overexpression of hypoxia-inducible factor 1alpha in common human cancers and their metastases. *Cancer Res.* **59**, 5830–5835.

Cellular Basis of Chronic Obstructive Pulmonary Disease in Horses

Darko Marinkovic, Sanja Aleksic-Kovacevic, and Pavle Plamenac

Department of Pathology, Faculty of Veterinary Medicine,
University of Belgrade, Belgrade, Serbia

Chronic obstructive pulmonary disease (COPD) is an inflammatory obstructive disease of the airways characterized with hypersensitivity of the airway tissues to various allergens, most commonly the fungi contained in the poor-quality hay and straw bedding—*Saccharopolyspora rectivirgula*, *Aspergillus fumigatus*, and *Thermoactinomyces vulgaris*. It is manifested clinically in middle-aged horses with recurrent episodes of dyspnea, chronic cough, and their reduced athletic and working capacity. Pulmonary emphysema and lack of pulmonary collapse are the most common gross lesion. Pathohistological findings in horses with COPD are chronic bronchitis/bronchiolitis, with characteristic changes in lumen, mucosa, submucosa, and smooth muscle layer and alveolar emphysema, both distensive and destructive form. Increased immunoreactivity in lungs and tracheobronchial lymph nodes is also noted. Most common lesions seen on cytology imprint smears from tracheal bifurcation is thick, viscous, PAS-positive mucus that forms Curschmann's spirals. Dominant cell population consists of desquamated airway epithelial cells, as well as eosinophils, neutrophils, mast cells, erythrocytes, and alveolar macrophages. Primary pulmonary pathogens as well as potential contaminants and secondary infection agents were isolated bacteriologically from lung samples. All of the aforementioned findings correlate pointing to the fact that chronic bronchitis/bronchiolitis represents a basic substrate of COPD, which have combined inflammatory and immunological etiology, and emphysema is secondary to airway obstruction.

KEY WORDS: Horse, Lungs, COPD, Pathohistology, Cytology. © 2007 Elsevier Inc.

I. Introduction

Because respiratory diseases are widely spread among the horse population and account for a substantial share of pathology of the animal species, study of chronic obstructive pulmonary disease (COPD) in horses is of great importance. COPD belongs to the group of chronic respiratory diseases that reduce the value of the sports animals and working capacity of the draught animals. The importance of the study is further illustrated by the fact that COPD is markedly similar to allergic, atopic, extrinsic asthma in humans. Study of pathogenesis and therapy of the COPD in horses may contribute to the body of knowledge in pulmonology and promote treatment of asthma and chronic inflammatory disease of airways occurring in humans hypersensitive to various known and unknowns environmental stimuli. COPD is an inflammatory obstructive disease of the airways characterized with hypersensitivity of the airway tissues to various allergens, most commonly the fungi contained in poor-quality hay and straw bedding (*S. rectivirgula*, *A. fumigatus*, and *T. vulgaris*). It is manifested clinically in middle-aged horses with recurrent episodes of dyspnea, chronic cough, and their reduced athletic and working capacity.

The disease is commonly called pursy or chronic alveolar emphysema, but there are many synonyms, because all authors studying this issue proposed a name for the disease: heaves, broken wind, RAO (Recurrent Airway Obstruction), chronic bronchiolitis-emphysema complex, chronic small airway disease, alveolar emphysema, chronic bronchiolitis, allergic bronchiolitis, asthma, asthmatic bronchiolitis, chronic cough, chronic pulmonary emphysema, chronic bronchitis/bronchiolitis, chronic pulmonary disease, hypersensitive pneumopathy, hyperreactive airway disease, chronic airway reactivity, and hay sickness (Rooney and Robertson, 1996).

This disease is encountered in horses that spend a lot of time in poorly aired dusty stables during winter, although there is a special type of the disease that also occurs in the summer. The reference literature states that the age at which the disease occurs for the first time varies from 4 to 8 years or more. It is most frequently encountered in sports horses in the following disciplines: show jumping, equestrian dressage, endurance (endurance race, cross-country riding with regular veterinary check-ups in which the horse pulse must not exceed 64 beats per minute), eventing (comprises show jumping, dressage, and cross-country with show jumping), but it also occurs in horses that are used for recreational riding, in riding schools, etc. (Art *et al.*, 1998).

The disease presents itself in two forms: (1) typical form of COPD in the winter months in horses that spend longer time in unaired, dusty stables and

are hay-fed; and (2) Summer pasture-associated obstructive pulmonary disease (SPAOPD)—this form of the disease is encountered in the southeast part of the United States, California, and the United Kingdom during the summer when the horses are grazing and when the weather is warm and humid (Costa *et al.*, 2001; Robinson, 2001; Seahorn and Beadle, 1993). Both in humans and horses the genetic base of COPD is considered to be very important. In the pathogenesis of equestrian COPD, an important role is played by T lymphocytes, CD4+ Th1 that release: IL-8, MIP-2, LTB-4, and ICAM-1, whereas CD4+ Th2 lymphocytes produce IL-4, IL-13, and IL-5.

Pathogenesis of the disease has not been fully elucidated, but some hypotheses have been proposed suggesting the development of the disease. With genetic predisposition, noxae (recurrent and uncured viral and bacterial infections of the airways, noxious effect of protease, and endotoxins) lead to lesions on the airway epithelium—loss of the cilia from the ciliary epithelium, desquamation of the epithelial cells of bronchioli and bronchi, as well as denudation of the basal membrane. Denudation of the basal membrane enables the antigen to establish a direct contact with the immunologically active tissues and as a result respiratory tissues become hypersensitive (McPherson and Lawson, 1974; Moore *et al.*, 2004; Trailovic, 2000).

The main role of CD4+ Th1 that produce IL-4, IL-5 and IL-13 activated mastocytes, platelets, epithelial cells, and substances originating from these cells—histamine, bradykinin, LTC-4, LTD-4, PAF, PGD₂, PGF₂ α —has been recognized in the pathogenesis of asthma. These substances lead to a series of pathological changes characteristic of both diseases. Macroscopically, appearance of the lung is mainly unchanged, but some authors suggest that in horses suffering from COPD the lungs usually do not collapse at exenteration from the chest or appear voluminous and excessively inflated, pale pink, and occasionally with imprints of the ribs seen. Sometimes there is emphysema as well as thick mucus that may be squeezed out of the lung section when pressed.

The pathohistological findings are very characteristic. The main pathohistological substrates of COPD include bronchitis and bronchiolitis that are characterized with changes on the mucosal and muscular layers of bronchi and bronchioli, in the peribronchial and peribronchiolar tissues as well as accumulation of content in the airways, their obstruction, and consequent development of secondary emphysema and atelectasis. Regardless of the fact that the disease was recognized long ago, few data exist on the pathogenesis, which makes the diagnosis establishing difficult. In addition to standard diagnostic methods, cytological smears obtained by bronchoalveolar and tracheobronchial lavage are also used. Moreover, imprints from the mucosal tissue in the tracheal bifurcation make postmortem diagnostic substantially easier and substantiates the diagnosis of the disease.

II. Morpho-Functional Features of Horse Lungs

A. Morphology

1. Lungs

Histology of the lungs is composed of conducting elements (lung conducting ways) composed of the bronchi and bronchioli; transitory elements composed of respiratory bronchioli; respiratory elements comprising alveolar channels, alveolar sacs, and alveoli; and stromal elements of the lungs represented by vascular and lymph vessels and nerves. The conducting elements start where the trachea branches into the right and main left bronchus that are initially extrapulmonary situated where in the lung hilar region they are covered by the lung parenchyma and continue to branch further intrapulmonarily. The conducting elements of the lungs are composed of the primary, secondary, and tertiary bronchi.

The wall of the extrapulmonary bronchus is similar to the tracheal architecture. The mucosa has an epithelial layer (*lamina epithelialis mucosae*) that is pseudostratified columnar, ciliated epithelium composed of stem, ciliary, goblet, and basal cells situated on the basal membrane (Banks, 1993). Below the basal membrane there is *lamina propria mucosae*—submucosal body, composed essentially from connective tissue rich with elastic fibers. The third layer is composed of elastic fibers, and it is believed to play the role of mucosal muscular layer. This is called *lamina elastica mucosae*. The *lamina propria* accommodates branched tubuloalveolar glands that spread in the cartilage and lymph follicles. The cartilage has a horseshoe shape. At the places where the cartilage ring is discontinued transversally spread smooth muscles may be seen. The whole extrapulmonary bronchus is covered with adventitia composed of connective tissue.

The intrapulmonary bronchus architecture differs somewhat from the extrapulmonary bronchus. The epithelial mucosal layer is also a pseudostratified in the type and mutual disposition of the cells present. It is also composed of stem, ciliary, goblet, and basal cells that cover the basal membrane. The fur is basically composed of elastic fibers. The smooth muscle fibers are distributed spirally and comprise the muscular layer of the mucosa (*lamina muscularis mucosae*). The submucosa is composed of connective tissue rich with collagen fibers accommodating the branched bronchial glands (*glandulae bronchales*) that are a combination of serous and mucinous cells, where the number of these cells decreases toward the tertiary bronchi. The submucosa also accommodates lymph nodes, that is, follicles (*lymphonodi bronchales*), nerve fibers, and ganglia of the neurovegetative system, blood and lymph vessels.

The bronchial cartilage in larger bronchi is semicircular but the cartilage rings get smaller and take the plaque shape or disappear completely at the site where the tertiary bronchi become the primary bronchioli. The epithelial mucosal layer of the bronchioli is composed of a single layer of squamous or columnar ciliary epithelium, where the number of cilia is higher in the primary, lower in the secondary bronchiole, whereas the tertiary bronchioli have no cilia at all. In addition to the ciliary, there are also cells without cilia called the Clara cells. The goblet cells are scarce. The bronchial and bronchiolar mucosa also contains neuroendocrine cells (in man called Feyerter, or Kulchitsky-like or K-cells) that exhibit neurosecretory type granules and contain bombesin, calcitonin, and in fetal lungs somatostatin (Banks, 1993; Rodriguez *et al.*, 1992). The *lamina propria* is composed of elastic and collagen fibers where mastocytes may be seen (Young and Heath, 2000). There is no cartilage in bronchioli.

Respiratory bronchioli in horses, as opposed to humans and some other species, are poorly developed and represent transitory elements of the lungs, establishing the link between the tertiary bronchioli and alveolar ducti and gas exchange takes place in them, as well. The epithelial layer of mucosa is columnar, the *lamina propria* is rich with elastic and collagen tissues with a layer of smooth muscles.

The respiratory elements of the lungs include alveolar channels (*ductus alveolaris*), alveolar sacs (*sacculus alveolaris*), and alveoli (*alveolae pulmonales*). The respiratory alveolae at the end split into numerous alveolar channels that are composed of alveoli. The alveolar channels also split and spread peripherally into the alveolar sacs. The alveolae are composed of two types of cells, pneumocytes type 1 (membranous pneumocytes, flat cells whose nucleus partially protrudes into the alveolar lumen) whose role is to communicate between air and blood to enable gas exchange, and pneumocytes type 2 (granular pneumocytes, circular or square cells that protrude into the alveolar lumen). Their role is secretory, meaning they produce and secrete pulmonary surfactant. The pulmonary surfactant is a secretory product of pneumocytes type 2 and is a kind of detergent primarily composed of a substance that reduces the surface tension called dipalmitoyl phosphatidyl choline (Young and Heath, 2000).

The lungs are permanently exposed to the influence of foreign materials inhaled with the air where the pulmonary macrophages (together with mucociliary apparatus of the lungs and protective substances in the bronchial fluid) are one of the defense mechanisms the body uses against foreign materials. Two types of pulmonary macrophages have been described, septal cells and alveolar macrophages where both conduct phagocytosis of foreign materials. The air-blood barrier is composed of pneumocytes, alveolar basal membrane, septal space, basal membrane of the blood vessels, and vascular endothelial vessels (capillaries).

The stromal elements of the lungs are composed of blood vessels, lymph vessels, and nerves (Banks, 1993). The immune system of the lungs is represented with six different types of lymphatic tissue: (1) free luminal lymphocytes present in smaller number in small bronchioli and alveolae; (2) intraepithelial lymphocytes present in the bronchi and bronchioli; (3) isolated lymphocytes in the mucosal fur that may be found in bronchi and bronchioli; (4) areas of densely packed lymphocytes occasionally present in small intrapulmonary bronchi; (5) lymphoid tissue with lymph noduli that may also be occasionally found in small intrapulmonary bronchi 4- to 8-mm wide (Mair *et al.*, 1987). As opposed to the local bronchus-associated lymphoid tissue (BALT), the presence of bronchiole-associated lymphoid tissue (BRLT) has been evidenced (Mair *et al.*, 1988); and (6) the last type of immunologically active tissue is represented with lymph nodes represented by the bronchial lymph center (*lymphocentrum bronchale*).

2. Lymph Nodes

In the course of embryonal development the lymph nodes develop after the thymus and spleen. The lymph nodes develop from the periarterial mesenchyme. Development of lymph vessels is followed by links between the lymph nodes and arteriolae where clusters of lymph cells occur, and periarteriolar reticular cells form a network that is an adequate environment colonized by lymphoblasts originating from the bone marrow or thymus. Foals are born with their lymph nodes formed, and in case of the presence of intrauterine infection they have germinative centers, as well (Valli, 1985).

The lymph nodes are clustered, encapsulated lymphatic tissues. The lymphatic tissue is encapsulated and from the capsule to the inner part of the lymph node, the partitions (trabeculae) are spread. The capsule and trabeculae are composed of connective tissue rich with collagen fibers, whereas the stromal elements are composed of reticular fibers secreted by the reticular cells (probably fibroblasts). These fibers, together with the cells, form a thick network within the lymph node. Formation of this network is supported by dendritic cells that are characterized with numerous cytoplasmic protrusions. These cells play the role of antigen presenting cells (APC) together with macrophages and exceptionally B lymphocytes, and depending on the localization site, they are termed interdigititation cells in the T-cell area of the lymph node, or follicular dendritic cells (FDC) in the B-cell zone. The lymphatic system is organized as primary and secondary lymph nodes (follicles). The primary follicles are composed of densely packed small lymphocytes. The secondary follicles have a central light region composed of macrophages and large lymphocytes with light cytoplasm and light chromatin in the nucleus, and the area is called the germinative center. The germinative center is

surrounded by the darker zone (mantle zone, corona) composed of small lymphocytes with reduced cytoplasm and darkly stained nuclear chromatin.

The lymph node cortex is divided into the nodular area accommodating the lymph follicles, internodal zone, and deep zone. The internodal and deep zones make the paracortical zone or paracortex. In horses, fusion of the follicles (nodular fusion) frequently takes place.

B lymphocytes are situated in the primary follicles and germinative centers of the secondary follicles, and the T lymphocytes are situated in the paracortex. The lymph node center, that is, medulla composed of branched trabeculas, reticular fibers, and cells (lymphocytes, plasmocytes, and macrophages) surrounded by the medullar sinuses and lymph capillaries, where these formations are termed the medullar bands. The afferent fibers of the lymph nodes enter the lymph node capsule in the medullar sinus. Lymph passes through the cortical sinuses, follicles into the medullar sinuses that subsequently merge and compose efferent lymph nodes that leave the lymph node in the hilar region.

In the hilar region arteries branch through the lymph node trabeculas to the capillary level entering a lymph node and venous drainage proceeds. The postcapillary venules play a role in lymph recirculation from the blood. Lymphocytes leave the blood through these and enter the follicles (B lymphocytes) or paracortex (T lymphocytes). These cells leave the lymph node via the efferent lymph vessels and via the thoracic ductus enter the venous system and subsequently, when they pass through the heart and small pulmonary circulation, they enter the systemic circulation. From the systemic circulation they re-enter a lymph node, and the cycle is repeated (Banks, 1993; Heath and Perkins, 1989). Lymph nodes participate in production of lymphocytes, lymph filtration, phagocytosis of foreign matter, and production of antibodies.

B. Physiology

Respiratory organs may be divided into the upper airways, respiratory muscles, chest wall and lungs, that is, production elements (conducting pulmonary ways) composed of the bronchi and bronchioli; transitory pulmonary elements composed of the respiratory bronchioli; and respiratory elements of the lungs including alveolar channels, alveolar sac, and alveolae (Banks, 1993). The upper respiratory airways comprise the nasal cavity, paranasal cavities—sinuses, nasopharynx, and trachea. The upper respiratory ways that together with the conducting parts of the lungs (bronchi and bronchioli) represent the “anatomically dead space” (in horses weighing 450 kg it amounts to 1.5–2.0 liters of air) meaning space in which no respiration takes place, but heating of the inspired air to the body temperature, enrichment of the air with humidity and its purification from larger particles, exceeding the

size of 5 μm that are halted in the nose and expelled into the external environment by secretion, while particles sized $<5 \mu\text{m}$ and $>0.5 \mu\text{m}$ enter the lower conducting parts of the lungs and are also expelled into the external environment by expired air, cough, bronchial or bronchiolar secretion (mucociliary lift), or phagocytic activity of alveolar macrophages (Art *et al.*, 2002). During inspiration, the inspired air is mixed with the air from the “physiologically dead space” composed of “anatomically dead space” (conducting air space) and “alveolar dead space” (space in the alveolae in which there is air but no gas exchange) so that the air from the atmosphere is not inspired alone, but mixed with the air from these spaces. Respiration is supported by the inspiratory muscles and expiratory muscles. The inspiratory muscles, diaphragm, *mm. intercostales externi*, *mm. scalene*, *m. sternomandibularis* help increase lateral, cranio-caudal and dorso-ventral diameters of the chest during inspiration and, consequently increase its volume, whereas the nasal muscles—*m. levator nasolabialis*, *m. caninus*, *mm. nasales* (*m. dilatator naris apicalis* and *m. lateralis nasi*) support preservation of the nasal diameter necessary for respiration because horses breathe through the nose.

Maintenance of the necessary diameters of the upper and lower airways is supported by the rigid structures such as the cartilage in the trachea and bronchi that prevent collapse of these structures. Interaction of the aforementioned muscles and pleura results in increased volume of the chest and negative intrapleural pressure, resulting in increased volume of the lungs, reduced intrapulmonary pressure, and when the value lower than the atmospheric one is reached, the air from the atmosphere via the conducting ways is “sucked into” the lungs. The suction is resisted by the elasticity of the lungs but the lungs spread, nevertheless, because the power of the inspiratory muscles exceeds that of the elasticity of the lungs, but during the inspirium, potential energy is deposited in the lungs and subsequently used for the expirium. Owing to that, the horses use the total of 2–5% of the total body energy for breathing, according to the state (rest or exercise). The expirium is mostly a passive process, but the expiratory muscles nevertheless take part: *mm. intercostales interni* as well as abdominal muscles that adhere to the ribs—*m. obliquus externus*, *m. rectus abdominis*, *m. transversus*. The intrapleural space is the space between the parietal and visceral pleural leaves, where the intrapleural pressure is, which may be either negative, (i.e., lower than the atmospheric pressure during inspirium) or positive, (i.e., higher than the atmospheric one during expirium).

During amble and trot the frequency of trot and breathing are not related, although some studies still suggest that they may be coordinated, whereas in the gallop the functions are always related (Art *et al.*, 2002). Normal respiratory frequency in horses is between 8 and 16 respirations per minute (may reach 110–130 during exertion, or maximum up to 148 respirations per minute). The largest amount of blood in horse lungs is situated in the dorsal parts of the

lungs, instead of the ventral ones as believed previously, because gravitation plays only a minor, almost negligible influence on distribution of blood in the lungs (Art *et al.*, 2002). The lungs play a role in respiration and maintenance of acid-base balance, metabolic function, endocrine function, defense function, thermoregulatory function, and excretory function—expelling volatile substances from the circulation: alcohol and acetone bodies, volatile anesthetics, methane, and other gases.

Breathing is regulated by activity of respiratory centers that are situated in the area of medulla oblongata and pons. There are four of these: inspiratory, expiratory, apneustic, and pneumotaxic. These centers are controlled by the higher parts of the vegetative nervous system—hypothalamus and limbic cortex. The inspiratory center is presented with the dorsal group of neurons of the medulla oblongata, belongs to the neurons of tractus solitarii that represents nuclei of the VII, IX, and X cranial nerves. It is tone-active, and receives the information from numerous chemo, baro, stretch, and other receptors. It spontaneously produces 8–16 rising signals per second.

The ventral group of neurons of the medulla oblongata operates concomitantly as the inspiratory and expiratory center, because it innervates both inspiratory muscles (*mm. intercostales internii*), and expiratory muscles (*mm. intercostales externii* and *mm. abdominales*). The apneustic center is situated in the lower part of the pons, it is also tone-active and is expected to prevent interruption of the rising signal from the inspiratory center. The pneumotaxic center is situated in the pons and is required to inhibit the apneustic and, indirectly the inspiratory center. It interrupts the inspirium and regulates the frequency and rhythm of respirations.

III. Cytological Features of Equine Lungs

The pulmonary parenchyma contain the subepithelial and free mastocytes that have, on the surface, incorporated E class immunoglobulins (IgE) and as a response to stimulation by specific antigen release histamine, heparin, arachidonic acid metabolites, platelet activation factor, and hemotoxic factors. Consequently, they play an important role in pathogenesis of some major equine diseases such as COPD and infection by pulmonary nematodes (Ainsworth and Biller, 1998).

Secretion of the lower airways reveals various kinds of cells. The cytologic finding is one of the most important parameters for diagnosis of various respiratory diseases. In clinically healthy horses the usual cytological finding in secretion originating from lower airways comprise usually sparse lymphocytes, macrophages, few cells from the bronchial epithelium, and a small amount of mucus. In horses suffering from miscellaneous diseases of the

bronchi, bronchioli, and alveolae, one may find macrophages, lymphocytes, neutrophil granulocytes, mastocytes, eosinophil granulocytes, erythrocytes, desquamated cells of bronchial and bronchiolar epithelia. In addition to the cells, smaller or larger amounts of mucus may also be found, as well as the bacteria that may be intracellular or extracellular, or may even form colonies.

The cytological smear presents alveolar macrophages as large cells, 15- to 40- μm diameter with high cytoplasm: nucleus ratio, 3:1. These cells are frequently vacuolized and may contain phagocytosed cellular debris (phagocytosed erythrocytes, hemosiderin, desquamated epithelial cells, apoptotic cells, fungal spores, pollen grains, etc.). The alveolar macrophages of horses present a low level of expression of major histocompatibility complex, class II antigen (MHC-II), and accessory molecules CD80 and CD86, so that presentation of antigen CD4 T cells is poor (Horohov, 2004).

Lymphocytes are cells with large oval- or kidney-shaped nucleus. There are two populations of lymphocytes: small, about 6- μm diameter, and larger, whose diameter is between 10 and 15 μm . Both types are encountered in clinically healthy horses and those suffering from respiratory diseases. There are two types of lymphocytes: (1) B lymphocytes that after activation are differentiated into M cells, memory cells and plasmocytes that produce specific antibodies (immunoglobulins) by way of which the B lymphocytes participate in humoral immunity; (2) T lymphocytes that may be Tc (cytotoxic) that may by way of substances they excrete (granzymes, perforines, TNF- β) directly kill microorganisms, virus-infected cells, and tumor cells; and Th (helper) lymphocytes that after contact with a certain antigen presented by macrophage (antigen presenting cell [APC]) depending on the subpopulation to which they belong exert effect on Tc lymphocytes or B lymphocytes (Th1 lymphocytes via cytokine IL-2 and TNF- β to Tc lymphocyte by potentiating their effect, and Th2 via IL-4, IL-5, IL-6, and IL-10 to B lymphocytes stimulating them to differentiate into memory cells and plasmocytes that produce immunoglobulins) (Banks, 1993). T lymphocytes also produce interleukin IL-8, interleukin MIP-2 (macrophage inflammatory protein 2), leukotriene LTB-4, and integrin ICAM-1, interleukins IL-4, IL-13, and IL-5 (Beadle *et al.*, 2002; Bowels *et al.*, 2002; Cunningham, 2001; Francini *et al.*, 2000; Geisel and Sandersleben, 1987; Giguere *et al.*, 2002; Halliwell *et al.*, 1993; Lavoie *et al.*, 2001, 2002; Mair *et al.*, 1988; Robinson, 2001; Schmallenbach *et al.*, 1998). Most lymphocytes (90%) found in secretion of the lower airways of horses are T lymphocytes, whereas B lymphocytes account for only 10%.

Neutrophil granulocytes are white cells, sized 10–12 μm and contain segmented nucleus. A nucleus of a mature neutrophilic granulocyte usually has three lobes, although the number of segments may vary by the age of the cells from 1–2 segments in young cells (shift to the left) to 4–5 segments in older cells (shift to the right). Cytoplasm of these cells contain granula filled with matter endowed with bactericidal activity (lysozyme, lactoferrin, and

defensins), proteolytic action (cathepsin, collagenase, and elastase), lipolytic action (phospholipase A1 and phospholipase A2), etc. (Kaneko, 1998).

Mastocytes (mast cells) are oval cells that may vary in size with small and light, centrally situated nucleus. Their cytoplasm is filled with secretory granules that contain heparin, histamine, serotonin, leukotrienes, platelet activation factor, and eosinophil chemotactic factor (ECF). Eosinophilic granulocytes are cells sized 10–15 μm with bilobar nucleus and large specific granules that in horses may reach the size of 1–2 μm (diameter) and are called Seamers granules and are stained red with eosin. These granules contain the main base protein, peroxidase, hydrolytic enzymes, acid phosphatase, aryl sulphatase, and collagenase (Zinkl, 2002). Epithelial cells originate from epithelial layer of bronchial and bronchiolar mucosa and are mostly highly columnar ciliary or less commonly low columnar without cilia (originating from tertiary bronchioli) (Hewson and Viel, 2002).

IV. Chronic Obstructive Pulmonary Disease (COPD) in Horses

In the respiratory system pathology COPD plays a very important role. COPD is an inflammatory obstructive disease of the airways that becomes clinically manifested in middle aged horses as recurrent episodes of dyspnea, chronic cough, and impaired sports and working capacity of horses (Robinson, 2001).

A. Etiology and Pathogenesis

1. Etiology

Etiology of the disease has not been fully elucidated but several factors are considered important for its occurrence.

Genetic predisposition plays an important role in the pathogenesis of the disease—studies conducted in two horse farms indicate a higher incidence of the occurrence of COPD in horses with one or both parents affected. It is suggested that numerous different genes participate in the occurrence of the disease. Genetic basis of the diseases has certain similarities with genetic basis of asthma in humans (Marti and Ohnesorge, 2002). Recurrent, inadequately managed bacterial and viral infections may also be considered in the etiology of this disease, particularly since correlation of the processes has been evidenced in both humans and experimental animals. Similar examples have been reported in horses, as well (Castleman *et al.*, 1990; Lopez, 2001; McPherson and Lawson, 1974; Trailovic, 2000).

Toxins have also been proposed as a possible cause of COPD more specifically, endotoxins (Pirie *et al.*, 2001) and exotoxins such as 3-methylin-dol (Derksen *et al.*, 1982). In humans, occurrence of pulmonary emphysema is closely related to protease (i.e., deficit of antiprotease factors [congenital α 1-antitrypsin deficiency] and smoking habit). In 1963, two Swedish researchers made a breakthrough in understanding the pathogenesis of lung emphysema in humans (Laurel and Ericsson, 1963). They have noted that serum α 1-antitrypsin deficiency and increased incidence of lung emphysema coincide in families with this genetic defect. Emphysema that they noted was the very destructive panacinar emphysema without accompanying bronchitis that used to be called "idiopathic." In horses also, activity of protease, both endogenous originating from neutrophilic granulocytes and epithelial cells and exogenous originating from microorganisms has been suggested, but it is believed they do not play as important of a role as in humans. Serine protease and matrix metalloproteinase 9 (MMP-9) have also been suggested (Gruning *et al.*, 1986; Raulo *et al.*, 2001; Winder *et al.*, 1990). Pulmonary nematode *Dictyocaulus arnfieldi* has also been suggested as a factor that may contribute to development of this disease (Ainsworth and Biller, 1998).

Undoubtedly most important and most commonly suggested etiological factor is hypersensitivity of the affected horses to specific antigens, that is allergic reaction. Among the suggested allergens fungi are the most common; their spores in the air originating from poor-quality hay, dusty hay bed, and poorly aired, usually humid stables in which the fungi flourish. *S. rectivirgula* (until it was termed *Faenia rectivirgula*, and in older literature it was referred to as *Micropolyspora faeni*) plays the most important role in the occurrence of COPD (Derksen *et al.*, 1988; Khan *et al.*, 1985). In addition to this fungus, *A. fumigatus* and *T. vulgaris* are also frequently suggested (McGorum *et al.*, 1993; Schmallenbach *et al.*, 1998). Other allergens, considered potential causes of the disease are also suggested: β D-glucan (integral part of cell walls of fungi and bacteria), nonparasite mite (*Lepidoglyphus destructor*), pollen of plants, miscellaneous allergens from grazing fields, particles of plants and feed, allergy to chicken, etc. (Ainsworth and Biller, 1998; McGorum, 2001).

2. Pathogenesis

Pathogenesis of the disease has not yet been fully elucidated, but some hypotheses have been proposed suggesting the development course of this disease. In addition to genetic predisposition of noxae (recurrent or unhealed viral and bacterial infections of airways, noxious effect of protease and endotoxin) lead to lesions of airways epithelium—loss of cilia from the ciliary epithelium, desquamation of epithelial cells of bronchioli and bronchi, and

denudation of the basal membrane. Denudation of the basal membrane enables direct contact of antigens with immunologically active tissues and consequent hypersensitivity of tissues in the airways (McPherson and Lawson, 1974; Moore *et al.*, 2004; Trailovic, 2000). Hypersensitivity of airways is characterized by persistent bronchospasm after the contact between the bronchioli and bronchi with allergens. This process may last for several days after a single contact with allergens (DerkSEN and Robinson, 2002; Hoffman, 2001). In horses with hypersensitivity of airway mucosa presence of larger number of T lymphocytes is also noted (CD4+, CD3+), as well as eosinophilic granulocytes and mastocytes (Slocombe, 2001; Watson *et al.*, 1997). When contact with the allergen takes place in these horses, combined allergic and inflammatory reactions occur.

Pulmonary alveolar macrophages (PAM) and T lymphocytes (CD4+ Th1) release cytokines: interleukin IL-8, interleukin MIP-2 (macrophage inflammatory protein 2), leukotriene LTB-4 and integrin ICAM-1, while CD4+ Th2 lymphocytes produce interleukins IL-4, IL-13, and IL-5. Interleukins IL-8, MIP-2, leukotriene LTB-4, and integrin ICAM-1 play a hemotoxic role so that neutrophilic granulocytes accumulate in the lumens of bronchioli and bronchus (Cunningham, 2001; Francini *et al.*, 2000; Lavoie *et al.*, 2002; Robinson, 2001). On the other hand, interleukins IL-4 and IL-13 play an important role in the switching of B lymphocytes to production of IgE, whereas IL-5 is responsible for tissue migration of eosinophilic granulocytes. In horses in which increased hypersensitivity is noted, increased concentration of IgE, IgA, and IgG in the airways is also present. Although increased production of IL-5 by CD4+ Th2 lymphocytes is also noted, massive infiltration of eosinophilic granulocytes does not take place, however the predominant cellular population is that of neutrophilic granulocytes (Beadle *et al.*, 2002; Bowels *et al.*, 2002; Geisel and Sandersleben, 1987; Giguere *et al.*, 2002; Halliwell *et al.*, 1993; Lavoie *et al.*, 2001; Mair *et al.*, 1988; Schmallenbach *et al.*, 1998). Also, nuclear transcription factor κ B (NF κ B) occurs, stimulating cytokine production, and thus accumulation of neutrophilic granulocytes. In addition to prolonged stimulation for accumulation, these neutrophilic granulocytes have prolonged apoptosis, they live longer, and this at least partially, explains the fact that after a single contact with allergen, development of allergic inflammatory process that last for several days ensues (Bureau *et al.*, 2000). Some reports suggest that oxidative stress, that is, substances that are released during the oxidative stress (isoprostanes—arachidonic acid derivatives) may play a certain role in pathogenesis of this disease (Kirschvink *et al.*, 2001). In affected horses increased level of nitrogen oxide synthetase (iNOS) has been recorded, playing a multiple role in inflammation (Costa *et al.*, 2001). Manifestation of increased sensitivity includes release of a large amount of mucus from goblet cells and from subepithelial cells into the lumen of airways where it is mixed with accumulated neutrophilic granulocytes and

cellular debris composed of desquamated epithelial cells of the airways. In the course of the allergic-inflammatory process that is the basis for development of COPD in parallel two processes take place in connection with goblet cells and subepithelial glands. At the sites where goblet cells and subepithelial cells physiologically are not present or are present in small amount their multiplication occurs. The process is called goblet cell metaplasia. At the sites where they normally occur, their number is significantly increased representing hyperplasia of the structures. It is believed that increased secretion of mucus results from increased number of mucosal cells where the actual mucus production is normal, increased production of mucus or reduced mucociliary clearance because of changes in the ciliary apparatus or changes in the physical features of the mucus (namely mucus secreted in this disease is thick, viscous, and sticky) (Hotchkiss, 2001).

Via IgE, the level of which is increased in horses suffering from COPD, allergens adhere to mastocyte membrane, the number of which is also increased in these horses, resulting in their degranulation. Mastocyte degranulation from their cytoplasmic granules results in release of biogenic amines—Inflammation mediators: histamine, arachidonic acid metabolites (prostaglandins and leukotrienes), platelet activation factor (PAF), serotonin, and hemotoxic factor (Hare *et al.*, 1999). Hemotoxic factors stimulate accumulation of neutrophilic granulocytes in the airway lumen. These reactions support the suggestion that hypersensitivity reaction type 1 plays a role in the pathogenesis of COPD, although hypersensitivity reaction type 3 has also been suggested as one of the causes of neutrophilic infiltration (Halliwell *et al.*, 1979; Lavoie, 2001; Lorch *et al.*, 2001). Serotonin, histamine, and leukotriene D4 (LTD-4) increase sensitivity of smooth muscles to endogenous acetyl choline (Ach) released from activated parasympathetic nerves and bound to M3-muscarinic receptors on smooth muscle cells of the muscular layer of bronchi and bronchioli. Additionally, histamine and serotonin promote increased release of acetyl choline from nerves. Lesions on epithelium of bronchus and bronchioli result in reduced production of epithelium-derived relaxing factor (EpDRF) whose physiological function is to control reactivity of bronchioli and bronchi and reduce the capacity for bronchospasm. Combination of these factors results in bronchospasm—contraction of smooth muscles of bronchioli and bronchi. Repeated episodes of effect of the allergen and persistent bronchospasm eventually result in hypertrophy—thickening of the muscular layer of the airways, particularly that of bronchioli (Derksen and Robinson, 2002; Robinson, 2001; Venugopal *et al.*, 2001; Wang *et al.*, 1995).

Due to permanent irritation, proliferation of bronchial and bronchiolar epithelium ensues, and subsequently squamous epithelial metaplasia follows in which the sensitive columnar ciliary epithelium is replaced by squamous epithelium. The squamous epithelium is more resistant to noxae, but because

it is devoid of cilia, function of mucociliary apparatus is affected, hindering expectoration of mucus, neutrophilic granulocytes and cellular debris from the lumen of small into the large airways and out in the environment. Increased accumulation of mucus, accumulation of neutrophilic granulocytes, desquamation of epithelial cells, proliferation of bronchiolar and bronchial epithelium and its squamous metaplasia, thickening of the smooth muscle layer, edema of the airway wall in the acute stage, as well as disruption of the function of mucociliary apparatus result in obstruction of the airways, hindering airflow through them, particularly in the expirium. Consequently, increased accumulation of air in the alveolae results, which secondarily leads to development of initially distensive emphysema (previously called compensatory), and subsequently when alveolar wall structure and interalveolar septae are disrupted, leads to development of destructive emphysema, compromising substantially gas exchange. Thus, emphysema is secondary in nature, and results from obstruction of airways (Geisel and von Sandersleben, 1987; Lopez, 2001; McPherson and Lawson, 1974) (Fig. 1).

B. Morphological Features of COPD

1. Macroscopic Findings

Voluminous and expanded lungs, pale pink, were found in 27.45% of studied horses, from our study, which is in concert with reference literature (Marinkovic, 2005; McPherson and Thompson, 1983; Robinson, 2001; Rooney, 1970; Slocombe, 2001). The rib imprints were not found in the

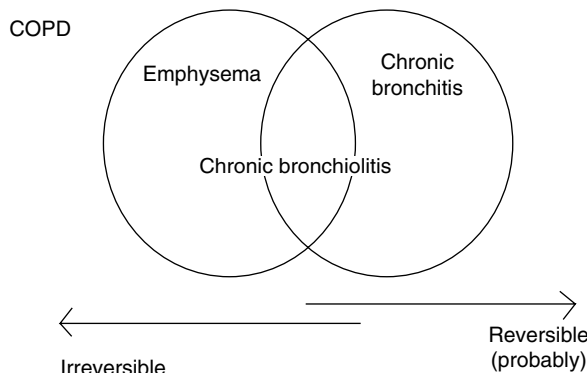


FIG. 1 Diagrammatic presentation of the overlap between the chronic inflammatory condition and COPD in horses.

studied horses. Emphysema was found in 11.76% of examined horses, coinciding with reports of other authors (Gerber, 1973; Lopez, 2001; McPherson and Lawson, 1974; Schoon and Deegen, 1983; Tyler *et al.*, 1971). Reference literature suggests that volume of the chest in deceased asthmatic patients is increased, the lungs are "inflated," frequently with marks of ribs on the surface.

2. Pathohistology

In the material examined for this study, bronchitis/bronchiolitis of various degree was diagnosed in 100% of studied horses (Marinkovic, 2005, 2007), coinciding with reports of Bracher and associates (1991) (Figs. 2 and 3). Reference papers by different authors differ only slightly in the percentage of histologically verified bronchitis/bronchiolitis from 37.4% (Winder and von Fellenberg, 1987) and 38% (McPherson *et al.*, 1978). Conversely, in a study conducted in Switzerland chronic bronchitis/bronchiolitis of various degrees of severity it was established in 62.3–100% of studied horses (Bracher *et al.*, 1991). In all studied horses loss of cilia, degeneration, necrosis, and desquamation of epithelial cells were found to various degrees, again in concert with reference literature (Kaup *et al.*, 1990a,b). Also, proliferation of bronchia/bronchiolar epithelium was recorded where these cells form papillomatous proliferations that protrude into the lumen as reported by many authors (Kaup *et al.*, 1990a,b; McPherson and Thompson, 1983; Slocombe, 2001; Winder and von Fellenberg, 1987, 1988). In humans during respiration or coughing these proliferates may fall off and enter the cytological material (sputum, bronchioaspirate) in the form of clusters (i.e., Creola bodies) (Naylor, 1962; Naylor and Railey, 1964) (Fig. 4).

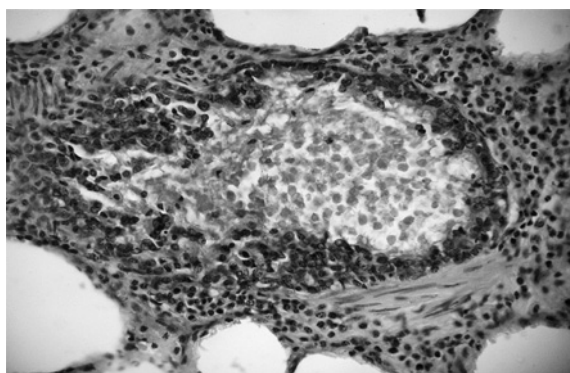


FIG. 2 Chronic bronchiolitis with epithelial proliferation, desquamation, and necrotic epithelial cells in the lumen (HE, $\times 400$).

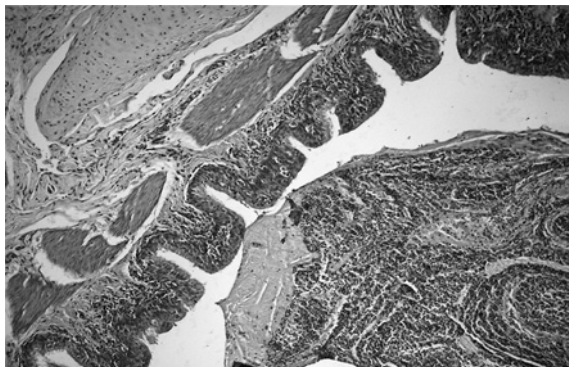


FIG. 3 Chronic bronchitis, muco-purulent plug in the bronchial lumen, and hypertrophic muscular layer (HE, $\times 200$).

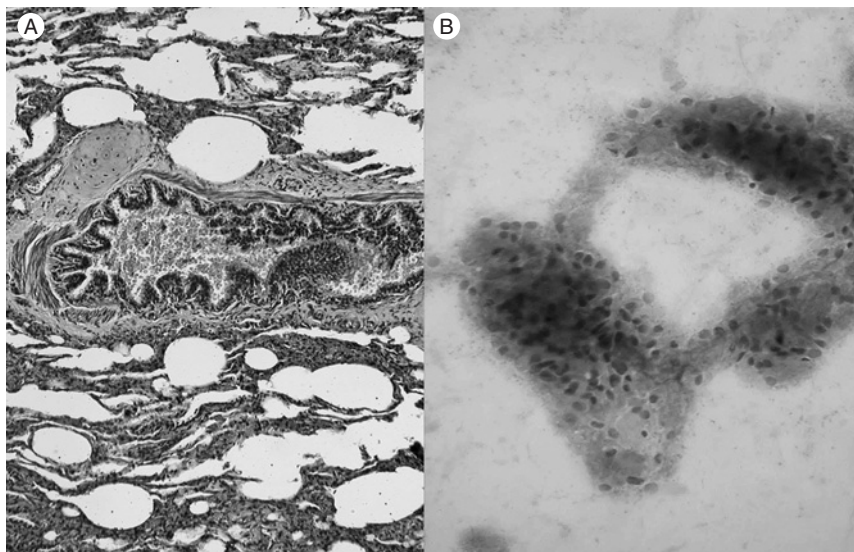


FIG. 4 (A) Chronic bronchiolitis with papillary proliferation in the lumen. (B) Tracheal imprint: Clusters of degenerated bronchial and bronchiolar epithelial cells (Creola body) (HE, $\times 200$).

Because the cells in these clusters are degenerated, frequently vacuolated cytoplasm and karyorrhectic nuclei, they may suggest adenocarcinoma of the lungs (Farber *et al.*, 1957). Careful observation reveals that some have residual cilia which adenocarcinoma cells never have. Although this finding is highly suggestive of asthma, it has been described in completely different

circumstances (e.g., sputa of workers in steel plants or sputa of pig breeders) (Djuricic *et al.*, 2001; Plamenac *et al.*, 1974). Due to chronic irritation squamous metaplasia (SM) developed in 7.84% of studied horses, in concert with reports of other authors (Robinson, 2001; Schoon and Deegen, 1983; Slocombe, 2003; Winder and von Fellenberg, 1988). Generally, findings of SM and other atypical proliferations of bronchial mucosa in persons exposed to various noxae (air pollution, smokers, miners in asbestos mines, truck drivers, etc.) are very common (Auerbach *et al.*, 1961; Berkheiser, 1959, 1963a,b, 1969; Couland and Kourilsky, 1953; Farber *et al.*, 1954; Lamb and Reid, 1968; Plamenac and Nikulin, 1969; Plamenac *et al.*, 1972a,b, 1973, 1978, 1980, 1981; Saccomano *et al.*, 1963, 1970; Sanderud, 1956; Weller, 1953). For a while, it was believed that there was a mutual link between degeneration and destruction of bronchial epithelium on the one hand and its SM and occurrence of lung cancer in humans on the other (Figs. 5–7).

Not every metaplasia is a precancer process and it may affect the respiratory epithelium widely (Auerbach *et al.*, 1961; Knudtson, 1960; Nasiell, 1967; Sanderud, 1958) and may even be taken as a physiological process in geriatric population (Plamenac *et al.*, 1970). It appears that carcinoma may develop in the bronchial epithelium regardless of the presence or absence of SM that may be considered as nonspecific reaction to various lesions that may or may not accompany cancerogenesis (Melamed *et al.*, 1977). Undoubtedly, metaplasia and precancer states of the bronchial epithelium play a minor role in pathology of horses compared to humans (Zinkl, 2002).

Finally, sporadic cases of lung cancer in horses are reported as casuistic rarities (Schultze *et al.*, 1988; Van Rensburg *et al.*, 1989) whereas SM is not such a rare phenomenon. Hyperplasia of goblet, mucus-producing cells established in 64.70% studied horses was reported by a series of authors

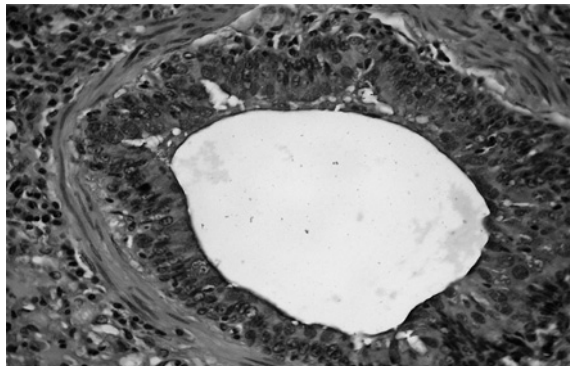


FIG. 5 Proliferation of bronchial epithelia with cellular atypia (HE, $\times 400$).

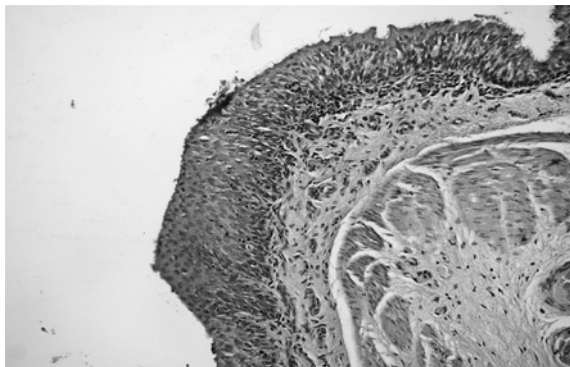


FIG. 6 Squamous metaplasia of the respiratory epithelium (HE, $\times 200$).

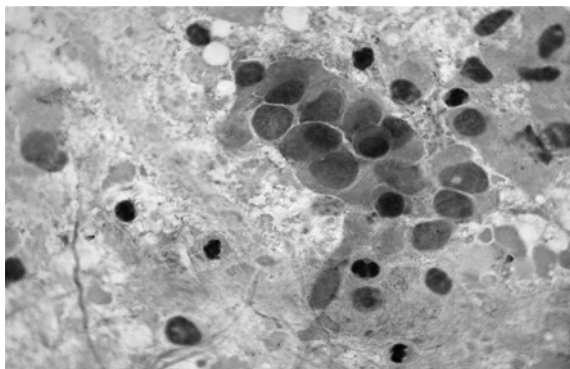


FIG. 7 Tracheal imprint: Cluster of squamous metaplastic cells (HE, $\times 1000$).

(Costa *et al.*, 2001; Kaup *et al.*, 1990a,b; McPherson and Thompson, 1983; Schoon and Deegen, 1983; Slocombe, 2001; Winder and von Fellenberg, 1987, 1988). In the lumen of bronchi and bronchioli of all studied horses accumulation of a large amount of thick viscous mucus that occasionally forms mucosal plugs obstructing the lumen of these airways, was reported by many other authors, as well (Costa *et al.*, 2001; Kaup *et al.*, 1990a,b; McPherson and Thompson, 1983; Robinson, 2001; Schoon and Deegen, 1983; Slocombe, 2003; Winder and von Fellenberg, 1987, 1988; Zinkl, 2002). In addition to hyperplasia of goblet cells, the increased amount of mucus in the lumen of bronchus is promoted by hyperplasia of subepithelial cells of the bronchi, as evidenced in 45.1% of these horses. In 60.78% of horses subepithelial structures revealed aggregation of lymphocytes, mastocytes, eosinophilic granulocytes, plasma cells, and macrophages that occasionally

form lymph follicles (Kaup *et al.*, 1990a,b; Schoon and Deegen, 1983; Slocombe, 2001). Hyperplasia of goblet cells, subepithelial mucus-producing glands has been described in patients suffering from asthma with consequent production of a large amount of thick, viscous, sticky, PAS-positive mucus that makes Curschmann's spirals (Jeffery, 2001). Eosinophilic granulocytes are a characteristic finding in the sputa of asthmatic patients, together with findings of Curschmann's spirals and Charcot-Layden's crystal (resulting from degradation of eosinophilic granulocytes under the influence of their phospholipases). The crystals are usually not recovered from the conventionally processed histological and cytological preparations, but only from plain sputum smears. There is no purpose in special search of these crystals because it has already been established that they are regularly recorded in all pathological states accompanied with eosinophilia, including some tumors. The mentioned triad (eosinophilic granulocytes, Curschmann's spirals, and Charcot-Layden's crystals) have remained a characteristic laboratory finding in cases of asthma. It is also well known that cytological diagnosis of this disease is more complex and that Creola bodies is the most important one. Also, findings of the Curschmann's spirals are not pathognomonic for asthma only: they may be found in numerous, other pathological conditions. Also, eosinophils and Charcot-Layden's crystals have been noted in the sputa of patients with pneumonia, echinococcus, lung tuberculosis as well as in patients with lung carcinoma.

Subsequent studies have shown that mucosal spirals, eosinophils, and crystals are not characteristic of asthma only, but may be seen also in other pathological conditions, including the sputa of smokers, former smokers, and persons exposed to noxious inhalants (Djuricic and Plamenac, 1998; Djuricic *et al.*, 2001; Plamenac *et al.*, 1972a,b, 1974, 1979b, 1981, 1985; Walker and Fullmer, 1970). Studies of numerous authors (Beadle *et al.*, 2002; Bowels *et al.*, 2002; Geisel and Sandersleben, 1987; Giguere *et al.*, 2002; Halliwell *et al.*, 1993; Lavoie *et al.*, 2001; Mair *et al.*, 1988; Schmallenbach *et al.*, 1998; Zinkl, 2002) have shown the predominant cellular population in the lumen of airways in horses is represented by neutrophilic granulocytes and desquamated epithelial cells, macrophages, and eosinophilic granulocytes may be seen. However, in the studied material of our research, desquamated epithelial cells and eosinophilic granulocytes with a large number of neutrophilic granulocytes were the predominant cellular population in the lumens of bronchi and bronchioli. As opposed to COPD in horses, in asthma the airways lumen has the predominant cellular population of eosinophilic granulocytes that are situated peribronchially. In addition to these cells, there are also lymphocytes, macrophages, mastocytes, and neutrophilic granulocytes. Thickening, hyalinization of the basal membrane of airway epithelium common in asthmatic patients has not been recorded in horses suffering from COPD (Huang *et al.*, 1999; Tiddens *et al.*, 2000), or have been noted in the material investigated within this study.

Hyalinization of basal membrane, epithelial changes, eosinophilic infiltration of the wall, hyperplasia of the glands and muscular wall of the bronchi are absolutely pathognomonic and allow decisive pathohistological diagnosis of bronchial asthma in human even without clinical substantiation in cases of sudden death without witnesses which may happen in cases of *status asthmaticus*. Hypertrophy of the smooth muscle layer is almost regular in airways of asthmatic patients (Huang *et al.*, 1999; Jeffery, 2001; Martin, 2001; Tiddens *et al.*, 2000).

Decisive cytopathological diagnosis of asthma is not possible, but may only be fairly reliably suggested. Hypertrophy of the muscular layer of the bronchi and bronchioli noted in 25.49% of studied horses has been reported by other authors, as well (Costa *et al.*, 2001; Robinson, 2001; Schoon and Deegen, 1983; Slocombe, 2001, 2003; Winder and von Fellenberg, 1987, 1988). Peribronchiolitis and peribronchitis diagnosed in 27.45% of studied horses as a characteristic and common finding in COPD has been suggested by other authors, as well (Costa *et al.*, 2001; McPherson and Thompson, 1983; Robinson, 2001; Watson *et al.*, 1997; Winder and Fellenberg, 1987, 1988). Intensive infiltration of the lungs by eosinophils has been recorded in 34 (66.66%) studied horses and reference literature links it with parasitic infections or within systemic eosinophilia (Dixon *et al.*, 1992; La Perle *et al.*, 1998; Latimer *et al.*, 1996; Nicholls *et al.*, 1978; Rooney and Robertson, 1996; Srihakim and Swerczek, 1978). Increased numbers of eosinophilic granulocytes, particularly in lung interstitium has also been suggested by other authors (McPherson and Thompson, 1983). Alveolar emphysema recorded in 70.59% of horses from our study were more common as distensive one (overinflation in 54.9%), and less commonly as destructive emphysema in 15.69% studied horses (Marinkovic, 2005, 2007), also in concert with other reports (Gerber, 1973; McPherson and Lawson, 1974; Schoon and Deegen, 1983; Slocombe, 2003; Tyler *et al.*, 1971).

American authors define human emphysema as a condition of the lungs that is characterized by abnormal and permanent increase of airways distally from terminal bronchioli, accompanied by destruction of their walls (American Thoracic Society, 1976; Thurlbeck, 1970). Expansion of airways not accompanied with destruction of the walls is, however, called overinflation, as is distension of airways after unilateral pneumectomy, which should more pertinently be called compensatory overfill of the airways, instead of emphysema (*emphysema compensatorium*). Some British experts (Fletcher, 1959; Reid, 1967) insist there are two categories of conditions of the lungs: dilation of the airways and dilation with destruction (distensive and destructive emphysema). As a consequence of airway obstruction accumulation of air in the lungs ensues, and secondary development of distensive emphysema follows, which may eventually evolve into destructive emphysema (Geisel and Sandersleben, 1987; Lopez, 2001; McPherson and Lawson, 1974). After emphysema has been

recognized in families with α 1-antitrypsin deficiency, research has focused the possible role of tissue proteolysis as a mechanism in the occurrence of emphysema in humans (Laurel and Ericsson, 1963). In 1965, Gross and colleagues induced the occurrence of emphysema in the rat by intratracheal administration of proteolytic enzyme papain. In subsequent papers it has been shown that enzymes with elastolytic activity are particularly effective (Blackwood *et al.*, 1973; Janoff *et al.*, 1977; Snider *et al.*, 1974). In an experiment, destructive emphysema was discovered in guinea pigs exposed to venom of spider *Latrodectus tredecimguttatus* (black widow), in absence of inflammatory changes on the parenchyma of the lungs and bronchi. Emphysema most probably resulted from hypoxia and hyperinflation (Ducic and Plamenac, 1984).

3. Immunohistochemistry

Numerous authors dealing with the problem of chronic respiratory infections within either immunodeficient and allergic diseases of humans and animals, or circumstances of mixed etiological attributes, have recognized in their work the distribution of lymphocyte subsets in the local lymphatic pulmonary tissue, airway epithelium, and mediastinal lymph nodes. In a study conducted by Watson *et al.* (1997) in all COPD-positive horses, a large number of CD3+ cells were identified in the airway epithelium, but replicate sections stained with CD4 and CD8 showed a few positively stained cells in the same region. This finding supports the presence of a population of CD4- CD8- CD3+ T lymphocytes in the pulmonary interstitial compartment of the horse (Watson *et al.*, 1997). In their study, the authors used Mabs specific for equine cell surface antigens to label lymphocyte subpopulations in the tissues. Our experience suggests it is possible to monitor distribution of T and B lymphocytes even using the murine Mabs specific for human cell surface antigens (CD3, CD79), in the lungs and mediastinal nodes of horses and other types of mammals: dogs, cats, pigs, as well as poultry (Aleksic-Kovacevic and Jelesijevic, 2001; Aleksic-Kovacevic *et al.*, 1999; Kovacevic, 1991; Velhner *et al.*, 2001).

In an comparative study of normal, allergic, and nonallergic asthmatic individuals, nonallergic asthmatics had a significantly higher CD4:CD8 ratio and a significantly lower number of CD8+ T cells in their peripheral blood than did either the normal or the allergic asthmatic individuals (Walker *et al.*, 1992). The ratio CD4:CD8 with prevalence of CD8 lymphocytes was also noticed in the local bronchial lymphatic tissue and mediastinal lymph nodes of immunocompromised cats with retroviral infections (Kovacevic, 1993; Kovacevic *et al.*, 1997).

Our investigations of COPD-positive horses showed large amount of lymphocytes that express CD3- and CD79-positive reaction in subepithelial regions of bronchi and bronchioli. These two populations of lymphocytes were also present in peribronchial and peribronchiolar tissue and less in the

pulmonary interstitium, alveolar septi, and perivascular. CD79-positive lymphocytes were present mostly in the germinative center of the cortex of tracheobronchial lymph node and CD3-positive lymphocytes were present in the marginal region of follicle and paracortex of the lymph node. Positive immunohistochemical reaction was visible in the form of marginal red membrane precipitate both on CD3 and CD79 lymphocyte populations in the lungs and in the tracheobronchial lymph node (Marinkovic, 2005).

In subepithelial structures of bronchioli and bronchi, as well as in peribronchiolar and peribronchial tissues and to a lesser extent in the interstitium of the lungs, alveolar septa, and perivascularly a large number of lymphocytes with positive CD3 reaction were recorded, complying with the reports of Winder and von Fellenberg (1988). CD79-positive lymphocytes were noticed mostly in the cortical region of lymph node, germinative centers of hyperplastic follicles, whereas CD3-positive lymphocytes were noticed in the marginal follicular region and lymph node paracortex, as reported by Searcy (2001) and Valli (1985). Presence of CD3+ lymphocytes in samples with morphological and histological signs of COPD should be observed from the point of view of various interleukins important for the development of COPD in horses and asthma in humans.

4. Cytology

In imprint preparations from the tracheal bifurcation in the studied material, the predominant cellular population comprises desquamated columnar cells recorded in 98.04% of studied horses (Marinkovic, 2005, 2007), in concert with other reference reports (Beech, 1975; Hewson and Viel, 2002; Zinkl, 2002). Other authors report preserved, unaffected neutrophilic granulocytes as a predominant cellular population in COPD in horses (Beech, 1975; Couetil *et al.*, 2001; Derkzen *et al.*, 1988; Hare *et al.*, 1999; Hewson and Viel, 2002; Lavoie *et al.*, 2001; Lorch *et al.*, 2001; Robinson, 2001; Seahorn and Beadle, 1993; Zinkl, 2002). In the studied imprint preparation from the tracheal bifurcation these cells were recorded in 19.6% of the studied horses. Desquamation and lesions of the columnar epithelium with loss of cilia from these cells, ciliocytophthoria (CCP), was registered by Hewson and Viel (2002), as well (Fig. 8).

Irritating forms or abnormal columnar cells of the respiratory epithelium may be found in miscellaneous acute or chronic inflammatory processes on the lungs (i.e., bronchi). The cells lose their regular cylindrical appearance, become stout, with increased amount of cytoplasm, and occasionally hyperchromatic or picnotic nuclei. These cells illustrate a nonspecific response to irritation of any kind and the incidence of this phenomenon is most common in lung cancer patients (Koss, 1979). However, this lesion has also been described in singers, players of wind instruments, and people in advanced

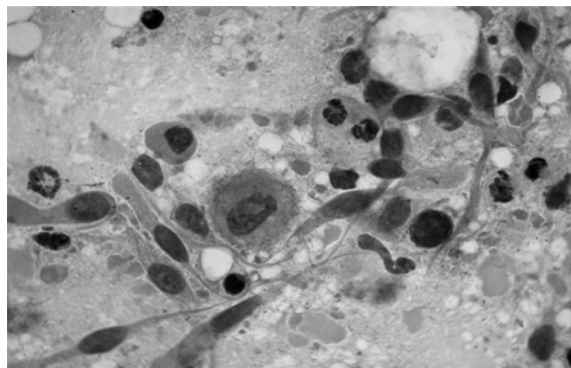


FIG. 8 Tracheal imprint: Alveolar macrophage and bronchial epithelial cells with ciliocytophthoria (HE, $\times 1000$).

age (Plamenac and Nikulin, 1969; Plamenac *et al.*, 1970). CCP is a term introduced in 1956 by Papanicolaou to signify severe lesion of columnar epithelial cell with its destruction and separation of the cytoplasm to the part that contains the nucleus and the one with remaining cilia. The process is frequently associated with eosinophilia of cytoplasm or nuclei or occurrence of small inclusions. At the beginning, viral inclusions were suggested, because the occurrence of CCP was registered in people suffering from viral pneumonia (Papanicolaou, 1956). Later, the same occurrence in pathognomonic incidence was seen in patients with lung carcinoma and other pulmonary diseases, whereby it lost its specific significance (Koss, 1979).

It was also seen in children smokers (Plamenac *et al.*, 1979), people exposed to air pollution (Plamenac *et al.*, 1979), and even in neonates with hyaline membrane disease (Doshi *et al.*, 1982). Eosinophilic granulocytes in cytological imprint preparations were recorded in a substantially larger number than in smears of healthy horses. Hewson and Viel (2002) suggest finding of these cells in cytological preparations is characteristic of COPD in horses. Conversely, Beech (1975) contests this and interprets findings of these cells in the smears by the presence of parasitic infection of the lungs. Erythrocytes recorded in 47.06% of the horses most probably result from inflammatory processes on the lungs or occurred as a result of blood aspiration when the animals were sacrificed (slaughtered). In 21.57% of studied horses alveolar macrophages were diagnosed, frequently with phagocytized bacteria, epithelial cells of phagocytized coal dust. The authors suggest that they occur in COPD horses less frequently than usual (Beech, 1975; Couetil *et al.*, 2001; Derkzen *et al.*, 1988; Hare *et al.*, 1999), although they account for the predominant cellular population in healthy animals. Findings of a larger number of mastocytes has been recorded in cases of immune hypersensitivity,

which is one of important features of COPD, in concert with reports of some other authors (Hewson and Viel, 2002), although some other authors suggest that COPD-affected horses have a reduced number of these cells (Couetil *et al.*, 2001; Derksen *et al.*, 1988; Hare *et al.*, 1999). Presence of mucus was recorded in 94.12% of studied horses (Marinkovic, 2005, 2007), less commonly as disorganized mucus, and more commonly as Curschmann's spirals composed of thick, viscous fluids producing spiral forms, networks, or bizarre shapes as described in some other published papers (Beech, 1975; Hewson and Viel, 2002; Zinkl, 2002).

The following bacteria were isolated from samples of lungs of horses with purulent pneumonia: *Streptococcus equi*, *Streptococcus pyogenes*, *Staphylococcus aureus*, as reported by some other authors (Chanter, 2002; Giguere, 2000; Harrington *et al.*, 2002; Karlstrom *et al.*, 2004; Leguillette *et al.*, 2002; Rooney and Robertson, 1996). Lungs of the studied horses yielded *Enterococcus sp.* in 11.76%, *Enterobacter sp.* in 33.33%, *Citrobacter sp.* in 5.88%, *Klebsiella sp.* in 9.8%, *Proteus mirabilis* in 37.25%, *Pseudomonas sp.* in 54.9%, and *Escherichia coli* in as many as 92.16% of studied horses. Although these bacteria have been suggested as possible causes of pneumonia (Chanter, 2002; Leguillette *et al.*, 2002) particularly in slaughtered animals or those subjected to postmortem examinations, their importance in secondary infections or contamination should not be overlooked (Ainsworth and Biller, 1998; Rooney and Robertson, 1996; Sweeney, 2002; Sweeney *et al.*, 1991). *Candida albicans* was isolated from 5.88% of the studied horses (lung samples) and it plays a role in the etiology of pneumonia in immunocompromised subjects, frequently within a systemic infection (Ainsworth and Biller, 1998; Hutchison, 1994; Reilly and Palmer, 1994). Fungi *S. rectivirgula*, *A. fumigatus*, and *T. vulgaris* have been suggested in reference literature as the most important factors in the occurrence of COPD. In the studied material here, however, these fungi have not been isolated because these fungi are not lung pathogens. Instead, they grow on feed (poor hay and grain), straw bedding (hay and straw) for horses, and participate in etiology of the disease as allergens (Derksen *et al.*, 1988; Khan *et al.*, 1985; McGorum *et al.*, 1993; Schmallenbach *et al.*, 1998).

Finally, based on results of our study and reference literature we may suggest that pathogenesis of COPD in horses and lung emphysema is somewhat different from the same disease and asthma in humans in spite of numerous similarities. Namely, in humans the main role in etiology is played by chronic bronchitis (etiology in horses is different), in which the predominant provoking factor is the smoking habit, but one may not overlook adverse environmental influences and air pollution (the same applies to horses). Also, in humans, a very important role is played by $\alpha 1$ -antitrypsin deficiency (emphysema without bronchitis), which is not the case in horses. There is no asthma in horses (at least not pathomorphologically) whereas in humans it represents an important component of COPD that in its pure form

(nonsmoker's asthma) rarely results in emphysema. The influence of smoking (cigarette smoking primarily) in the development of emphysema in humans may be compared with the influence of poor-quality hay, straw bedding, and poor ventilation of stables in horses. In horses, the disease most probably begins with recurrent bronchitis that spreads, resulting in the development of more or less diffuse bronchiolitis, after which distension follows and subsequent destruction of alveolar spaces, that is, COPD is accompanied with emphysema with all pertinent consequences.

V. Conclusions and Perspectives

Cytological analysis of mucosal imprints of the tracheal bifurcation suggests the presence of an asthmatic pattern analogous to that of humans (a large number of eosinophils, mucosal spirals, Creola bodies) but histological examinations of pulmonary parenchyma and bronchi do not correspond to human asthma, because hyalinization of the basal membrane is missing (Dunnill, 1960; Salvato, 1968; Sanerkin and Evans, 1965). Obviously, allergic component plays a very important role in the pathogenesis of COPD. The diagnosis is established according to history, clinical presentation, general clinical examination, and specialized diagnostic procedures.

The history suggests this disease occurred usually in advanced age, 4- to 8-years old (sometimes even later). The owner or caretaker of animals usually recognize chronic cough as the most important complaint, usually intensified after exposure of the animal to the allergen (dust during feeding or cleaning in classic forms of COPD, or allergens in grazing fields in the form of SPAOPD). Horses breathe with difficulty, tire easily, and after the animals are exposed to physical activities, heart and respiration frequencies return to the physiological values slowly—the resting time is prolonged.

Clinical presentation is characterized with chronic cough, dilated nostrils, mucopurulent nasal excretion, accelerated respirations—tachypnea, prolonged inspirium, abdominal breathing, “anal breathing,” abnormal respiratory sounds in the lungs (barely auscultable because of poor air flow, or wheezing), enlarged percussion area of the lungs, hypertrophy of abdominal muscles (*m. obliquus externus abdominis*)—“heave line,” and loss of body weight (even cachexia) resulting from the fact that they eat less.

The procedures used in the diagnostic of COPD include bronchoscopy, determination of blood gas levels (O₂, CO₂), cytology (BAL, TBL), radiography, intradermal allergic tests, allergic testing by nebulization of hay dust suspension (HDS), whole blood analysis, blood biochemistry, lung biopsy, etc. (Ainsworth and Biller, 1998; Hewson and Viel, 2002; McPherson *et al.*, 1978; Pirie *et al.*, 2002a,b,c; Robinson, 2001; Rose and Hodgson, 1993;

Trailovic, 2000; Wilson *et al.*, 1993). Therapy of the disease usually comprises systemic and inhalatory corticosteroids (e.g., dexamethasone, prednisolone) and bronchodilators (usually clenbuterol and albuterol, but some others as well). Bronchosecretolytic agents may also be used (dembrexin-chloride, acetyl cysteine), nebulization of physiological saline that is associated with bronchosecretolytic effect, hyperfusion, disodium chromoglycate (Chromelin), furosemide, antihistaminics etc. (Ainsworth and Biller, 1998; Robinson, 2001; Rose and Hodgson, 1993; Rush, 2001; Trailovic, 2000).

The main point in prevention of the disease and reduction of the associated clinical symptoms comprises reduction or complete elimination of exposure of the animals to the allergen that provokes the disease. This implies taking the animals out of the stables for pasture, feeding on quality hay, spraying or wetting hay used for feed, use of silage and haylage, pelleted and bracketed feed instead of hay, spraying grains with molasses to reduce the amount of dust in the feed, etc. Also, care should be taken on selecting bedding so that instead of poor-quality straw and hay, use of carton, paper, and specially treated wood shavings is recommended (Ainsworth and Biller, 1998; Robinson, 2001; Rose and Hodgson, 1993; Trailovic, 2000).

- The most common macroscopic finding in the studied horses combines emphysema and absence of lung collapse. Pathohistologically in all studied horses chronic bronchitis/bronchiolitis was evident with characteristic changes in the lumen, mucosa, fur, and smooth muscle layer.
- Alveolar emphysema was evident in 70.59% of the studied horses, more commonly as distensive emphysema (54.9%), and less commonly as destructive emphysema (15.69%).
- Increased immune reactivity in the subepithelial region of bronchioli and bronchus, in peribronchiolar and peribronchial tissues and less perivascularly, and in lung interstitium and alveolar septa suggest their importance in the development of COPD. Population of CD79+ lymphocytes was evidenced in the cortical region, in germinative centers of hyperplastic follicles, whereas the population of CD3+ lymphocytes was identified in the marginal region of the follicles and paracortex of the lymph nodes.
- The primary finding on cytological imprint preparations from the tracheal bifurcation is the thick, viscous, PAS-positive mucus that make curly Curschmann's spirals; the predominant cellular population is composed of desquamated epithelial cells of the airways with the presence of eosinophilic and neutrophilic granulocytes, mastocytes, erythrocytes, and alveolar macrophages. This suggests the presence of asthmatic pattern analogous to that found in humans.
- *Streptococcus equi*, *Streptococcus pyogenes*, and *Staphylococcus aureus* were isolated from lungs of horses that suffered from pneumonia in addition to COPD; in addition to numerous pathogenic bacterial flora potential

contaminants and causative organisms of secondary infections were also present—*Enterococcus* sp., *Enterobacter* sp., *Citrobacter* sp., *Klebsiella* sp., *Proteus mirabilis*, *Pseudomonas* sp., *E. coli*, and fungus *Candida albicans*.

- Pathohistological, cytological, immunohistochemical, and bacteriological findings are mutually correlated suggesting that chronic bronchitis/bronchiolitis is the main substrate of COPD in horses and that it has combined inflammatory and immune etiology, in which emphysema occurs secondarily, as a result of airway obstruction.

REFERENCES

Ainsworth, D. M., and Biller, D. S. (1998). Respiratory System. In "Equine Internal medicine" (S. M. Reed and W. M. Bayly, Eds.), 1st ed. W.B. Saunders, Philadelphia.

Aleksic-Kovacevic, S., and Jelesijevic, T. (2001). Morphological, histopathological and immunohistochemical study of canine malignant lymphoma. *Acta Vet.* **51**, 245–254.

Aleksic-Kovacevic, S., Gagic, M., Lazic, S., and Kovacevic, M. (1999). Immunohistochemical detection of infectious bursal disease virus antigen in bursa of fabricius of experimentally infected chickens. *Acta Vet.* **49**, 13–19.

American Thoracic Society (1976). Chronic bronchitis, asthma, and pulmonary emphysema. Statement by ehs Committee on Diagnostic Standards for Non-Tuberculous respiratory Disease. *Am. Rev. Resp. Dis.* **85**, 762–772.

Art, T., Bayly, W., and Lekeux, P. (2002). Pulmonary function in the exercising horse. In "Equine Respiratory Diseases" (P. Lekeux, Ed.). International Veterinary Information Service, Ithaca, New York.

Art, T., Duvivier, D. H., Votion, D., Anciaux, N., Vandenput, S., Bayly, W. M., and Lekeux, P. (1998). Does an acute COPD crisis modify the cardiorespiratory and ventilatory adjustment to exercise in horses? *J. Appl. Physiol.* **84**, 845–852.

Art, T., McGorum, B. C., and Lekeux, P. (2002). Environmental control of respiratory disease. In "Equine Respiratory Diseases" (P. Lekeux, Ed.). International Veterinary Information Service, Ithaca, New York.

Auerbach, O., Stout, A. P., Hammond, E. C., and Garfinkel, L. (1961). Changes in bronchial epithelium in relation to cigarette smoking and in relation to lung cancer. *N. Engl. J. Med.* **256**, 253–267.

Banks, W. J. (1993). "Applied Veterinary Histology," 3rd ed., Mosby Year Book, St. Louis.

Beadle, R. E., Horohov, D. W., and Gaunt, S. D. (2002). Interleukin-4 and interferon-gamma expression in summer pasture-associated obstructive pulmonary disease affected horses. *Equine Vet. J.* **34**, 389–394.

Beech, J. (1975). Cytology of tracheobronchial aspirates in horses. *Vet. Pathol.* **12**, 157–164.

Berkheiser, S. W. (1959). Bronchial proliferation and metaplasia associated with bronchiectasis, pulmonary infarcts and anthracosis. *Cancer* **12**, 499–508.

Berkheiser, S. W. (1963a). Bronchial proliferation and metaplasia associated with thromboembolism. A pathologic and experimental study. *Cancer* **16**, 205–211.

Berkheiser, S. W. (1963b). Epithelial proliferation of the lung associated with cortisone administration. A pathologic and experimental study. *Cancer* **16**, 1354–1364.

Berkheiser, S. W. (1969). Bronchiolar epithelial changes associated with congenital heart diseases. *Am. Rev. Res. Dis.* **100**, 735–737.

Blackwood, C. E., Hosannal, Y., Permen, E., Keller, S., and Mandl, J. (1973). Experimental emphysema in rats: Elastolytic titer of inducing enzyme as determinant of the response. *Proc. Soc. Exp. Biol. Med.* **144**, 450–459.

Bowels, K. S., Beadle, R. E., Mouch, S., Pourciau, S. S., Littlefield-Chabaud, M. A., LeBlanc, C., Mistric, L., Fermaglich, D., and Horohov, D. W. (2002). A novel model for equine recurrent airway obstruction. *Vet. Immunol. Immunopathol.* **87**, 385–389.

Bracher, V., von Fellenberg, R., Winder, C. N., Gruening, G., Hermann, M., and Kraehenmann, A. (1991). An investigation of the incidence of chronic obstructive pulmonary disease (COPD) in random populations of Swiss horses. *Equine Vet J.* **23**, 136–141.

Bureau, F., Bonizzi, G., Kirschvink, N., Delhalle, S., Desmacht, D., Merville, M.-P., Bours, V., and Lekeux, P. (2000). Correlation between nuclear factor- κ B activity in bronchial brushing samples and lung dysfunction in an animal model of asthma. *Am. J. Respir. Crit. Care Med.* **161**, 1314–1321.

Castleman, W. L., Sorkness, R. L., Lemanske, R. F., and McAllister, P. K. (1990). Viral bronchiolitis during early life induces increased numbers of bronchiolar mast cells and airway hyperresponsiveness. *Am. J. Pathol.* **137**, 821–831.

Chanter, N. (2002). Bacterial infections including mycoplasmas. In "Equine Respiratory Diseases" (P. Lekeux, Ed.). International Veterinary Information Service, Ithaca, New York.

Costa, L. R. R., Seahorn, T. L., Moore, R. M., Oliver, J. L., and Hosgood, G. L. (2001). Plasma and bronchoalveolar fluid concentrations of nitric oxide synthesis in the lungs of horses with summer pasture-associated obstructive pulmonary disease. *Am. J. Vet. Res.* **62**, 1381–1386.

Couetil, L. L., Rosenthal, F. S., DeNicola, D. B., and Chilcoat, C. D. (2001). Clinical signs, evaluation of bronchoalveolar lavage fluid, and assessment of pulmonary function in horses with inflammatory respiratory disease. *Am. J. Vet. Res.* **62**, 538–546.

Couland, E., and Kourilsky, R. (1953). Modification des epithelium et des parois bronchiques produites chez le cobaye par inhalation des vapeurs parafine. *Rev Tuberc. (Paris)* **17**, 1153–1164.

Cunningham, F. (2001). Inflammatory mediators, including leukotriens. – International Workshop on Equine Chronic Airway Disease, Michigan State University 16–18 June 2000. *Equine Vet. J.* **33**, 5–19.

DerkSEN, F. J., and Robinson, N. E. (2002). Overview of the Equine Respiratory System. In "Equine Respiratory Diseases" (P. Lekeux, Ed.). International Veterinary Information Service, Ithaca, New York.

DerkSEN, F. J., Robinson, N. E., Scott, J. S., and Stick, J. A. (1988). Aerosolized *Micropolyspora faeni* antigen as a cause of pulmonary dysfunction in ponies with recurrent airway obstruction (heaves). *Am. J. Vet. Res.* **49**, 933–938.

DerkSEN, F. J., Robinson, N. E., Slocum, R. F., and Hill, R. E. (1982). 3-Methylindole-induced pulmonary toxicosis in ponies. *Am. J. Vet. Res.* **43**, 603–607.

Dixon, P. M., McGorum, B. C., Long, K. J., and Else, R. W. (1992). Acute eosinophilic interstitial pulmonary disease in a pony. *Vet. Rec.* **130**, 367–372.

Djuricic, S., and Plamenac, P. (1998). Cytological changes of the respiratory tract in young adults related to high levels of air pollution exposure. *Cytopathology* **9**, 23–28.

Djuricic, S., Zlatkovic, M., Babic, D., Gligorijevic, D., and Plamenac, P. (2001). Sputum cytopathological findings in pig farmers. *Pathol. Res. Pract.* **197**, 145–155.

Doshi, N., Kanbour, A., Fujikura, T., and Klionsky, B. (1982). Tracheal aspiration cytology in neonates with respiratory distress: Histopathologic correlation. *Acta Cytol.* **26**, 15–21.

Ducic, V., and Plamenac, P. (1984). Experimentally induced pulmonary emphysema in guinea pigs by venom (cephalothoracic macerate) of spider *Latrodectus tredecimguttatus*. *Acta Med. Jug.* **38**, 99–109.

Dunnill, M. S. (1960). The pathology of asthma, with special reference to changes in the bronchial mucosa. *J. Clin. Path.* **13**, 27–30.

Farber, M. S., Wood, D. A., Pharr, S. L., and Person, B. (1957). Significant cytologic findings in non-malignant pulmonary disease. *Dis. Chest.* **31**, 1–13.

Farber, S. M., Rharr, S. L., Traunt, H. F., Wood, D. A., and Gorman, R. D. (1954). Metaplasia and dysceratosis of bronchial epithelial cells following inhalation of trypsin and desoxyribonuclease. *Lab. Invet.* **3**, 333–338.

Fletcher, C. M. (1959). Terminology, definitions and classification of chronic pulmonary emphysema and related conditions. *Thorax* **11**, 268–273.

Francini, M., Gill, U., von Fellenberg, R., and Bracher, V. D. (2000). Interleukin-8 concentration and neutrophil chemotactic activity in bronchoalveolar lavage fluid of horses with chronic obstructive pulmonary disease following exposure to hay. *Am. J. Vet. Res.* **61**, 1369–1374.

Geisel, O., and von Sandersleben, J. (1987). Pathomorphology of chronic obstructive lung disease in the horse. *Tierarztl. Prax. Suppl.* **2**, 52–56.

Gerber, H. (1973). Chronic pulmonary disease in the horse. *Equine Vet. J.* **5**, 26–33.

Giguere, S. (2000). Rhodococcus equi Infections. In "Equine Respiratory Diseases" (P. Lekeux, Ed.) International Veterinary Information Service, Ithaca, New York.

Giguere, S., Viel, L., Lee, E., MacKay, R. J., Hernandez, J., and Francini, M. (2002). Cytokine in pulmonary airways of horses with heaves and effect of therapy with inhaled fluticasone propionate. *Vet. Immunol. Immunopathol.* **85**, 147–158.

Gross, P., Pfitzer, E. A., Tolker, E., Babyak, M. A., and Kaschak, M. (1965). Experimental emphysema. Its production with papain in normal and silicotic rats. *Arch. Environm. Hlth.* **11**, 50.

Gruning, G., von Fellenberg, R., Maier, R., and Corboz, L. (1986). Elastase-producing microorganisms in horse lungs: Their possible role in the pathogenesis of chronic pulmonary disease in the horse. *Equine Vet. J.* **18**, 396–400.

Halliwell, R. E., McGorum, B. C., Irving, P., and Dixon, P. M. (1993). Local and systemic antibody production in horses affected with chronic obstructive pulmonary disease. *Vet. Immunol. Immunopathol.* **38**, 201–215.

Halliwell, R. E. W., Fleischman, J. B., Mackay-Smith, M., Beech, J., and Gunson, D. E. (1979). The role of Allergy in Chronic Pulmonary Disease of Horses. *J. Am. Vet. Med. Assoc.* **174**, 277–281.

Hare, J. E., Viel, L., Conlon, P. D., and Marshall, J. S. (1999). *In vitro* allergen-induced degranulation of pulmonary mast cells from horses with recurrent airway obstruction (heaves). *Am. J. Vet. Res.* **60**, 841–847.

Harrington, D. J., Sutcliffe, I. C., and Chanter, N. (2002). The molecular basis of *Streptococcus equi* infection and disease. *Microb. Infect.* **4**, 501–510.

Heath, T. J., and Perkins, N. R. (1989). Pathways between lymph vessels and sinuses in lymph nodes: A study in horses. *Anat. Rec.* **223**, 420–424.

Hewson, J., and Viel, L. (2002). Sampling, microbiology and cytology of the respiratory tract, In "Equine Respiratory Diseases" (P. Lekeux, Ed.) International Veterinary Information Service, Ithaca, New York.

Hoffman, A. (2001). Does measurement of airway reactivity assist in population definition? – International Workshop on Equine Chronic Airway Disease, Michigan State University 16–18 June 2000. *Equine Vet. J.* **33**, 5–19.

Horohov, D. W. (2004). Immunology of the equine lung. In "Equine Respiratory Diseases" (P. Lekeux, Ed.) International Veterinary Information Service, Ithaca, New York.

Hotchkiss, J. (2001). What do we know about mucus?—International Workshop on Equine Chronic Airway Disease, Michigan State University 16–18 June 2000. *Equine Vet. J.* **33**, 5–19.

Huang, J., Olivenstein, R., Taha, R., Qutayba, H., and Ludwig, M. (1999). Enhanced proteoglycan deposition in the airway wall of atopic asthmatics. *Am. J. Respir. Crit. Care Med.* **160**, 725-729.

Hutchison, J. M. (1994). Candidiasis in foals. *J. Am. Vet. Med. Assoc.* **205**, 1114-1115.

Janoff, A., Sloan, B., Weinbaum, G., Damiano, V., Sandhaus, R., Elias, J., and Kimbel, P. (1977). Experimental emphysema induced with purified human neutrophil elastase. *Am. Rev. Resp. Dis.* **115**, 461-469.

Jeffery, P. K. (2001). Remodeling in asthma and chronic obstructive lung disease. *Am. J. Respir. Crit. Care Med.* **164**, 28-38.

Kaneko, J. J. (1998). "Clinical Biochemistry of Domestic Animals." 4th ed. Academic Press, San Diego, California.

Karlstrom, A., Jacobsson, K., Flock, M., Flock, J.-I., and Guss, B. (2004). Identification of a novel collagen-like protein, SclC, in *Streptococcus equi* using signal sequence phage display. *Vet. Microbiol.* **104**, 179-188.

Kaup, F. J., Drommer, W., and Deegen, E. (1990a). Ultrastructural findings in horses with chronic obstructive pulmonary disease (COPD) I: Alterations of the larger conducting airways. *Equine Vet. J.* **22**, 343-348.

Kaup, F. J., Drommer, W., and Deegen, E. (1990b). Ultrastructural findings in horses with chronic obstructive pulmonary disease (COPD) II: Pathomorphological changes of the terminal airways and the alveolar region. *Equine Vet. J.* **22**, 349-355.

Khan, Z. U., Misra, V. C., and Randhawa, H. S. (1985). Precipitating antibodies against *Micropolyspora faeni* in equines in north-western India. *Antonie Van Leeuwenhoek* **51**, 313-319.

Kirschvink, N., Bureau, F., Art, T., and Lekeux, P. (2001). Bronchoconstrictive properties of inhaled 8-epi-PGF_{2 α} in healthy and heaves-susceptible horses. *Vet. Rec.* **32**, 397-407.

Knudtson, K. P. (1960). The pathogenic effects of smoking tobacco on the trachea and bronchial mucosa. *Am. J. Clin. Path.* **33**, 310-317.

Koss, L. G. (1979). "Diagnostic Cytology and its Histopathologic Bases." 3rd ed. J.B. Lippincott, Philadelphia-Toronto.

Kovacevic, S. (1991). Imunocitohemjska ispitivanja lokalnog imunoloskog sistema pluca miseva pri eksperimentalno aktivisanoj latentnoj *Pneumocystis carinii* infekciji Magistar thesis, Univerzitet u Beogradu, Fakultet veterinarske medicine.

Kovacevic, S. (1993). Ispitivanja lokalnog imunoloskog sistema pluca macaka sa spontanim retrovirusnim infekcijama Dissertation, Univerzitet u Beogradu, Fakultet veterinarske medicine.

Kovacevic, S., Kipar, A., Kremendahl, J., TeebkenSchuler, D., Grant, C. K., and Reinacher, M. (1997). Immunohistochemical diagnosis of feline leukemia virus infection in formalin-fixed tissue. *Eur. J. Vet. Pathol.* **3**, 12-21.

La Perle, K. M. D., Piercy, R. J., Long, J. F., and Blomme, E. A. G. (1998). Multisystemic, Eosinophilic, Epitheliotropic Disease with Intestinal Lymphosarcoma in a Horse. *Vet. Pathol.* **35**, 144-146.

Lamb, D., and Reid, L. (1968). Mitotic rates, goblet cell increase and histochemical changes in mucus in rat bronchial epithelium during exposure to sulphur dioxide. *J. Path. Bact.* **96**, 97-111.

Latimer, K. S., Bounous, D. I., Colatos, C., Carmichael, K. P., and Howert, E. W. (1996). Extreme eosinophilia with disseminated eosinophilic granulomatous disease in a horse. *Vet. Clin. Pathol.* **25**, 23-26.

Laurel, C. B., and Ericsson, S. (1963). The electrophoretic α 1-globulin pattern of serum in α 1-antitrypsin deficiency. *Scand. J. Clin. Invest.* **15**, 132-137.

Lavoie, J. P. (2001). Antibody and cytokine profiles.—International Workshop on Equine Chronic Airway Disease, Michigan State University 16-18 June 2000. *Equine Vet. J.* **33**, 5-19.

Lavoie, J.-P., Leguillette, R., Pasloske, K., Charette, L., Sawyer, N., Guay, D., Murphy, T., and Hickey, G. J. (2002). Comparison of effects of dexamethasone and the leukotriene D4 receptor antagonist L-708,738 on lung function and airway cytologic findings in horses with recurrent airway obstruction. *Am. J. Vet. Res.* **63**, 579–585.

Lavoie, J.-P., Maghni, K., Desnoyers, M., Taha, R., Mertin, J. G., and Hamid, Q. A. (2001). Neutrophilic airway inflammation in horses with heaves is characterized by a Th2-type cytokine profile. *Am. J. Crit. Care Med.* **164**, 1410–1413.

Leguillette, R., Roy, M. F., and Lavoie, J.-P. (2002). Foal pneumonia. In "Equine Respiratory Diseases" (P. Lekeux, Ed.). International Veterinary Information Service, Ithaca, New York.

Lopez, A. (2001). Respiratory system, thoracic cavity, and pleura. In "Thomson's Special Veterinary Pathology" (M. D. McGavin, W. W. Carlton, and J. F. Zachary, Eds.), 3rd ed. Mosby, St. Louis.

Lorch, G., Hillier, A., Kwochka, K. W., Saville, W. J., Kohn, C. W., and Jose-Cunilleras, E. (2001). Results of intradermal tests in horses without atopy and horses with chronic obstructive pulmonary disease. *Am. J. Vet. Res.* **62**, 389–397.

Mair, T. S., Batten, E. H., Stokes, C. R., and Bourne, F. J. (1987). The histological features of the immune system of the equine respiratory tract. *J. Comp. Path.* **97**, 575–586.

Mair, T. S., Stokes, C. R., and Bourne, F. J. (1988). Increased local IgA production in chronic obstructive pulmonary disease. *Equine Vet. J.* **20**, 214–216.

Marinkovic, D. (2005). Morfoloska ispitivanja hronicnog opstruktivnog oboljenja pluca konja. Magistar thesis, Univerzitet u Beogradu, Fakultet veterinarske medicine.

Marinkovic, D., Aleksic-Kovacevic, S., and Plamenac, P. (2007). Morphological findings in lungs of horses with chronic obstructive pulmonary disease. *Acta Vet.* **57** (in press).

Marti, E., and Ohnesorge, B. (2002). Genetic basis of respiratory disorders. In "Equine Respiratory Diseases" (P. Lekeux, Ed.). International Veterinary Information Service, Ithaca, New York.

Martin, J. (2001). Human asthma and chronic obstructive pulmonary disease (COPD) – International Workshop on Equine Chronic Airway Disease, Michigan State University 16–18 June 2000. *Equine Vet. J.* **33**, 5–19.

McGorum, B. (2001). Environmental factors as aetiological agents – International Workshop on Equine Chronic Airway Disease, Michigan State University 16–18 June 2000. *Equine Vet. J.* **33**, 5–19.

McGorum, B. C., Dixon, P. M., and Halliwell, R. E. (1993). Responses of horses affected with chronic obstructive pulmonary disease to inhalation challenges with mould antigens. *Equine Vet. J.* **25**, 261–267.

McPherson, E. A., and Lawson, G. H. K. (1974). Some aspects of chronic pulmonary diseases of horses and methods used in their investigation. *Equine Vet. J.* **6**, 1–6.

McPherson, E. A., and Thompson, J. R. (1983). Chronic obstructive pulmonary disease in the horse I. Nature of disease. *Equine Vet. J.* **15**, 203–206.

McPherson, E. A., Lawson, G. H. K., Murphy, J. R., Nicholson, J. M., Fraser, J. A., Breeze, R. G., and Pirie, H. M. (1978). Chronic obstructive pulmonary disease (COPD): Identification of affected horses. *Equine Vet. J.* **10**, 47–53.

Melamed, M. R., Zaman, M. B., Flehinger, B. J., and Martini, N. (1977). Radiologically occult in situ and incipient invasive epidermoid lung cancer: Detection by sputum cytology in a survey of asymptomatic cigarette smokers. *Am. J. Surg. Path.* **1**, 5–16.

Moore, J. E., Matsuda, M., Yamamoto, S., and Buckley, T. (2004). Hypersensitivity pneumonitis in the horse: An undiagnosed condition?. *J. Equine Vet. Sci.* **24**, 510–511.

Nasiell, M. (1967). Abnormal columnar cell findings in bronchial epithelium. A cytologic study of lung cancer and non-cancer cases. *Acta Cytol.* **11**, 387–403.

Naylor, B. (1962). The shedding of the mucosa of the bronchial tree in asthma. *Thorax* **17**, 69–72.

Naylor, B., and Railey, C. (1964). A pitfall in the cytodiagnosis of sputum of asthmatics. *J. Clin. Pathol.* **17**, 84–89.

Nicholls, J. M., Clayton, H. M., Pirie, H. M., and Duncan, J. L. (1978). A pathological study of the lungs of foals infected experimentally with *Parascaris equorum*. *J. Comp. Path.* **88**, 261–274.

Papanicolaou, G. N. (1956). Degenerative changes in ciliated cells exfoliating from bronchial epithelium as cytologic criterion in diagnosis of disease of lung. *N.Y. State J. Med.* **56**, 2647–2650.

Pirie, R. S., Collic, D. D., and McGorum, B. C. (2002a). Evaluation of nebulized hay dust suspensions (HDS) for the diagnosis and investigation of heaves. 2: Effects of inhaled HDS on control and heaves horses. *Equine Vet. J.* **34**, 337–342.

Pirie, R. S., Dixon, P. M., and McGorum, B. C. (2002b). Evaluation of nebulized hay dust suspensions (HDS) for the diagnosis and investigation of heaves. 3: Effect of fraction of HDS. *Equine Vet. J.* **34**, 343–347.

Pirie, R. S., Dixon, P. M., Collie, D. D., and McGorum, B. C. (2001). Pulmonary and systemic effects of inhaled endotoxin in control and heaves horses. *Equine Vet. J.* **33**, 311–318.

Pirie, R. S., McLachlan, G., and McGorum, B. C. (2002c). Evaluation of nebulized hay dust suspensions (HDS) for the diagnosis and investigation of heaves. 1: Preparation and composition of HDS. *Equine Vet. J.* **34**, 332–336.

Plamenac, P., and Nikulin, A. (1969). Atypia of the bronchial epithelium in wind instrument players and singers. *Acta Cytol.* **13**, 274–278.

Plamenac, P., Nikulin, A., and Kahvic, M. (1970). Cytology of the respiratory tract in advanced age. *Acta Cytol.* **14**, 526–530.

Plamenac, P., Nikulin, A., and Pikula, B. (1972b). Cytology of the respiratory tract in former smokers. *Acta Cytol.* **16**, 256–300.

Plamenac, P., Nikulin, A., and Pikula, B. (1973). Cytological changes of the respiratory tract in young adults as a consequence of high levels of air pollution exposure. *Acta Cytol.* **17**, 241–244.

Plamenac, P., Nikulin, A., and Pikula, B. (1974). Cytologic changes of the respiratory epithelium in iron foundry workers. *Acta Cytol.* **18**, 34–40.

Plamenac, P., Nikulin, A., Pikula, B., and Markovic, Z. (1972a). Cytology of the respiratory tract in asbestos miners. *Acta Med. Jug.* **32**, 297–309.

Plamenac, P., Nikulin, A., Pikula, B., and Markovic, Z. (1979a). Cytologic changes in the respiratory tract in children smokers. *Acta Cytol.* **23**, 389–391.

Plamenac, P., Nikulin, A., Pikula, B., and Vujanic, G. (1979b). Cytologic changes of the respiratory tract as a consequence of air pollution and smoking. *Acta Cytol.* **23**, 449–453.

Plamenac, P., Nikulin, A., Pikula, B., Gmaz-Nikulin, E., and Kafedjic, A. (1980). The influence of air pollution and smoking on cytologic changes of the respiratory epithelium of professional truck drivers. *Folia Med. Univ. Sar.* **15**, 49–61.

Plamenac, P., Nikulin, A., Pikula, B., Gmaz-Nikulin, E., and Zeljo, A. (1981). Cytological changes of the respiratory tract in children as consequence of high levels of air pollution exposure. *Folia Med. Univ. Sar.* **16**, 41–50.

Plamenac, P., Santic, Z., Nikulin, A., and Serdearevic, H. (1985). Cytologic changes of the respiratory tracs in vineyard spraying workers. *Eur. J. Respir. Dis.* **67**, 50–55.

Raulo, S. M., Sorsa, T., Tervahartiala, T., Pirila, E., and Maisi, P. (2001). MMP-9 as a marker of inflammation in the tracheal epithelial lining fluid (TELF) and in bronchoalveolar fluid (BALF) of COPD horses. *Equine Vet. J.* **33**, 128–136.

Reid, L. (1967). "The pathology of emphysema." Lloyd-Luke Medical Books Ltd., London.

Reilly, L. K., and Palmer, J. E. (1994). Systemic candidiasis in four foals. *J. Am. Vet. Med. Assoc.* **205**, 464–466.

Robinson, N. E. (2001). Recurrent Airway Obstruction (Heaves). In "Equine Respiratory Diseases" (P. Lekeux, Ed.). International Veterinary Information Service, Ithaca, New York.

Rodriguez, A., Pena, L., Flores, J. M., Gonzalez, M., and Castano, M. (1992). Immunocytochemical study of diffuse neuroendocrine system cells in equine lungs. *Anat. Histol. Embryol.* **21**, 136–145.

Rooney, J. R. (1970). "Autopsy of the Horse." Williams & Wilkins, Baltimore.

Rooney, J. R., and Robertson, J. L. (1996). "Equine Pathology." 1st ed. Iowa State University Press, Ames, Iowa.

Rose, R. J., and Hodgson, D. R. (1993). "Manual of Equine Practice—Respiratory System." W.B. Saunders, Philadelphia.

Rush, B. (2001). Corticosteroid therapy.—International Workshop on Equine Chronic Airway Disease, Michigan State University 16–18 June 2000. *Equine Vet. J.* **33**, 5–19.

Saccomano, G., Saunders, R. P., Archer, V. E., Auerbach, O., Kuschner, M., and Beckler, P. A. (1963). Cytology of the lung: The cytology of sputum prior to the development of carcinoma. *Acta Cytol.* **9**, 413–423.

Saccomano, G., Saunders, R. P., Klein, M. G., Archer, V. E., and Brennan, L. (1970). Cytology of the lung in reference to irritant, individual sensitivity and healing. *Acta Cytol.* **14**, 377–381.

Salvato, G. (1968). Some histological change in chronic bronchitis and asthma. *Thorax* **23**, 168–173.

Sanderud, K. (1956). Squamous epithelial metaplasia in the respiratory tract in uremics. *Brit. J. Cancer* **10**, 226–231.

Sanderud, K. (1958). Squamous metaplasia of the respiratory tract epithelium. An autopsy study of 214 cases. Incidence, age and sex distribution. *Acta Pathol. Scand.* **42**, 247–264.

Sanerkin, N. G., and Evans, D. N. D. (1965). The sputum in bronchial asthma: Pathognomonic patterns. *J. Path. Bacteriol.* **89**, 535–541.

Schmalenbach, K. H., Rahman, I., Sasse, H. H. L., Dixon, P. M., Halliwell, R. E. W., McGorum, B. C., Crameri, R., and Miller, H. R. P. (1998). Studies on pulmonary and systemic *Aspergillus fumigatus*-specific IgE and IgG antibodies in horses affected with chronic obstructive pulmonary disease (COPD). *Vet. Immunol. Immunopathol.* **66**, 245–256.

Schoon, H. -A., and Deegen, E. (1983). Histopathologie der chronisch obstruktiven Bronchitis bei klinisch manifest erkrankten Pferden. *Tierarztl. Prax.* **11**, 213–221.

Schultze, A. E., Sonea, I., and Bell, T. G. (1988). Primary malignant pulmonary neoplasia in two horses. *J. Am. Vet. Med. Assoc.* **193**, 477–480.

Seahorn, T. L., and Beadle, R. E. (1993). Summer pasture-associated obstructive pulmonary disease in horses: 21 cases (1983–1991). *J. Am. Vet. Med. Assoc.* **202**, 779–782.

Searcy, G. P. (2001). The hemopoietic system. In "Thomson's Special Veterinary Pathology" (M. D. McGavin, W. W. Carlton, and J. F. Zachary, Eds.), 3rd ed. Mosby, St. Louis.

Slocombe, R. (2001). Pathology of the airways.—International Workshop on Equine Chronic Airway Disease, Michigan State University 16–18 June 2000. *Equine Vet. J.* **33**, 5–19.

Slocombe, R. F. (2003). Diagnosis of equine respiratory disease: Postmortem methods and lesion interpretation. In "Equine Respiratory Diseases" (P. Lekeux, Ed.). International Veterinary Information Service, Ithaca, New York.

Snider, G. L., Hayes, J. A., Franzblau, C., Kagan, H. M., Stone, P. S., and Karthy, A. L. (1974). Relationship between elastolytic activity and experimental emphysema inducing properties of papain preparations. *Am. Rev. Resp. Dis.* **110**, 254–261.

Srihakim, S., and Swerczek, T. W. (1978). Pathologic changes and pathogenesis of *Parascaris equorum* infection in parasite-free pony foals. *Am. J. Vet. Res.* **39**, 1155–1160.

Sweeney, C. R. (2002). Equine restrictive lung disease. Part 3: interstitial diseases. In "Equine Respiratory Diseases" (P. Lekeux, Ed.). International Veterinary Information Service, Ithaca, New York.

Sweeney, C. R., Holcombe, S. J., Barningham, S. C., and Beech, J. (1991). Aerobic and anaerobic bacterial isolates from horses with pneumonia or pleuropneumonia and antimicrobial susceptibility patterns of the aerobes. *J. Am. Vet. Med. Assoc.* **198**, 839–842.

Thurlbeck, W. M. (1970). Present concepts of the pathology and pathogenesis of pulmonary emphysema. *Pathol. Microbiol. (Basel)* **35**, 130–133.

Thurlbeck, W. M., Dunnill, M. S., Hartung, W., Heard, B. E., Heppleston, A. G., and Ryder, R. C. (1970). A comparison of three methods of measuring emphysema. *Hum. Pathol.* **1(2)**, 215–216.

Tiddens, H., Silverman, M., and Bush, A. (2000). The role of inflammation in airway disease. *Am. J. Respir. Crit. Care Med.* **162**, 7–10.

Trailovic, D. R. (2000). Hronico opstruktivno oboljenje pluca konja. In “Respiratorne bolesti konja” (D. R. Trailovic, Ed.). Fakultet veterinarske medicine, Univerzitet u Beogradu.

Tyler, W. S., Gillespie, J. R., and Nowell, J. A. (1971). Modern functional morphology of the equine lung. *Equine Vet. J.* **3**, 84–94.

Valli, V. E. O. (1985). The haetopoietic system. In “Pathology of Domestic Animals” (K. V. F. Jubb, P. C. Kennedy, and N. Palmer, Eds.), 3rd ed., Vol. 3. Academic Press, Orlando.

Van Rensburg, I. B. J., Stadler, P., and Soley, J. (1989). Bronchioloalveolar adenocarcinoma in a horse. *J. S. Afr. Vet. Assoc.* **60**, 212–214.

Velhner, M., Lazic, S., Petrovic, T., and Aleksic-Kovacevic, S. (2001). Protection of the chickens with maternally derived antibodies after challenge with very virulent IBDV. *Acta Vet.* **51**, 219–227.

Venugopal, C. S., Moore, R. M., Holmes, E. P., Koch, C. E., Seahorn, T. L., and Beadle, R. E. (2001). Comparative responses of bronchial rings to mediators of airway hyperreactivity in healthy horses and those affected with summer pasture-associated obstructive pulmonary disease. *Am. J. Vet. Res.* **62**, 259–263.

Walker, C., Bode, E., Boer, L., Hansel, T. T., Blaser, K., and Virchow, J. C., Jr. (1992). Allergic and nonallergic asthmatics have distinct patterns of T-cell activation and cytokine production in peripheral blood and bronchoalveolar lavage. *Am. Rev. Respir. Dis.* **146**, 109–115.

Walker, K. R., and Fullmer, C. D. (1970). Progress report on study of respiratory spirals. *Acta Cytol.* **14**, 396–398.

Wang, Z. W., Robinson, N. E., and Derkisen, F. J. (1995). Acetylcholine release from airway cholinergic nerves in horses with heaves, an airway obstructive disease. *Am. J. Respir. Crit. Care Med.* **151**, 830–835.

Watson, J. L., Stott, J. L., Blanchard, M. T., Lavoie, J. -P., Wilson, W. D., Gershwin, L. J., and Wilson, D. W. (1997). Phenotypic characterization of lymphocyte subpopulations in horses affected with chronic obstructive pulmonary disease and in normal controls. *Vet. Pathol.* **34**, 108–116.

Weller, T. W. (1953). Metaplasia of bronchial epithelium, postmortem study. *Am. J. Path.* **23**, 768–774.

Wilson, D., Watson, J., Lapointe, J., and Lavoie, J. (1993). Transthoracic biopsy and bronchoalveolar lavage for diagnostics of equine COPD. *Vet. Pathol.* **30**, 441.

Winder, C., Gruning, G., Hermann, M., and von Fellenberg, R. (1990). Fibrin/fibrinogen in lungs and respiratory secretions of horses with chronic pulmonary disease. *Am. J. Vet. Res.* **51**, 945–949.

Winder, N. C., and von Fellenberg, R. (1987). Chronic small airway disease in horses slaughtered in Switzerland. *Schweiz. Arch. Tierheilkd.* **129**, 585–593.

Winder, N. C., and von Fellenberg, R. (1988). Chronic airway disease in the horse: Immunohistochemical evaluation of lungs with mild, moderate and severe lesions. *Vet. Rec.* **122**, 181–183.

Young, B., and Heath, J. W. (2000). “Wheater’s Functional Histology—a text and colour atlas,” 4th ed. Churchill Livingstone, London.

Zinkl, J. G. (2002). Lower respiratory tract. In “Diagnostic Cytology and Hematology of the Horse” (R. L. Cowel and R. D. Tyler, Eds.), 2nd ed. Mosby, St Louis.

This page intentionally left blank

INDEX

A

Actin, 150, 157
Action potential (AP), 43–75. *See also* Calcium channels; Chloride channels; Compartment manipulation; Patch clamps
in charophytes, 49–74
agonists during, 65–66
antagonists during, 65–66
 Ca^{2+} channels and, 54–55, 57–60
capacitance during, 68
 Cl^- channels and, 57–61
compartment manipulation for, 50–52
cytoplasmic streaming in, 54–55
inhibitors during, 65–66
ion concentrations during, 63–64, 69–70
 K^+ channels and, 56, 61–62
patch clamp technique for, 52
pH levels during, 64–65
proton pumps and, 62–63
signal propagation in, 67
signal transmission for, 49
stimulus for, 53–54
tonoplasts in, 55–57, 68–69
voltage-clamp technique for, 49–50
early models of, 68–71
two-state hypothesis, 68
features of, 43–44, 46–47
HH model of, 44, 46–47, 70–71
PD in, 43
plant *v.* animal, 44, 45, 46–47, 49
simulated, 46
temperature effects on, 47, 66–67
turgor regulation and, 73–74
in wound signaling, 73

Advanced glycated end products (AGEs), 159
Angiopoietin, 146
Anode break excitation, 53
Antigen presenting cells (APC), 218
AP. *See* Action potential
APC. *See* Antigen presenting cells
Apoptosis
inflammation and, 144–145
myofibroblasts and, 168
Arabidopsis thaliana (*A. thaliana*), 85
synapsis proteins in, 103–104
Articular chondrocytes, 17–18
growth plate *v.*, 17
Atherosclerosis, 11

B

Biliary atresia, 11
Bone growth 1–31. *See also* Cartilage development; CCN protein family
CCN2 proteins in, 12–30
angiogenic potential of, 16
BMP and, 19
bone damage and, 28
CAESAR and, 25, 26–27
cell surface protectors and, 20–21
chondrocytes and, 17–18
endocytotic incorporation of, 22–23
expression of, 14–15, 23–24
HSPG and, 18
integrins and, 20, 22
mesenchymal cells and, 12
osteoblasts and, 16–17
phenotypes of, 19–20
posttranscriptional regulation of, 26–27

Bone growth (*continued*)

- as proximal promoter, 24–26
- skeletal development and, 12–14
- structural/functional conservation of, 14
- CCN5 protein and, 7
- CCN6 protein and, 8
- CTGF and, 2
- “dry sockets” and, 30
- vascular endothelial cells and, 15–17
- Bone morphogenetic protein (BMP), 19
- Breast cancer, 11, 151
- CCN2 proteins and, 23

C Ca^{2+} . *See Calcium (Ca^{2+}) channels*

Caenorhabditis elegans (*C. elegans*), 101–103

- structure of, 102
- terminal domains in, 102

CAESAR. *See Cis-acting element of structure-anchored repression (CAESAR)*Calcium (Ca^{2+}) pumps, 72–74

Calcium (Ca^{2+}) channels, 54–55

- during AP, 57–60
- calmodulin as binding agent for, 65
- extracellular, 61
- internal stores for, 70–73
- mobility of, 74
- pumps, 72–74
- simulated concentrations for, 75

Calmodulin, Ca^{2+} channels and, 65

Cancers. *See also* Breast cancer; Carcinomas; Chondrosarcoma; Colorectal cancer; Melanomas; Pancreatic cancer; Skin cancer; Tumors

stromal myofibroblasts in, 152–154

Carboxyl terminal cysteine knot (CT), 3, 4

Carcinomas

CCN4 and, 6

Cardiac fibrosis, 11, 151

Cartilage development

CCN2 and, 28–30

CCN6 and, 8

regeneration of, 29

CCN protein family, 2–31

CCN1, 4–5

integrin-associated cell adhesion

mediation by, 4

tumor phenotypes and, 5

CCN2, 5, 8–31

- bone cell biology and, 12–30
- cartilage regeneration and, 28–30
- development of, 9

ECM component production and, 10

echogenic, 5

endochondral ossification and, 9, 13

endogenous production of, 28

exogenous production of, 28

fibrotic disorders and, 10–11

HSPG and, 18

in kidneys, 9

LRP-1 and, 21

MAPK and, 21–22

tissue distribution of, 8–10

in tumors, 11–12

vascular endothelial cells and, 8–9

wound healing and, 10

CCN4, 6–7

carcinomas and, 6

osteoblastic differentiation regulation from, 6

CCN5, 7

adhesion from, 7

bone growth and, 7

cell proliferation from, 7

osteoblastic differentiation from, 7

CCN6, 3, 7–8

bone growth from, 8

cartilage development from, 8

overexpression of, 8

Cefl0, 4–5

CT and, 3, 4

CTGF, 5

Cyr61, 2, 4–5

IGFBP and, 3, 4

NOV, 2, 5–6

angiogenic properties of, 6

MAV and, 5

nuclear localization of, 6

Nov, 5–6

structure of, 2–4

terminology for, 2–4

TSP1 and, 3, 4

VWC and, 3, 4

WISP-1, 6–7

WISP-2, 7

WISP-3, 7–8

CCN2 proteins, 5, 8–31

bone growth and, 12–30

angiogenic potential in, 16

BMP and, 19
CAESAR and, 25, 26–27
cell surface protectors and, 20–21
damage during, 28
endocytotic incorporation in, 22–23
expression in, 23–24
integrins and, 20
mesenchymal cells and, 12, 19
phenotypes for, 19–20
posttranscriptional regulation in, 26–27
proximal promoter in, 24–26
breast cancer and, role in, 23
cartilage regeneration and, 28–30
chondrocytes and, 9, 15–16
development of, 9
ECM component production and, 10
endochondral ossification and, 9, 13, 23–24
endogenous production of, 28
ERK and, 21
exogenous production of, 28
fibrotic disorders and, 10–11
in kidneys, 9
LRP-1 and, 21
MAPK and, 21–22
tissue distribution of, 8–10
TRENDIC and, 24, 25
in tumors, 11–12
vascular endothelial cells and, 8–9
wound healing and, 10

CCN3 protein. *See* Nephroblastoma-overexpressed gene

CCP. *See* Ciliocytophthoria

Charge distributions
along synapsis proteins, 99–101
models of, 101

CHARGE program, 99

Charophytes. *See also* Action potential; Compartment manipulation; Patch clamps

AP in, 49–74
 Ca^{2+} channels and, 54–55, 57–60
capacitance during, 68
 Cl^- channels and, 57–61
compartment manipulation
during, 50–52
cytoplasmic streaming in, 54–55
ion concentrations during, 63–64, 69–70
 K^+ channels and, 56, 61–62
patch clamp technique for, 52
pH levels during, 64–65
proton pumps and, 62–63

signal propagation in, 67
signal transmission in, 49
temperature effects on, 66–67
tonoplasts in, 55–57, 68–69
voltage-clamp technique for, 49–50

Chemotherapy, for tumor hypoxia, 182, 199–201

Chloride (Cl^-) channels, 57–61
ethacrynic acid and, 66
patch-clamp technique and, 61
turgor regulation and, 73

Chondrocytes, 2
articular, 17–18
in bone growth, 15–18
CCN2 proteins and, 9
growth plate, 17
hypertrophy, 19
tissue development and, 10
TRENDIC and, 24, 25

Chondrosarcoma, 11

Chromosomes
compact, 87
during meiosis, in plants, 86

Chronic bronchiolitis, 228, 229

Chronic obstructive pulmonary disease (COPD), in horses, 214–238
bacteria in, 237, 239
CCP and, 236
chronic bronchiolitis and, 228, 229
diagnostic procedures for, 238–239
EpDRF and, 226
etiology of, 223–224
hyperplasia of goblet cells in, 230–232
morphological features of, 227–238
cytology of, 235–238
immunohistochemistry for, 234–235
macroscopic findings for, 227–228
pathohistology for, 228–234

PAM and, 225

pathogenesis of, 215, 224–227
symptoms of, 214
therapies for, 239

Ciliocytophthoria (CCP), 236,
Cis-acting element of structure-anchored
repression (CAESAR), 25, 26–27
location of, 27

Cl^- . *See* Chloride channels

Cohesins, 115–122. *See also* Rad51 proteins;
RecA proteins
conversation of, 118
homologs of, 117

Collagen
fibroblasts and, 164–165
fibronectin and, 165

Colorectal cancer, 11, 151

Compartment manipulation
(during AP), 50–52
cytoplasm-enriched fragments during, 52
plasma-membrane permeabilization, 52
tonoplast removal, 51–52
vacuolar perfusion, 50–51

Connective tissue growth factor (CTGF), 5.
See also CCN protein family
bone growth and, 2

Connexins, 124–126
molecular configurations for, 125
TMDs in, 124–125

Contraction, 165–166

COPD. *See* Chronic obstructive pulmonary disease

CT. *See* Carboxyl terminal cysteine knot

CTGF. *See* Connective tissue growth factor

Cyr61 protein. *See* Cysteine-rich protein 61

Cysteine-rich protein 61 (Cyr61), 2, 4–5. *See also* CCN protein family

Cytoplasm-enriched fragments, 52

Cytoplasmic streaming, during AP, 54–55

D

Deoxyribonucleic acid (DNA)
RecA protein interaction with, 111
during recombination, 110

Dmc1 proteins, 112–113
expression of, 112

DNA. *See* Deoxyribonucleic acid

Drosophila melanogaster
(*D. melanogaster*), 85, 90
recombinant constructs within, 99
synapsis proteins in, 98–99
synaptonemal complex for, 95

“Dry sockets,” 30

E

ECF. *See* Eosinophil chemotactic factor

ECM. *See* Extracellular matrix

“Ecogenin.” *See* CCN2 proteins

EGF. *See* Epidermal growth factor

Electron microscopy (EM), 87

EMT. *See* Epithelial-mesenchymal transition

Endochondral ossification, 1–2, 19, 30.
See also Bone growth
CCN2 protein and, 9, 13, 23–24

Endoplasmic reticulum (ER), 149

Eosinophil chemotactic factor (ECF), 223

EpDRF. *See* Epithelium-derived relaxing factor

Epidermal growth factor (EGF), 145
HIF and, 187

Epithelial-mesenchymal transition (EMT), 156
alveolar, 156
renal, 156

Epithelium-derived relaxing factor (EpDRF), 226

ER. *See* Endoplasmic reticulum

ERK. *See* Extracellular signal-regulated kinase

Ethacrynic acid, 66

Eukaryotes
RecA proteins and, 111–112
in tumor hypoxia gene therapies, 192–194

Extracellular matrix (ECM), 10, 144
degradation of, 168
as fibrogenic mediator, 159–160
AGEs and, 159
fibronectin and, 159
metalloproteinases in, 168–169

Extracellular signal-regulated kinase (ERK), 21

F

FAK. *See* Focal adhesion kinase

FDC. *See* Follicular dendritic cells

Fibroblast growth factor (FGF), 146

Fibroblasts, 143–144, 148–149, 154–170.
See also Myofibroblasts
antisera for, 150
collagen and, 164–165
downregulating therapies for, 169–170
ECM molecules and, 144
ER as part of, 149
FGF and, 146
origins of, 154–156
circulatory, 154, 156
EMT, 156
resident, 154
responses, 162–166

contraction, 165–166
differentiation, 162–163
matrix synthesis, 164–165
migration, 163–164
mitogenesis, 164
thrombin in, 163
signal transduction in, 160–161, 160–162
nonreceptors and, 162
receptor binding as part of, 161
second messenger pathways in, 162
statins and, 169
ultrastructures for, 149

Fibrogenesis
mediators for, 157–160
ECM, 159–160
inhibitors of, natural, 160
integrins as, 161
mechanical tension and, 160
probiotic cytokines, 157–159
regulation of, 166–170
remodeling as, 168–169
resolution as, 166–168

Fibronectin, 159
collagen and, 165

Fibrotic disorders
atherosclerosis, 11
biliary atresia, 11
cardiac, 11, 151
CCN2 protein and, 10–11
hepatic, 151, 157
inflammatory bowel disease, 11
myofibroblasts in, 151–152
pancreatic, 11
pulmonary, 11, 151
renal, 11

Focal adhesion kinase (FAK), 20

Follicular dendritic cells (FDC), 218

G

GDEPT. *See* Suicide gene therapies

Gene therapies
suicide, 188–189
for tumor hypoxia, 184–201, 196
with chemotherapy, 182, 199–201
eukaryotic delivery vehicles in, 192–194
HREs, 188–189
nonviral agents in, 193
prokaryotic delivery vehicles in, 194–195
with radiotherapy, 182, 196–199, 200

signaling modification in, 185–188
survivin in, 188
viruses as part of, 189–190

Gene-directed enzyme/prodrug therapy (GDEPT). *See* Suicide gene therapies

GM-CSF. *See* Granulocyte macrophage-colony stimulating factor

Granulocyte macrophage-colony stimulating factor (GM-CSF), 158

Growth plate chondrocytes, articular v., 17

H

Heparan sulfate proteoglycans (HSPG), 18

Hepatic fibrosis, 151, 157

Herpes simplex virus (HSV), 191

HIF. *See* Hypoxia-inducible factor

Hodgkin-Huxley (HH) model, 44, 45, 46–47, 70–71
adaptations of, 70–71
AP in, 44, 46–47
axon excitation in, 44, 46

Horses
COPD in, 214–238
bacteria in, 237, 239
CCP and, 236
diagnostic procedures for, 238–239
EpDRF and, 226
etiology of, 223–224
factors for, 214
hyperplasia of goblet cells in, 230–232
morphological features of, 227–238
pathogenesis of, 215, 224–227
therapies for, 239
toxins as factor in, 224

lungs, 216–218
cytological features of, 221–223
immune system for, 218
structure of, 216–217

lymph nodes in, 218
APC in, 218
FDC in, 218
structure of, 218–219

respiratory physiology for, 219–221
SPAOPD in, 215

HREs. *See* Hypoxia responsive elements

HSV. *See* Herpes simplex virus

Hypoxia. *See* Tumor Hypoxia

Hypoxia responsive elements (HREs), 183–184
in gene therapies, 188–189
Hypoxia-inducible factor (HIF), 182–189
domain structures of, 184
EGF and, 187
heterodimerization of, 187
HREs and, 183–184
inhibition of, 186
ODN and, 186
overexpression of, 186
siRNA technology for, 186
synthesis regulation of, 185
VHL proteins and, 183

I

IGFBP. *See* Insulin-like growth factor-binding protein module
Inflammation, 144–145
apoptosis and, 144–145
fibrogenesis from, 145
Kupffer cells and, 145
platelets' role in, 144
polymorphs during, 144
tissue destruction during, 145
wound healing and, 144–145
Inflammatory bowel disease, 11
Innexins, 124–126
Inositol 1,4,5,-triphosphate (IP₃) internal stores, 71–73
Insulin-like growth factor-binding protein module (IGFBP), 3, 4
Integrins, 20, 22
FAK, 20
as fibrogenic mediators, 161
MAPKs and, 20
Internal stores
for Ca²⁺ channels, 70–73
for IP₃, 71–73
Ion concentrations, in charophytes, 63–64, 69–70
IP₃ internal stores, 71–73
in cytoplasm, 74

K

K⁺. *See* Potassium channels
Keratinocyte growth factor (KGF), 145
KGF. *See* Keratinocyte growth factor

Kidneys, CCN2 protein in, 9
Kinetochore proteins, 123
Kupffer cells, 145

L

Lampreys, 12
Law of Homologous Series in Hereditary Variation (Vavilov), 84–85
Lentiviruses, 193
Leptotene, 87
Low-density lipoprotein receptor-like protein 1 (LRP-1), 21
LRP-1. *See* Low-density lipoprotein receptor-like protein 1
Lungs, in horses, 216–218
cytological features of, 221–223
ECF in, 223
lymphocytes in, 222
mastocytes in, 223
neutrophil granulocytes in, 222
immune system for, 218
structure of, 216–217
Lymph nodes, in horses, 218
APC in, 218
FDC in, 218
structure of, 218–219
Lymphocytes, 222
Lytic viruses, 189

M

Manganese (Mn²⁺) channels, 60
MAPKs. *See* Mitogen-activated protein kinases
Mastocytes, 223
Meiosis, 83–132
for *A. thaliana*, 85
in *C. elegans*, 101–103
structure of, 102
terminal domains in, 102
chromosomes during, 86
3D structure of, 88
compact, 87
cytological pattern of, 84–89
EM use for, 87
homomorphism of, 86–89
for *D. melanogaster*, 85, 90
leptotene and, 87
molecular basis of, 84

morphogenetic proteins in, 89–109
nodules during, 91
organelle morphology during, 130–132
protein homology within, 85
recombination during, 109–114
 in *D. melanogaster*, 99
DNA and, 110
Rad51 proteins and, 111–114, 119, 120
rates of, 111
RecA proteins and, 111–114, 119, 120
RNAs and, 109–111
for *S. cereale*, 85
for *S. cerevisiae*, 85
secondary proteins in, 122–130
 connexins as, 124–126
 innnexins as, 124–126
 kinetochore, 123
 NPC as, 126–130
 pannexins as, 124–126
 structure of, 122–123
SMC proteins during, 114–122
 cohesins and, 114–122
synapsis proteins in, 92–109
 in *A. thaliana*, 103–104
 in *C. elegans*, 101–103
 charge distribution within, 99–101
 evolution of, 108–109
 lateral elements in, 105–109
 in *O. sativa*, 104–105
 SCP1, 93, 94, 95–96
 Zip1, 93, 94, 96–98
synaptosomal complexes and, 87–88
 3D model of, 91
 ultrastructure of, 90–92
for *Z. mays*, 85
Melanomas, 11
Mesenchymal cells, 12. *See also* Chondrocytes
 bone marrow, 19
Metalloproteinases, 168–169
Mitogen-activated protein kinases
 (MAPKs), 20–22
 Mn^{2+} . *See* Manganese channels
Myeloblastosis-associated virus (MAV),
 NOV and, 5
Myofibroblasts, 143, 149–154, 156–157
 actin in, 150, 157
 apoptosis and, 168
 differentiation markers for, 150–151
 marker staining for, 153
 in organ fibrosis, 151–152
 origins of, 156–157

smoothelin and, 149
stromal, in tumors, 152–154
in tissue repair, 149, 155
ultrastructures for, 149, 151
wound healing and, 145

N

Nephroblastoma-overexpressed gene
 (NOV), 2, 5–6. *See also* CCN protein
 family
 angiogenic properties of, 6
 MAV and, 5
 nuclear localization of, 6
Neutrophil granulocytes, 222
NOV. *See* Nephroblastoma-overexpressed
 gene
Nuclear pore complex (NPC)
 proteins, 126–130
Nups, 128, 129
POMs, 128

O

ODN. *See* Oligodeoxynucleotides
Oligodeoxynucleotides (ODN), 186
Oncolytic viruses, 190
Oryza sativa (*O. sativa*), 104–105
Osteoblasts
 bone growth and, 16–17
 tissue development and, 10

P

Pancreatic cancer, 11, 151
Pancreatic fibrosis, 11
Pannexins, 124–126
 TMDs in, 124–125
Patch clamps, 52
 Cl^- channels and, 61
 plasma membranes and, 52
 tonoplast membranes and, 52
PD. *See* Potential difference
PDGF. *See* Platelet-derived growth factor
Pedomorphosis, 14
Perfusion, vacuolar, 50–51
pH levels
 during AP, 64–65
 voltage-clamp techniques and, 64

Plasma-membrane permeabilization, 52

Platelet-derived growth factor (PDGF)
as probiotic cytokine, 146, 158, 161
wound healing and, 146

Platelet-rich plasma (PRP), 10

Platelets. *See also* Platelet-derived growth factor
during inflammation, 144
thrombin in, 163

POMs. *See* Pore membrane proteins

Pore membrane proteins (POMs), 128

Potassium (K^+) channels, 56, 61–62

Potential difference (PD), in AP, 43

Probiotic cytokines, 157–159

- GM-CSF, 158
- PDGF, 146, 158, 161
- TGF β , 145–146, 158, 161

Prokaryotes, in tumor hypoxia gene therapies, 194–195

Proteins. *See also* Bone morphogenetic protein; CCN protein family; CCN2 proteins; Nephroblastoma-overexpressed gene

- BMP, 19
- collagen, 164–165
- connexins, 124–126
molecular configurations for, 125
TMDs in, 124
- Dmcl, 112–113
fibronectin, 159, 165
homology of, during meiosis, 85
innexins, 124–126
kinetochore, 123
MAPKs, 20–22
morphogenetic, in meiosis, 89–109
NPC, 126–130
 - Nups, 128, 129
 - POMs, 128
- pannexins, 124–126
TMDs in, 124
- Rad51, 111–114
 - Dmcl proteins and, 112–113
- RecA, 111–114
shugoshin, 121–122
SMC, 114–122
 - cohesins within, 115–122
- smoothelin, 149
statins, 169
survivin, 188
synapsis, 92–105
 - SCP1, 93, 94, 95–96

Zip1, 93, 94, 96–98

3D structures of, 131

VHL, 183

WISP-1, 6–7

WISP-2, 7

WISP-3, 7–8

Zip1, 93, 94, 96–98

Proton pumps, 62–63

PRP. *See* Platelet-rich plasma

Pulmonary alveolar macrophages (PAM), COPD and, in horses, 225

Pulmonary fibrosis, 11, 151

R

Rad51 proteins, 111–114

- Dmcl proteins and, 112–113
evolution of, 113–114
expression of, 112
phylogenetic tree for, 119, 120

Radiotherapy

- TPZ in, 197–198
for tumor hypoxia, 182, 196–199, 200

RecA proteins, 111–114

- conserved motifs of, 120
DNA interaction with, 111
eukaryotes and, 111–112
evolution of, 113–114
phylogenetic tree for, 119, 120

Recombination, 109–114

- within *D. melanogaster*, 99
DNA during, 110
during meiosis, 109–114
Rad51 proteins and, 111–114
 - Dmcl proteins and, 112–113
evolution of, 113–114
expression of, 112
phylogenetic tree for, 119, 120

rates of, 111

RecA proteins and, 111–114

- conserved motifs of, 120
DNA interaction with, 111
eukaryotes and, 111–112
evolution of, 113–114
phylogenetic tree for, 119, 120

RNs, 109–111

- Shugoshin proteins and, 121–122
localization of, 121

Recombination nodules (RNs), 109–111

Renal fibrosis, 11

RNs. *See* Recombination nodules

S

Saccharomyces cerevisiae (*S. cerevisiae*), 85, 90
Zip1 protein in, 93, 94, 96–98
Scar tissue, 147
Scarring, 146, 147–148
cellular basis of, 148
wound healing v., 146, 147–148
SCP1 proteins. *See* Synaptonemal complex 1 proteins
Secale cereale (*S. cereale*), 85, 86
synaptonemal complexes in, 89
Shugoshin proteins, 121–122
localization of, 121
Skeletal development, 12–14. *See also*
 Bone growth
 of clavicle, 12
 of cranium, 12
 intramembranous ossification and, 12
Skin cancer, 11
Small interfering RNA (siRNA)
 technology, 186
SMC proteins. *See* Structural maintenance of chromosome proteins
Smoothelin, 149
SPAOPD. *See* Summer pasture-associated obstructive pulmonary disease
Statins, 169
Stimulus (for AP)
 mechanical, 53
 subthreshold, 53
Structural maintenance of chromosome (SMC) proteins, 114–122
cohesins and, 115–122
conservation of, 118
homologs of, 117
phylogenetic tree for, 119
formation of, 116
heterodimers and, 115
Suicide gene therapies, 188–189
Summer pasture-associated obstructive pulmonary disease (SPAOPD), 215
Survivin, 188
Synapsis proteins, 92–109
 in *A. thaliana*, 103–104
 in *C. elegans*, 101–103
 charge distribution within, 99–101
 in *D. melanogaster*, 98–99
 evolution of, 108–109
 lateral elements in, 105–109
 in *O. sativa*, 104–105

SCP1, 93, 94, 95–96
 domains of, 94
 hypothetical scheme for, 95
 structure of, 93
Zip1, 93, 94, 96–98
 Zip2 and, 96
Synaptonemal complex 1 (SCP1) proteins, 93, 94, 95–96, 132
Synaptonemal complexes, 87–88, 92.
 See also Synapsis proteins
3D model of, 91
central space of, 96, 97
for *D. melanogaster*, 95
in *S. cereale*, 89
ultrastructure of, 90–92

T

Temperature, AP influenced by, 47, 66–67
TGF β . *See* Transforming growth factor-beta
3D models
 of chromosomes, during meiosis, 88
 of protein structures, 131
 of synaptonemal complexes, 91
Thrombin, 163
Thrombospondin type 1 repeat module (TSP1), 3, 4
Tirapazamine (TPZ), 197–198
Tissue development
 CCN2 protein and, 8–10
 chondrocytes, 10
 fibroblasts, 10
TMDs. *See* Transmembrane domains
Tonoplasts
 in charophytes, 55–57, 68–69
 patch clamps and, 52
 removal of, during AP, 51–52, 56
 excitation during, 57
 in two-state hypothesis, 68
TPZ. *See* Tirapazamine
Transcriptional enhancer dominant in chondrocytes (TRENDIC), 24, 25
Transforming growth factor-beta (TGF β), 145–146
 as probiotic cytokine, 158, 161
Transmembrane domains (TMDs), 124–125
TRENDIC. *See* Transcriptional enhancer dominant in chondrocytes
TSP1. *See* Thrombospondin type 1 repeat module

Tumor hypoxia, 181–201
 cellular signaling and, 182–184
 chemotherapy for, 182, 199–201
 chronic, 182
 gene therapies for, 184–201
 eukaryotic delivery vehicles in, 192–194
 nonviral agents in, 193
 prokaryotic delivery vehicles in, 194–195
 signaling modification as, 185–188
 suicide, 188–189
 survivin in, 188
 vectors in, 189–192
 viruses in, 189–190

HIF and, 182–189
 domain structures of, 184
 EGF and, 187
 heterodimerization of, 187
 HREs and, 183–184
 inhibition of, 186
 ODN and, 186
 overexpression of, 186
 siRNA technology for, 186
 synthesis regulation of, 185
 VHL proteins and, 183
 radiotherapy for, 182, 196–199, 200
 transient, 182

Tumors
 CCN1 protein in, 5
 CCN2 protein in, 11–12
 myofibroblasts in, 152–154

Turgor regulation, 73–74
 Cl^- channels and, 73

V

Vacuolar perfusion, 50–51

Vascular endothelial cell growth factor (VEGF), 17, 20
 during wound healing, 145–146

Vascular endothelial cells
 bone growth and, 15–17
 CCN2 protein and, 8–9
 tissue development and, 10
 in VEGF, 17, 20

Vavilov, N.I., 84–85

VEGF. *See* Vascular endothelial cell growth factor

VHL proteins. *See* von Hippel-Landau proteins

Viruses, in hypoxia-targeted gene therapy, 189–190

HSV, 191
 lentiviruses, 193
 lytic, 189
 oncolytic, 190

Voltage-clamps, 49–50
 pH levels and, 64

von Hippel-Landau (VHL) proteins, 183
 HIF and, 183

von Willebrand factor type C (VWC), 3, 4
 VWC. *See* von Willebrand factor type C

W

Wnt 1-inducible secretory proteins (WISP-1), 6–7

Wnt 2-inducible secretory proteins (WISP-2), 7

Wnt 3-inducible secretory proteins (WISP-3), 7–8

Wound healing, 144–148
 angiopoietin during, 146
 AP and, 73
 CCN2 protein and, 10
 cellular basis of, 148
 contraction in, 165–166
 EGF during, 145
 fetal, 147
 FGF during, 146
 inflammation and, 144–145
 apoptosis during, 144–145
 fibrogenesis from, 145
 Kupffer cells during, 145
 platelets' role in, 144
 polymorphs during, 144
 tissue destruction during, 145
 myofibroblasts and, 145
 PDGF during, 146
 PRP and, 10
 scarring v., 146, 147–148
 TGF β and, 145–146
 thrombin in, 163
 VEGF during, 145–146

Z

Zea mays (*Z. mays*), 85

Zip1 protein, 93, 94, 96–98
 in *S. cerevisiae*, 93, 94, 96–98
 Zip2 and, 96